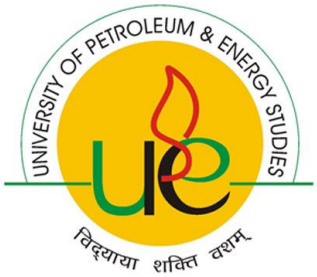

UNIVERSITY OF PETROLEUM AND ENERGY STUDIES

Ph.D. Thesis

FLOW AND CRITICALITY ANALYSIS OF FAST NEUTRON KINETICS OF GASEOUS CORE SUPERCRITICAL REACTORS IN SPACE PROPULSION FOR INTERSTELLAR FLIGHT UNDER MICROGRAVITY AND SEMI-RELATIVISTIC THRUST CONDITIONS

By
VELIDI VENKATA SUBRAHMANYA SURYA GURUNADH

Thesis Supervisors:

Dr. UGUR GUVEN
Professor Aerospace Engineering

Dr.KAMAL BANSAL
Professor & Director College of Engineering

Programme : DOCTORATE OF PHILOSOPHY

DEPARTMENT OF AEROSPACE ENGINEERING

FLOW AND CRITICALITY ANALYSIS OF FAST NEUTRON KINETICS GASEOUS CORE SUPERCRITICAL REACTORS IN SPACE PROPULSION FOR INTERSTELLAR FLIGHT UNDER MICROGRAVITY AND SEMI-RELATIVISTIC THRUST CONDITIONS

A DISSERTATION

SUBMITTED TO THE DEPARTMENT OF AEROSPACE ENGINEERING

AND THE COMMITTEE ON DOCTORAL STUDIES

OF UNIVERSITY OF PETROLEUM AND ENERGY STUDIES

IN PARTIAL FULFILLMENT OF THE REQUIREMENTS FOR THE DEGREE OF

DOCTORATE OF PHILOSOPHY

GURUNADH VENKATA SUBRAHMANYA SURYA VELIDI

DECEMBER 2013

THESIS COMPLETION CERTIFICATE

This is to certify that the thesis on **"FLOW AND CRITICALITY ANALYSIS OF FAST NEUTRON KINETICS GASEOUS CORE SUPERCRITICAL REACTORS IN SPACE PROPULSION FOR INTERSTELLAR FLIGHT UNDER MICROGRAVITY AND SEMI-RELATIVISTIC THRUST CONDITIONS"**Velidi V S S Gurunadh in Partial completion of the requirements for the award of the Degree of Doctor of Philosophy is an original work carried out by him under our supervision and guidance.

It is certified that the work has not been submitted anywhere else for the award of any other diploma or degree of this or any other University.

Dr.Ugur Guven
Thesis Supervisor
Professor Aerospace Engineering

Dr.Kamal Bansal,
Thesis Supervisor
Professor& Director, CoES

ACKNOWLEDGMENTS

My prayers to Shri.Guru Madavandha Swamiji and his ashram has given me peace of mind and glimpse of light towards knowledge and structured life. First and foremost I want to thank my thesis supervisors Dr.Ugur Guven and Dr.Kamal Bansal. It has been a great honor to be their Ph.D. student; Dr.Ugur Guven has taught me both fundamental aspects of nuclear engineering and advanced aspects of gas core reactors and neutronics. I am happy to complete my Masters and Doctoral work under Dr.Kamal Bansal Director College of Engineering, who has been a mentor for my career. I am thankful for the technical contributions, time, ideas, and support to complete this work. He always supported me whenever I have difficulties and he is a nice guide to work with. I am also greatly thankful to University of Petroleum and Energy Studies for funding my research and supporting with financial assistance.

The joy of work and research enthusiasm has been encouraged by the Chancellor Dr.S.J Chopra, even with the busy schedule Dr.Parag Diwan spends time in reviews and supports with the administrative and technical needs of the doctoral students. I am also happy to express my thanks to Prof.Utpal Ghosh for support while carrying the research work. Dr.Shrihari has spent time in suggesting me the various methods of solving the heat transfer problem and also in terms of moral and logistics support. The university IT team is always supported me with the technical help for running simulations in the lab.

I am also thankful to Dr.Ozoner who supports me in development of code and helping me out in creating specific libraries to simplify the problem, which is helped me in completing the given problem with in the planned time. The University Faculty Research Committee continuously advised me in every review, I am thank full to each and every

committee membered in spending time and giving valuable suggestions. In the process of completing the desired research on neutronics and the heat transfer aspects of the current thesis my team members from the aerospace departments has a special role. I should mention my gratitude to Dr.Rajesh Yadav for his support in structuring the thesis; Mr.Pavan Kumar Nanduri is always with me when I have difficulties. I am also thanking full to other team members Mr.Sourab Bhat, Mr.Karthick Sundarraj and Mr.Linsu Sebastian.

My family members, my father V.G. V Subrahamanyam who is teacher by profession and he is always supports me like a friend. My mother V.S.L.V Kameswari, and My sister Abhizna Velidi, who supported me in all possible aspects while continuing this work. Continuous motivation from Mr.Sonti Sundaram and family helped in concentrating on the aimed work and I am very much grateful to them. Special Thanks to other family members who shows special interest in me. Last but not least all my friends and students who worked with me have a special place in my heart.

Velidi V S S Gurunadh
University of Petroleum and Energy Studies
December 2013

DEDICATED TO MY PARENTS

DECLARATION

I do hereby declare that this submission is my own work and that, to the best of my knowledge and belief, it contains no material previously published or written by another person nor material which has been accepted for the award of any other degree or diploma of the university or other institute of higher learning, except where due acknowledgment has been made in the text.

Gurunadh Velidi

Doctoral Research Fellow
University of Petroleum and Energy Studies
Dehradun-248007

TABLE OF CONTENTS

LIST OF TABLES

LIST OF FIGURES

ABBREVIATIONS

IMF	Interplanetary Magnetic Field
LASL	Los Alamos Scientific Laboratory
LISM	Local Interstellar Medium
LLL	Lawrence Livermore Laboratory
LTE	Local Thermodynamics Equilibrium
MHD	Magneto Hydro Dynamics
NASA	National Aeronautics and Space Administration
NASDA	National Space Development Agency
NERVA	Nuclear Engine for Rocket Vehicle Applications
NER	Nuclear Electric Rocket
NENL	Near Earth Neutral Line
NRDS	Nuclear Rocket Development Station
NTR	Nuclear Thermal Rocket
QPO	Quasi-Periodic Oscillation
SEP	Solar Energetic Particles
SSC	Strom Sudden Commencement
STJ	Superconducting Tunnel Junctions
WNAL	Westing House Astronuclear Laboratory

NOMENCLATURE

A_e	Nozzle Exit Area
c	Speed of sound
C_p	Specific heat at constant pressure
C_v	Specific heat at constant volume
e	Total energy per unit volume
F	Thrust
f_z	Distant
p_a	Static Pressure
p_e	Exit Pressure
t	Time
m_a	Mass of the system
v	Absolute velocity
n	Neutron density
p	Core propellant pressure
T	Propellant Temperature
T_c	Reactor core temperature
ν	Neutron Velocity
E	Energy released per fission
Σ_f	Fission cross section
C_i	Concentration of delayed-neutron precursors for ith group
λ_i	Decay constant for ith group
β	Total fraction of decayed neutrons
δk	Excess multiplication factor
l^*	Mean effective neutron lifetime
ρ	Propellant mass density

P_i	Propellant core inlet pressure
Q	Heat generation per unit volume
h_f	Fluid-Side Local heat transfer coefficient
T_w	Wall Surface Temperature
T_f	Local Fluid Temperature
q_{rad}	Radiative Heat Flux
k_s	Thermal Conductivity of the solid
Δn	Distance between wall surface and the solid cell center
T_s	Local Solid Temperature
T_w	Temperature of the radiating surface
A	Core cross-sectional Area
a	Maximum Eigen Value
a_R	Rosseland Mean opacity
D	Diameter
D_h	Hydraulic Diameter
e	Total Energy per unit Volume
f_z	Distance Correlation for Nusselt Number
f_p	Property Correlation of Nusselt Number
h	Enthalpy or heat Transfer Coefficient
k	Thermal Conductivity
I	Unit Matrix
l, L	Length of the Core
m	Mass flow rate
Nu	Nusselt Number, hD/k
Pr	Prandtl Number, $C_p\mu/k$
q''_c	Conductive Heat Flux

q''_c	Radiative Heat Flux
q''_w	Wall Heat Flux
q''_t	Total Heat flux
q''''	Volumetric Heat Generation Rate
r	Radial Position Measured from the center line
Re	Reynolds Number, $\mu L/\nu$
T	Temperature
t	Time
T_s	Surrounding Temperature
u	Axial Velocity z component
v	Radial Velocity r component
z	Axial Position measured from the core Inlet
γ	Ratio of Specific Heat
Φ	Function of Separation Angle

ABSTRACT

The needs of traveling beyond the current limitations will be addressed through nuclear space propulsion. The basic advantage in choosing nuclear energy is to address the propulsion needs, because of the developments in reactor technology today with the generation VI reactors. The possibility of creating controlled fission reaction even in a moving reactor will be a safe option in terms of operation. In the advanced propulsion methods from the physics of the propulsion point of view there are much stronger ways of creating energy like nuclear electric propulsion, antimatter propulsion. The only advantage in choosing fission based methods is because of technological feasibility as on date and faster development possibilities in terms of real system. The basic approach of creating a nuclear rocket system will be dependent on heating the propellant through fission based heat source and higher specific impulse will be generated. The functionality of thermal propulsion system is much simple since it will use fission based nuclear reactor to heat the hydrogen propellant and it will be expanded through the nozzle. In the total system architecture the propellant is used to force through various channels in the rector using a turbo pumping system.

The initial stages of the work is revolved around solid core nuclear reactors as heat source and various configuration has been developed and their experimental results are quite encoragive. Whereas rocket is a compact space traveling device which needs to be as stable as possible and weight of the system configuration reduces the payload capability. Also with the solid core systems due to the metallurgical limitations with the fuel elements the reactor operation need to be restricted a core temperature range of 2500k-3500k and in many of the cases the secondary cooling system like helium need to be introduced across the wall to

maintain the effective safety conditions with the operation. With the above problems the method of adopting vapor core in place of solid core reactor system attracted the thermal propulsion system and it lead to the development of open gaseous core reactor system as well as closed core gaseous reactor system based on its operational parameters.

This work is chosen on open cycle gaseous core reactor system to examine the fluid dynamics of the vapor core as well as the neutrons under microgravity with the semi relativistic speeds. In the open gaseous core reactors the fuel will be in the core region and the propellant will be passed through buffer region of the reactor. The secondary flow channels will be connected to the reactor before it reaches the nozzle. The effective flow conditions are examined with various configurations for vortex chamber using computational fluid dynamics. The fuel region is treated as generating sauce and convective and radiative models are solved under various conditions to supply parameters to the neutronics analysis.

Numerical Heat Transfer analysis is conducted to address the key aspects of the reactor core Temprature and pressure variations with the fuel plasma Temprature. For high energy conversion systems like nuclear rockets the convective and radiative heat transfer analysis between the fuel and the propellant should be high to generate moderated specific impulse of order 3618 sec. the analysis is conducted on a two directional reactor model for different heat generation rates obtained from the fission energy equation. Two different propellants are considered to compare the effectiveness of the core performance and hydrogen has many advantages. The analysis is conducted with respect to the fuel enrichment of 50% where the GCR core has a potential of producing 100 MW/m^3 is to be consider to justify the needs of interstellar travel. In the other case the fuel enrichment varied from 60 MW/ m^3 and the 40 Mw/m^3 of generation rates are possible with 5 % and 30 % fuel enrichment. Where the generation rates are not

directly related to the percentage of enrichment also the pressure variation and the reactor core size effects the complete design. In case of helium as propellant the similar generations rates are considered with the change in fuel composition due to the vaporization effects the percentage of fuel composition with the U-C-F compounds are varied with respect to the percentage of enrichment. The analysis is accounted for the behavior of the fluid in various changes in parameters inside the GCR core and the deseeded Temprature and pressure levels for fission to occur are investigated. The flow domain is divided into 500000 elements to identify the changes in the core and the heat transfer process. The Temprature distribution and the pressure variations are studied at the constant wall Temprature boundary condition to support the reflector Temprature limitations. The maximum reflector Temprature is considered at 1900 K and it has lower limit of 200 k, it is only possible in case of ideal conditions. This work considered the most optimum reflector Temprature limitation possible for the graphite reflector at 1200K. The combined convective and radiative heat fluxes can give the overall idea of Temprature distribution in different zones at a given generation rate.

Neutronics analysis is conducted on a one dimensional core model for three different cases with the change in its fuel composition and the fuel enrichment with in the compounds of U-C-F. The original form of the fuel composition is derived from depleted uranium obtained in a uranium enrichment process and UF_4, UF_5 and UF_6 compounds are produced. These three compounds are most suitable for the GCR reactor operations. In the analysis conducted on GCR the percentage of variation is consider with 50%, which is an ideal case and most practical case is considered at 5% enrichment levels. Neutronics analysis conducted on the GCR core can describe the fuel gas density effects on the fuel Temprature and the neutron production effects of criticality with various parameters are obtained using a Monte Carlo code developed in Visual C++ for a

two group diffusion theory to account for the neutron interactions in a 150 cm core region. The core model is divided into 54 regions inside the infinite cylinder with a diamond differencing method and the behavior of the thermal and fast neutrons are considered. The grid is developed in the form of user library to call for different programs in future, besides grid.h there are several libraries. The relative error in the iterations and the error levels in the reactor criticality are analyzed for all the three cases and the accuracy of the solution are discussed in the thesis.

Since the analysis is conducted on GCR model which is likely to operate for space needs the criticality is much higher than the regular power reactors. The consideration of actinides formation is not an appropriate method for the following case since fast neutron groups and the thermal neutron groups are considered and also reactor criticality is much higher. In case of using solid core reactors these considerations are applicable due to the fuel interaction with the materials used for reactor fuels. The connection between the heat transfer analysis and the neutronics established with the radial Temprature distribution to maintain effective criticality values, since the behavior of the propellant gas and the fuel it will change, In case of rocket applications the flow regulations can be done remotely. The reactor operating parameters are considered from Van Booman model and the variations are analyzed for the moderated conditions. The reactivity coefficient and the fuel density variations are large in case of gas core reactors. The keff values are studies for different cases at a specific variation the Temprature profile. The peak values are considered from CFD analysis and inputted to the code is designed and T_f and ρ_f are given as inputs and the neutron flux density is calculated using probability functions and Keff values are compared for various T (r) and ρ (r) the keff varied with the enrichment levels and the tempratures distribution.

CHAPTER 1: NUCLEAR SPACE PROPULSION

The idea of nuclear propulsion is to use light rector system to generate required energy for the space travel. The light nuclear reactor is used for heating a low molecular weight propellant, coolant. The advantage in depending upon atomic energy to use for rocket/space allocation is because of larger magnitude of energy density. There are various means of converting atomic energy in the rockets, like most of the work concentrated on nuclear electrical propulsion and nuclear thermal propulsion. There are mixed means of creating higher energies for traveling to the distances in space, which needs technological systems development and temperature handling up to 50,000 K are the major constrains (G.M Piacentino, 2008). Using nuclear rockets, interplanetary missions travel time can be significantly reduced as a same time payload carrying capacity will increase due to compactness of the propellant and the fuel tanks. It can also support onboard power requirements at a capacity of 250-300 kWe(Gunn SV, 1989). This additional feature can support more scientific missions through instrumentation; wide range of experiments can be planned in shorter mission duration.

Travel beyond the solar system is a scientific challenge under the means of current technology as well as economically it's a higher objective. Traveling distances which are in light years need a propulsion technology which can complete one particular mission like reaching nearest star in once life time will be an effective result. Such kinds of mission required a rocket system which will travel with semi-relativistic speeds within the range of 0.2-0.3c (Dann G, 2004). These speeds are not attainable with the existing propulsion systems as well as the considerations from relativistic space mechanics and

external space radiation are going to a challenge. The experimentation which is going to be planned will become absolute with the time since we will advance during the mission travel time. Conventional rocket systems will be having (ΔVs) in few hundreds of kilometers per second, where are nuclear rockets are having higher order of (ΔVs).

To design a spacecraft which can travel with significant fraction of the light speed needs at least 4×10^{15} J/kg of kinetic energy of the order which it will change along with the distance and acceleration of the travel (D F Spencer, 1963). The idea of dealing with nuclear propulsion instead of high energy density propulsion, antimatter propulsion and Ion propulsion, since nuclear thermal propulsion work is in progress from 1960's in the countries like United states as well as in USSR. The developments so far were also discuss in the thesis to give complete idea over the problem and its analysis. This thesis majorly concentrates on nuclear thermal propulsion using gas core reactor, based on the past work the design parameters were considered and the computation analysis over neutronics and Heat transfer aspects are the major focus.

1.1 NUCLEAR THERMAL PROPULSION

The controlled fission is the major principle in the nuclear rockets, propellant will gain heat energy through fission process and rest of the rocket principles applies. The early days of work on nuclear thermal propulsion is quite encouraged the space community. The solid core reactor development for rocket applications and their designs were successful with LASL as well as with USSR. The famous programs like NERVA and Rover created a great impact in various systems development. In the rocketry point of view these rockets will have double the specific impulse compared to chemical rockets.

This factor comes from the energy density rate which is high for fission process when compared to chemical combustion and the second factor is with the selection of propellant and coolant for the reactor chamber. In most of the designs the recommendations lies with Hydrogen since it will be helpful for duel purposes. These rockets will produce high trust with good specific impulse since both energy density and low molecular weight of the propellant is the major for them. In the process of conducting research on nuclear thermal rockets, there are various models proposed to make design more versatile for space travel.

The initial stages of the design are more likely same as power generation reactor but developed for limited energy generation to reduce the size of the reactor configuration. In the course of development reactors have been built without control rods and propellant pumping mechanisms are integrated to the reactor system. But solid course reactors could not able to cater the needs of space travel, since few limitations with the temperature of the fuel rods, reactor core temperature limitations and control problems effected the design and the current developments in the solid core reactors can only support core temperature ranges from 2000 K-3500K (Gurunadh V, 2012).

1.1.1 SYSTEM CONFIGURATION

The nuclear thermal rocket configuration is likely same as chemical rockets, the difference in design comes to support nuclear fission in the reactor core. Base on type of fuel used neutron reflectors, moderator, fuel rods in case of solid core reactors and flow channels will describe a complete configuration. The neutron reflector plays an important role to have a controlled chain reaction that is a steady-state operation when neutrons are produced, they should be equally participating in fission. In general various energy levels of

neutrons are produced and only thermalized neutrons participate in nuclear fission (Anghaie S, 1986). The Kinetic energy of the neutrons will be lost in the collisions and neutrons will thermalize. The major objective of this work is to work with the neutron reflector material and its thickness of the reflector to reduce size of the reactor. Eventually the objective of designing nuclear rocket is to reduce the overall weight of the configuration to support heavy payloads and long distance travel. These neutron reflectors will be made with specific material for a particular configuration and shape to prevent neutrons from escaping the core. The reactor pressure vessel is designed to maintain required pressure varies from 3MPa to 8 MPa(Bissel W R, 1992). It will be made up of aluminum or composite materials to withstand high radiation, heat flux and high pressure inside the reactor.

Solid core reactors normally said to be thermal or fast reactors depending upon the neutron energy with which fission is taking place. In order to see the probability of neutrons to participate in fission the energy levels should below 1ev and the energy range of the neutrons produced in reaction will be from 10-15 Mev(G M Grayanzov, 1994). To slow down these neutrons and to make fission self-sustained, one has to use moderator with assembly systems made up of a martial with low atomic number. In fast reactors the range of energy will vary from 100Kev to 15Mev, in such cases we should avoid using moderators (G M Piacentino, 2008). In most of the space reactors usage of moderator is not an effective method. The energy levels we want maintain will be much higher than the power generation reactors.

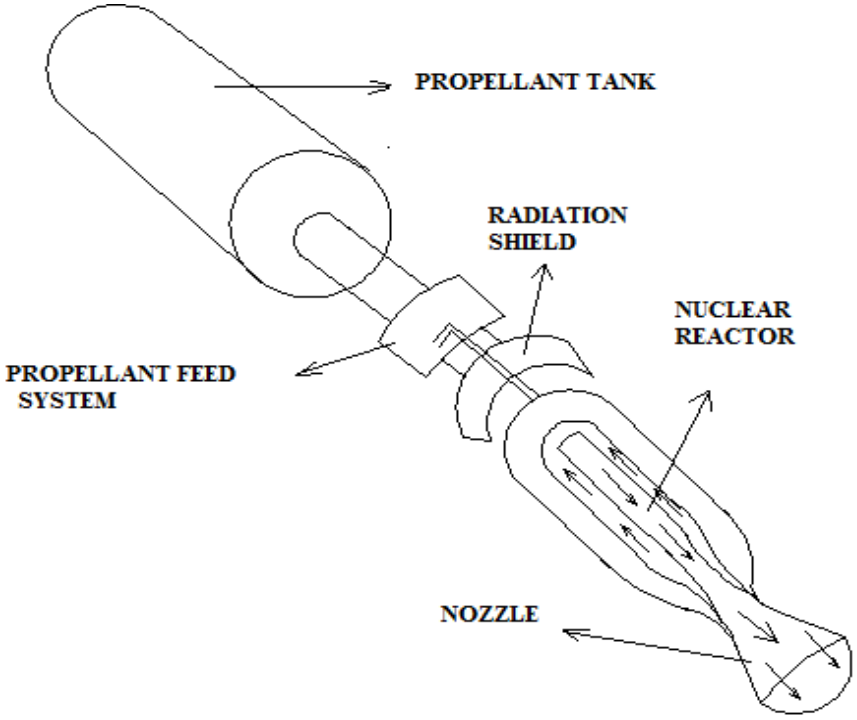

Figure 1.1: Nuclear Thermal Reactor Configuration Model

In some special cases moderators will be mixed with fuel elements, so that operation range of the reactor will come to average range of energy levels of the neutrons. A schematic diagram of the thermal rocket system is illustrated in the figure 1. The fuel arrangement for various configurations differs with the principle of operation, in case of most of the models tested for space propulsion applications are solid core reactors. In solid core fuel assembly system is little complex since it has to have coolant/propellant flow channels in between the configuration. It takes advantage of surface area to transfer the heat to the propellant and allows some sort of barrier to the fission products (G L Bennett, 1994). System configuration becomes more complex in solid core reactors with reflectors, flow channels and control rods around the fuel rods, so that it controls the neutronics as well the flow rate of the propellant.

In case of solid core reactors even control rods or drums are arranged to control the fission reaction when and where it is required. Unlike ground reactor it needs controlled reaction in case of traveling to long distances the mechanism of operation will be acceleration and deceleration by its distance (Dann G, 2004). These are can be used a control mechanism to balance the neutron population to maintain desired energy levels in the reactor core, in some configurations dual purpose design is used to control as well as to reflect the neutrons. In case of rotating interstation one side is beryllium and other side is born one will act as a control surface and other will act as a reflecting surface. This mode reduces its size by grater magnitude in terms of system configuration.

Most of the thermal rocket systems independent of core configuration only hydrogen is chosen as a propellant to reduce the tank size and weight, in case of solid core reactors propellant will enter in the form of vapor to avoid the thermal shocking and boiling issues at high temperature. In case of gas core reactors buffer region allows propellant to exchange heat with great time interval. The overall size of the solid core reactor system is not so attractive due to the above described system configuration and supporting mechanisms and their setups, so the overall size of the system increase by volume as well as by weight. There are various limitations of the solid core reactors in terms of operational temperature and problems associated with hydrogen handling at high temperatures. Later days of research turned the focus towards gaseous core reactors to address the above problems. In the nuclear thermal rockets the strategy is to use the heat released in the core to pressurize the second passage through the reactor the core walls. The model solid core reactor configuration using in the figure below, this consists of main propellant channel through the core surface to maintain initial conditions to enter the flow channels.

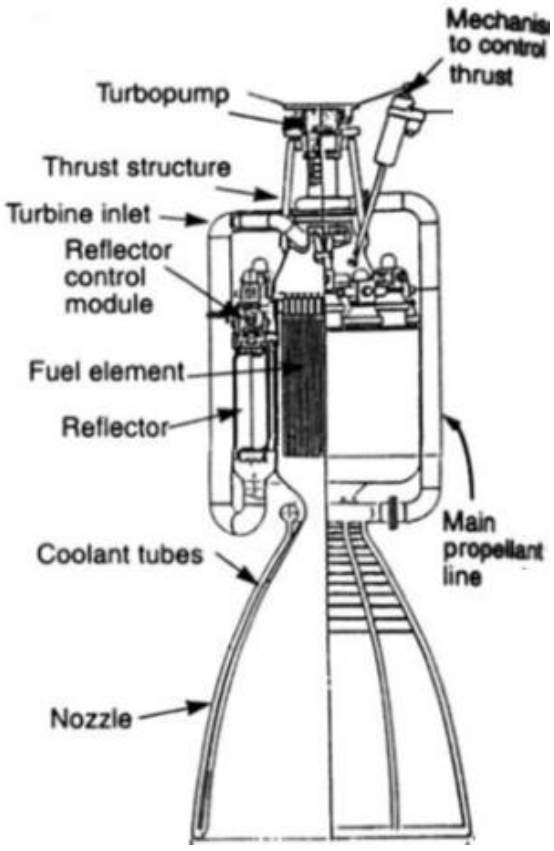

Figure 1.2: Nuclear Rocket Engine using Solid-Core Configuration

The eject mass from the secondary stage of the rocket will be pressurized from the secondary stage of energy conversion. This mass can be treated as fission fragments with is $\mu=0$, sometime it can also be treated as inert mass and its leads to the formation of actinides in the reactor core. In general these reactors consists μ in the order of 10^3 to 10^6, which allows them to maintain increased thrust and moderated temperatures. In the third stage of the reaction this energy will convert into macroscopic kinetic energy to expand from the nozzle (G M Gryanzov, 1991). Most of the configuration developed and tested is with solid core reactor system with three stages of operation as a replica of chemical rocket system.

1.2 GAS CORE REACTORS

Gas core or vapor core reactor is a fission based reactor in which fuel will be in the form of gas instead of fuel rods. The actual core design will be completely different for gaseous core reactors since the temperature limitation for nuclear fuel rods will not be applicable, for the same reason solid core reactors cannot be operated above 3500K (G L Bennett, 1994). Because the fuel rods can melt, vaporize, ruptured or destroyed due to core temperature. Whereas gas core reactors can be operated near about temperature limit of 10000K, only constrain will be wall temperature but it is not as critical as core temperature. Another aspect of handling reactor core at above 10000k will be a challenge since high level ionization will be realized in the fuel and it becomes plasma. Usage of nuclear fuel in the gaseous form can be wise way of reducing system complexity, which is intern going to support space travel needs as a rocket vehicles (G M Piacentino, 2008). Unlike conventional reactors oxidant and the propellant volume will be less, and reactor system will become compact and powerful for the payload carrying. Because of this GCR are having more potential in considering for rocket application and which can be designed for quite high temperature with in the current technological possibilities. In the fission based rocket reactor system only GCR are having highest core temperature of all exiting designs.

The main benefit of a GCR is with its core design and reflector arrangement, since there is no dividing wall between the fuel and the propellant heat transfer will be more effective through both convection and radiation. The arrangement in the core will be explain in the figure below, the injection of hydrogen and gaseous uranium will be injected in radial direction that vortex generation can happen to protect the uranium hexafluoride inside the reactor core (Gurunadh, 2012). The reactor will be dividing into two different zones

to differentiate the process, the core region where nuclear fission takes and the buffer region for hydrogen to expand and to create effective kinetic energy. Reactor model illustrated in the below figure can give us the specific idea over vortex generation and radial entry of the fuel systems.

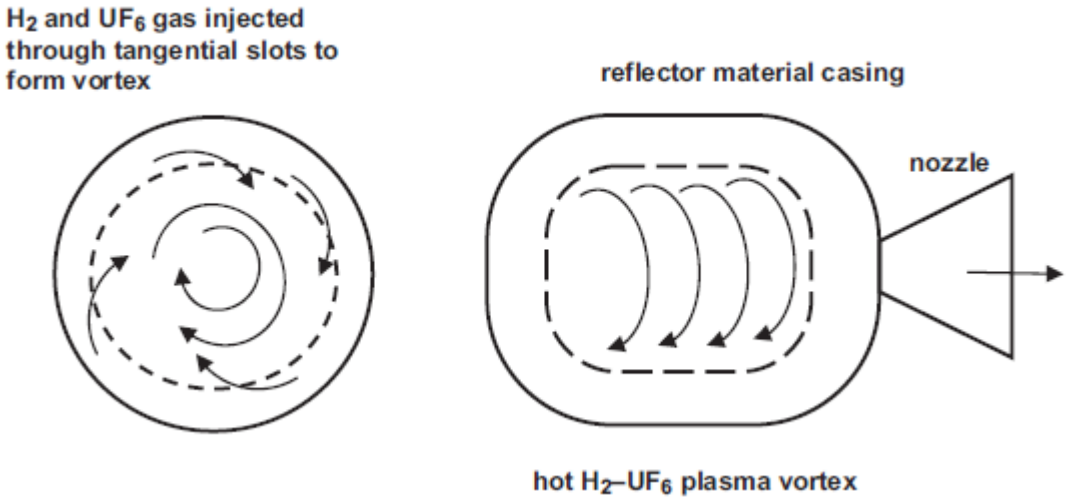

Figure 1.3: Flow configuration in GCR

1.2.1 GASEOUS FORM OF NUCLEAR FUEL

In the fission process we do use radioactive materials in various forms, due to the power reactors the development of fuel rods technology is well established and effective fissionable fuel rods can be made with required enrichment for solid core reactors. In case of reactors that can be used for rocket applications also have different way of developing fuel pins to reduce the weight and size of the system configuration, and various other reactor models are also proposed using fuel rods. Whereas in case of gas core reactors we use highly enriched fuel nearly above the weapon grade enrichment and in the form of Uranium hexa fluoride, Uranium tetra fluoride as well as in the form of mixed configurations like U-F-C are

common in usage. The specific application describes the means of development of gaseous form on nuclear fuel since the process associated with the depleted uranium in uranium enrichment process. The only work available in uranium processing to gaseous from is with 1940 data, before that crude based processing used to be an unreliable technique and the data is not so reliable on UF_6 models. Uranium hexafluoride or tetra fluoride is stored in semi-solid state due to its safety constrains (Anghaie.S, 1986). When it will be entered into the fission chamber, it will be converted into the liquid state and eventually into gas before it travels through the overall length of the chamber. Even the vortex generated in the flow path will allow periodic participation of the fuel in the reactor core.

Since the material processing and handling is more costly the amount of fuel we need to use for each application need to be taken care. The major constraint it to protect the fuel inside the chamber so that fuel will not be expelled out through propellant, there are various means of protecting the fuel inside the chamber. The fundamental idea in the initial days of development is to use MHD generator to create magnetic field and to ionize the propellant so that higher kinetic energies can be attainable (G L Bennett, 1994). In this thesis vortex generation approach will be considered and there will not be any physical containment between the fuel and propellant. This approach is considered from Kerrebrock, 1961 and the analysis is conducted on the similar reactor model with the effective conditions. This can be created with radial injection into the reactor chamber and the pressure difference in the core system. This approach develops pre-fission conditions with the fuel gas inside the core so that fission reaction is self-sustained.

1.3 DEVELOPMENTS IN NUCLEAR SPACE PROPULSION

The theoretical work on rockets which can travel beyond earth atmosphere started from the Konstantin Tsiolkovskii in the period of 1857, he described about space travel, weightlessness and exhaust velocity. The paper published in 1903 by Tsiolkovskii given a derivation for rocket equation in the form of delta for the use of reaching distances, also he described about the multistage rocket systems and liquid propulsion system by using alcohol and liquid oxygen (Bissel WR, 1992). This work identified exhaust velocity as an important performance parameter; also he concluded that higher temperature produced by lower molecular weight liquid fuels would be an important method for producing higher exhaust velocities.

The next stages of the theoretical work continued by Herman Obreth and he examined the use of liquid propelled rockets in given a design in his doctoral thesis in 1923, by using his work in Germany lot of amateur rocket scientists started creating systems using liquid oxygen and alcohol. The actual engineering and scientific work originated from the year 1914 from Robert Goddard, who got a patent for a liquid propelled rocket combustion chamber and a nozzle. The overall experimentation and theoretical work from this professor resulted in getting 214 patents for the development of various systems for rocket propulsion (Stanley, 2001). His inventions include use of vanes in the jet stream to steer the rocket, gyroscope, turbo-pump to drive the propellant to the combustion chamber, cooling system for the rocket nozzle using liquid oxygen. Goddard lunched his first rocket in 1926 with the weight of 5 kg using petrol and liquid oxygen as a fuel and successfully attained a height of 12.5 meters and he presented a paper on his experimental work and mentioned the possibility of sending unmanned rocket vehicle to the moon (Goddard, 1919).

The idea of using non chemical sources for propulsion applications started again by Goddard, who has written a paper for a conference held in 1906, France. Where he described about using radium as an energy source for creating higher energy in the rocket engines, later he realized the emitted power will be insufficient for reaching longer distances in space. Which leads to an idea of using atomic energy to rocket applications to create powerful rocket engines, the theoretical work was proposed by Esnault-Pelterie in 1912.

The technological support to create nuclear rockets started in the year of 1950's , and the experimental testing was done successfully in 1960's on aground based reactor , below table describes the various reactor models tested and their date of testing.

Table 1.1: NERVA: Reactor and Engine Systems Tests

Name	**Date of Testing**
Phoebus 1B (one-Power test)	Feb.1967
Phoebus 2(cold-flow tests)	July 1967-Aug.1967
NRX-A6(one Power test)	Dec.1967
XECF(cold-flow test)	Feb.1968-Apriil 1968
Phoebus-2A(Three-Power tests)	Jan.1968-July 1968
Pewee-1(Two Power Tests)	Nov.1968-Dec.1968
XE(28 Starts)	Dec.1968-Aug.1969

1.3.1 SUMMARY OF CONTRIBUTIONS

The cold war between Americans and Russians lead to various scientific accomplishments on the field of aerospace and rockery sciences. With the same intentions the nuclear propulsion program started in 1950's and continued till 1970's, in United States the program is names as nuclear energy for rocket applications called NERVA. This program successfully tested its first reactor and given a greater hope among American community, the model reactor that was tested is given in the figurer below. The technical details of the complete reactors tested are tabulated in the table2, the maximum specific impulse recorded in the testing is 971 sec which is twice the specific impulse from chemical rockets. The NERVA rockets reactors designed for 1570 MW of power but it obtained only 825sec specific impulse(Stanley, 2001). Later stages of the NERVA program research focused on developing higher specific impulse with in the designed reactor power, but its performance characteristics are limited to some extent. In the reactor developments most of the focus given to solid core reactor till 1965 with the hope that power reactor experience will help in converting it to mobile reactor system. In part of NERVA program KIWI and TROY programs are established in LASA with the support of Lawrence Livermore Laboratory. In the above programs research followed in the direction of searching alternative working fluids to address the problem in the potential chemical interaction with the fuel elements and the hot hydrogen (G M Gryanzov, 1991). In KIWI 1 reactor design ammonia was proposed as a working fluid, whereas with Troy reactors they tried with nitrogen. To operate the reactors at high temperature both the reactors have graphite requited fuel rods. The idea of using graphite have multiple advantages, it can handle high temperatures in the reactor core as a

same time it can also act a moderator in controlling neutrons, so that population of thermalized neutrons concentration increase.

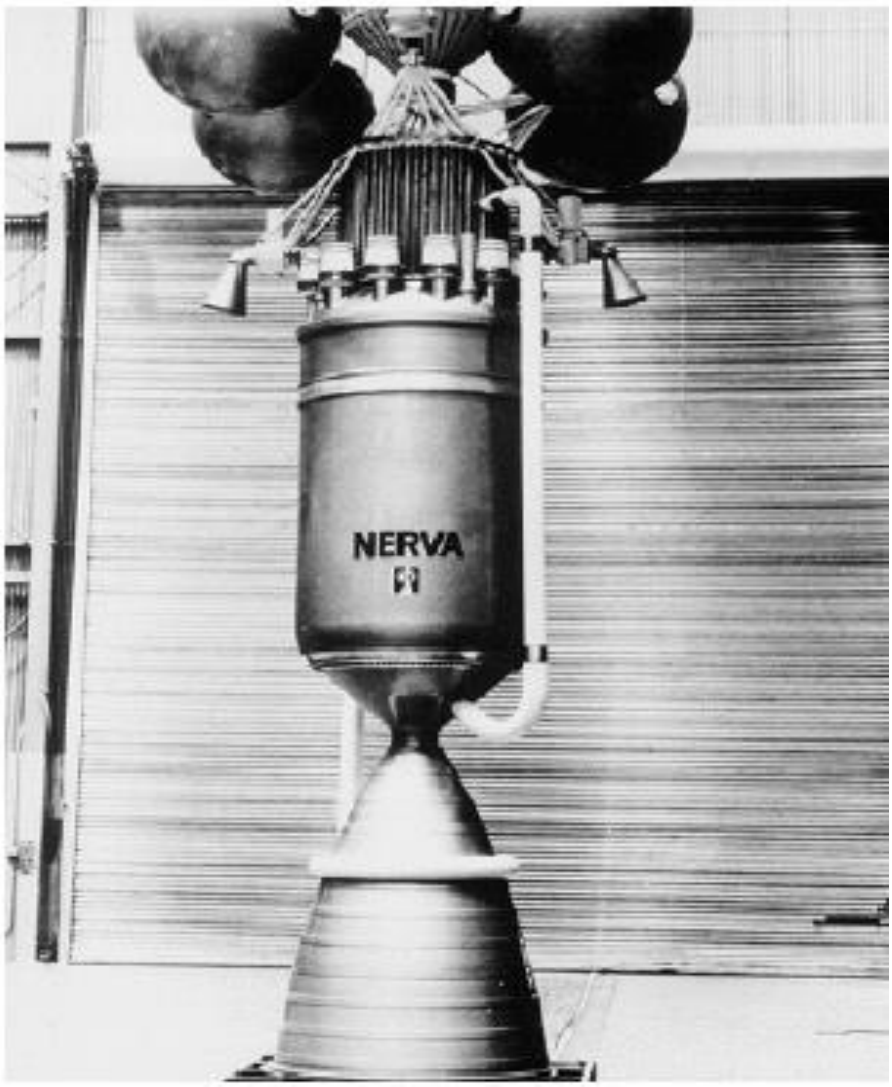

Fig 1.4: Source: NERVA 1 as it stands in Huntsville, Alabama, Space Park[Dewar, 2004]

Characteristics	NERVA	Particle bed	CERMET
Power, MW	1.570	1945	2000
Thrust, N	334.061	333.617	445.267
Propellant	H2	H2	H2
Fuel Element	Solid Rod	Pours Particle bed	Solid Rod
Maximum Propellant Temperature , K	2361	3200	2507
Isp,s	825	971	930
Chamber Pressure, Mpa	3.102	6.893	4.136
Nozzle Expression Ration	100	125	120
Engine Mass, kg	10138	1705	9091
Total Shield mass, kg	1590	1590	1590
Engine thrust/weight (no shield)	3.4	20.0	5.0

Table 1.2: DIFFERENT DESIGN PARAMETER UNDER TEST CONDITIONS

Besides the scientific organizations, US military was also shown specific interest in the similar periods to develop a system which has higher ΔV and heavy payload applications. Rocketdyne with US air force started working on nuclear rocket systems design with the hope that it can strengthen their capabilities. Later the direction shifted towards development of single stage ballistic missile, hydrogen as a working fluid. Unfortunately technological limitation created a huge impact on outcome, rocket dyne focused in developing a propellant pumping system. With the development of propellant pumping system all the agencies shared the contact and started working in KIWI A reactor with 100 MW power range to verify the performance of various systems (Bissel W R, 1992). This reactor was design to operate at 100 Psi pressure range and maximum temperature of 4500 ^{o} R. Since hydrogen used as working fluid and the reactor pressure is compared to be low, designing a nozzle became a challenge. RocketDyne was given a contract to design nickel coted nozzle for the designed chamber pressure with water cooled configuration (Dan, 1997).

These efforts have given a grate focus on future plans and the success in KIWI A directed LASL towards KIWI B reactor development program to develop high power density. The design made in KIWI A is limited to 100 MW, where in KIWI B focused on developing 1000 MW reactor system with 50000 lb of thrust, 500 psi operating pressure with a hydrogen flow rate of 66 lb/s (Stanly, 2001). The effective designed concluded that controlled fission can be attainable in solid core reactors, but the compactness of the reactor configuration and the higher power densities have become a challenge in reactor research. With the aims of reaching mars NASA mission planner identified the thrust requirements from nuclear rocket in a range of 200000-250000lb, which has set a goal of designing 5000 MW propulsion reactor

(Poston, 1994). The next program in meeting above performance characteristics lead to start Phoebus which is a developed setup from KIWI B-4E fuel elements based reactor system. This analysis was conducted computational and resulted in grater increase of 50% in power density, in the similar lines experimental investigations started with Phoebus reactor. LASL proposed Phoebus 1 and 2 reactors with improvement from the fuel elements of KIWI B-4E configuration to operate at 1500 MW power with a chamber pressure of 75000 lb that is aimed to attain 750 psi chamber pressure to increase 50 % heating of the propellant in the nozzle region. This model lead to the development of heat load evolved tubular nozzle at a new state of art level. The modification done in Phoebus 2 is of meeting 5000 MW/ 250000lb thrust based on increased core diameter to 55-inch in which 4068 fuel elements are bundled(G M Piacentino, 2008). This reactor systems development has given a grate thrust to the rocket engine program and lead to the development of 2001-Vintage NTR design to utilize NERVA-Rover fuel elements with tie tube cooling system. The test was conducted on the developed system for 10.5 minutes and able to attain 900 sec of specific impulse with the moderated pressure and the chamber temperatures. These developments could not able to meet NASA's projections in planning a MAR's mission using nuclear thermal rocket. Besides these programs from LASL, Russian community also worked in the similar lines and the developments are not so attractive. Due to these limitations in 1974 the funding to the reactor development programs has been ceased.

1.4 MOTIVATION FOR RESEARCH

Within the current technology one can plan missions to nearest planets around the solar system; but the vision of the human is to reach stars and to understand the dynamics of the universe with in a possible man's life time.

The nearest start human can reach is at a distance of 4.3 light years or 2.52×10^{13} miles. If we start traveling at a speed of 25000 miles per hour by a spacecraft it would take 114000 years to reach alpha century (Richard F. Tinder. 1967). There are various observations over the nearest stars like Proxima Century, Alpha Century-C, Bernard Star, Epsilon Eradani and Lalande-21185, which takes much longer period since their distances are above 10 light years. The need to find opportunities to complete such kind of missions with in a human life time needs greatest spacecraft which can travel at relativistic speeds. With idea of four years of research with nuclear rocket propulsion, the near future possible propulsion system that can support such kinds of missions can be with gas core reactors.

This indicates traveling in deep space is going to be challenge where we have to be dependent on the time that we can encounter on the earth one humans life time. And completing such ambitious missions need effective propulsion system Nuclear energy is one of the considerable sources for replacing chemical rockets; the idea of using nuclear energy for rocket applications was established from the success of controlled fission reaction. In space travel distances and time are two major contains which need to be addressed from rocket science. The conventional rocket propulsion methods are quite suitable to reach moon or near earth orbits with specific payloads. The space community in the current generation is looking at interplanetary manned missions, to reduce the travel time to protect human from space environment as well as from radiation. The competitive feasible solution with in the aimed time line is going to be nuclear thermal rocket. The first glimmers of a chance to convert fanciful notions of extraterrestrial flight into an idea with engineering significance came with the invention of rocket (Robert, 1958). The idea of creating nuclear thermal rocket is to strengthen the spacecraft's

with higher energy potential. In nuclear thermal rocket nuclear fission based rector will be used to produce energy and low molecular weight propellant like hydrogen will be used as a propellant to extract heat from the reactor. The major developments in designing reactor system for nuclear rockets are tied with safety and cost effectiveness as well as engineering possibilities over material contains. The operational temperature range starts from 3000k and it can be upgraded to effective values based on the fluid limitations. Traveling with grater speeds in space is more of a relativistic space mechanics problem than a systems development problem. The theoretical attainable speed by manmade object internes of fraction of light speeds is 0.37c. Which needs a greater level of kinetic energy producing device and carrying such a huge mass of fuel and propellant will be a challenge. The reactor technology developments supporting nuclear thermal rockets can eventually support travel up to nearest star system, if not a complete mission but at least robotic probe can change the overall idea with its observations.

The gas core reactor development will be based on neutronics and establish collisional cross-section between the neutron and the nuclei with in the core geometry. Unfortunately there is not much information available on gas phase neutronics and thermalized kinetics. LASL is active for two decades in the investigation of neutronics with the hope that it can give a day of light for nuclear thermal rocket development. The theoretical studies in the research indicate that gas core neutronics is viable, but practical developments need more understanding. The idea of working on gas core neutronics is to at least develop a system which can accommodate 10000K core temperature so that the specific impulse that can be achieved will reach to 1500 sec at least, since the theoretical studies are revolving around 2400-2800 sec. In a way fuel selection choices are also limited, may be uranium hexafluoride, uranium

tetrafloride and 242 Am can only be used. This study over two group neutron theory will develop an idea over gas core neutronics with heat transfer model.

1.5 OBJECTIVE OF THE THESIS

In most of the neutron investigations and heat transfer models for various reactors uniform temperature and density distributions are assumed, for heat transfer analysis assumed uniform flux distribution with in the reactor chamber. The objective of looking in this aspect is to increase neutron mean free path length so that low fuel density can be maintained. The neutron mean free path and density effects can also be correlated with the geometry change and diameter as a characteristic variable. This approach neglects fluctuations in the core and correlates with the average value of the neutrons inside the core. Since the neutron mean free path length is large the power density is to be considered as a proportional parameter to the uranium density inside the core. The errors from the above assumptions are considered to be small compared with the variable density distribution system and applicable to specific cylindrical geometry under consideration.

This research is conducted as a doctoral thesis in the field of reactor development for nuclear propulsion from university of petroleum and energy studies. Research was conducted on a graphite-walled GCR with fuel gas consisting of carbon fluorides as a mixture of uranium and which they are chemical equilibrium. The gaseous from of uranium was considered to be uranium tetrafloride. In this thesis two different reflector material are considered, on will be with graphite and other will be with Beo. The investigation comprise of variation in the gas mixture composition with the reflector thickness.

A one dimensional infinite cylindrical core model solution is obtained from in house developed two group diffusion theory based program in visual C++ and the fuel flow was not considered to be an obstructer for neutron transport. The main objective of this research is to quantifying Neutronics and heat transfer effects inside the core with flat temperature, density and uniform flux distribution. The interaction of fuel density and temperature with neutronics is important; the process of fission depends upon the initial conditions of the uranium tetra fluoride and hydrogen pre mixing zones. For investigating transient GCR model coupled neutronics and computational fluid dynamics need to be developed, whereas this aspect will be beyond the scope of this work. The current research focuses on investigating the parameters affecting the neutronics and heat transfer separately, followed by synthesis that will read the effects of fuel redistribution on the reactivity inside the core.

1.6 ORGANIZATION OF THE THESIS

This thesis starts with the nuclear space propulsion introduction and its development aspects and technical parameters investigated in the past research. The sold core reactor systems development and maximum attainable rocket performance and its limitations are briefly discussed. The need for research in the area of gas core reactors development and future mission plans and their propulsion needs were described. The development aspects in nuclear space propulsion in the past four decades will give a magnified prospective to the reader of the thesis. The silent features of the gas core reactors and the importance of neutron investigation also described.

Chapter two deals with the review on nuclear thermal rockets to strength the parametric considerations of the current research work. It also describes various experimental results so far available on solid core reactors and

neutronics investigation analysis of various reactor configurations. It also described the mode of solving heat transfer problem for gas core reactors and the pioneered work in the field is available. This chapter is the basis for the considerations of the parameters in the current research for both neutronics as well as for CFD. Various gas core reactors proposed theoretical models were described along with the most suitable model for the current research. Study on thermodynamics aspects of the gas core reactors is also taken into account to support fluid dynamic analysis with the physio- chemical data of gaseous uranium fuels.

Heat transfer analysis is conducted on Van dam and Hoogenboom cylindrical core model and parameters calculated are verified as per the results obtained from the heat transfer analysis. The temperature variations are investigated for the different core models with the ideal variation in the enrichment of uranium and corresponding temperature are considered from the neutronics calculation. The ideal case investigated for the enrichment level of 50 %, since highly enriched uranium is an unaffordable aspect. The specific cases investigated are for flat temperature and uniform density with the moderated enriched fuel. The objective of investigation heat transfer model is to illustrate both convective and radiative heat transfer rate between the fission region and to hydrogen propellant. This will give a clear idea over kinetic energy gain by the propellant as well as it describes dissociation of large fuel molecules into small once at higher temperatures. The calculations are validated against Van Dam and Hoogenboom models (Van, 1983). This idea is to evaluate the temperature and density profiles inside the three core cases considered in this work. It will also give us some idea over other parameters like core pressure, maximum temperature and entropy developed in the system and heat losses due to the walls.

In fourth chapter neutronics analysis on gas core reactor models were conducted using one dimensional fission code developed based on Monte Carlo method. This chapter described the need of investigating neutronics and its criticality calculations for interpreting the heat transfer and neutronics results together to develop a profile for average fuel density effects on core temperature. The criticality parameters like Keff factor and fuel gas density; this will create profile for neutron flux distribution on heat production. The change in reflector material on the GCR core and its parameters change were compared against the graphite model. In this work three models are investigated with variation in fuel enrichment varying from 50% to 5%.

Finally Chapter five gives the conclusions drawn from the work and the correlations made between heat transfer and neutronics and the inferences are taken from the parameters and interpreted them for development of GCR. The conclusions are made from the core density calculations and comparing them for various models with the validation of results and justification of assumptions made were described. This also includes future scope of the work and recommendations for various problems in the development of GCR models were discussed. This work is also supported by appendix, in which a model input for the code and code itself are added to it. The graphs and table which are used in both heat transfer and neutronics calculations are also attached.

CHAPTER 2: REVIEW ON NUCLEAR THERMAL ROCKETS

Man Kind's destiny point is towards quest of the stars, which is very much difficult to achieve with the current space propulsion technology. The question of travel beyond the solar system will only become practice if we address the needs as time and energy through a powerful space travel mechanism. The prospects of space physics and nuclear propulsion are two coherent branches which have to go forward in this direction; the Use of nuclear energy for space propulsion was under study as early as 1946, when R.Serber from Douglas Aircraft Company published some fundamental considerations of the applications of fission energy for the rocket propulsion in a safest possible manner. The greatest reason to concentrate in this approach is because of the vast distances in the solar system which makes travelling is a very difficult prospect for the astronauts involved in such a mission (Dana, 2004). With today's standards, even a simple mission to far planets such as Jupiter, Saturn or even a nearby planet like Mars would take a long time, from the NASA mission planers the travel time with chemical propulsion is around 436 days. Even in the case of Mars, you would need to commit more than one year for such a mission. In the case of Jupiter or other far away planets in our Solar System, the travelling times can be more than a decade. It is clear that space propulsion requirements for manned missions are more prominent, in the current scenario the probes that actually can attain a mean speed of 340.0000 and 115.000Km/h. At present no technology, but through a nuclear one can provide accelerations of the order of 0.5-0.3 g (Giovanni, 2003).

However, if you consider out of solar system destinations such as Proxima Centauri, you would need to travel for hundreds of years just to reach there. So, as a result, a more advanced means of travel is required for deep space missions.

Luckily, the option of nuclear energy provides a way to obtain such a mission since the specific impulse of a rocket can be raised by several magnitudes. Moreover, besides the space propulsion applications, it is also imperative to understand that continuous power will need to be provided to the astronauts involved in such a mission. For example, if you were to provide continuous power for three astronauts who are involved in a three year mission, you would have to consider their life support requirements, as well as the operational power for the onboard systems such as navigation, communications as well as various other systems which require electric power (Gunn, 2003). This would accumulate tremendously over time and it could not be met by conventional chemical batteries or even by Nuclear Isotopic Thermal Generators. You would need a full scale nuclear reactor in order to function. The effective specific impulse need to reach specific destinations tabulated in 2.1 and the maximum specific impulse is in the range of 1200 sec and which is quite manageable through gas core reactor systems.

Table 2.1: Possible In Situ NTP Propellant Source and their I_{Sp} Potential

Propellant	Destination	I_{sp} Potential (s)
CO_2	Martain atmosphere, Martain frost, Earth	160-380
CH_4	Asteroids, Phobus and Deimos, Earth, Outer Planets	460-670
H_2	Lunar polar Ice, Lunar Silane, NEO Asteroids, Earth, outer Planest	800-1200
NH_3	Earth, Outer planets	350-700
He	Lunar Ice, Martian Ice, Planetary Moons	160-240

The idea of using nuclear energy for the space applications goes back to R.Goddard at the time 1906-1907, he started using radium as energy source and realized it emits energy. But the level of energy produced from it will be insufficient for the propulsion applications.. Esnault- Pelterie concluded that nuclear energy was indispensable for space travel in 1912.There is specific developments by ash in 1965, Bussard and DeLauer in 1958. The dynamic measurements are reported by Bodenschatz et al. 1966. The there is a two-path flow feedback model was used by smith and stenning in 1961, 1962, 1964, and by wiberg and Woyski in 1968. The reactor core is a homogenous mixture of U^{235} and graphite penetrated by propellant passages.

2.1 THE KIWI and Troy Program

At the inception of the KIWI and Tory programmers, the choice of a working fluid was influenced by concerns over the potential for chemical interactions between the fuel elements and the working fluid. The first major program decision made by the SNPO was the creation of the Nuclear Engine for Rocket Vehicle Application (NERVA) program in 1961. NERVA focused on utilizing and integrating the KIWI B reactor designed into a flight-packaged nuclear rocket engine. Aerojet and Westinghouse were the selected engine system and reactor contractors. NERVA testing Facility In this arrangement the earlier MK 9 liquid hydrogen pumping systems were utilized to support the testing of the NRX A-2, A-3 and A-5 reactors between 24 September 1964 and 23 June 1966. The KIWI test program initially concentrated on relatively modest power-density reactors (KIWI A, A0 and A3), which were rated at 100MW. In 1965 Maxwell R. Morton addresses the problems related to the nuclear space propulsion in his paper named facility design problems associated with static firing of large nuclear rocket stages which is published in nuclear structural engineering. It address the use of nuclear reactors for the interplanetary travel, the capacity that this work suggest is

between 10,000 MW to 20,000 MW for different nuclear rocket stages. He also addressed radiation effects from the reactor core as well from the outer space. In 2001 A Nedaivod produced a work on the comparative analysis of the forecast of development of rocket prolusion facilities and he addressed the need for developing nuclear thermal propulsion systems and which is published in Acta Astronautica

In 1972 J.W PYM conducted analysis on minimum time trust start-up of a nuclear rocket with Integro- Differenecial Constrains and he could not able to address the rocket startup problem under critical conditions due to time lag in the neutrons propagation. *Nuclear Rocket Propulsion,* edited by Clayton W. Watson, his description continues with reviews of heat transfer and fluid dynamics, reactor physics and kinetics, materials and radiation effects, and turbines, mid concludes by consideration of the methods and concepts used in rocket engine design. Oleksii. M.Krytonove in his work published in Acta Astronautica in 2011 he analyzed Finite-thrust optimization of interplanetary transfers of space vehicle with bimodal nuclear thermal propulsion and he concluded. The formulation of the problem of optimization of the interplanetary transfer with the combination of high- and low-thrust arcs was presented. The high-thrust burns were considered using finite-thrust approach instead of traditional impulsive approach that is especially important for NTR propulsion.

2.2 LITERATURE REVIEW ON NUCLEAR PROPULSION

In 1947, the Orion project proposed by Stanislaw Ulam suggested dropping little thermonuclear or fission explosive at a distance of 60 m rare of the vehicle shield and to use the mechanism of thick steel platter designed to catch the blast and to propel the vehicle forward by absorbing the impulse from the plasma wave using large multi-story high shock absorbers. This is the first step in testing physical

configuration beyond the theories on nuclear propulsion. In early stages USA and Russian space agencies started activates in addressing the problems of nuclear propulsion. The US nuclear rocket program was named as Rover program which is started on 2nd November 1955 through which two national laboratories has been established to work on specific problems namely Los Alamos National Laboratory (LANL) and Lawrence Livermore National Laboratory (LLNL). These laboratories build some 20 more reactors and successfully tested as a part of ROVER/NERVA (Nuclear Engine for Rocket Vehicle Applications) program showing the long duration operation during ground testing conditions. The overall performance of the solid graphite reactors was established and they demonstrated the possibilities and success of early nuclear rocket engine program.

2.3 THE NUCLEAR ROCKET

The basic nuclear rocket engine concept is very simple and is consists of nuclear reactor which is used to heat low molecular weight propellant like hydrogen gas to a high temperature as possible, a nozzle through which the gas is expanded and a turbo pump to force it through the system. The reactor must operate at very high temperature and high power densities to minimize the effect of overall system weight. This combination of high temperature and high power densities are going to be a real challenge to reactor designers and material researchers. Under the current conditions that reactors which have been tested for research purposes which are made to be used in nuclear rocket are around at a range of 2500^0 C, this testing is done at LASL (Los Alamos Scientific Laboratory) (Gunn, 2003). There are few materials under use to develop reactor interior systems like refractory metals and graphite. The metals should be strong neutron reflectors, whereas graphite is good temperature handling capability but not neutron absorbing strength. But it acts as a neutron moderator in a way it will minimize the amount of enriched uranium required in the reactor core. The only

disadvantage with the graphite in the reactor core is its reactive ability with hot hydrogen to form gaseous hydrocarbons, this problem can be handled by providing a protecting coatings. But one of the biggest challenge in this approach lies with the high temperature resistance of the protective coating under critical stages of nuclear fission reaction.

2.3.1 DESIGN OF NUCLEAR REACTOR FOR ROCKETS

The basic considerations in the reactor design stand on many factors, but the fundamental factors that govern the nuclear fission reaction will be taken into the account to make sure elemental problems are addressed in the microgravity fission analysis, such as neutronics, heat transfer requirements from the core, high mechanical loading, and the complex problem of start-up, control and shutdown. David Bunden , 1992 addressed the safety aspects in using nuclear reactors for rocket applications and important parameters that effect the design in safety aspects. Unplanned nuclear criticality preventive measure and control mechanisms, stable thrust conditions for the safety of the on board systems, core integrity in case of re-entry as well as planetary or interstellar space travel, radiological safety in case of random impact location (Vulpetti, 1985). This work is concentrated and specified NERVA reactor system safety considerations and future improvements in selection of nuclear reactor core designs.

Frank E Rom and Robert G Ragsdale described the heat transfer importance in designing the nuclear rocket reactor systems and compared the difference in using gaseous core instead of solid core reactors. In solid core reactors the limitation of fuel rods are set to be at 4400K, whereas the specific impulse that can be obtained from higher temperature operation of core is very high. In his work the specific impulse that can be reached at 20000 K is above 3456 sec. This is an interesting parameter for mission planners, when a rocket operates at the specific values the

time of travel will reduce by grater fractions. Frank has raised concern towards the development of gaseous core reactor technology by experimenting the reactor model, but a serious problem that need to be addressed before design the reactor is associated with the thermal-hydraulics of the reactor core and the neutron behavior inside the reactor sue to the use of gaseous fuel and propellant. The effective areas to address these problems is to conduct extensive study on hydrodynamics of the reactor core and the heat transfer analysis to investigate radiative and convective heat transfer problems along with the neutron behavior in specific conditions.

Milton Klein conducted a study on nuclear thermal systems developments in 2004, the experimental data was presented for the NERVA program and the different reactors tested at various power ranges. The maximum specific impulse recorded in these testes is at 760 sec which is twice as high as chemical rockets, and the reactor was operated for a period of 10 minutes and able to record 245 KN thrust from the system. The problems addressed in this particular design are related maximum power density and these reactors have an ability to operate over wide range of power conditions, without having any external source the reaction becomes self-sustained in the reactor core (Bussard, 1958). The KIWI series started at 70 MW power range and can able to reach 1096 with the KIWI B 4 E Reactor and all the operations are conducted for 28 times in different time intervals. The next level of work continued and ultimately XE Prime EST 1 could able to attain higher power range compared with all the designs tested, it could able to operate at 1140 MW (Brengel, 1992). Milton described that the level of improvements that can be made from solid core reactors are quite limited so there is a need to establishing a program to develop gas core reactors.

2.3.2 PHYSICS OF FISSION FOR SPACE REACTORS

In fission reactors the energy is released slowly through a radioactive reaction in a highly controlled manner. If a very heavy nucleus has a neutron added to it then it will become so unstable, it will be split into two or more species a process called nuclear fission. In the fission process it releases more neutrons; it will be useful in self-sustaining chain reaction. The kinetics of the reactor core also studied to identify the rate of fission and the interactions with the neutrons with the propellant and the reflector core.

2.3.3 PARTICLE BED REACTORS

H.Ludewig from 1996 considered the design for the particle bed reactor for nuclear thermal propulsion applications. The methods of analysis and their validations are outlined for physics of the reactor analysis using Monte Carlo methods for neurotics of the reactor; several algorithms were developed in order to handle fluid dynamics and heat transfer and transient analysis for the reactor core. In case of simulating structural and thermal aspects of the core as well as shielding is done through commercial codes (Anghaie, 1986). An experiment was also conducted using prototype of PBR to analyses the physics and neutronics of the reactor experiments were also conducted to examine blow down power extraction capabilities, material and Mechanical design aspects validation, and design concepts for fuel elements.

2.4 GAS CORE REACTORS EVALUSTION

The first idea of using gas core fission reactors have evolved from Arthur C. Clark as a way of separating the nuclear reactor and the human habitation module. This is an even more advanced concept, initially proposed at the Scientific-Research Institute of Thermal Processes (now Keldysh Research Center), in

Russia [Koroteevet al., 2002]. Studies started in 1954, and somewhat later also NASA-Lewis (now NASA-Glenn Research Center) began to investigate it as well. The original suggestion for gas-phase fission (as opposed to fission in solid materials) actually goes back to 1949 [Bussard and DeLauer, 1958, pp. 322–327],

Jerry Gray in 1959 in his paper described about the possibilities of experimentation for gaseous core reactors for nuclear thermal propulsion in place of solid core reactors. The aspects considered are more on the theoretical level demonstration on exhaust velocity improvements through reaching higher core temperatures so that plasma state of operation can result greatest fraction of specific impulse. In fact this work also suggests the direct interaction of fission region to the propellant so that maximum heat transfer can takes place through convection and radiation. But this work did not demonstrate the methods through which the interactions need to be obtained. This paper also explains the development of cooling system that can keep wall temperature limited, since core is exposed to higher temperatures and the wall do get affected by the thermal radiation. The second aspect is quite interesting part over this thesis, controlling the fission reaction at criticality condition by maintaining the effective temperature (Black, 1991). The third concern raised in his work is to control the propellant flow rate without effecting exhaust velocity, since the radioactive material should not be expelled out when flow becomes turbulent. The basic design need that can make interstellar space propulsion possible is to design at least 1g acceleration attainable vehicle and second aspect is to create small thrust to weight ratio. The proposals from the work on theoretical base have given a cavity reactor model which can work with mixture of propellant and fissionable gas in a dense neutron reflector core.

Samim Anghaie, 2005 worked on optimum utilization of fuel in gas core reactors which are externally reflected and moderated by creating a force to keep fuel with

in the reactor chamber by means of magneto hydrodynamics. The advantage in GCRs is with operating reactor at higher temperatures and actinide formation can be avoided due to the propellant/ coolant circulation. Samin proposed GCR-MHD concept for closed cycle gas core reactors through a bypass flow channel in the reactor system. The MHD Generator cycle will directly convert the fission liberated heat to power and the operational temperature suggested in his design are around 1800-2500K. This work did not mention any specific working fluid in terms of operation but it suggests He, KF, LiF, or BeF_2 are going to be effective solution (Spencer, 1963). The development in the field of gas core reactors good amount of work supports hydrogen and MHD cycle is a budding concept to secure uranium vapor inside the core. Convectional solid core reactors have limited applicability of MHD generator system, this direction limited amount of work was available. The suggestion made in this work is to make use of MHD to create high neutron flux to achieve non-equilibrium ionization.

S D Howe, 1997 conducted feasibility study on gas core rocket design based on the concept of using fluid dynamics inside the core by creating a vortex. The objective of creating vortex is to contain the nuclear fuel to create high power levels. The power levels vary with the effectiveness of kinetic energy change with in the working fluid with a radiative couplin (Dunn, 1991). This parameter studied for understanding the potential of using gas core reactors for long range missions.

P Sforza, professor at Brooklyn Polytechnic Institute created a clod flow experimental setup to create initial geometry of the core to establish vortex inside the core. He followed annular injection to create a vortex through a base plate, in the initial stages this experiment was conducted with the help of air. This experimental data helped in creating vortex models for gaseous fuel formation requirements to generate the similar phenomena and separate shedding. In case of

fuel injection the base line fuel injection was controlled to establish oscillation to create bleed flow, so that fuel will be contained in the fission region.

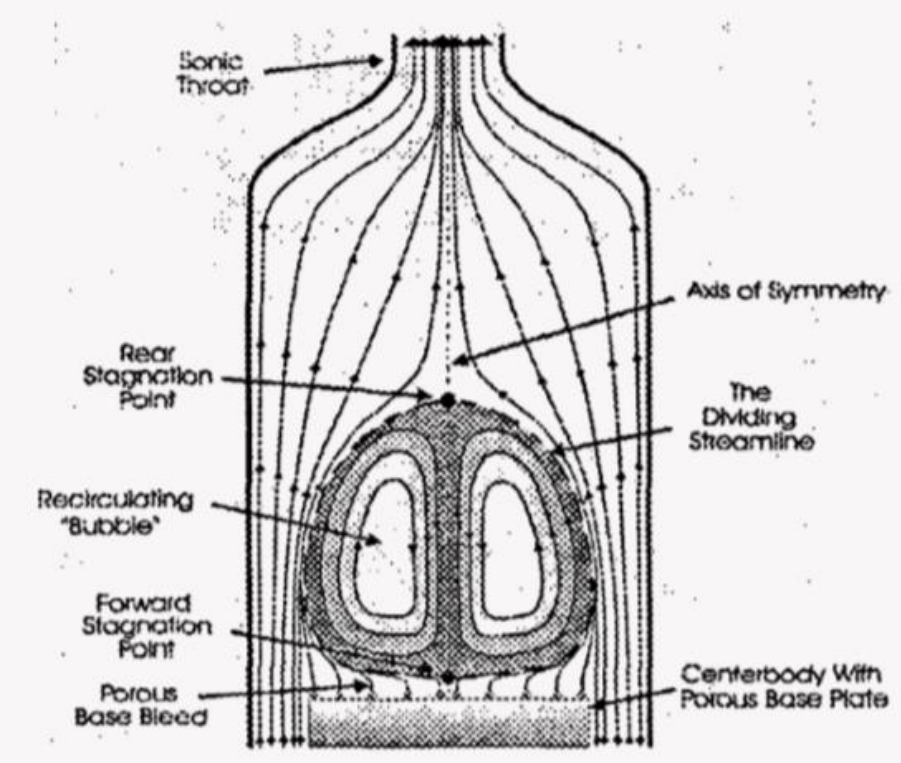

Figure 2.1: Experimental Setup Used by Prof. Sforza to Create Cold-Fluid Vortex Region

This work is an important determination in the later stages to design active control mechanisms that can be employed in a reactor core. The chamber that contains high pressure plasma with high temperature hydrogen, the behavior of vortex generation studies is quite difficult in understanding (Edelman, 2001). This experiment created a relationship between the injection velocity of the fuel and the axial position of the inlets, at high injection velocities the axial position of the inlet can be dragged as near as the core region. With the same chamber if nozzle is also attached to study the stability of the vortex a time-independent injection

velocity with an in viscid flow demonstrated the vortex settle down to a fixed axial position. To maintain the uranium criticality inside the code the vortex size need to be defined from the geometry, if the vortex is large then hydrogen and uranium starts mixing inside the chamber. In case of smaller vortex with a bigger core geometry uranium criticality starts degrading so that fission reaction is no more self-sustained. The geometrical modifications based on results obtained by simulating vortex formation in a cylindrical chamber with a base plate described the mechanism of altering the vortex location by controlling the flow through axial injection (Frank, 2012). The annular injection is major parameter in defining the strength of the vortex formed; no shading and vortex breakup in order to maintain uniform fission rate.

2.4.1 METHODS FOR RETAINING FUEL

Various mechanisms have been proposed in creating a mechanism to stop fissionable material from the reactor flow. The first mechanism is based on creating a magnetic bottle kind of approach, since the temperatures high in the core gas can be ionized easily there by using a low molecular weight propellant so that the flow is always on the corner of the core. The second approach suggest is to use difference in atomic mass numbers, like all the nuclear fuels are having higher atomic mass number compared to the propellants like hydrogen or helium as a same time its heat carrying capacity should be impressive (Marx, 1963). On the similar grounds creating a uni-directional flow to create a vortex by which fuel can be contained within the chamber. The third approach is to choose magnetic hydrodynamics approach is to create Vortex Street to protect the gaseous fuel inside the core by providing the centrifugal acceleration for fuel separator. The major consideration in selecting above approaches should also focus on heat-transfer and the thermal emissivity should not be low inside the core.

Vortex containment is commonly used approach in gas core reactors to protect nuclear fuel from expelling out through the propellant. Physical containment introduction is an obstructer to the heat transfer. Jack L Kerrebrock, 1961 has done work on vortex containment mechanism to use them in nuclear rockets. Vortex generation is done through creating a pressure field by diffusing low molecular weight propellant radially into the reactor chamber. In this work a 2-D laminar vortex flow is studied and the fuel is introduced tangentially so that vortex generation can happen due to pressure difference and the circulation happens with low molecular weight propellant (Glasston, 1955). The parameters need to be developed to generate such kind of containment chamber are purely controlled by pressure difference, the mass flow capacity of the vortex per unit of vortex length (Jack, 1961). The entire phenomenon worked out in this concept is independent of vortex diameter since the mass flow rate becomes negligible when it reaches the fission region. So that small diameter vortices filling the given volume, if the tangential Mach number of the radial flow reaches unity in the mixture gaseous fuel and the propellant mass flow capacity will reach 0.01 pounds per second-foot. If the pressure gradient decrease due to the molecular weight difference still the fuel can be maintained inside the core, the difficulty that can occur is due to control over the pump mechanism used for fuel. However at very high temperature ratios and the pressure gradients it cannot be decreased unless the fission dies (Goel, 1991). The problems described through is work are associated with containment mechanism, like the radial heat transfer, difficulty in maintain nuclear fuel in gaseous form, generation of vertices with low radial mass flow rates at high tangential velocities.

Robert V, 1961 formulated a diffusion problem for the vortex containment chamber analysis to address the problems mentioned by Jack he studied the variation of density ration with dimensionless radius by considering the diffusion

velocity of the heavy gas in the ration of 0.7 and two peak comparative variations are obtained at 0.17 and 0.34 under critical conditions. Similarly the energy equation was solved to get the variation of dimensionless temperature to the radius of the core under the assumption that heat rate is proposal to the concentration of the fissionable material. This solution is obtained by solving three first-order differential equations with three variables under constant dimensional radius. This results in terms of observing variation of density ratio along the core radius, through which critical and maximum heating rates can be found, the maximum heating rate value is observed inside the vortex (Howell, 1965). In this work variation of dimensionless fuel concentration across the geometry also investigated and the core is having grater fuel concentration in the vortex region. Significant results are obtained from the analysis described the performance characteristics of the reactor core through vortex generation. Over all temperature ration examined the relative mass flow capacity which indicates overall enthalpy rise of the gas mixture due to the fraction carried by radiation.

2.5 THERMODYNAMIC PERFORMANCE OF GAS CORE REACTORS

W. Boersma-Klein, 1985 preformed analysis on gas core fission reactors to investigate the thermodynamic behavior of the fission products, the rocket engine is visualized as a constant pressure stagnation chamber containing the energy source. The analysis conducted on 1200 MW Power Reactor, with a pressure range of 0.1 MPa and 2.5 Mpa at a temperature range of 1300 K to 10000K for a U-F-C core. The significance of the work comes from usage of plutonium compound in the form of PuF_4 which is recycled with UF_4. The results from the work demonstrated the partial pressure variations after 200 hours of reactor operation at 1200 MW thermal power at a 2.5 MPa with a temperature range of 2500K to 2800 K (Piacentino, 2008). This indicates these are no condensation of fission products inside the reactor core. The thermodynamic behavior of

plutonium with rare earth compounds is limited due to variation in the partial pressure. The plutonium compound can essaly be reprocessed with UF_4 and the whole mixture is easily dissociated and Uranium atoms can be ionized about 65%, so that the exact velocity of the propellant gains the kinetic energy.

Thermodynamic Performance study of possible fluid for nuclear thermal reactors was conducted by Kenneth E.Kissell, the main focus of the study is to analysis the ionization and dissociation effects of the various working fluids. The idea comparison is made with the hydrogen as a working fluid which can have a potential of producing exhaust velocities exceeding 32,000 ft/sec. Liquid hydrogen energy equalence in terms of heat of formation. The ionizing hydrogen's equilibrium composition over a temperature range is computed up to 15000 K using thermochemical data. The data plotted from equilibrium composition to obtain entropy and enthalpy relationship at two distinct regions. To generate the data for practical range of rocket chamber pressure from 1 to 500 atm at a pressure ratio of 10 to 1000 from expansion processes. The total enthalpy of hydrogen mixture at 3000 K is nearly intensive to chamber pressure (Kenneth, 1989). In this besides hydrogen water vapor and air is considered as a working fluid, comparing all the physo-thermal properties hydrogen behavior at higher pressure and its variation of exhaust velocities are giving effective relation between entropy and enthalpy.

2.6 GASEOUS FUEL FOR ROCKETS

W Boersema conducted analysis on gaseous core reactors and the behavior of the gaseous fuels inside the reactor and their chemical reactors at various tempratures are investigated. The temperature range considered in this particular work in 1989 by considering 2000 K-10000k, for a pressure range varying from 1 bar to 100 bar. The U-C-F system was analyzed by changing the floride concentration in the

composite system. In this work a dissociation energy levels are determined by creating a mixture of compounds in the fuel. The identifications done from this work is a trendsetter to conduct future research on UF_4 based systems as well as UF_6 developments.

2.7 FLOW ANALYSIS ON GAS CORE REACTORS

Computational fluid dynamic and heat transfer analysis is conducted on gaseous core and gas cooled space power and propulsion reactor system by S. Ahghaie and G.Chen from university of Florida in 1996. This work concentrated in solving a computational model based on the axisymmetric thin layer Navier- Stokes equations and investigated radiative and conductive heat transfers in nuclear reactors using implicit-explicit finite volume, MacCormack method along with Gasuss-Seidel line iteration process for solving governing equations. The considerations are the flow is both subsonic as well as supersonic for hydrogen gas and uranium hexafluoride under variable boundary conditions. The boundary condition consider in S.Ahghaie system are at constant heat flux the process is adiabatic, isothermal to simulate the propellant flow in nuclear reactor core. To obtain the convergent solution an enthalpy-rebalancing scheme is implemented for the wall heat flux. The outcomes of the above work can be a path way to solve thin layer Navier-Strokes equations, radiative heat transfer model using Roseland diffusion approximation, Baldwin and Lomax two layer turbulence models and can be a reliable computational tool for a space nuclear core models. The model reactor system is shown in the figure below. This model was suggested by Kerrebrock and Meghreblian that a multiplicity of vortex chamber can contain the fuel inside the reactor core.

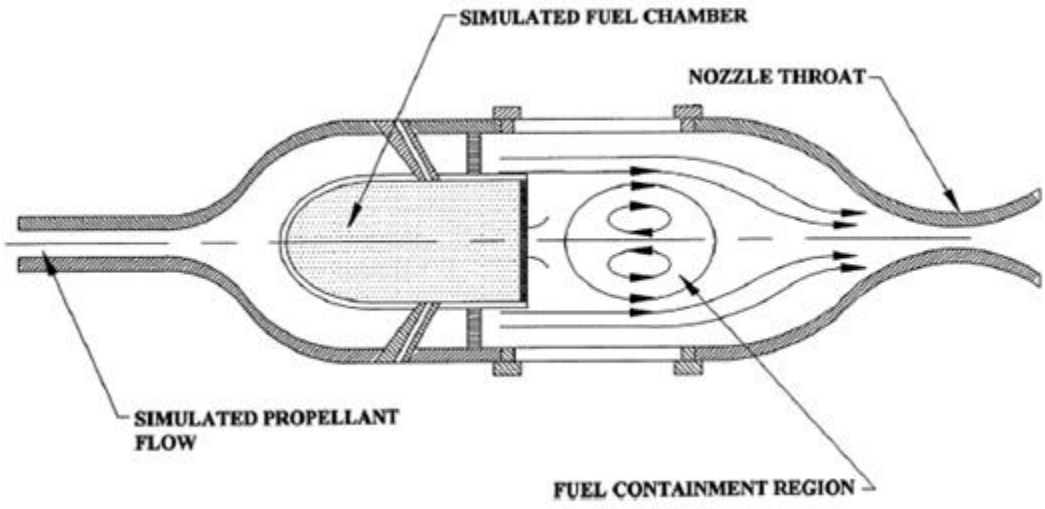

Figure 2.2: Gas Core Nuclear Reactor Core Flow Model with Vortex Generation

The thermal hydraulic analysis conducted by kammash in 1994 considered Navier- stokes energy, and species diffusion equations for the propellant flow inside the reactor core. The assumptions made in his analysis on constant mass flow rate of the fuel as well as the propellant, thereby it occupies the shape of a cylindrical annul and converts the radioactive fuel into plasma with reduced cross section near to the throat (Huth, 1960). The propellant enter through channel attached to the wall surrounded by the reflector so that it can act as a coolant to the core as well as it can take the initial heat before entering into the chamber. Depending upon the heat flux the propellant flow rate was regulated and he identified that, at maximum heat flux the buffer region is having highest rate of heat transfer. The parameters of interest in the analysis are likely to develop effective pressure and temperature values inside the core, this work demonstrated the effect of pressure on K_{eff}. The value getting affected based on density factor of the fuel, since the analysis was conducted under ideal conditions the maximum value of the temperature is at 50,000k (Hsia, 1991). At the same grounds the K_{eff}

value is reaching 1.2 at 1000 atm pressure, which cannot be searched under current conditions.

The second consideration made in this work is to keep the temperature of the core constant at 10000K and start varying the density of the propellant, poor performance was observed under these conditions since the value of K_{eff} started decreasing and above a certain point it started increasing. This indicates that hydrogen started behaving like a neutron moderator inside the core; this effect was not visible at higher temperatures since the neutrons starts reflecting in reactor core above 10000k (Palaniswamy, 1991). The reflector thickness has its own effects on K_{eff} it also effects the propellant behavior inside the core, since the reflector thickness is a question of maintaining the fission under control. This work gives a specific idea over the effect of temperature on reactor criticality between 10000K -20000k, the future analysis also done in the similar lines to investigate helium behavior and the effects over the neutronics. The attractive propellant can be hydrogen in case of using high temperature reactor operations.

David I Poston and Terry Kammash, 1994 have done an analysis on thermal hydraulic model of gas core reactors using open cycle nuclear rocket. The solution was obtained by two dimensional Navier-Stokes Equations, species diffusion; energy equation was solved for high temperatures. The analysis provided effective understanding of the fluid dynamics of the core. In this work David considered uranium hexafluoride as a fuel which is heated through fission and plasma region going to created, heat there by transfers to hydrogen propellant. Gas core reactors major problem associated with the mixing of propellant and the fuel. If mixing can be avoided through some mechanism without having any solid boundary the performance of the reactor system will improve and the reactor power that can be produced is at 3000 MW that can produce 3160 sec specific impulse with a thrust of 125 kN (Palaccio, 1950). This analysis conducted on a

code developed by using Navier -Stokes equations by considering constant heat flux, when the wall heat flux becomes maximum the flow rate of propellant will increase. Turbulence model is introduced of eddy viscosity, as an input the turbulent transport coefficients of mass, momentum and heat are specified. The results are presented for 500 MW open cycle GCR design the contours presented in the work are ranging from 5000K to 50000 k (Michal Plavee, 2011).

2.8 NEUTRONICS OF GAS CORE REACTORS

In the area of gas core reactors design and analysis limited amount of work can be found since the availability of expertize and data from the scientific agencies are not accessibly for everyone. Few special cases can be found from the university level research, University of Florida, Delft University and University of Michigan some work was published into research papers. David I, 1994 conducted a study of neutronics on open cycle gas core reactors. This work investigated keff variations as a function of design parameters. The major dependent factor can be temperature, composition of the fuel and propellant along with reflector thickness. This work also investigated coupled thermal-hydraulics which is obtained by solving 2-D steady state conservation of mass equations, species, energy, radial momentum and axial momentum (Michael, 2009). The specific design considered in the solution results various parameters like neutron flux, variation in power density, neutron energy spectra are the outcomes of the solution. The changes that can occur by changing the fuel composition and by changing different fuels along with variety of propellants have been considered. In model the solution is obtained for the core without considering any physical barrier between uranium plasma and to the propellant. Ideal operational parameters includes 3000 MW reactor which can able to produce a specific impulse of 3160 sec with a thrust of 125 kN, it related to maximum heat flux of 100MW/m^2. In this work the solver chosen to investigate neutronics was TWODANT code, 50 group cross-sections

are the range of material and temperatures in the library. The input requirements for the code are Up scattering, many energy groups, Highly in Homogenous mesh and output Tailoring. This code solves isotropic and linearly anisotropic differential scattering matrix for all cases at an order of S_{ON}=4 (Spence, 1965). The fuel material considered are U-235, U-233, Pu-239 with a Beo reflector and the pressure vessel material was considered as Ti with the various propellants like H, D, He.

Volken seker in 2004analysed neutronics of HTR-10 reactor core using MCNP code, HTR-10 is a high temperature gas cooled reactor. The reactor analysis is performed to cheak intial criticality for a pebble bed core and the equations solved in obtaining the effectiveness factor is neutron transport equation. The reactor model considered in this analysis is from jing et al 2002, VOSS code was used in jings model and the volken compared MCNP results aginest VOSS for validation. Tuechurt, 1994 conudced neutronics analysis on the same code but for a pebble bed reactor with a different configuration, in fact helium also has some considerable characteristics but it is not a good neutron moderator there by criticality can't be controlled in high temperature operations (Stanley, 2001). Goltsev 2005 studded neutronics of a pressurized water reactors system, the analysis focused on kernel inside the fuel system. The reactor parameters considered for analyzing neutronics in the HTR-10 is having a power capacity of 10 MW with 197 cm of core height, 180 cm of core diameter. In the current system helium was used as coolant with an inlet temperature of 350 ^{0} C and the reactor exit tempratures is 850 ^{0}C, the operation pressure of the reactor system is at 3Mpa (Sforza, 1992). In the HTR-10 reactor graphite was used as a neutron reflector, keff values are studied for various conditions like vacuum, helium, air. The highest value is passed in vacuum with improved core height, the analysis conducted on HTR-10 core given a relationship between the loading height of the

reactor and the keff factor. With full height the reactors critical value is continuously growing, whereas with the critical height it starts declining.

Summer shin in 1998 conducted an analysis on neutronics in space reactors which can be used for power and propulsion applications. The reactor was controlled by B_4 C drums attached with a Beo reflector, Uranium Carbide used as a fuel. The idea of investigating the neutronics in this core configuration is to estimate the heating on control drums due to neutron interactions. The reactor is designed to develop a thermal thrust of 5000 N with a specific impulse of 760 sec. Hydrogen is used as a propellant and the core exit temperature of the propellant is at 1900 K. The neutronics analysis is conducted using ANISN code which can solve one-dimensional, two dimensional transport equations with the fission groups S_{16}-P_3 and S_8-P (Taub, 1975). The reflector thickness considered for the core is around 16 cm with the 14 cm control drum thickness the delta Keff is resulted on the fast reactor is around 13.56%, The operational power levels of the rector is around 50 KWe with a reactor height of 35 cm and its radius is given around 22 cm. This analysis indicates the maximum amount of heat generated in the fission process is used in propulsion phase and the heat is carried by Hydrogen propellant.

2.9 PROPELLANTS FOR GAS CORE REACTORS

Ron J. Litchford conducted analysis on hot hydrogen exposer to various materials and he studies effects of high temperature and pressurized gas behavior inside the reactor core using a non-nuclear means of heating system with the help of arc heater driven by hyper convective and radiative environment. The facility later modified to study the behavior of hydrogen under high temperature in a pressure vessel. The test data available up to 3500k in a 3Mpa environment to support the solid core reactors operation within the temperature range of fuel material limitations (Spence, 1965). The hydrogen performance was estimated at various

mass flow rates varying from 5-10 g/s and various levels of efficiencies have been recorded with variation in pressure inside the chamber the maximum pressure that can improve the performance of the system was recorded at 35 atm (Thomas, 1993). The behavior starts deteriorating with increase in temperature the power density starts decreasing from the chamber. This work demonstrated the effective operational range and the maximum floe rate levels of the hydrogen.

LASL report on possible propellants for use in nuclear rockets describes the use of Hydrogen, methane, ethane, helium, propane, mixture of hydrazine and these hydrocarbons, ammonia, methanol, ethanol and propanol. The dissociation products and their compounds with in the temperature range of 1000-3000 K (Chen, 1996)., among all the suggested propellants Hydrogen has a highest mole fraction when temperature starts increasing, methane shows poor performance in terms of thermodynamic aspects. Due to the low molecular weight and the higher mole fraction this study recommends hydrogen as a most suitable propellant for rocket reactors design.

CHAPTER 3: HEAT TRANSFER ANALYSIS OF GAS CORE REACTOR

Heat transfer in a nuclear rocket system is a complex engineering design aspect, since in the gas core nuclear reactors the propellant and coolant is same. The operational temperature is much higher compared to the conventional systems, and in the microgravity condition the process is not so favorable to the common operations. In order to analyze the specific process that takes place in space propulsion systems whereas gaseous core model, a numerical heat transfer analysis for the high temperature energy conversation system is need. The general heat transfer process from the fission to the propellant as well as to the system walls will be through conduction, convection and radiation. This study is focused on solving the heat transfer aspects numerically under the microgravity supercritical fission reactions. The reactor is modeled without having any control rods and the pressure will be continuously fluctuating to control and to slow down the neutrons and so that reactor will be under the control.

The idea is to improve the specific impulse of the nuclear rocket by allowing the reactor to generate power at temperatures much higher than the conventional reactors. The greatest challenge to operate gaseous core reactors under these conditions will be controlling the high temperature and as well as the super critical fission. The wall cooling also needs to be taken care by the external cooling system to idealize the process, which is characterized by the convective flow of a radiating gas (Anghaie, 1996). The cooling is obtained by propellant itself in the reactor core model. The schematic diagram of flow process in gaseous core reactors is shown in the figure 3.1, the fuel is entered into the system with a minute inlet and the propellant gas passes through the reflector walls to absorb heat from the reflector and enters into the reactor chamber. Initially the liquid

hydrogen is pumped into the reactor walls and the absorption of heat from the reflector walls converts the hydrogen into gaseous state. The hydrogen enters into the buffer region through which the convective radiative heat transfer takes place.

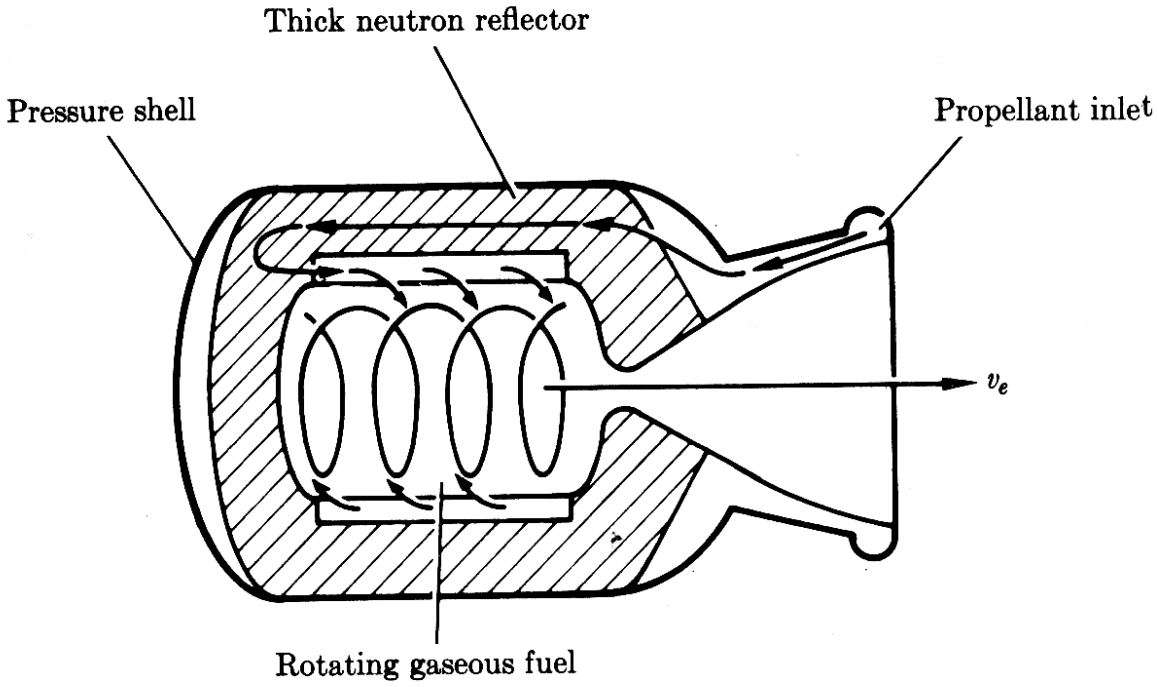

Figure 3.1: Gaseous Core Reactor system with Propellant Inlet through radial direction

In this thesis two- dimensional axis-symmetry model was considered to analyses the radiative and convective problem. Two different cases are analyzed to compare the effectiveness of the process. In most of the cases hydrogen is selected as a propellant due to its low molecular weight. In some of the reactor models to maintain criticality even helium is considered due to its inertness. There thermo chemical reactions between the graphite reflector and the hydro have its

own disadvantages. From the experimental results in handling hydrogen at above 3500 K is quite difficult in a closed system (Anghaie, 1986). The facility yet to be developed to conduct experiments in this direction. The idea of analyzing hydrogen and helium is to choose effective fluid with more positive characteristics to operate in space reactors under the given pressure and tempratures ranges. The coupled solution might have given a better idea of even neutron behavior with the propellant.

3.1 NUMERICAL MODELING

The numerical analysis is conducted using computational fluid dynamics, with a commercially available package called ANSYS Fluent. This work is conducted at university of Petroleum and Energy Studies, which has research license for Andy's fluent. The package works with the fundamental aspects of fluid dynamics by solving continuity, momentum equation, Energy Equation. The detailed explanation is given below with the equations solved to analyses each pentameter and the turbulence models are discussed. The model section based on the conditions while solving the problem is also included in the methodology. The heat transfer model solved in the problem and the boundary conditions used are included. The constant parameters with respect to the fuel and the propellant operational characteristics are added in the appendix d.

3.1.1 THE CONTINUITY EQUATION

The divergence form of the global continuity equations can be obtained by applying the law of conservation of mass to an infinitesimally small volume of fluid fixed in space. It is written in vector form as in equation 3.1

$$\frac{\partial \rho}{\partial t} + \nabla.(\rho \vec{V}) = 0 \qquad (3.1)$$

In the Cartesian coordinate system, with *u*, *v* and *w* representing the *x*, *y* and *z* components, respectively, of the velocity vector $\vec{V}$ and ρ representing the density of fluid, the above equation becomes

$$\frac{\partial \rho}{\partial t} + \frac{\partial (\rho u)}{\partial x} + \frac{\partial (\rho v)}{\partial y} + \frac{\partial (\rho w)}{\partial z} = 0 \qquad (3.2)$$

3.1.2 THE MOMENTUM EQUATIONS

The gradient form of the momentum equation can be obtained by applying Newton's second law of motion to an infinitesimal control volume of fluid fixed in space. This momentum equation is the statement of the conservation of linear momentum of the fluid volume as can be written as

$$\frac{\partial (\rho V)}{\partial t} + \nabla.(\rho \boldsymbol{V})\boldsymbol{V} = \rho.\boldsymbol{f} + \nabla.\prod_{i,j} \qquad (3.3)$$

In equation 3.3, $\rho.\boldsymbol{f}$ is the body force per unit volume and $\boldsymbol{\Pi}_{i,j}$ is the stress tensor which consists of normal and shearing stresses which in turn are represented by the components of stress tensor as expressed in equation 3.4.

$$\prod_{i,j} = -p\delta_{ij} + \mu\left(\frac{\partial u_i}{\partial x_j} + \frac{\partial u_j}{\partial x_i}\right) + \delta_{ij}\lambda\frac{\partial u_k}{\partial x_k} \qquad (i, j, k=1, 2, 3)\ (3.4)$$

Where p is the pressure and δ_{ij} is the Kronecker delta function; $u_1, u_2\ and\ u_3$ represents the three components of the velocity vector ***V***; μ is the molecular viscosity coefficient and λ is the second coefficient of viscosity.

The molecular viscosity coefficient and the second viscosity coefficient are related to each other through the coefficient of bulk viscosity κ, as hypothesized by Stokes, given in equation 3.5.

$$k = \frac{2}{3}\mu + \lambda \qquad (3.5)$$

However, the coefficient of bulk viscosity is often negligibly small for Newtonian fluids, yielding equation 3.6

$$\lambda = -\frac{2}{3}\mu \qquad (3.6)$$

With above relation the momentum equation can be rewritten with substantial derivative notation as equation 3.7.

$$\rho\frac{D\boldsymbol{V}}{Dt} = \rho.\boldsymbol{f} - \nabla.p + \frac{\partial}{\partial x_j}\left[\mu\left(\frac{\partial u_i}{\partial x_j} + \frac{\partial u_j}{\partial x_i}\right) - \frac{2}{3}\delta_{ij}\mu\frac{\partial u_k}{\partial x_k}\right] \qquad (3.7)$$

Or,

$$\rho \frac{D\boldsymbol{V}}{Dt} = \rho . \boldsymbol{f} - \nabla . p + \frac{\partial}{\partial x_j}\left[\boldsymbol{\tau}_{ij}\right] \tag{3.8}$$

Where $\boldsymbol{\tau}_{ij}$ is the viscous stress tensor?

In Cartesian coordinate system, the above equation can be written, with *u*, *v* and *w* respectively as the *x*, *y* and *z* component of the velocity, as

X-momentum:

$$\frac{\partial(\rho u)}{\partial t} + \nabla.(\rho u \boldsymbol{V}) = -\frac{\partial p}{\partial x} + \frac{\partial \tau_{xx}}{\partial x} + \frac{\partial \tau_{yx}}{\partial y} + \frac{\partial \tau_{zx}}{\partial z} + \rho . \boldsymbol{f}_x \tag{3.9a}$$

Y-momentum:

$$\frac{\partial(\rho v)}{\partial t} + \nabla.(\rho v \boldsymbol{V}) = -\frac{\partial p}{\partial y} + \frac{\partial \tau_{xy}}{\partial x} + \frac{\partial \tau_{yy}}{\partial y} + \frac{\partial \tau_{zy}}{\partial z} + \rho . \boldsymbol{f}_y \tag{3.9b}$$

Z-momentum:

$$\frac{\partial(\rho w)}{\partial t} + \nabla.(\rho w \boldsymbol{V}) = -\frac{\partial p}{\partial z} + \frac{\partial \tau_{xz}}{\partial x} + \frac{\partial \tau_{yz}}{\partial y} + \frac{\partial \tau_{zz}}{\partial z} + \rho . \boldsymbol{f}_z \tag{3.9c}$$

In above equations the components of the viscous stress tensor are given by

$$\tau_{xx} = \lambda(\nabla . \boldsymbol{V}) + 2\mu \frac{\partial u}{\partial x} \tag{3.10a}$$

$$\tau_{yy} = \lambda(\nabla.\boldsymbol{V}) + 2\mu\frac{\partial v}{\partial y} \tag{3.10b}$$

$$\tau_{zz} = \lambda(\nabla.\boldsymbol{V}) + 2\mu\frac{\partial w}{\partial z} \tag{3.10c}$$

$$\tau_{xy} = \tau_{yx} = \mu\left[\frac{\partial v}{\partial x} + \frac{\partial u}{\partial y}\right] \tag{3.10d}$$

$$\tau_{xz} = \tau_{zx} = \mu\left[\frac{\partial w}{\partial z} + \frac{\partial u}{\partial x}\right] \tag{3.10e}$$

$$\tau_{yz} = \tau_{zy} = \mu\left[\frac{\partial w}{\partial y} + \frac{\partial v}{\partial z}\right] \tag{3.10f}$$

3.1.3 THE ENERGY EQUATION

The energy equation for viscous internal flows can readily be obtained by applying the law of conservation energy i.e. the first law of thermodynamics to an infinitesimally small volume of fluid fixed in space(Schnitzler, 1986). The energy equation in conservation form is given by equation 3.11.

$$\frac{\partial}{\partial t}(\rho E) + \nabla(\vec{V}(\rho E + P) = -\nabla\left[\sum_j h_j J_j\right] + S_h \tag{3.11}$$

Where E_t is the total energy per unit volume of fluid and is given by

$$E_t = \rho\left(e + V^2 + potential\,energy + vibrational\,energy + ...\right) \quad (3.12)$$

With *e* as the internal energy per unit mass.The first term of the left hand side of the energy equation 3.11 represents the rate of change of total energy per unit volume of the fluid while the second term on the same side is the energy lost per unit volume by convection through the control surfaces. The term $\frac{\partial Q}{\partial t}$ represents the rate at which heat is supplied to the unit volume of fluid and term $\nabla.\boldsymbol{q}$ denotes the rate at which heat is lost through the control surfaces, per unit volume, by the process of conduction (Brengle, 1992). The heat transfer per unit volume $\boldsymbol{q}$ is related to the temperature gradient by the Fourier Law expressed as

$$\boldsymbol{q} = -k\nabla.T \quad (3.13)$$

Where $k$the coefficient of thermal conductivity and T is the temperature and the third and fourth term of the energy equation (3.11) represent the work done on the fluid per unit volume by the body forces and the surface forces respectively.

For a Cartesian coordinate system, the conservation form of the energy equation can be rewritten as

$$\frac{\partial E_t}{\partial t} - \frac{\partial Q}{\partial t} - \rho\left(f_x u + f_y v + f_z w\right) + \frac{\partial}{\partial x}\left(E_t u + pu - u\tau_{xx} - v\tau_{xy} - w\tau_{xz} + \boldsymbol{q}\right)$$
$$+ \frac{\partial}{\partial y}\left(E_t v + pv - u\tau_{xy} - v\tau_{yy} - w\tau_{zy} + \boldsymbol{q}\right) \qquad (3.14)$$
$$+ \frac{\partial}{\partial z}\left(E_t w + pw - u\tau_{xz} - v\tau_{yz} - w\tau_{zz} + \boldsymbol{q}\right) = 0$$

In the above equation, the heat flux vector,

$$\boldsymbol{q} = q_x i + q_y j + q_z k \qquad (3.15)$$

Where,

$$q_x = -k\frac{\partial T}{\partial x} \qquad (3.16a)$$

$$q_y = -k\frac{\partial T}{\partial y} \qquad (3.16b)$$

$$q_z = -k\frac{\partial T}{\partial z} \qquad (3.16c)$$

3.1.4 THE ENERGY EQUATION FOR HIGH TEMPERATURE GAS

The energy equation and the closure equations given in section 3.1.3 are valid only up to moderate temperatures. In viscous flows it is generally associated with very high temperatures of the order of thousand degrees Celsius (Poston, 2006). As the temperature of the gas is increased to higher values, the assumption of calorifically perfect gas is no longer valid and the gas becomes *thermally perfect*. A thermally perfect gas is one whose specific heats are functions only of temperature.

Taking into account the effect of high temperatures, the governing energy equation should be modified to accommodate the diffusion terms. The total energy E_t should now include the vibrational, rotational, translational and electronic energies as well (Kammash, 2005). The resultant Energy equation can be given in substantial derivative form by equation 3.21.

$$\rho\frac{DE_t}{Dt}=\frac{\partial Q}{\partial t}-\nabla.\boldsymbol{q}-\nabla.p\boldsymbol{V}+\frac{\partial}{\partial x}\left(u\tau_{xx}\right)+\frac{\partial}{\partial y}\left(u\tau_{yx}\right)+\frac{\partial}{\partial z}\left(u\tau_{zx}\right)+\frac{\partial}{\partial x}\left(v\tau_{xy}\right)$$
$$+\frac{\partial}{\partial y}\left(v\tau_{yy}\right)+\frac{\partial}{\partial z}\left(v\tau_{zy}\right)+\frac{\partial}{\partial x}\left(w\tau_{xz}\right)+\frac{\partial}{\partial y}\left(w\tau_{yz}\right)+\frac{\partial}{\partial z}\left(w\tau_{zz}\right) \quad (3.17)$$

Where the heat flux vector $\boldsymbol{q}$ also includes the energy flux due to diffusion and radiation as given by equation 3.22

$$\boldsymbol{q}=-k\nabla T+\sum\nolimits_i \rho_i U_i h_i+\boldsymbol{q}_R \quad (3.18)$$

In equation 3.22, the second term represents the energy flux due to diffusion is the summation energy fluxes due to diffusion of all species present in the mixture. The variables ρ_i, U_i, and h_i respectively are the density, diffusion velocity and the enthalpy of the i^{th} species in the mixture. The term $\boldsymbol{q_R}$ represents the energy transport though the phenomenon of radiation.

3.1.5 THERMODYNAMIC PROPERTIES OF A CHEMICALLY REACTING MIXTURE

For most of the chemically reacting gases, each species in the mixture can be assumed to obey the perfect gas equation of state with negligible intermolecular

forces. Additionally the gas can be assumed to be a mixture of thermally perfect gases. The equation of state for a mixture of perfect gases can be given by

$$p = \frac{\mathcal{R}}{\mathcal{M}} T \tag{3.19}$$

Where $\mathcal{R}$ is the universal gas constant (8314..34 J/kg mol K) and $\mathcal{M}$ is the molecular weight of the mixture. The molecular weight of the mixture in equation (3.24) can be calculated using equation 3.24

$$\mathcal{M} = \left(\sum_{i=1}^{n} \frac{c_i}{\mathcal{M}_i} \right)^{-1} \tag{3.20}$$

In equation (3.2o) c_i is the mass fraction of the i^{th} species and $\mathcal{M}_{\text{i}}$ is the molecular weight of each species.

The thermodynamic properties of a mixture of gases in thermo-chemical equilibrium is a function two state variable only viz. Temperature and pressure. The thermodynamic properties of a mixture of perfect gases in thermal equilibrium and chemical non-equilibrium on the other hand are dependent on the mass fraction of each species as well (Dunn, 1991). The specific enthalpy and specific heat of each species in the mixture are given respectively by equations 3.25 and 3.26.

$$h_i = C_{1,i} T + h_i^0 \tag{3.21}$$

$$c_{p,i} = C_{2,i} \tag{3.22}$$

Where the coefficients $C_{1,\text{i}}$ and $C_{2,\text{i}}$ for each species is a functions of temperature and h_i^0 is enthalpy of formation of individual species. The coefficients for the

curve fits of piecewise polynomial variations of specific heats and enthalpy of individual species is readily available in the literature. The enthalpy and specific heat of the mixture of perfect gases in turn are given by equations 3.27 and 3.28.

$$h = \sum_{i=1}^{n} c_i h_i \tag{3.23}$$

$$c_p = \sum_{i=1}^{n} c_i c_{p,i} \tag{3.24}$$

3.1.6 TURBULENT FLOWS

The unsteady Navier-Stokes equations are generally sufficient to solve the turbulent flow field completely in a continuum regime. All levels of turbulence can be captured by the *Direct Numerical Simulation* (DNS) of the transient Navier stokes equations. The DNS require that all length scales of turbulence are resolved, from the smallest eddies to scales of the order of the physical dimensions of the problem under consideration. For the direct numerical simulation, all computations need to be done in three dimensions with grid and time step small enough to capture the small scale motions in a time accurate manner. These requirements put a large demand on the computer resources and such simulations are practically impossible for any real engineering problem with present day computer capabilities. Thus, the present day researches intend to capture the turbulence flow through the time averaged Navier-Stokes equations. In this statistical method, commonly called as *Reynolds averaged Navier-Stokes* (RANS) equations, the time averaging of flow variables is carried out in order to separate the time-mean quantities from the fluctuations (Marx, 1963). This averaging introduces new variables in the system of equations, thus require additional equations to close the system of equations. The new equations can be

formulated by what is called the *turbulence modelling*. Two types averaging is currently in use viz. classical Reynolds averaging and mass weighted averaging, of which the latter is primarily used for compressible flows.

3.1.7 EQUATIONS FOR TURBULENCE

The mass weighted (Favre) averages for any variable f is given by

$$f = \tilde{f} + f''$$

(3.25)

Where the mean quantity $\tilde{f}$ and the fluctuating part f'' are respectively given by

$$\tilde{f} = \frac{\overline{\rho f}}{\rho} \tag{3.26}$$

$$f'' = \frac{\overline{\rho' f'}}{\rho}$$

(3.27)

And the fluctuating part has the property

$$\overline{\rho f''} = 0$$

(3.28)

With mass averages for the dependent variable the Navier-Stokes equations can be written as

Continuity equation:

$$\frac{\partial \bar{\rho}}{\partial t} + \frac{\partial(\bar{\rho}\tilde{u})}{\partial x} + \frac{\partial(\bar{\rho}\tilde{v})}{\partial y} + \frac{\partial(\bar{\rho}\tilde{w})}{\partial z} = 0 \tag{3.29}$$

Momentum Equations(x-only):

$$\frac{\partial}{\partial t}\left(\bar{\rho}\tilde{u}\right)+\frac{\partial}{\partial x}\left(\bar{\rho}\tilde{u}\tilde{u}\right)+\frac{\partial}{\partial y}\left(\bar{\rho}\tilde{u}\tilde{v}\right)+\frac{\partial}{\partial z}\left(\bar{\rho}\tilde{u}\tilde{w}\right)=-\frac{\partial\tilde{p}}{\partial x}+\frac{\partial}{\partial x}\left(\tilde{\tau}_{xx}-\overline{\rho u''u''}\right)+\frac{\partial}{\partial y}\left(\tilde{\tau}_{yx}-\overline{\rho u''v''}\right)+\frac{\partial}{\partial z}\left(\tilde{\tau}_{zx}-\overline{\rho u''w''}\right) \tag{3.30}$$

Where the mean viscous stresses $\tilde{\tau}_{ij}$ can be given, neglecting the fluctuations in viscosity, as

$$\tilde{\tau}_{ij}=\mu\left[\left(\frac{\partial\tilde{u}_i}{\partial x_j}+\frac{\partial\tilde{u}_j}{\partial x_i}\right)-\frac{2}{3}\delta_{ij}\frac{\partial\tilde{u}_k}{\partial x_k}\right]+\mu\left[\left(\frac{\partial\overline{u_i''}}{\partial x_j}+\frac{\partial\overline{u_j''}}{\partial x_i}\right)-\frac{2}{3}\delta_{ij}\frac{\partial\overline{u_k''}}{\partial x_k}\right] \tag{3.31}$$

Where *i*, *j*, *k* are dummy variables representing *x*, *y* and *z* directions respectively.

3.1.8 Energy equation:

The energy equation for turbulent flows in compact tensor notation employing Einstein summation convention can be written as

$$\frac{\partial}{\partial t}\left(\bar{\rho}c_p\tilde{T}\right)+\frac{\partial}{\partial x_j}\left(\bar{\rho}c_p\tilde{T}\tilde{u}_j\right)=\frac{\partial\bar{p}}{\partial t}+\tilde{u}_j\frac{\partial\bar{p}}{\partial x_j}+\overline{u_j''\frac{\partial p}{\partial x_j}}+\frac{\partial}{\partial x_j}\left(k\frac{\partial\tilde{T}}{\partial x_j}+k\frac{\partial\overline{T''}}{\partial x_j}-c_p\overline{\rho T''u_j''}\right)+\overline{\Phi} \tag{3.32}$$

Where

$$\overline{\Phi} = \overline{\tau_{ij} \frac{\partial u_i}{\partial x_j}} = \tilde{\tau}_{ij} \frac{\partial \tilde{u}_i}{\partial x_j} + \overline{\tau_{ij} \frac{\partial u_i''}{\partial x_j}} \tag{3.33}$$

3.1.9 Turbulence Modelling

Turbulence models to close the Reynolds averaged N-S equations can broadly be divided into two groups depending on whether the model is based on *Boussinesq assumption* or otherwise. As per Boussinesq assumption, the apparent turbulent shearing stresses are related to the rate of mean strain through an eddy viscosity. For a general Reynolds stress, the Boussinesq assumption gives

$$\overline{-\rho u_i' u_j'} = 2\mu_T S_{ij} - \frac{2}{3}\delta_{ij}\left(\frac{\mu_T \partial u_k}{\partial x_k} + \rho \bar{k}\right) \tag{3.34}$$

Where μ_T is the turbulent viscosity? The turbulent kinetic energy $\bar{k}$ and the rate mean strain tensor S_{ij} in equation 3.54 are respectively given by

$$\bar{k} = \frac{\overline{u_i' u_j'}}{2} \tag{3.35}$$

And

$$S_{ij} = \frac{1}{2}\left(\frac{\partial u_i}{\partial x_j} + \frac{\partial u_j}{\partial x_i}\right) \tag{3.36}$$

The above assumption is commonly known as eddy- viscosity approach. By applying the eddy-viscosity approach to the Favre-averaged Navier Stokes

equations, the dynamic viscosity coefficients in viscous stress tensor (equations 3.10 a-f) is simply replaced by the sum of a laminar and a turbulent component i.e.

$$\mu = \mu_L + \mu_T \tag{3.37}$$

In above formulation, the laminar viscosity can be computed using the kinetic theory of gases or by some empirical formulations like the Sutherland's formula. Similarly, using the Reynolds Analogy the thermal conductivity in equations 3.15 (a-c) can be evaluated as

$$k = k_L + k_T = c_p\left(\frac{\mu_L}{\mathrm{Pr}_L} + \frac{\mu_T}{\mathrm{Pr}_T}\right) \tag{3.38}$$

Where Pr_L and Pr_T are laminar and turbulent Prandtl numbers corresponding to laminar and turbulent viscosities μ_L and μ_T. Once the value of eddy viscosity μ_T is known, the Navier Stokes equations for turbulent flows can be solved by adding the eddy viscosity to the laminar viscosity terms.

The turbulence models that use Boussinesq eddy-viscosity assumption are referred as first order models and those not based on this assumption are referred to as second order models. Most of the engineering simulations at present are done with first order models (Goel, 1990). Further the first order models can be classified as zero-equation, one equation and two-equations depending on the number of closure equations.

3.1.10 SHEAR STRESS TRANSPORT (SST) *K-* Ω TURBULENCE MODEL

The second model used in this research, primarily to do the turbulence model independence study, is shear stress transport model proposed by Menter (Halloran, 1990) . This model overcomes the freestream turbulence intensity dependence of the standard *k-ω* model while retaining the robust near-wall formulation of the standard *k-ω* model. The SST model incorporates the transport of turbulence kinetic energy (*k*) and specific dissipation rate (*ω*).

$$\frac{\partial}{\partial t}(\rho k)+\frac{\partial}{\partial x_i}(\rho k u_i)=\frac{\partial}{\partial x_j}\left(\Gamma_k \frac{\partial_k}{\partial x_j}\right)+\tilde{G}_k-Y_k+S_k \tag{3.54}$$

and

$$\frac{\partial}{\partial t}(\rho \omega)+\frac{\partial}{\partial x_i}(\rho \omega u_i)=\frac{\partial}{\partial x_j}\left(\Gamma_k \frac{\partial_\omega}{\partial x_j}\right)+G_\omega-Y_\omega+D_\omega+S_\omega \tag{3.55}$$

Modeling the Production of Turbulence

In equation (3.11) the term $\tilde{G}_k$ represents the production of turbulent kinetic energy and G_ω in equation (3.52) represents the generation of ω, given respectively by equations (3.56) and (3.57)

$$\tilde{G}_k=\min\left(G_k,10\rho\beta^* k\omega\right) \tag{3.56}$$

$$G_\omega=\frac{\alpha}{\nu_T}\tilde{G}_k \tag{3.57}$$

with

$$G_k = -\rho\overline{u_i' u_j'}\frac{\partial u_j}{\partial x_i} \tag{3.58}$$

Calculation of the Effective Diffusivity

The effective diffusivities of k and ω appearing in equations (3.51) and (3.52) is computed using,

$$\Gamma_k = \mu + \frac{\mu_T}{\sigma_k} \tag{3.59}$$

$$\Gamma_\omega = \mu + \frac{\mu_T}{\sigma_\omega} \tag{3.60}$$

Where turbulent Prandtl numbers for turbulence kinetic energy and the specific dissipation rate σ_k and σ_ω and the turbulent viscosity μ_t are computed respectively using the relations 3.61 (a)-(c).

$$\sigma_k = \frac{1}{F_1/\sigma_{k,1} + (1-F_1)/\sigma_{k,2}} \tag{3.61a}$$

$$\sigma_\omega = \frac{1}{F_1/\sigma_{\omega,1} + (1-F_1)/\sigma_{\omega,2}} \tag{3.61b}$$

$$\mu_T = \frac{\rho k}{\omega}\frac{1}{\max\left[\frac{1}{\alpha^*}, \frac{SF_2}{\alpha_1\omega}\right]} \tag{3.61c}$$

In above equations the coefficient α* and the blending functions F_1 and F_2 are the calculated respectively using,

$$\alpha^* = \alpha_\infty^* \left(\frac{\alpha_0^* + \mathrm{Re}_T / R_k}{1 + \mathrm{Re}_T / R_k} \right) \tag{3.62}$$

$$F_1 = \tanh\left(\phi_1^4\right) \tag{3.63}$$

$$F_2 = \tanh\left(\phi_2^4\right) \tag{3.64}$$

with

$$\phi_1 = \min\left[\max\left(\frac{\sqrt{k}}{0.09\omega y}, \frac{500\mu}{\rho y^2 \omega} \right), \frac{4\rho k}{\sigma_{\omega,2} D_\omega^+ y^2} \right] \tag{3.64}$$

$$D_\omega^+ = \max\left[2\rho \frac{1}{\sigma_{\omega,2}} \frac{1}{\omega} \frac{\partial k}{\partial x_j} \frac{\partial \omega}{\partial x_j}, 10^{-10} \right] \tag{3.65}$$

and

$$\phi_2 = \max\left[2 \frac{\sqrt{k}}{0.09\omega y}, \frac{500\mu}{\rho y^2 \omega} \right] \tag{3.66}$$

where y is the distance next to the surface and the $D^+{}_\omega$ is positive component of the cross diffusion term. Also the coefficient α_∞ appearing in equation (3.66) is evaluated as

$$\alpha_{\infty} = F_1 \alpha_{\infty,1} + (1 - F_1)\alpha_{\infty,2} \tag{3.67}$$

where, with κ=0.41

$$\alpha_{\infty,1} = \frac{\beta_{i,1}}{\beta^*_{\infty}} - \frac{\kappa^2}{\sigma_{w,1}\sqrt{\beta^*_{\infty}}} \tag{3.68}$$

$$\alpha_{\infty,2} = \frac{\beta_{i,2}}{\beta^*_{\infty}} - \frac{\kappa^2}{\sigma_{w,2}\sqrt{\beta^*_{\infty}}} \tag{3.69}$$

3.1.11 HEAT TRANSFER MODEL

In the reactor core the heat transfer is going to happen through both convection and radiation. The energy equation is solved to account the rise in heat in the propellant region from the fission process. The study flow energy equation is expressed by using non dimensional numbers to account for nussult number for given geometry is expressed.

$$Nu = F_1\left(\mathrm{Re}, \mathrm{Pr}, M, \frac{\Delta T_{ad}}{T_W - T_b}\right) \tag{3.70}$$

It is expressed as a function of Reynolds number, Prandtl number, Mach number and total adiabatic stagnation tempratures rise. The energy equation solved to express the h eat transfer in the given geometry is written as

$$\frac{\partial}{\partial t}(\rho E) + \nabla \cdot (\vec{v}(\rho E + p)) = \nabla \cdot \left[k_{eff} \nabla T - \sum_j h_j \vec{J}_j + (\overline{\overline{\tau_{eff}}} \cdot \vec{v}\right] + S_h \tag{3.71}$$

The energy accounted by E and the viscous dissipation, sensible enthalpy and diffusion fluxes indicates heat transfer, which can be found from the turbulence model selected.

$$E = h - \frac{p}{\rho} + \frac{v^2}{2} \qquad (3.72\ a)$$

$$h = \sum_j Y_j h_j \qquad (3.72\ b)$$

$$h_j = \int_{T_{ref}}^{T} c_{p.j}\, dT \qquad (3.72\ c)$$

In the solution the boundary condition used at the wall is adiabatic wall with a constant wall tempratures, since in the space heat transfer is through convection and radiation and the reflector tempratures is also maintained with in the specified range. In the pressure based solution the species diffusion equation is also add to the solver in the form of diffusion energy source.

$$\nabla \cdot \left[\sum_j h_j \overrightarrow{\vec{J}_j} \right] \qquad (3.73)$$

Radiation also included in the solution since the overall heat transfer is accounted as the convection and radiation together in a reactor core. The radiation equations are express below; since the radiative flux is comparatively large the convection and radiation are included as mixed phenomena

$$Q_{rad} = \sigma\left(T_{\max}^4 - T_{\min}^4\right) \qquad (3.74)$$

In the solution surface to surface radiation model is used since the heat transfer through radiation is from the plasma source and which is at the center of the core

and some of the heat is transfer through interactions of the regions and some of it is due to radiation between the fission sources to the buffer region. The equation written for accounting for radiation is in the form of

$$\frac{dI(\vec{r},\vec{s})}{ds}+(a+\sigma_s)I(\vec{r},\vec{s})=an^2\frac{\sigma T^4}{\pi}\int_0^{4\pi}I(\vec{r},\vec{s}')\Phi(\vec{s}\cdot\vec{s}')d\Omega' \qquad (3.75)$$

In the solution fixed tempratures conditions are applied to the walls since the reflector tempratures need to be maintained with in the limit and variations are more likely to be with propellant tempratures.

$$q=h_f(T_w-T_f)+q_{rad} \qquad (3.76a)$$

$$q_{rad}=\varepsilon_{ext}\sigma(T_\infty^4-T_w^4) \qquad (3.76b)$$

In the fixed wall condition the fluid side local heat transfer coefficient is accounted along with the radiative fluxes. In the interface the heat transfer is accounted from solid cells and it can be expressed as

$$q=\frac{K_s}{\Delta n}(T_w-T_s)+q_{rad} \qquad (3.77)$$

The radiative heat transfer equation can be solved based on surface absorption and the emission, absorption and scattering is accounted from

$$\frac{\partial I_{si}}{\partial x_i}+(\sigma+\sigma_s)I(r,s)=an^2\frac{\sigma T^4}{\pi}+\frac{\sigma_s}{4\pi}\int_0^{4\pi}I(r,s')\Phi(s,s')d\Omega' \qquad (3.78)$$

Wall functions need to be calculated to define heat transfer coefficient to the source, based on the turbulent kinetic energy the energy equation is enabled to account the convection

$$h_{eff} = \frac{\rho c_p C_\mu^{\frac{1}{4}} k^{\frac{1}{2}}}{T^*} \tag{3.79}$$

The dimensionless temperature need to be calculated to supply T^* to the above equation

$$T^* = \frac{(T_w - T_P)\rho c_p k_p^{\frac{1}{2}}}{\dot{q}} = \begin{cases} \Pr y^* + \frac{1}{2}\Pr \frac{C_\mu^{\frac{1}{4}} k_p^{\frac{1}{2}} U_P^2}{\dot{q}} U_P^2 (y^* < y_T^*) \end{cases} \tag{3.80 a}$$

$$T^* = \frac{(T_w - T_P)\rho c_p k_p^{\frac{1}{2}}}{\dot{q}} = \begin{cases} \Pr_t \left[\frac{1}{k} \ln(EY^*) + P \right] + \frac{1}{2} \frac{\rho C_\mu^{\frac{1}{4}} k_P^{\frac{1}{2}}}{\dot{q}} \{\Pr_t U_P^2 + (\Pr - \Pr_t) U_c^2\} (y^* > y_T^*) \end{cases}$$

$$P = 9.24 \left[\left(\frac{\sigma}{\sigma_t} \right)^{\frac{3}{4}} - 1 \right] \left[1 + 0.28 e^{\frac{-0.007\sigma}{\sigma_t}} \right] \tag{3.80b}$$

The major assumption made while considering the radiation model is that the radiation intensity decomposed into series of spherical harmonics. The first term in the equation 3.80 b on right hand side indicates series represented in P1 model. It includes effect of scattering, while solving this equation it assumes all surfaces are diffuse. In the process if accounting radiation heat transfers in the mixed model the solver predicts the localized radiative heat fluxes and calculate the non-dimensional tempratures (Dunn, 1967). The variation in tempratures and pressure inside the reactor is varied in stream wise direction and the values are accounted for the specific heat flux. In calculating the heat fluxes the radial heat conduction is neglected, the propellant gas absorbs and emits radiation. The phase change of

the propellant takes place before entering into the reactor core itself, and the scattering effects of the propellants are neglected.

The axisymmetric form of mass averaged time-dependent compressible Navior-Stokes equations can be considered in the following form.

$$\frac{\partial \overline{U_i}}{\partial t} + \frac{\partial \overline{F_i}}{\partial z} + \frac{\partial \overline{G_i}}{\partial r} = \frac{\partial \overline{G_v}}{\partial r} + \overline{H} \tag{3.81}$$

Where

$$\overline{U_i} = \begin{bmatrix} \rho \\ \rho u \\ \rho v \\ e \end{bmatrix}, \quad \overline{F_i} = \begin{bmatrix} \rho u \\ \rho u^2 + P \\ \rho uv \\ (e+P)u \end{bmatrix}, \quad \overline{G_i} = \begin{bmatrix} \rho v \\ \rho uv \\ \rho v^2 + P \\ (e+P)u \end{bmatrix} \tag{3.82}$$

Thermal and Viscous Source Terms are

$$\overline{H} = \begin{bmatrix} 0 \\ 0 \\ 0 \\ \dot{Q} \end{bmatrix} \tag{3.83}$$

And

$$\overline{G_v} = \begin{bmatrix} 0 \\ \mu_T \dfrac{\partial u}{\partial r} \\ 4\dfrac{\mu_T}{3}\dfrac{\partial v}{\partial r} - \dfrac{2}{3}\mu_T \dfrac{v}{r} \\ \mu_T u \dfrac{\partial u}{\partial r} + \dfrac{4}{3}\mu_T v \dfrac{\partial v}{\partial r} - q_c'' - q_r'' \end{bmatrix} \tag{3.84a}$$

$$e = \rho[\varepsilon + \frac{1}{2}(u^2 + v^2)] \tag{3.84 b}$$

Total viscosity

$$\mu = \mu_m + \mu_e \tag{3.85}$$

Fourier's Law of conduction heat flux

$$\dot{q}_e = -k_c \frac{dT}{dr} \tag{3.86}$$

Where

$$k_c = C_P\left(\frac{\mu_m}{P} + \frac{\mu_c}{P}\right) \tag{3.87}$$

$$P = \rho RT\ ,\ \varepsilon = C_v T\ ,\ h = C_P T\ ,\ \gamma = \frac{C_P}{C_V} \tag{3.88}$$

The equations that can be obtained by using the above relations by interchanging the terms from equation number 3.85.

$$P = (\gamma - 1)\left[e - \frac{1}{2}\rho(u^2 + v^2)\right] \tag{3.89}$$

$$T = \frac{(\gamma - 1)}{R}\left[\frac{e}{\rho} - \frac{1}{2}(u^2 + v^2)\right] \tag{3.90}$$

$$\frac{\partial\left(\frac{\partial U}{\partial t}\right)}{\partial t} + \frac{\partial A_i\left(\frac{\partial U}{\partial t}\right)}{\partial z} + \frac{\partial B_i\left(\frac{\partial U}{\partial t}\right)}{\partial r} = \frac{\partial B_v\left(\frac{\partial U}{\partial t}\right)}{\partial r} + \frac{\partial H}{\partial t} \tag{3.91a}$$

Where

$$A_i = \frac{\partial F_i}{\partial U},\ B_i = \frac{\partial G_i}{\partial U},\ B_v = \frac{\partial G_v}{\partial U} \qquad (3.91\ b)$$

The equations can be written in terms of nth coefficient to convert them into implicate form to find the Jacobian of A_i, B_i, B_v

$$\Delta U^n = \Delta t\left(\frac{\partial U}{\partial t}\right)^n,\ \Delta H^n = \Delta t\left(\frac{\partial H}{\partial t}\right)^n,\ \delta U^{n+1} = \Delta t\left(\frac{\partial U}{\partial t}\right)^{n+1} \qquad (3.20)$$

3.2 GEOMETRIC MODELING AND GRID GENERATION

The problem taken for solving analysing the fluid flow and heat transfer, the geometries are constructed using Catia V5 and then imported into Gambit in using STEP format and scaled according to the dimensions of the problem. In gambit grid is generated, since its state of art pre-processor to support CFD problems. In gambit the interfacing of the mesh surfaces are easy and the quality of the mesh generated is quite attractive. It can accept different CAD models in diversified formats and coordinate miss matching is limited compared to the other solvers. The complex geometries can be created in the form of volumes and can be tightly integrated for the desired shape. The mesh generation part in the gambit modeller functions with automated size function driven tools for mexh generation. It can generate both structured and unstructured mesh with highest quality, the skewness values are below 40 percent and the ratio of elements can be taken as per the requirement of the solution domine.

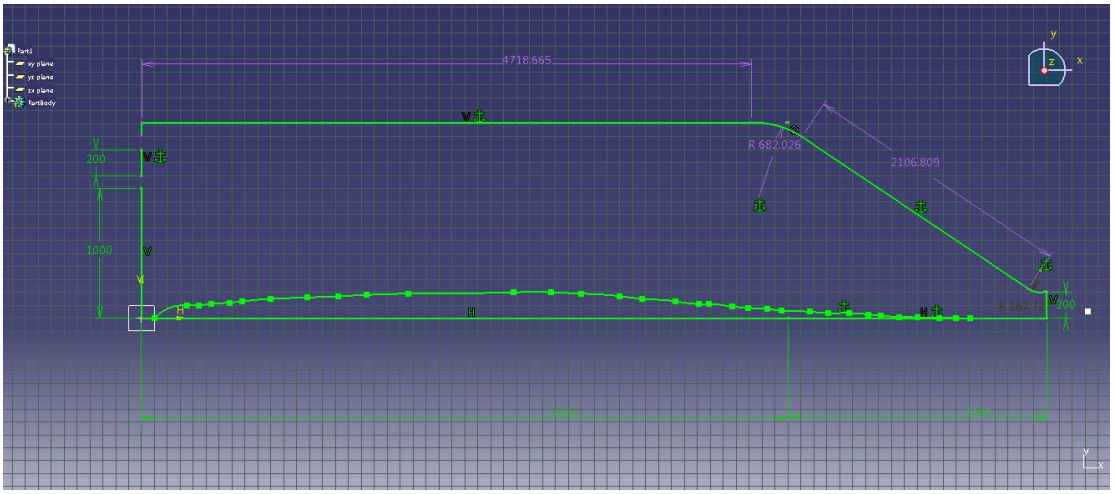

Figure 3.2: Model Used For Solving Heat Transfer Problem with the Fuel Region

The mesh generation part include creation of geometry and the specifying solver based on its units selection, mesh generation on the edges and creation of face mesh/ volume mesh. To examine the created mesh and to see the quality of the mesh at various places gambit options and it can be remodifyed. Finally zone assignment is done to set the boundaries, in case of fluid problems the flow boundary conditions, in heat transfer problems thermal boundary conditions can be set.

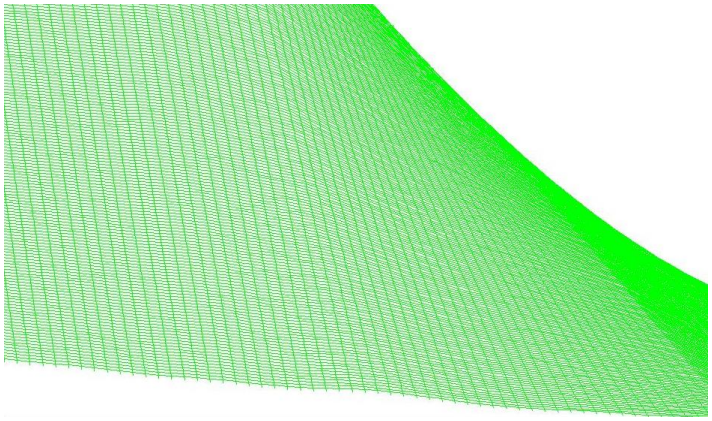

Figure 3.3: Dense Grid Generated Inside the Axisymmetric Core Model

The geometry can be exported in various formats once the c reaction and meshing and other things are completed based on solver the format will change. In case of fluent the gambit geometry need to be exported as msh file. In fluent msh file can be read and grid cheak and boundaries can be verified, if conditions need to be changed fluent have options for it. The model designed in the catia is shown in the figure below. The complete length of the chamber with the throat portion is considered with an axisymmetric model. The diameter of the section is at 3 meters and the throat is designed to have Mach 1. The dense mesh created on the geometry using gambit mesh generator is shown in the figure 3.3, the total number of elements created are 500000, based on grid independent study the number of elements are considered to be an effective, and the results are accurate for the given boundary conditions. At the walls the thermal boundary conditions is given so the grid generated with concentrated grid points.

3.3 SOLVER SELECTION AND BOUNDARY CONDITIONS

The equations governing fluid flow and heat transfer forms an initial boundary value problem, in order to solve such kind of problems we need to solve partial differential equations with the help of boundary conditions by iterative methods. The solver used in calculating the flow variations and heat transfer effects in gas core reactor chamber with various heat generation rates are analysis for different propellant properties. In solver due to the heat generation rate with the given geometry it predicts p^* the pressure field in the flow domain and it solves the continuity, Momentum and Energy Equations. The values are correlated with p' and the final pressure rise at the throat due to the rise in kinetic energy is obtained from the solver. The velocity correlation is used from the mass flow at the inlet and the u,v,w values are obtained. In case of convective and radiative heat transfer problems with a specific heat generation rate due to the source with moderated heat flux need to be treated as a special case of momentum equation to solve ϕ at

general boundary conditions. The solver follows implicit- explicit based finite volume method to discretize the fluid flow equations.

In the physical means of operating gas core reactor is based on nuclear fission and which involves subatomic particles and their behavior. This solution concentrated on solving Navior-Stokes equation on flow domain inside the reactor core, the fission part and the plasma part of the problem is solved in the next chapter to investigate the neutronics and fission energy rate. The idea of conducting numerical experimentation on the current model is to create the behavior of the propellants and to understand the operations conditions to obtain the peak values in case of different enrichments and the results are used to conduct neutronics analysis as an input the reactor core tempratures and pressure conditions are used along with the fuel tempratures maintained in the process. The scope of the problem is limited to deal with operations conditions of the reactor system and modeling uranium hexafluoride for fission cannot be considered in the solver due to the numerical limitations (Jack, 1961).

The fission region is considered as a gaseous uranium flow field and can be contained in the reactor chamber through vortex generation through the radial and axial entries of the fuel at different flow properties. In solution using turbulence model affects the accuracy of the solution, in the current problem k-ε model to obtain the turbulent kinetic energy effects throughout the length scale by using one and two equation models. In the solution the product of effective viscosity and the mean strain rates are replaced by mean momentum equation to with turbulent shear stress, this yield to faster convergence and the accurate solution. Diffusion equations are solved to calculate the convective and radiative heat transfer rates under high tempratures conditions. This problem considers rossland radiation model to obtain the flow patterns through radiation. The multiple inlets are provided for hydrogen to enter the chamber and fixed wall tempratures is used

to maintain the reflector tempratures with in the upper limit it varied with the multiple cases and the consideration are made from Van Booman model to correlate reflector tempratures limitations for graphite. In one of the case the upper limit is set to be 2200k and in other case it was limited to 1900k. Since the reactor criticality affects by reflector tempratures selection. In figure 3.4 the detailed approach followed in solving N-S equations on a flow domain is explained using a flow chart. In the problem the heat transfer analysis between fissioning gas and propellant analyzed, for identifying the behavior in the core chamber a convective and radiative model is solved for different operating conditions. The consideration of different heat fluxes for hydrogen and helium and their operating pressure are tabulated below. In the analysis the solution is obtained based on set solution parameter and can be initialized on a modeled grid and the values are compared with the exact solution or experimental predictions.

In case of solving numerical heat transfer problems using convection and radiative flow domain, the geometrical modeling and grid generation plays an important role. In the current work a 2D axisymmetric model is developed with a structured grid capable of handling complete flow domain. Boundary conditions are specified on each edge of the computational 2D domain, the material properties are specified for the propellants used in the flow path. The variation of physical properties as per the change in temperature taken as a piecewise polynomial order and the coefficents are add to the case. The numerical procedure and the solution algorithms are presented in the figure 3.4, the starting values for the flow field in a given domain are supplied as intial conditions. The residuals can be thought of as a measure of how much the solution to a given transport equation deviates from exact and we monitor average residuals for the each transport equation solved. The convergence criteria depends on the solution methods incorporated with the transport equations.

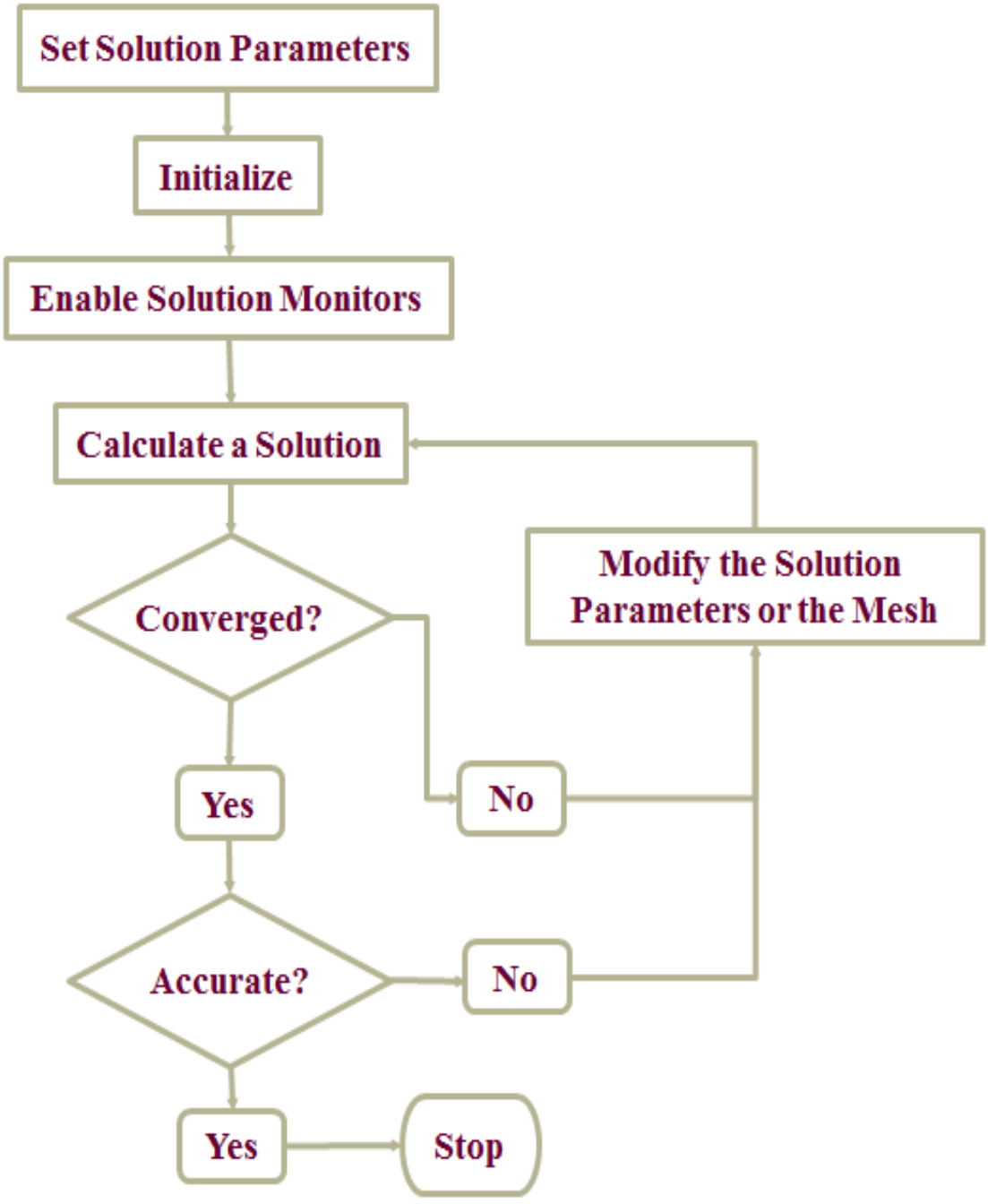

Figure 3.4: Method of Solving Navior-Stokes Equations

The solutions are obtained by various trails to reach desired effectiveness and the result should be as accurate as possible. The intial boundary value problem is solved by iterations through partial differential equations applicable to the physics of the problem using a numerical method. Specific boundary conditions need to be identified with in the solver limitations based on the system application. If the solution gets converged with in the given limits results need to be verified across the different parameters. Most possible errors in numerical investigations are related to the discretization, geometry modeling. If the solution is not accurate the process of reconsidering the geometry or changing the boundary conations will optimize the quality of the solution. Sometimes iterative convergence error occurs due to the limits of the solution and the CFL number is varied to reach convergence.

Table 3.1: Boundary Conditions Considered for Solution

Type	Propellant	Thermal Boundary Condition K(T_{Wall})	Heat Generation Rate	U-C-F Enrichment %	Mass Flow rate of Propellant
Case 1	Hydrogen	1900	1000 MW/m^3	50%	4.2 Kg/s
Case 2	Helium	1850	1000 MW/m^3	50 %	4.2 Kg/s
Case 3	Hydrogen	1600	620 MW/m^3	30 %	3.6 Kg/s
Case 4	Helium	1600	620 MW/m^3	30 %	3.6 Kg/s
Case 5	Hydrogen	1200	280 MW/m^3	5 %	3 kg/s
Case 6	Helium	1200	280 MW/m^3	5%	3 Kg/s

Physical modeling errors are taken care after every solution, with the expected variations and the trends in the plots obtained are cross verified. In case of CFD problems the physical modeling errors can occur in considering the specific dimensions in geometry preparations. The second possibility is thought he boundary conditions selected and the models chosen. The only method of validation in case of geometry is through literature and comparing the dimensions with the work. The truncation error is generally visible in the solution because the partial differential equations are solved using approximate methods.

The problem is solved using the tabulated boundary conditions the geometry is considered from the parameters discussed through literature and the conditions are applied as per the need of the solution. There are six cases analyzed using CFD to identify the GCR core behavior, in that two different propellants are chosen. Most commonly used rocket propellant with less molecular weight is hydrogen and due to the inertness and in terms of higher het handling capacity fluid as Helium as considered. The analysis is conduced based on the heat generation rate obtained in the reactor with the fuel enrichment and the peak values are chosen for conducting neutronics analysis. In case one, hydrogen is considered as propellant and the fuel enrichment is chosen at 50 % for generation rate of 100 MW/m^3 is selected in the similar manner the analysis is conducted on Helium gas for the same boundary conditions. The mass flow rate selected for all the cases kept similar to compare the Temprature and pressure variations in the core chamber with respect to the fission heat generation rate. Mixed boundary condition is used with the ideal gas density properties, and the thermal conductivity and viscosity are varied with the piecewise polynomial profile so that different zone are having different values as per the change in generation rate. The thermal boundary condition is set to the reflector wall to limit the Temprature, with in the desired ratio.

3.4 RESULTS AND DISCUSSIONS

Numerical heat transfer is an interesting study in nuclear reactors which operates at high pressure and high Temprature conditions. In order to achieve higher rate of energy conversion from fission to the maximum Ve, the propellant selection and investigation of heat transfer in a GCR core can develop an idea for reactor operations. In case of GCR core propellant selection and the rate at which heat transfer taken place are investigated at different heat generation rates. An axisymmetric model was solved with a throat designed to operate at Mach 1, the stream lines of the flow domain is shown is the figure 3.4. The flow is smooth at the wall and the tempratures limitation applicable with a thermal boundary condition, back flow is visible near the vortex region to separate the propellant and the gaseous fuel from mixing.

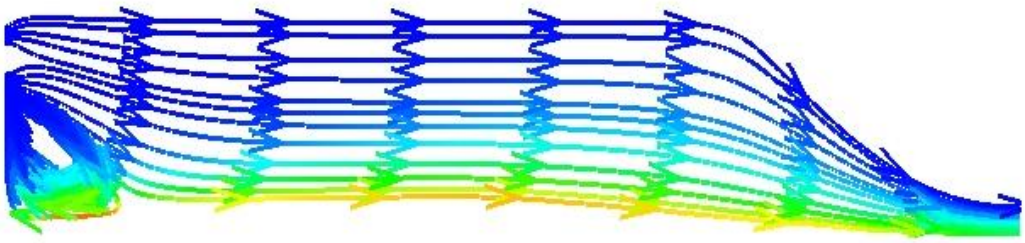

Figure 3.5: The Stream Lines of the Flow Pattern inside the core

In case one the analysis is conducted for the GCR core which is operated with the 50 % enriched gaseous fuel, the heat generation rate in case of GCR is obtained from the design parameters. The analysis is conducted using a pressure based solver for examining the core behaviour and the heat transfer between the fuel gases to the propellant. Radiative and convective heat transfer is considered with a temperature limitation to the core containment, since the propellant takes the heat from the walls and enters the reactor chamber.

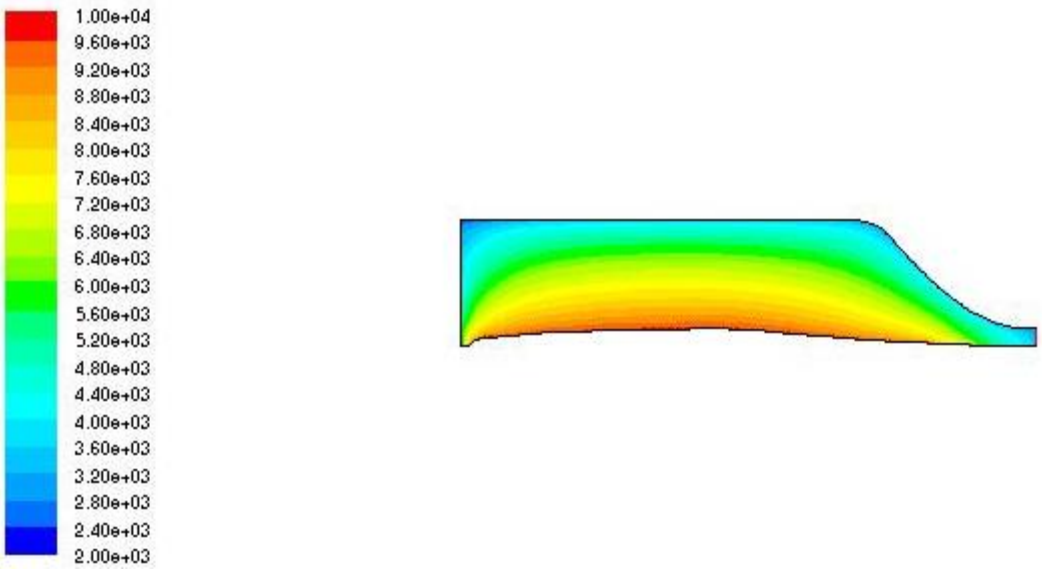

Figure 3.6: Static Temperature in Variation in case 1 with Hydrogen Propellant

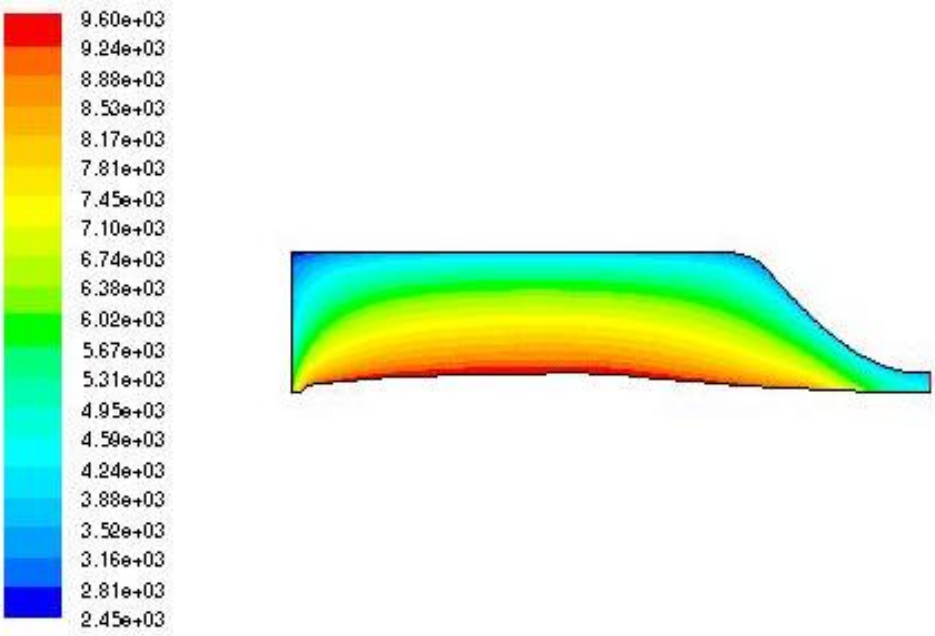

Figure 3.7: Total tempratures Variation in Case 1 with Hydrogen Propellant

In the case 1 Hydrogen is considered as a propellant and the static temperature and total temperature variations in case of 1000 MW/m^3 generation rate. The maximum temperature at the core is reaching 10000 K and which is considered as a core reaction temperature in case of solving 50 % enriched fuel in neutronics. The temperature rise in the reactor core can be explain with the help figure 3.5, at the inlet hydrogen enters the core at 2000k and the it occupies the buffer region and the overall temperature rise for the working fluid is ranging up to 10000k. The idea of using hydrogen is take dual advantage as coolant to the reflector walls and as well as the rocket propellant. The variation in total temperature is also presented in the plot 3.6, which indicates the stagnation points and their temperature changes due to the reverse flow in the flow domain. The total loss in source temperature to the propellant is within the range of 300 K and the heat transfer is effective in case 1.

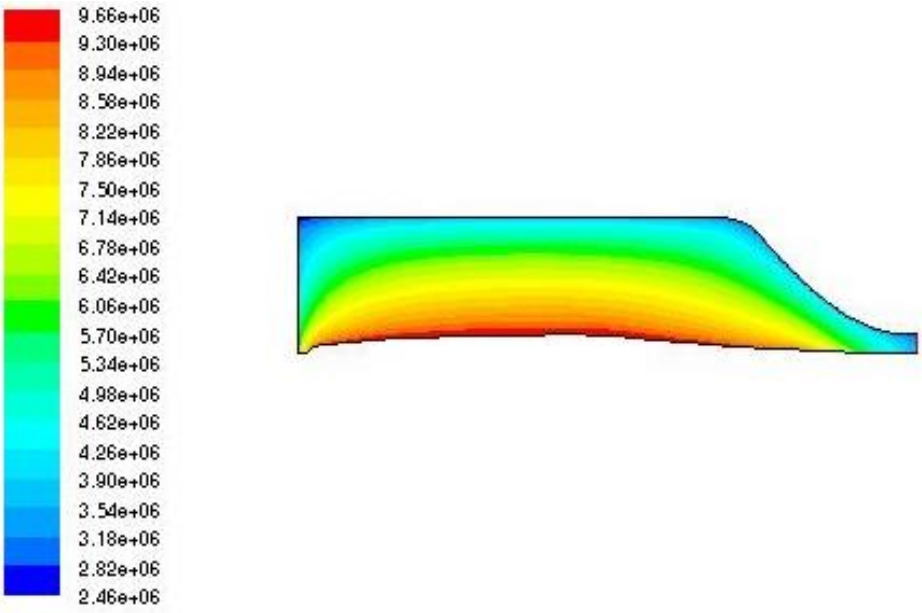

Figure 3.8: Enthalpy Change in Case 1 for Hydrogen Propellant

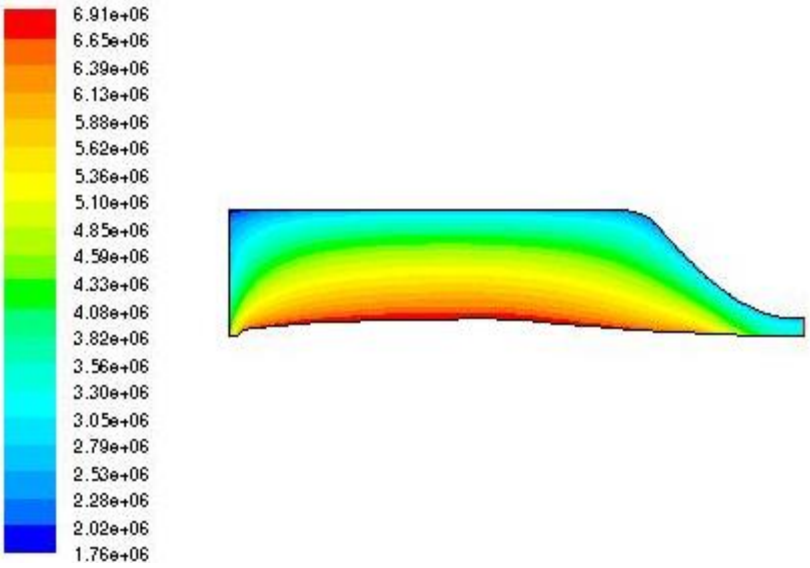

Figure 3.9: Total Energy Variation in case 1 with Hydrogen Propellant

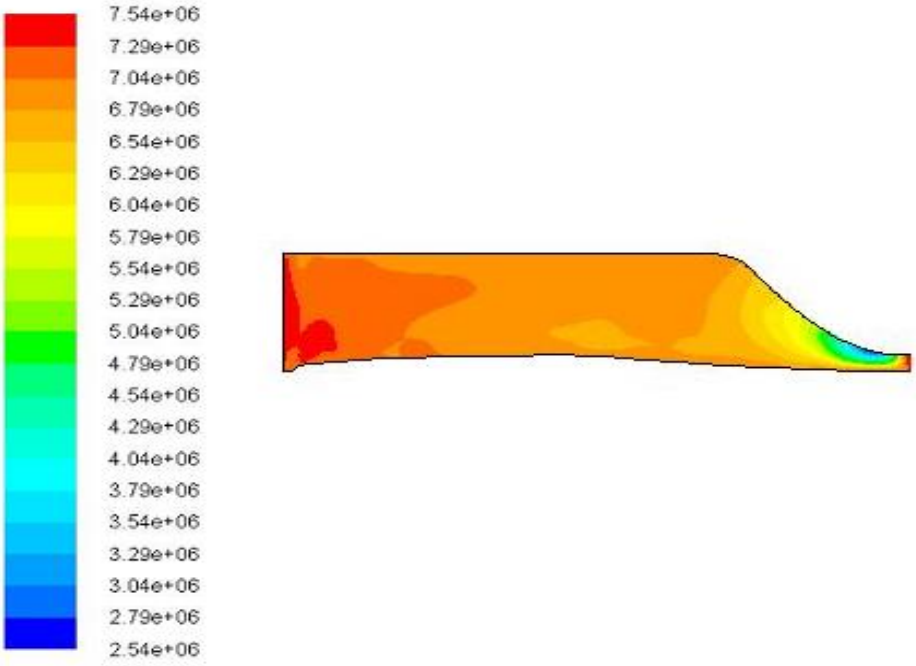

Figure 3.10: Total Pressure Variation in Case 1 for Hydrogen case 1

The enthalpy change in the reactor system with respect to source is indicated in the figure 3.7; the variation is in j/kg due to the back flow from the source and the maximum enthalpy this variation is occurring due to the sensitiveness of the wall function in heat transfer analysis. The thermal boundary condition applied to the reflectors walls is to maintain Temprature constant, an isothermal boundary condition with a specified temperature based on the reflector wall temperature limitation is applied. In case 1 the temperature is limited to 2000 K, in reality it affects the criticality and the neutron reflection. But in case of highly enriched reactor cores the operational tempratures are very high and the propellant circulation rate in the buffer region also creates viscous heating. The energy levels are very much high at the center of the core, the radial position if we consider the maximum energy levels are at 6.38 MJ/kg, since the source energy levels are high the buffer region takes more heat from the fission. In case of radiation heat transfer the total radiation source temperature is at 10000 K and it is limited at the wall due to thermal boundary condition.

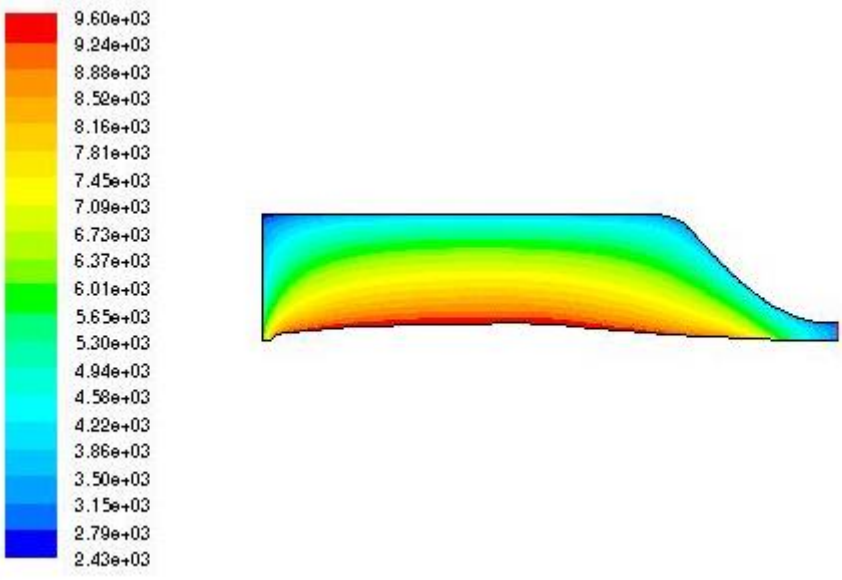

Figure 3.11: Radiation Temperature Variation in Case 1 with Hydrogen

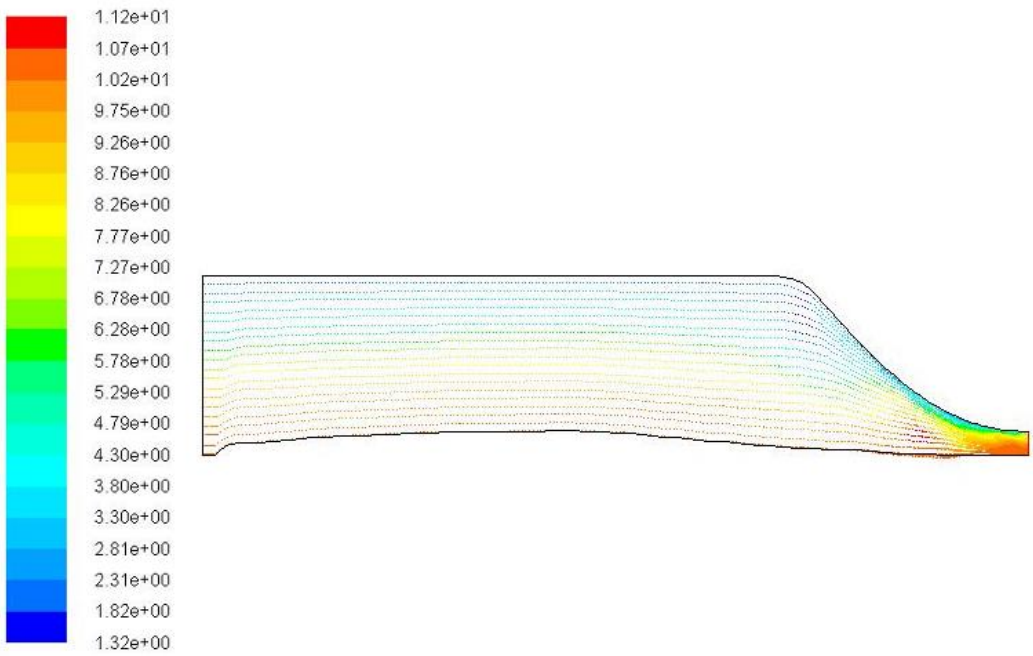

Figure 3.12: Velocity Vectors for the Case 1 with Hydrogen Propellant

The velocity magnitude in the GCR core for the case 1 is shown in the figure 3.12, the velocity variation is from 1.32 m/s to 11.2 m/s, at the throat maximum velocity is obtained. The stream lines of the propellant in a high temperature conditions for the case 1 is shown in the figure 3.13.

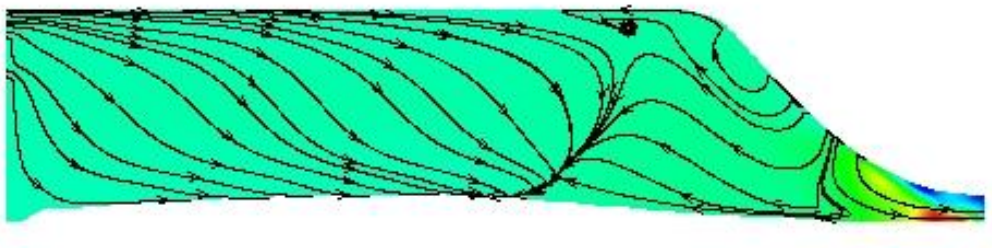

Figure 3.13: Velocity Strum lines in case of Hydrogen with back flow

The core is exposed to the heat from the fission source and the total heat transfer is a result of both convection and radiation. The convective heat fluxes are the result of fluid flow near the source and the radiative heat changes with the radial distance. The flow velocity changes with the increase in temperature with the fluid and it becomes supersonic flow and it reaches Mach 1 at the throat. Since the ratio of the throat to the nozzle is considered as 1:36 in terms of Mach number. The incident radiation profile along the core is plotted in the figure 3.13 and which indicates the sudden rise in the radiation levels when the fluid reaches the source and the variation are depends on the scattering and the absorption of the total radiation emitted from the source. In case of gases the absorption coefficents is very less since the density of the high temperature gas is very less, as a same time the scattering coefficient is high.

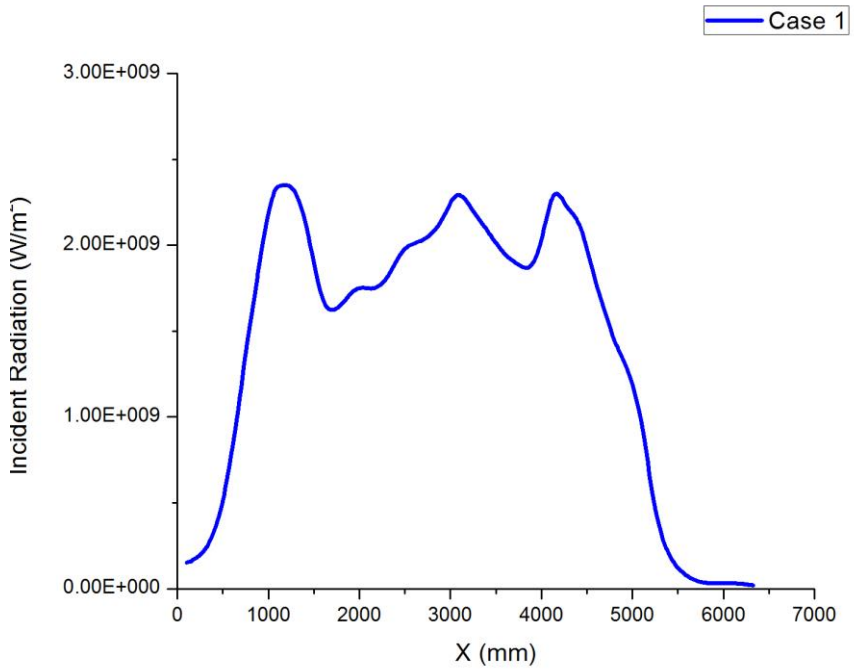

Figure 3.14: Incident Radiation in GCR from the source in Case 1

In case 2 the boundary conditions are similar as case one and the mass flow inlet applied with a 3 kg/s mass flow rate and propellant is changed to helium to see the effectiveness of the heat transfer and the behavior of the core. In most of the gas cooled nuclear reactors helium is preferred as a coolant due to its inertness and due to less absorption coefficient. So that reaction with the core material is limited, in the current case graphite is used as a reflector material. In the solution two different thermal boundary conditions are used, in spite of source the iso-thermal wall limits the heat flow in the radial direction and the distribution of the heat for the propellant in the buffer region is comparatively low in case 2. The static temperature variation is visible in the graph 3.14, the variation the static temperature behavior in the core between two different propellants is related to their thermal conductivity.

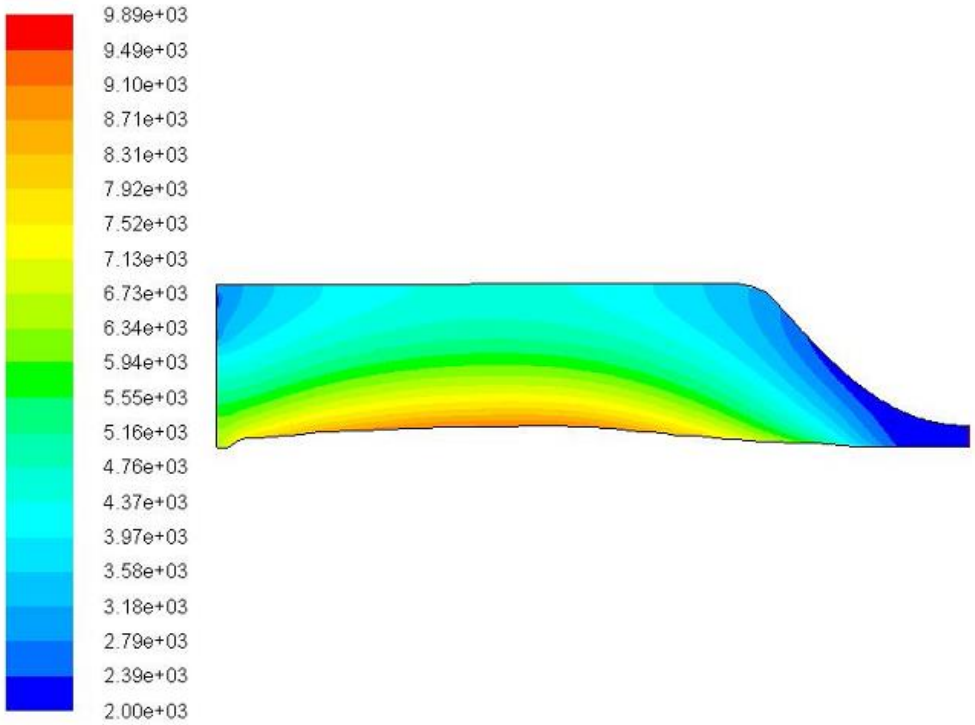

Figure 3.15: Static Temperature in Case 2 with Helium Propellant

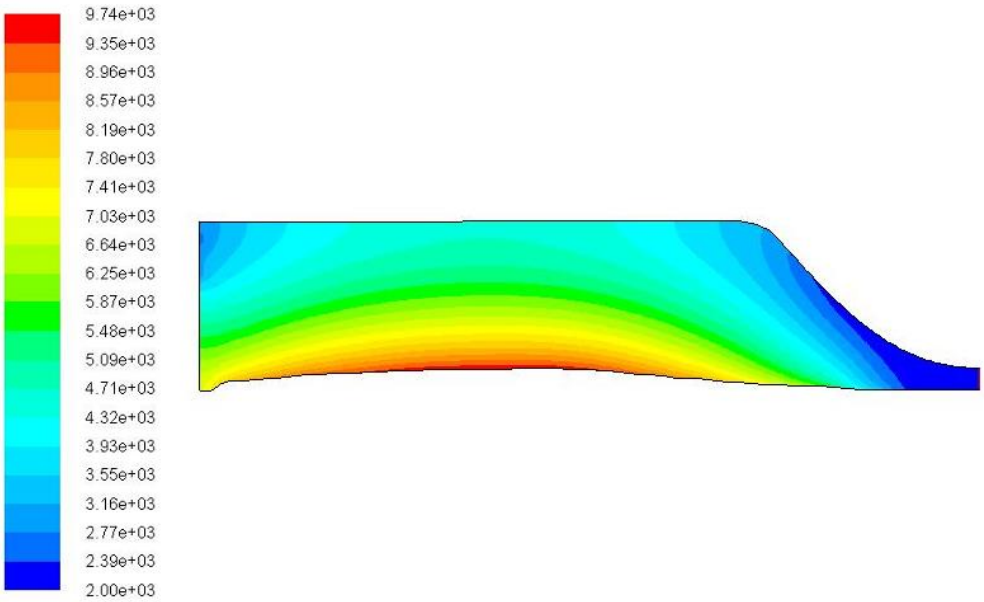

Figure 3.16: Total Temperature in Case 2 with Helium as a Working Fluid

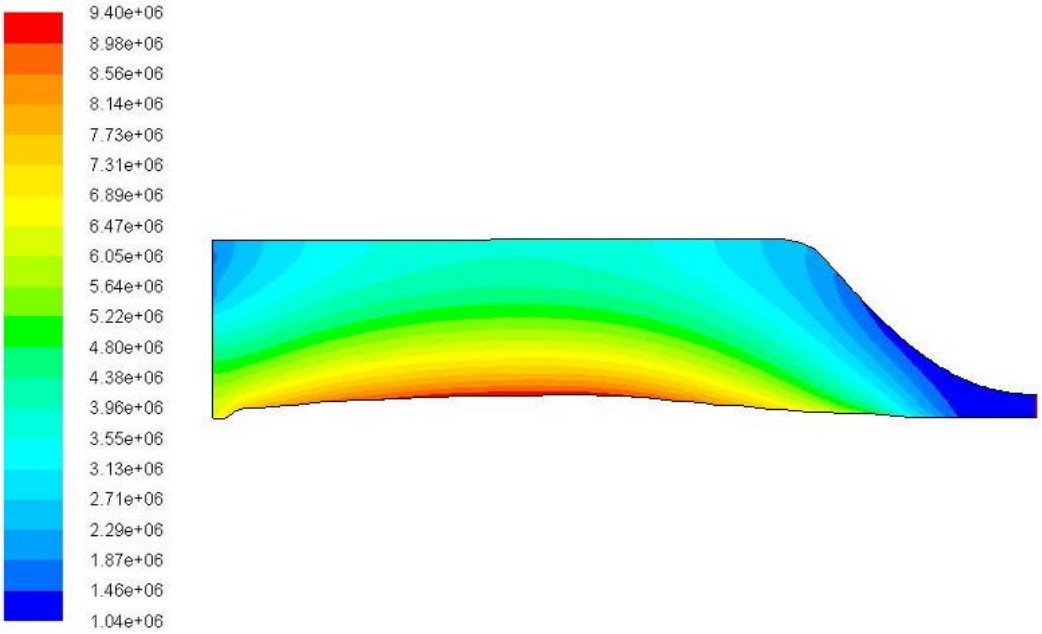

Figure 3.17: Enthalpy Change in J/kg for Case 2

The total temperature variation and the static temperature variation there is likely to have a temperature difference both the working fluids. In case of hydrogen the thermal conductivity is high and the inlet temperature is kept similar for both the working fluids. In case of helium the possibility of allowing the working fluid at lower temperature can result better heat transfer. In case of enthalpy change the total heat content from the source is indicated at the core and the variation is visible along the buffer region. The total variation in the enthalpy and energy content between Inlet and to the outlet is in the range of 1.04 MJ/kg to 9.40 MJ/kg, some parts of the buffer region is also showing the limited values due to the stagnation in the flow created by the pressure difference. The total energy is high at the fission source and the energy distribution in the throat and the buffer region is comparatively limited. The maximum energy levels maintained inside the core is in the range of 1.62 MJ/kg to 6.38 MJ/kg, in the reservoirs region there is a bypass flow which also takes away the heat content.

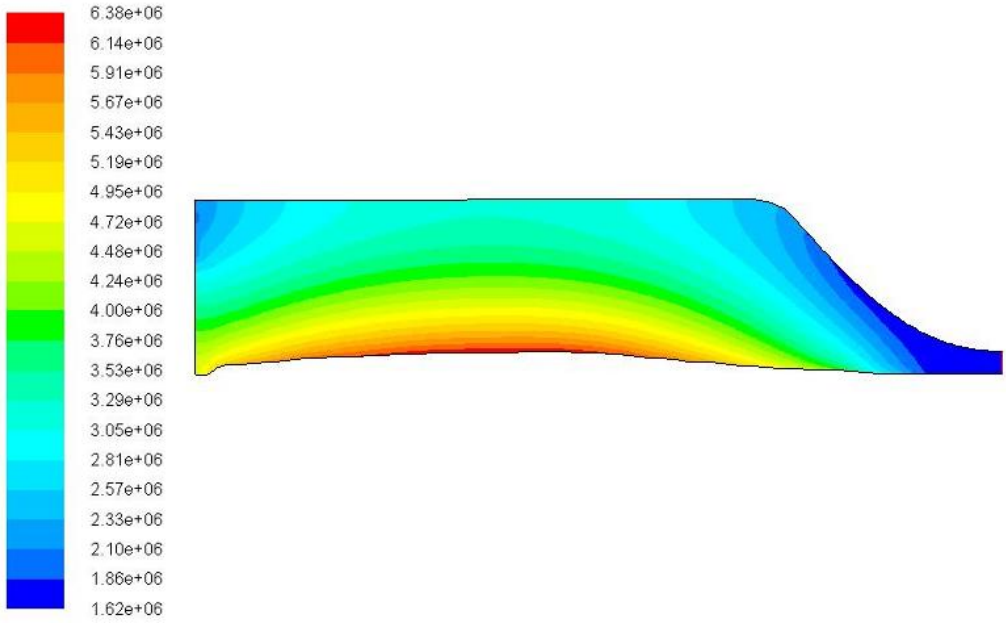

Figure 3.18: Total Energy Variation in J/Kg in Case 2 with Helium

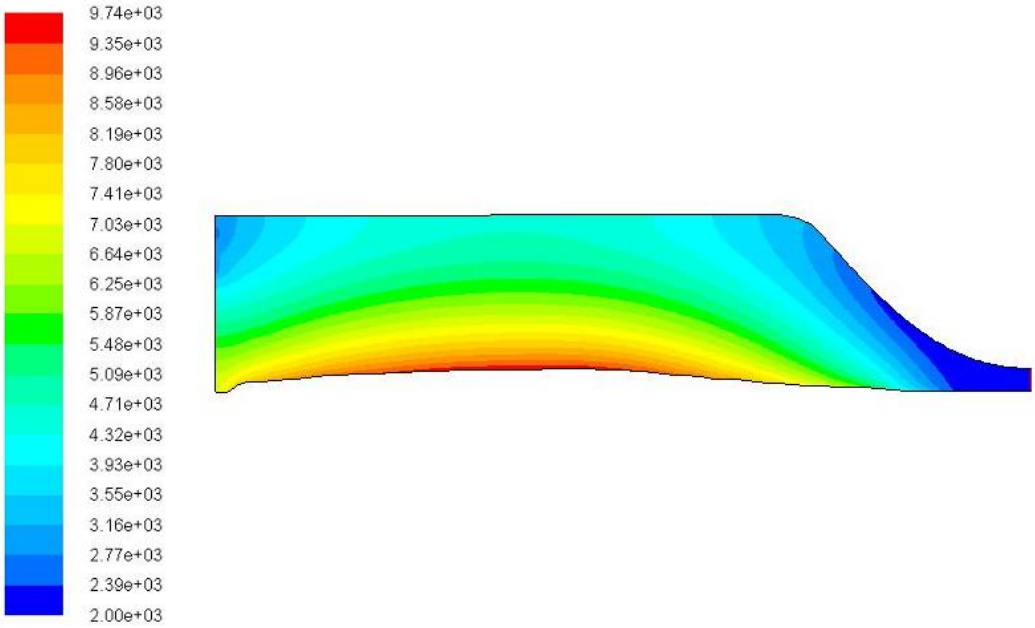

Figure 3.19: Radiation Temperature in case 2 with Helium

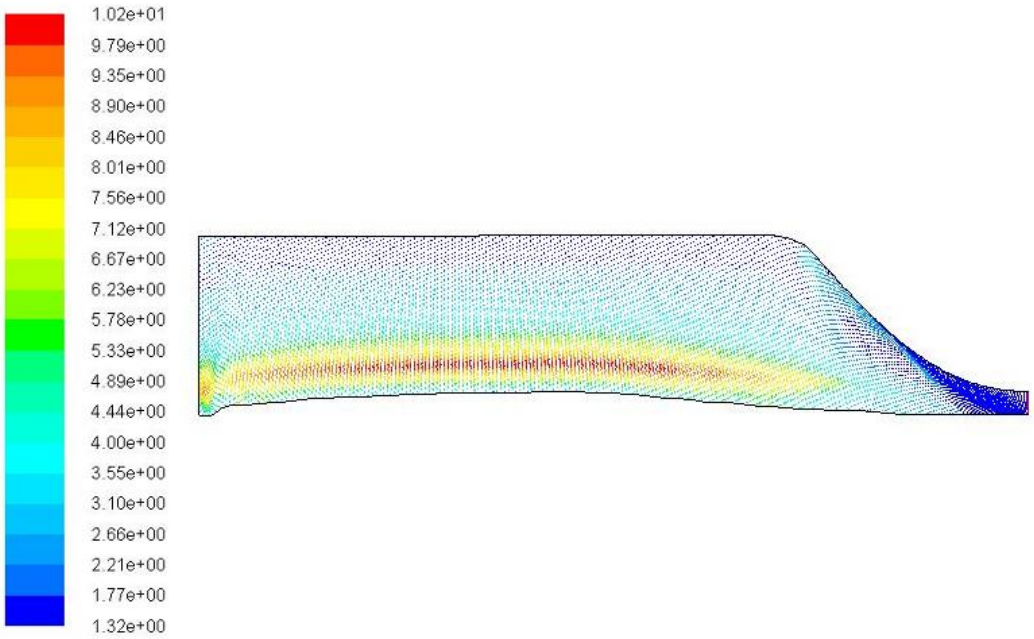

Figure 3.20: Velocity magnitude for the case 2 with Helium

The radiative heat transfer needs to be effective since there is no physical containment that differentiates the fuel flow and the propellant circulation region. The pressure difference govern the flow and the vortex is created to contain the fuel inside the chamber, the radiative heat contours are shown in the figure 3.18 the maximum temperature variation in case of helium is reaching 9760 K. It indicates that the source temperature is much higher and the heat transfer is effective. If we compare the similar operating conditions with the different working fluids in terms of effectiveness, hydrogen shows better performance since the absorption coefficient is comparatively low with the helium. The velocity variation is shown in the figure 3.20, the maximum velocity attained by the helium is in the reservoir region and it is reaching 12.0 m/s. The pressure variation in the case 2 is visible in the figure 3.21, the inlet pressure conditions of the working fluid is at 2.54 Mpa and the heat generation in the chamber is also increasing the total pressure to 7.42 Mpa.

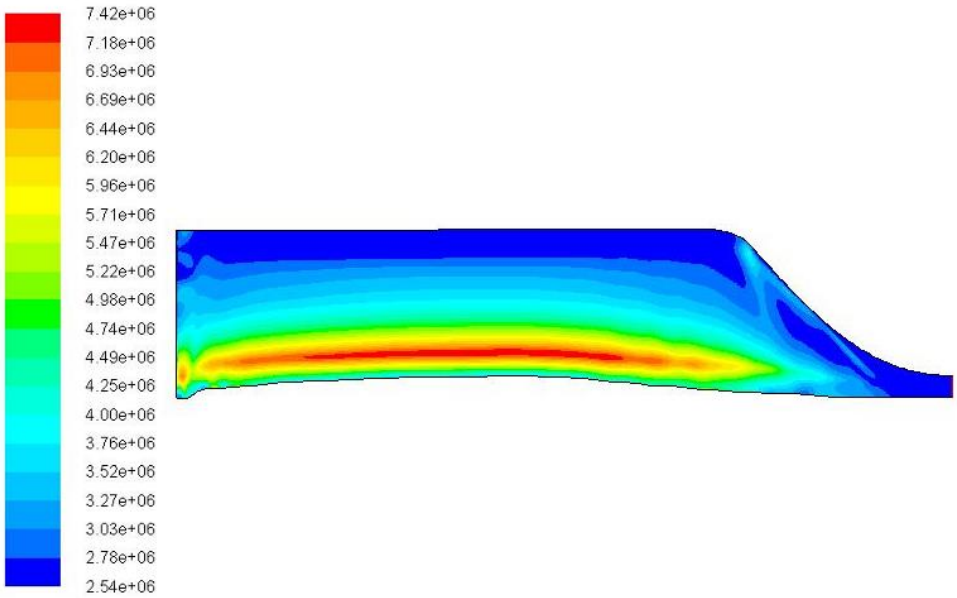

Figure 3.21: Total Pressure Variation for Case 2 with Helium

The incident radiation in the case two is comparatively less with the case 1 since the absorption coefficients and the scattering coefficients of both the working fluids are varying. Since both are gases the variation is limited, but the overall change in density in the core is affecting the radiation. The incident radiation with respect to change in position along the core is plotted in the figure 3.22, at the inlet the variation is little effective and at the source it is reaching to peak and in the throat region it is low. The maximum incident radiation at the source is reaching at 3e03 MW/m^3, which is trice from reactor heat generation rate at the interface. The solution is limited by constrains used in the solution, since the direct fission source cannot be modeled in the computational fluid dynamics approach. The incident radiation is limited at the wall boundaries due to the isothermal boundary condition and the solver limits the heat transfer.

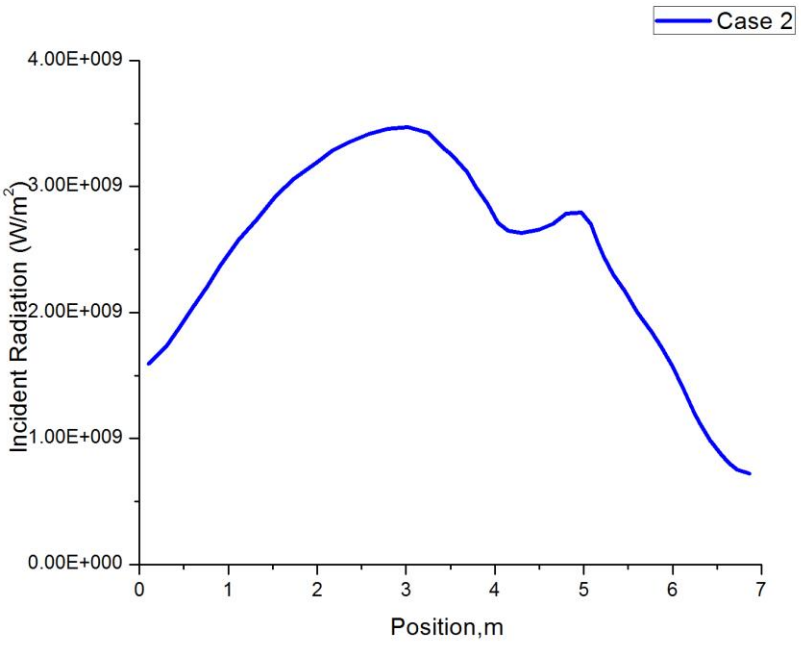

Figure 3.22: Incident Radiation in Case 2 for Helium

The thermal boundary conditions applied to replicate the physical phenomena are likely to create the heat generation rate by constant heat generation rate at the source and the constant temperature at the wall boundaries. Due which the pressure variation is also occur only at the center of the core and the wall are maintained limited variations. The total pressure variation in along the core between the case 1 and case 2 are plotted in the figure 3.22 to compare the effectiveness of the working fluid inside the core. In case 1 the pressure variation is high at the source due to the high heat transfer rate and the variation in fluid density. The pressure variations are plotted in the figure 3.23 to understand the behavior of the working fluids along the length of the core.

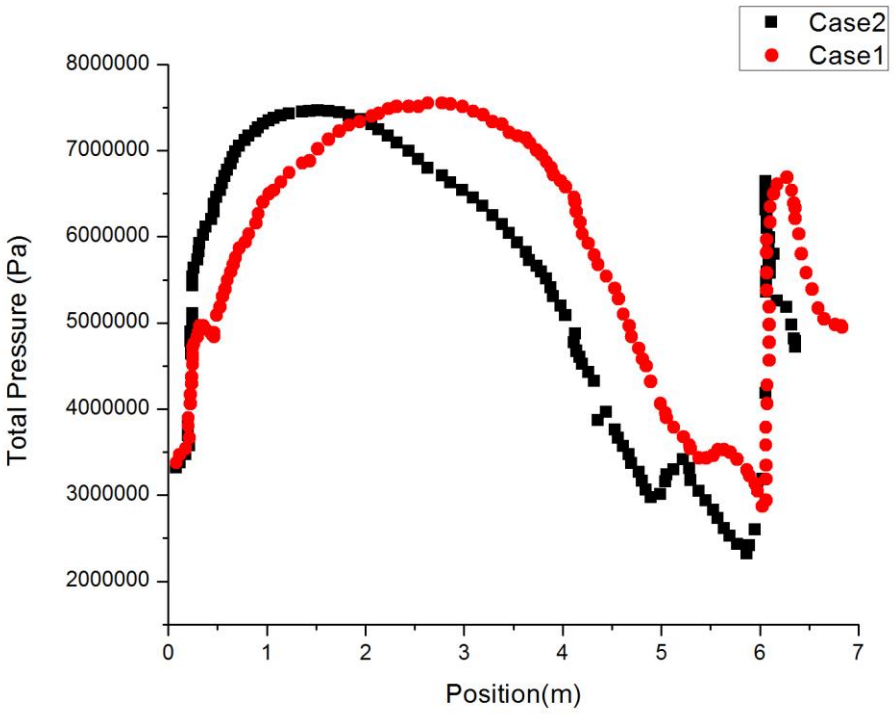

Figure 3.23: Total Pressure Variation in Case 1 and Case 2 along the Core

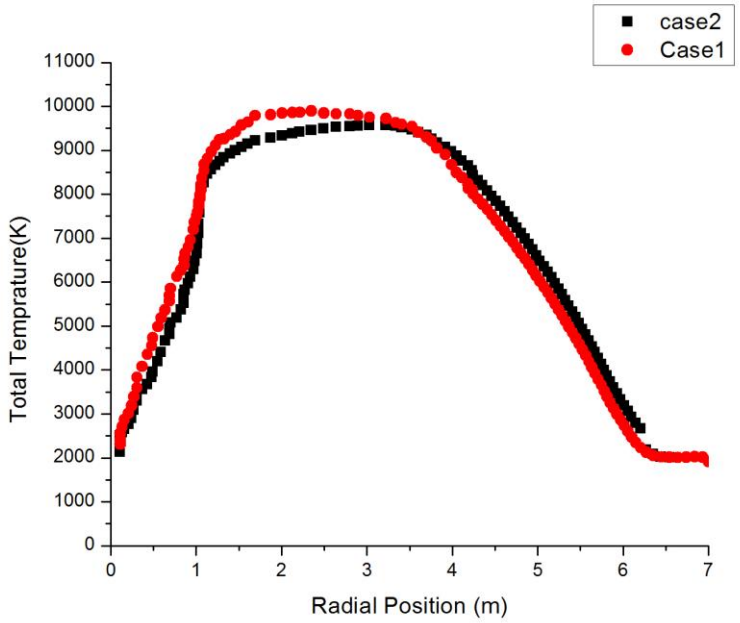

Figure 3.24: Total Temperature Variation along the Length of the Core

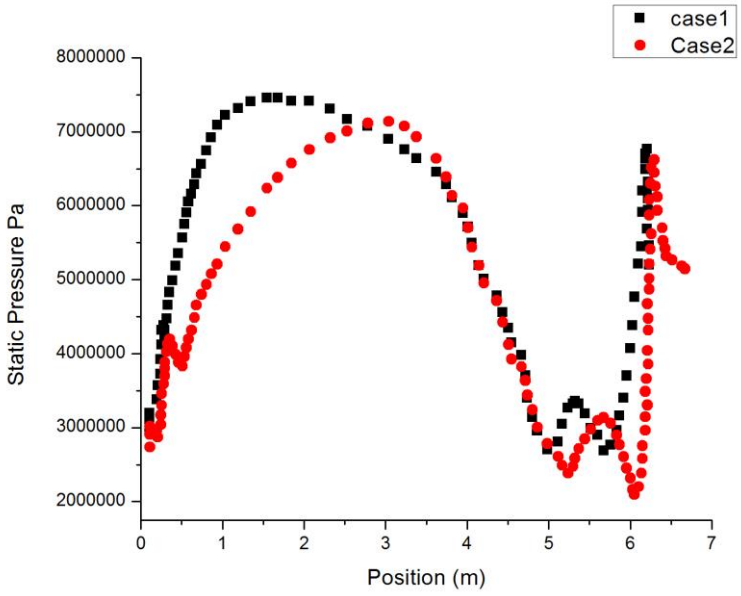

Figure 3.25: Static Pressure Variation in Case 1 and Case 2

The hydrodynamics of the fluid motion affects the behavior of the working fluid under high temperature and pressure conditions. In hydrogen the molecular weight is less and the thermal conductivity is comparatively high and which is likelier to be preferred as a rocket propellant. The total temperature variation and the static pressure variation in both the cases are shown in the figure 3.24 and the 3.25, the thermal conductivity and the viscosity are varied with respect to the temperature since the piecewise polynomial coefficents are selected from the graphs shown in the appendix D. The incident radiation is compered in the graph shown in the figure 3.26, in case of hydrogen the incident radiation is comparatively low since the convective heat fluxes are more and the remaining heat is transferred to the radiation. In case of helium the radiative heat fluxes are high so and the convective heat fluxes are comparatively low.

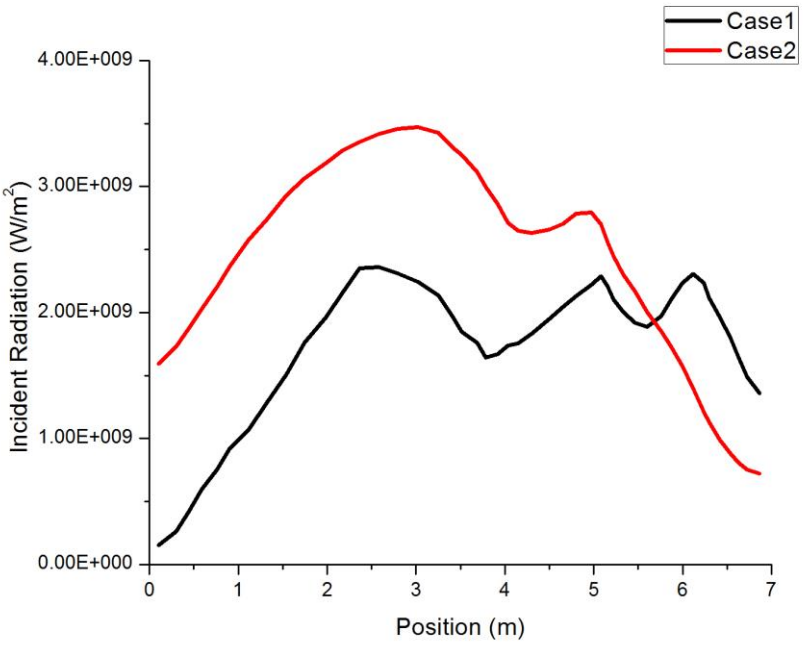

Figure 3.26: Incident Radiation for case 1 and Case 2

In case 3 the propellant selected for solving 30 % enriched GCR core with a uniform density distribution of the fuel along the core. The heat generation rate at the interface is considered as constant with 620 Mw/m^2 with an isothermal boundary condition. The temperature is limited to 1600 K at the core reflector wall to improve the buffer region fluids kinetic energy; also it supports more neutron reflection behavior of the graphite material at lower tempratures. The inlet temperature reduced to 1800 K due to the variation in pressure and the pre heating temperature limitation. The convective and radiative fluxes are considered to generate the heat and to evaluate the heat transfer between the propellant and the fuel gas. The static temperature variation is shown in the figure 3.27, the maximum temperature attained in the fission region is at 7800 K, and the maximum temperature maintained is the propellant from the source is limited to 7250 K.

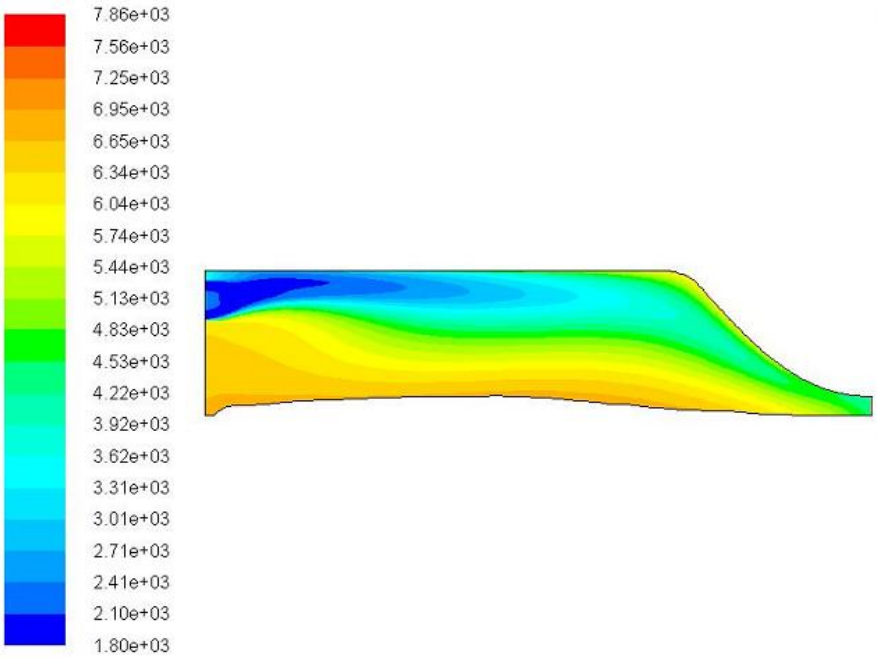

Figure 3.27: Static Temperature in Case 3with Hydrogen Propellant

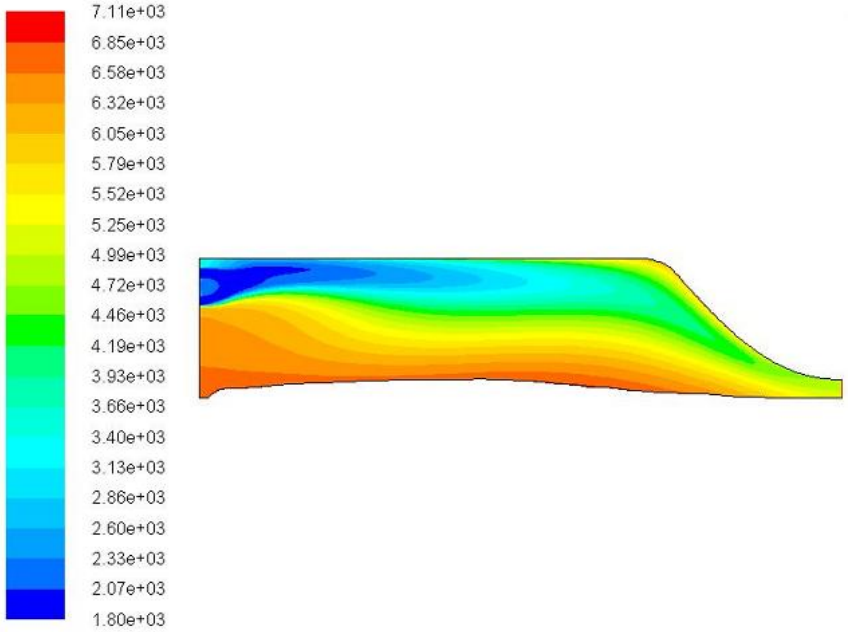

Figure 3.28: Total Temperature in Case 3with Hydrogen Propellant

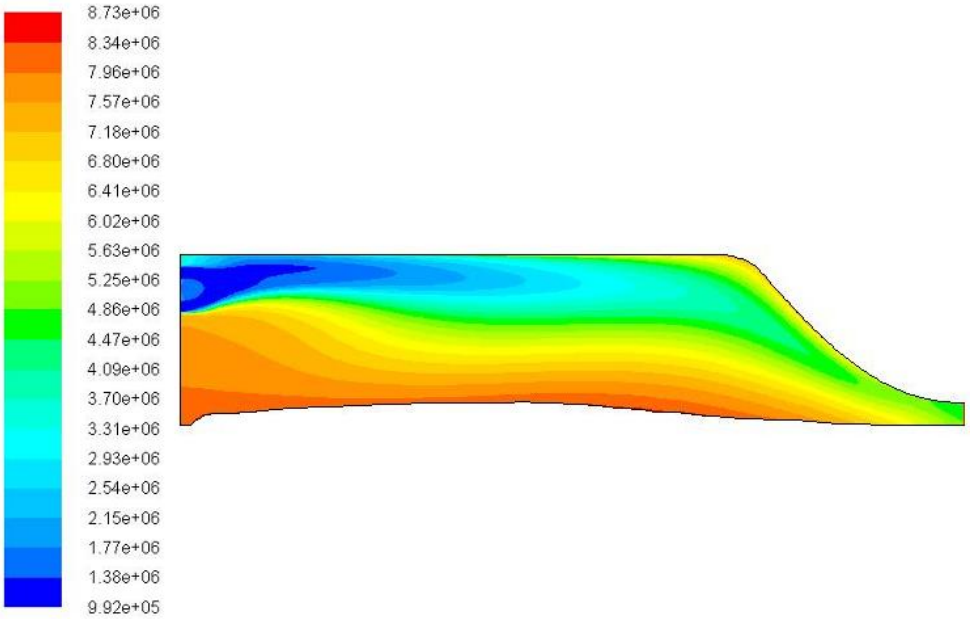

Figure 3.29: Total Enthalpy in Case 3 with Hydrogen Propellant

The total temperature variation along the stagnation points in the flow region is shown in the figure 3.28, in case 1 and 2 the maximum temperature raise is due to the higher energy content in the fission. The variation in the fuel enrichment is greatly affecting the total heat content and the generation rate. The advantage in using moderated generation rates with an affective temperature does help in maintain the GCR chamber within the limits and eventually the better thrust conditions can attain. In case 3 with the hydrogen propellant the maximum enthalpy maintained near the fuel surface is in the range of 8.73 MJ/kg. The ionization of propellant is a major problem in case of high temperature GCR core; many fuel inlet channels are added in operation at the throat region. In the current case the propellant flow is effectively maintained with in the targeted mass flow rate.

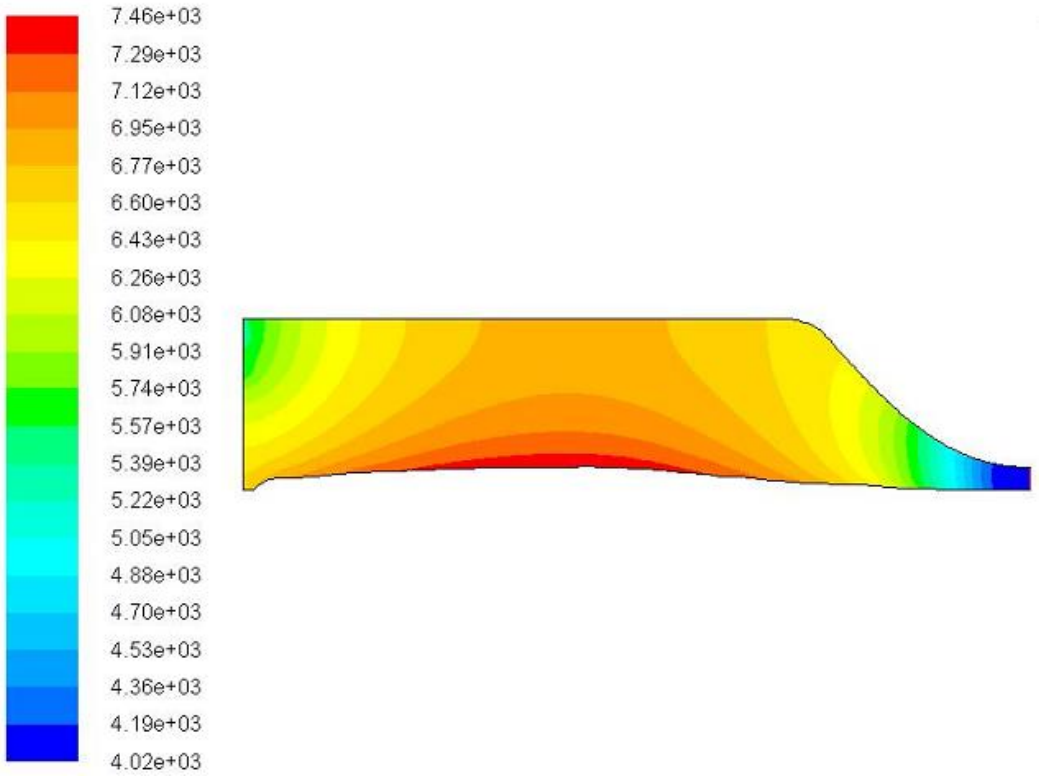

Figure 3.30: Radiation Temprature in Case 3 with Hydrogen Propellant

The heat transfer from the radiation can be compared for the current case from the figure 3.30, the maximum radiation temperature in the flow stream can be found at the source. The absorption coefficient t of the hydrogen gas is low, as a same time the scattering coefficient is high. In GCR core to get the advantage of high energy fission the heat transfer need to be affectively high through radiation so that the mixing for propellant and fuel can be minimized. The maximum temperature attained is at 7460K with an intial propellant temperature of 4020, with convective heat transfer. It indicates the radiative heat flux is higher by a fraction two compared from convective heat flux. Since the criticality of the reactor chamber is maintained at the designed value and pressure variations are limited due to the continuous generation of heat.

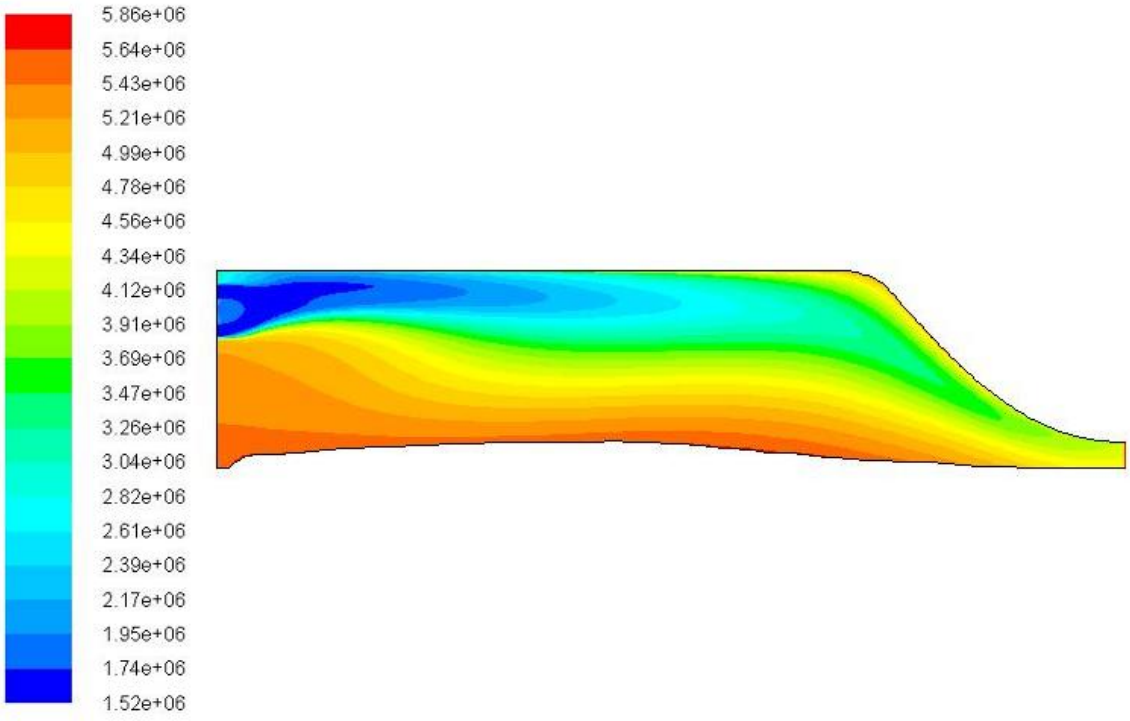

Figure 3.31: Total Energy in Case 3 with Hydrogen Propellant

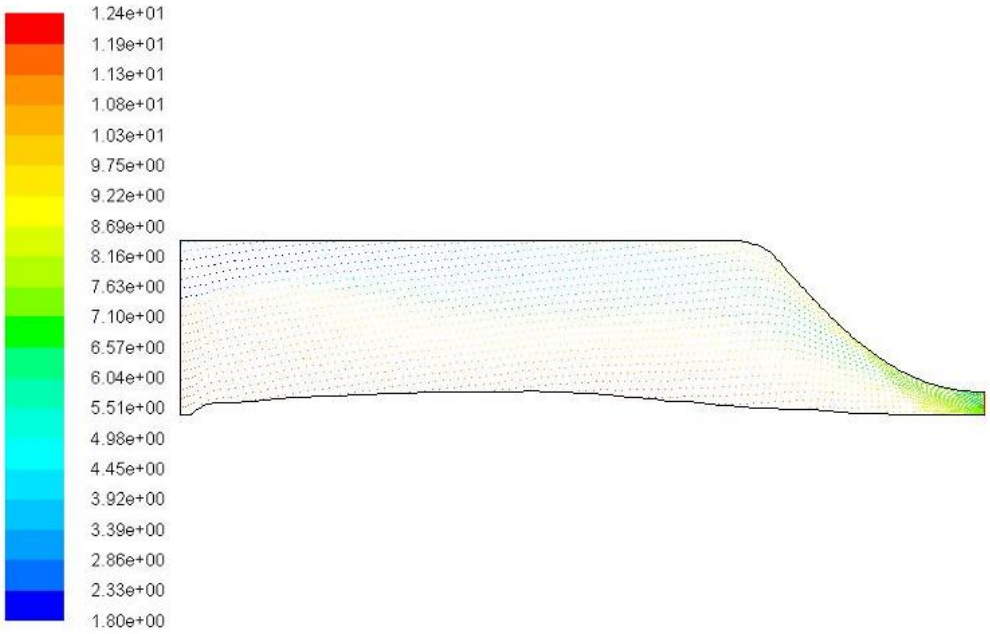

Figure 3.32: Velocity Vectors in Case 3 with Hydrogen Propellant

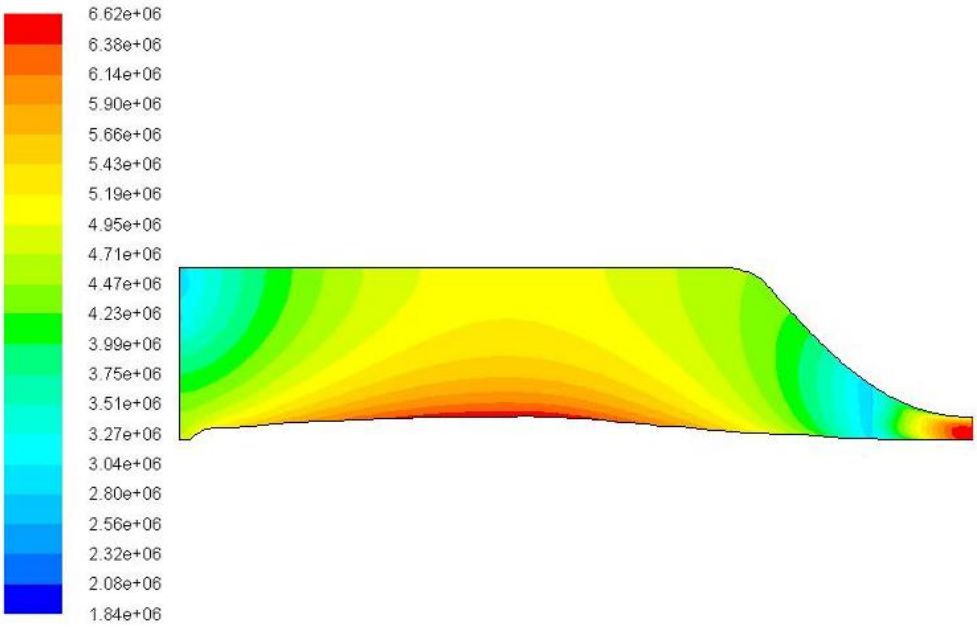

Figure 3.33: Static Pressure in Case 3 with Hydrogen Propellant

In the boundary conditions of all the case the solution is obtained at the constant mass flow rate with the addition of flow channels in the reservoir region to compensate for the ionization of the propellant. The velocity magnitude is represented in the figure 3.32 and static pressure variations are shown in the figure 3.33. The maximum velocity obtained in the 30 % enriched GCR core with a maximum temperature is at 12.4 m/s. The static pressure variations are from the input pressure of 1.84 Mpa is used and the pressure rise due to the fission and the wall flux is at 6.62 Mpa. At the higher pressure incident radiation scattering will be limited; in the current case the incident radiation is showing higher value along the core at 600Mw/m2.

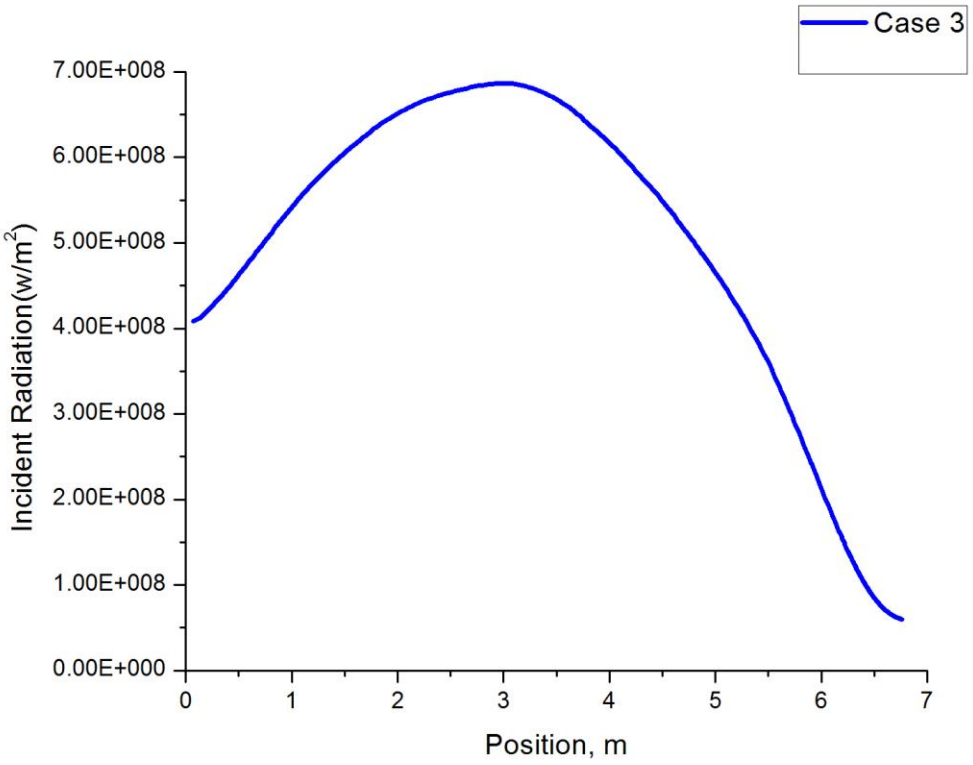

Figure 3.34: Incident Radiation in Case 3 with Hydrogen Propellant

In case 4, helium is selected for the same boundary conditions as the 30% enriched GCR core model heat generation temperature. The uniform fuel gas density is considered in the core to investigate the effectiveness of the heat transfer by the propellants. The behavioral changes that are going to be observed in the analysis is depends on the mode of heat transfer and the flux distribution along the radial length. In case 4 the heat generation rate is in the range of 620 MW/m^3, the maximum temperature reached with the calculated heat generation rate is shown in the below figure 3.35, it indicates the static temperature variation along the core. The maximum temperature at the center of the core is observed to at 7680 K with an inlet temperature of 1600 K. The isothermal temperature condition is enforced while calculating the below profile to improve neutronics in GCR core.

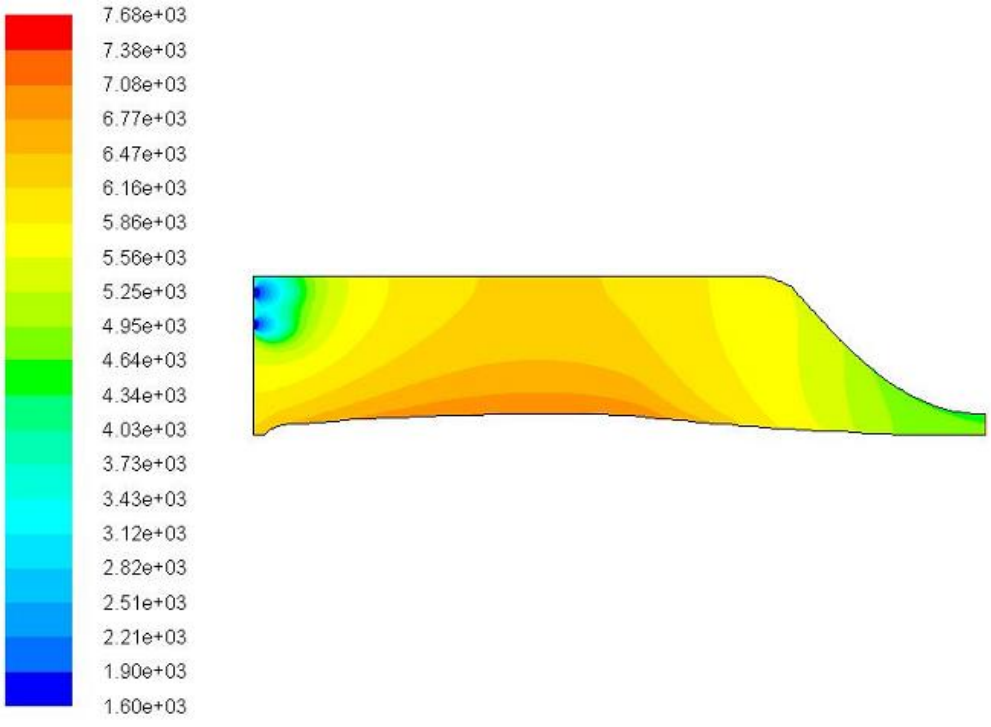

Figure 3.35: Static Temperature in Case 4 with Helium Propellant

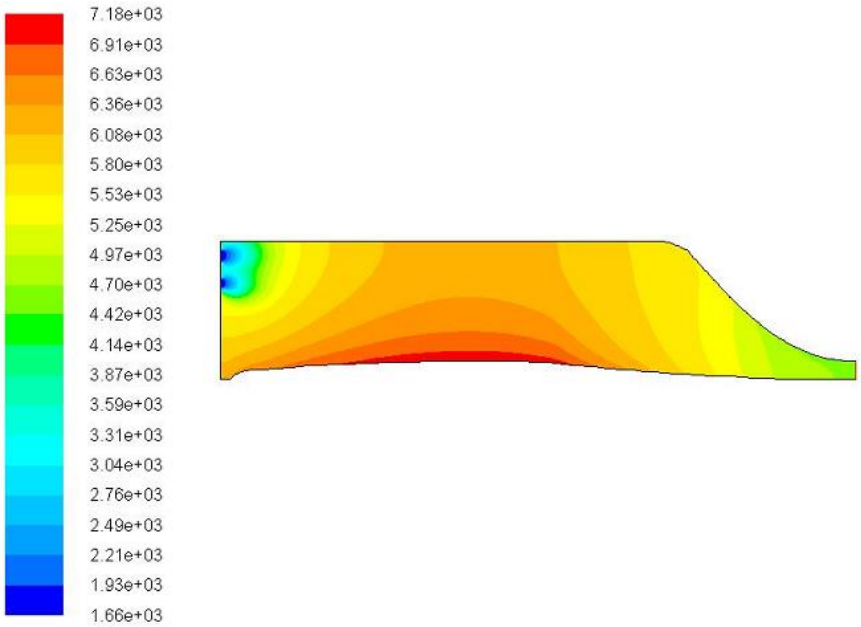

Figure 3.36: Total Temperature in Case 4 with Helium Propellant

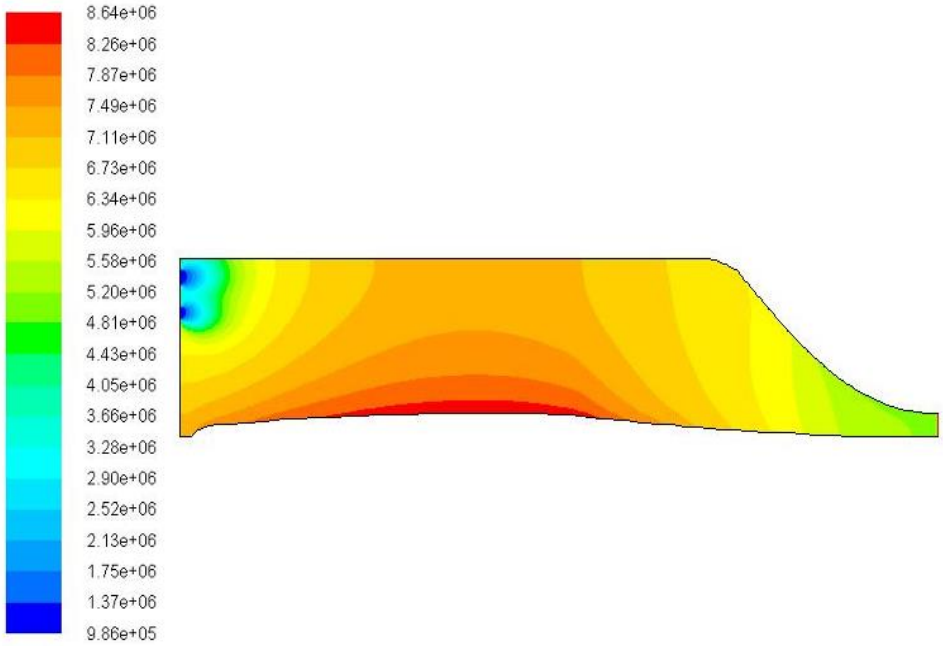

Figure 3.37: Total Enthalpy in Case 4 with Helium Propellant

In case 4 the difference is visible with the maximum temperature maintained in the core and eventually the kinetic energy generation is low. The energy levels indicate in the figure 3.39 shows the maximum energy at the interface between the fuel and the propellant with 5.67 MJ/kg, which is maintained to keep self-sustained fission with neutron criticality. In order to improve the specific impulse of the rocket system which operates with 30 % nuclear fuel enrichment the exhaust velocity need to be high. In the current case the maximum energy that is available at 5.04 MJ/kg can be directly covered in the nozzle. In the current case the maximum heat transfer is through radiation along the core, the figure 3.38 indicates the maximum radiation temperature between the sources to the propellant with 7150 K of interface temperature.

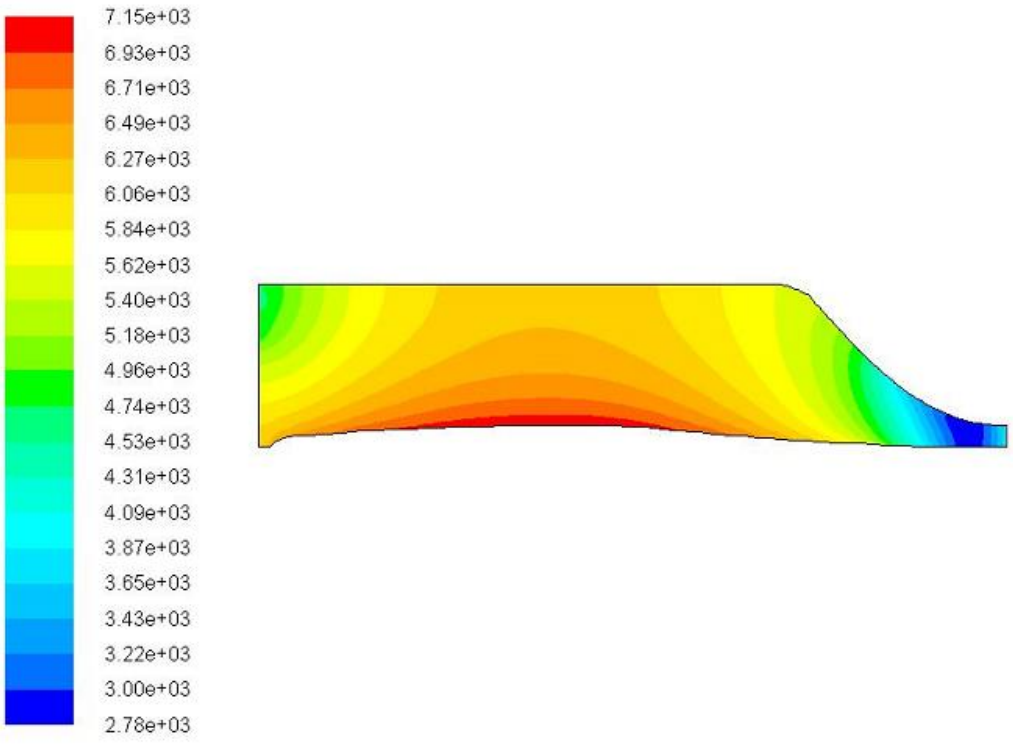

Figure 3.38: Radiation Temprature in Case 4 with Helium Propellant

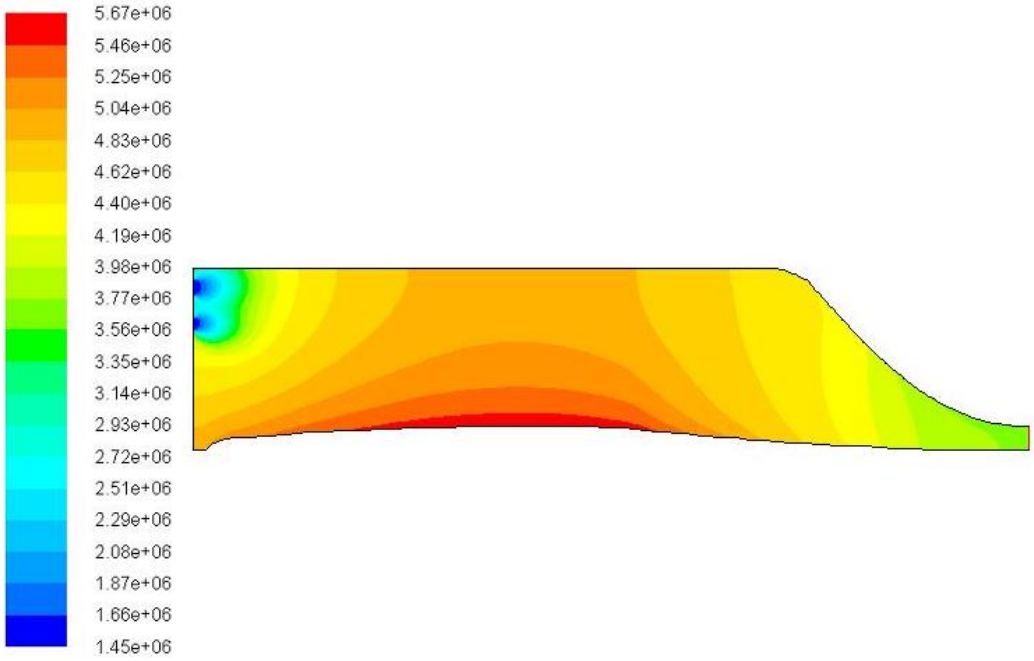

Figure 3.39: Total Energy in Case 4 with Helium Propellant in J/kg

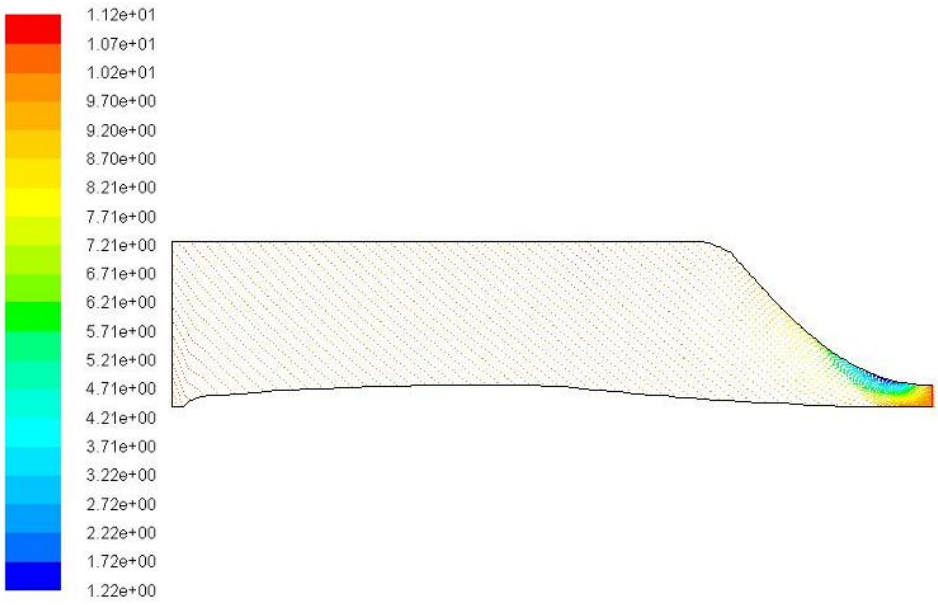

Figure 3.40: Velocity Magnitude in Vector form for Case 4

In order to maintain unique fuel composition the pressure need to be maintained in the reactor core; in case of helium absorption of heat at higher tempratures are more affective. In the middle section the propellant absorbs the heat to improve enthalpy of a buffer region fluid, where at the propellant surrounded in the wall region is adopted as a coolant. The wall cooling mechanism is more affective in the current case, since helium itself is an effective coolant in gas cooled nuclear reactors. The thermal wall condition applied in the current case to limit the reflector temperature is at 1600 K, so the buffer region fluid gets benefited more to improve the specific impulse. The mass flow rate is also varied along the core due to the variation in the core enrichment, in case 1 and 2 there is no targeted mass flow rate.

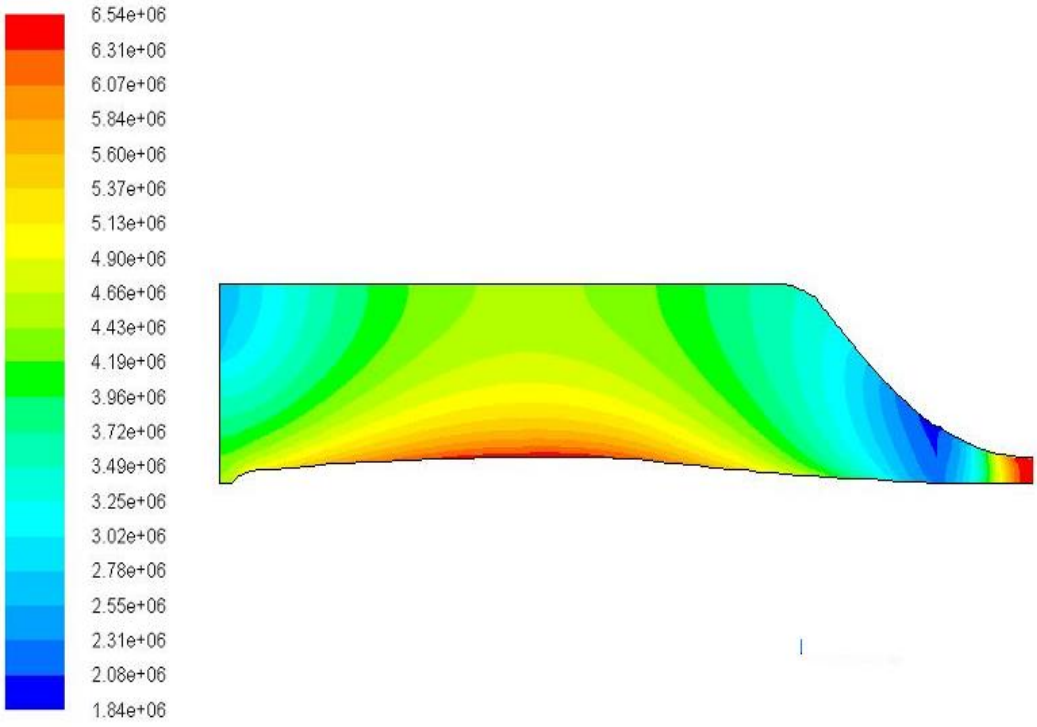

Figure 3.41: Static Pressure in Case 4 with Helium Propellant

In order to contain the nuclear fuel with in the reactor chamber, without mixing with the propellant a mechanism which is governed by the pressure difference is adopted. The static pressure variation shown in the figure indicates the maximum variation of the pressure in the current case with the 1.84 Mpa of inlet to the pressure rise of 6.54 Mpa. The idea is to improve the radiation heat transfer, so that the fuel is contained without mixing. The result obtained with the current case solution for incident radiation is shown in the figure 3.42, and which indicates the maximum incident radiation is at 5.8 MW/m^2 along the length of the core. This indicates the generation of energy from the GCR operates with the above mentioned values can capable of production 1200 Mwth energy to effective thrust with a moderated specific impulse.

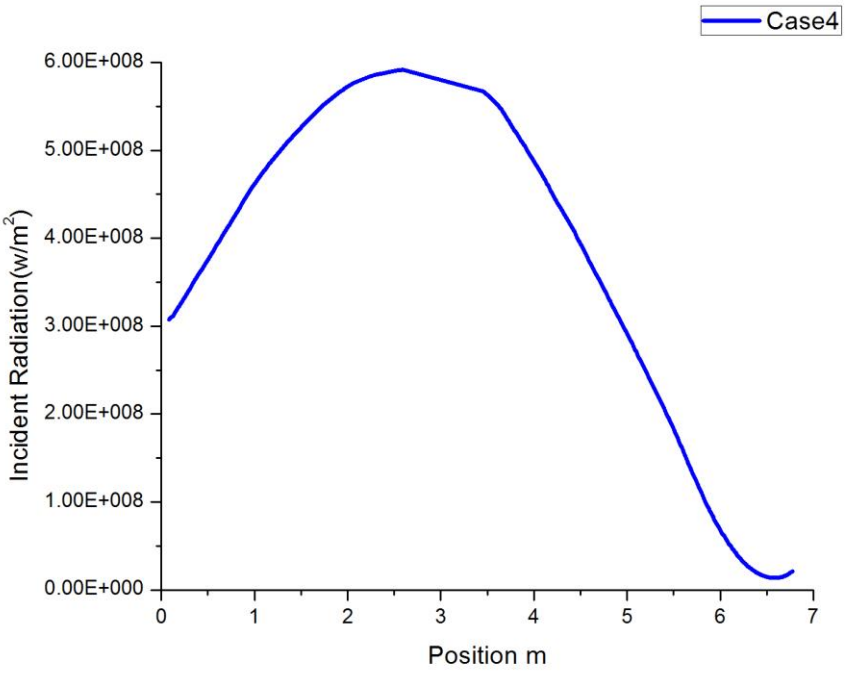

Figure 3.42: Incident Radiation in Case 4 with Helium Propellant

In case 3 and case 4 the analysis is conducted to understand the behavior of two different propellants which are more suitable to use in gas core nuclear rockets. The inlet pressures are similar in both the cases and the variation starts from the source position as shown in the figure 3.43. In case 3 the value reaches slightly high compared with the helium propellant case. In variation is not so high in terms of throat functionality and still the ratio of 1:36 of Mach can be maintained but only difference visible is due to the rise in temperature in the fluid and the reverse flow in the reservoir region. In case of hydrogen the heat addition at the constant pressure is visible, so that is more likely to be as an isobaric process and the variation is happening at reservoir due to change in cross section. This pressure helps to maintain the optical thickness of the uranium gaseous fuels in the core.

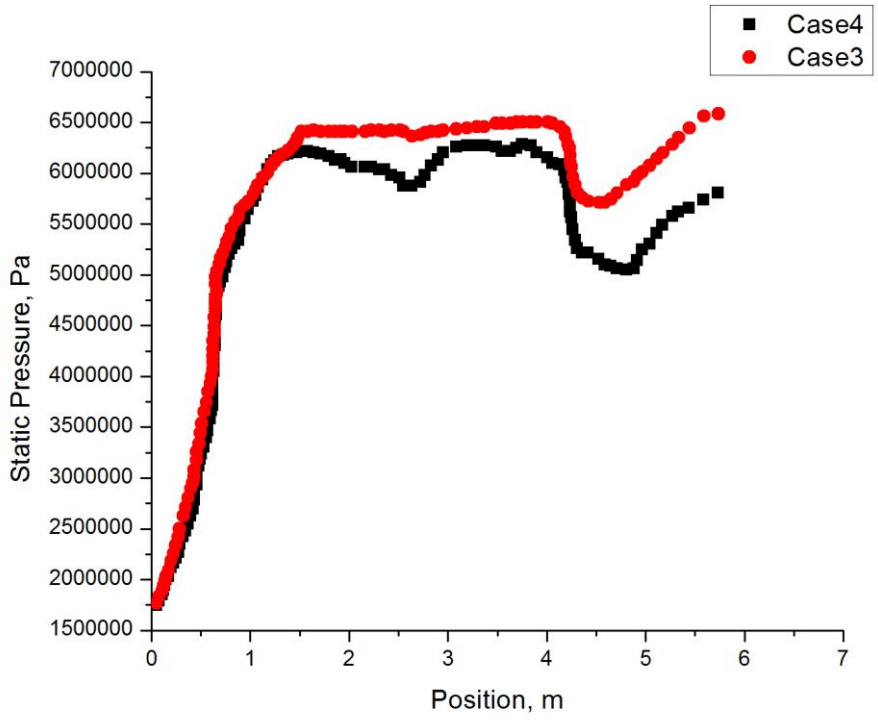

Figure 3.43: Static Pressure in case 3 and Case 4

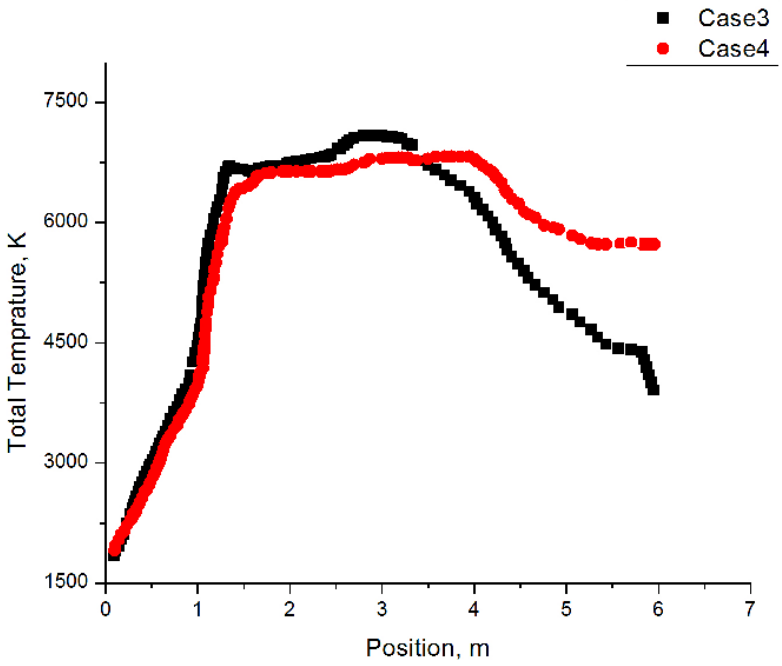

Figure 3.44: Total Temperature in Case 3 and Case 4

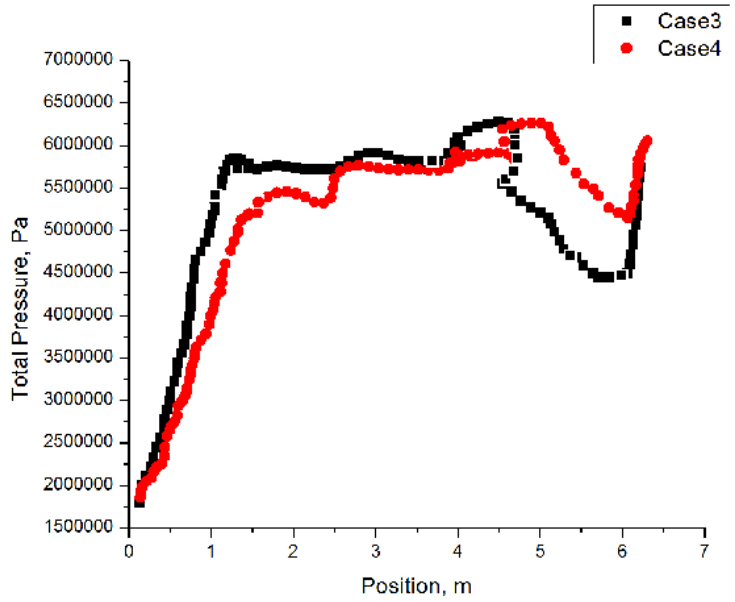

Figure 3.45: Total Pressure in Case 3 and Case 4

In case 3 and 4 the total temperature variation is indicating the difference in source temperature and the propellant at the reservoir region. The difference in both the cases is very limited since the generation rate is reduced by a fraction of 0.5 and that clearly shows the difference in incident radiation also. In case 3 the maximum incident radiation at the source is reaching to 6.8MW/m^2 and whereas in case of helium, since the convective heat flux is dominant the incident radiation is limited to 5.67 Mw/m^2. The total pressure variation trends show the maximum pressure rise in both the case at a value of 6.25 Mpa is attained in GCR core. The problem in maintain the higher radiative heat fluxes in GCR core is related to the reflector temperature limitation due to scattering of radiation

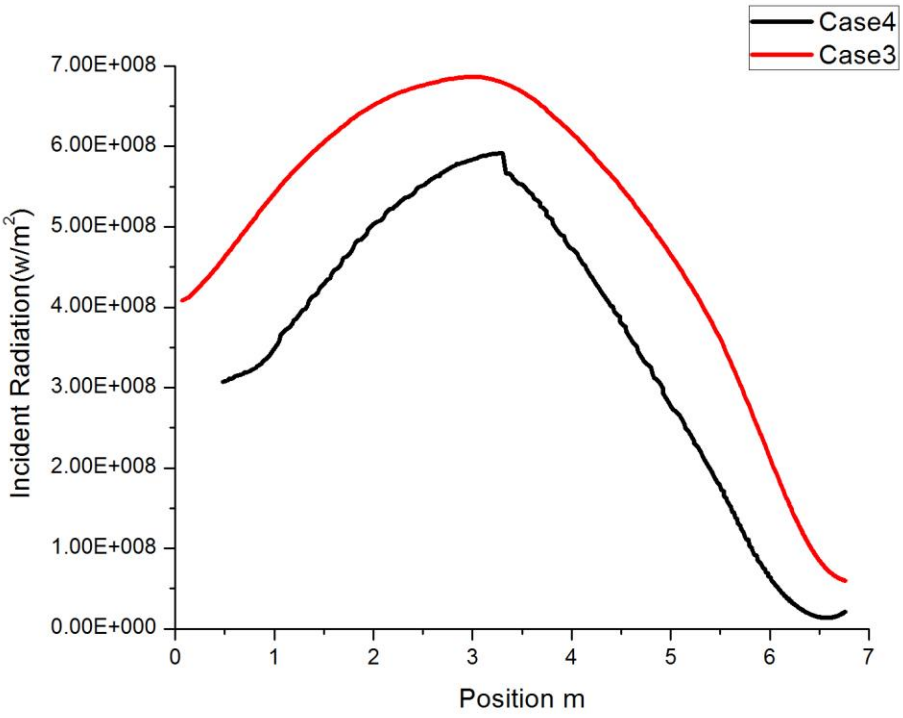

Figure 3.46: Incident Radiation Case 3 and Case 4

In case 5, hydrogen is selected as a propellant for the 5 % enriched GCR core, to investigate the propellant behavior. The constant heat generation rate considered for the analysis is at 280 MW/m^3, the material properties are based on piecewise polynomial and the scattering coefficents and absorption coefficents are considered for the higher temperature hydrogen from the experimental data at higher tempratures above 3500, the plots are added in the appendix D.The static temperature variations in the case five are shown in the figure below, which is changing from 1600 K to 5960 K. In the current case the inlet temperature of the hydrogen is at 1600 K with a specific mass flow rate of 3 kg/s. The variation in the temperature at the core is reaching around 4400 K and the maximum tempratures shown in the figure is in the fuel gas.

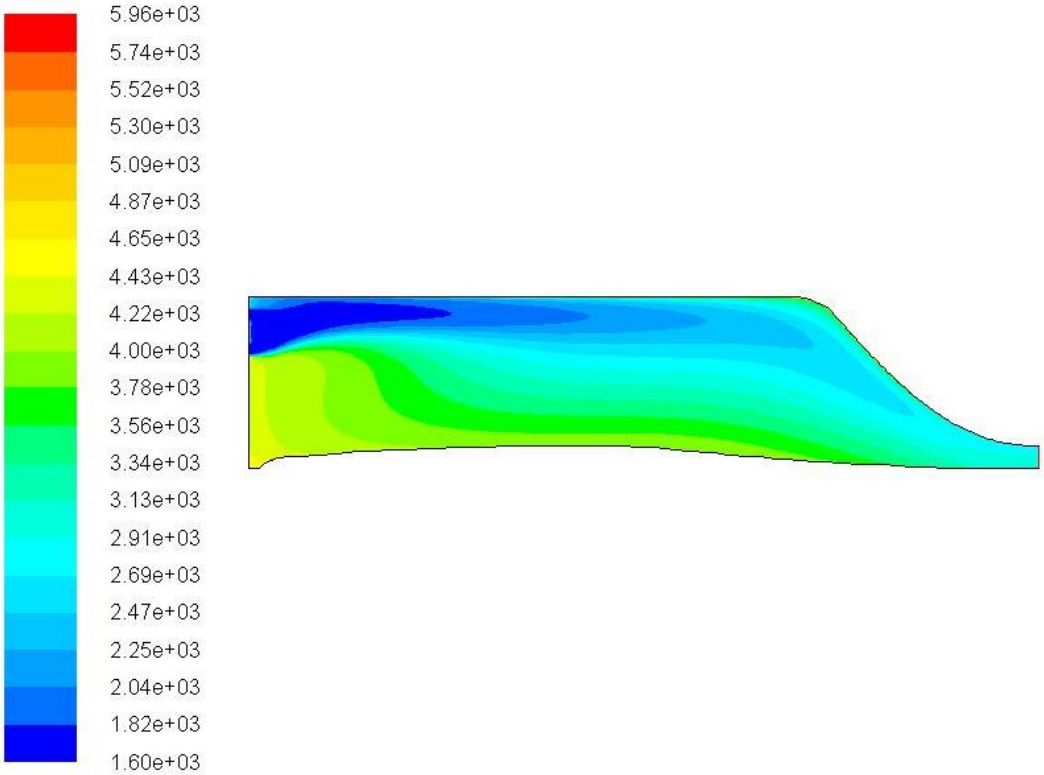

Figure 3.47: Static Temperature Variation in Case 5 with Hydrogen

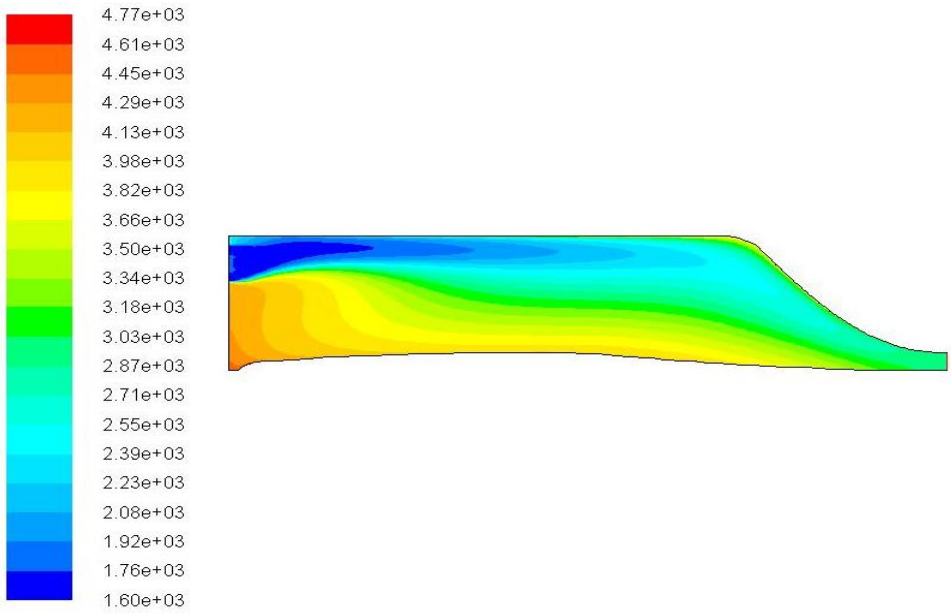

Figure 3.48: Total Temperature Variation in Case 5 with Hydrogen Propellant

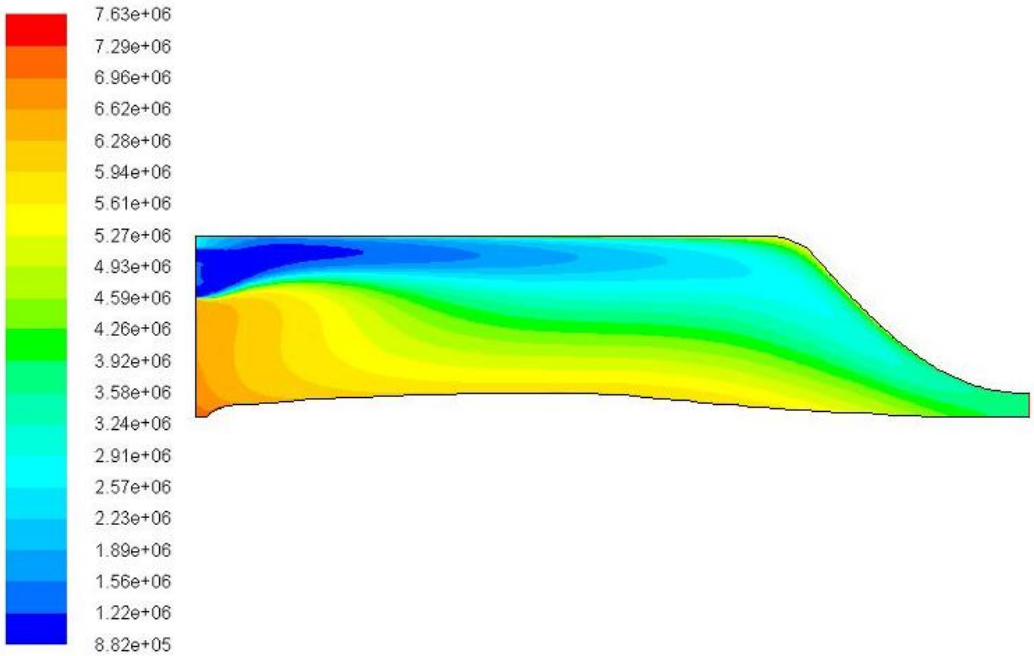

Figure 3.49: Total Enthalpy in Case 5 with Hydrogen Propellant

The total Temprature variation shown in the figure 3.48 indicates the available Temprature for the buffer region and the variation is uniform along the core with the maximum temperature of 4700 K. Since the propellant starts expending after the throat region the maximum pressure and temperature available is converted into the kinetic energy as the expense of loss of pressure in the supersonic nozzle used in the nuclear rocket. The total energy variation indicates the difference in source energy levels to the propellant energy in the buffer region. In order to analyze the thermodynamic performance of the gas core fission reactors, the total enthalpy change and the energy variation described the efficiency of the conversion system along with the thermodynamic cycle.

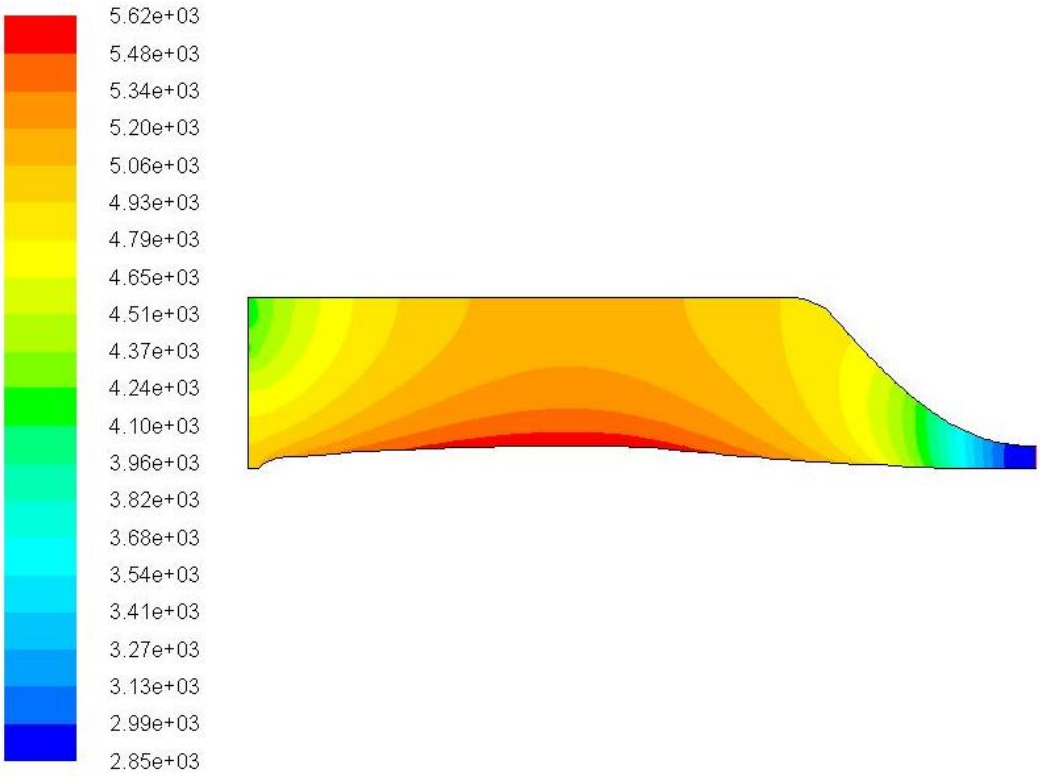

Figure 3.50: Radiation Temprature in Case 5 with Hydrogen Propellant

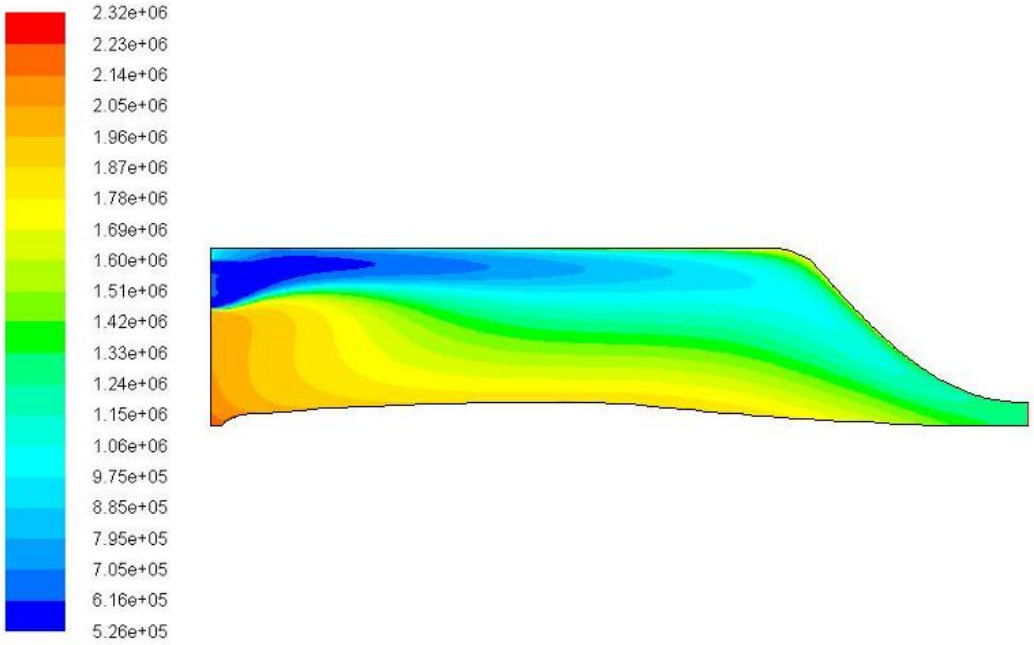

Figure 3.51: Total Energy Variation in Case 5 with Hydrogen Propellant

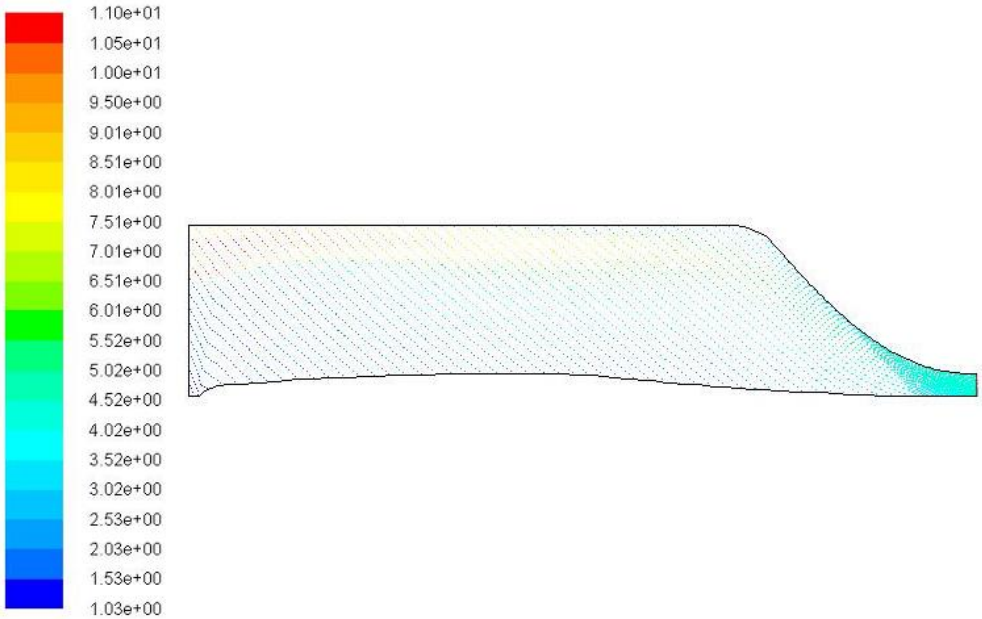

Figure 3.52: Velocity Magnitude Vector Plot for Case 5 with Hydrogen

The radiation temperature shown in the figure 3.50 indicates the maximum temperature attained by the radiation in the GCR core at 5060 K. The resection exposed to the incident radiation is direct and the counters are showing the maximum temperature at the wall in the radial direction also. Which need to be absorbed by the propellant, in case of obtaining the constant heat generation rate the free energy function is considered from the data, from the desired values of the composition mentioned in the table 4.2 the heat of formation is calculated. The operating pressure is obtained from the standard free energy formation from the fission in the range of 0.1 Mpa to 2.5 Mpa. Based on the energy release and the heat addition to the propellant operation pressure can be raised. The equilibrium compositions mentioned in the GCR analysis is with the U-C-F percentage variation and the attainable fission energies with the formed atomic ratios. The mole fraction of the condensed species is referred as a pure compound.

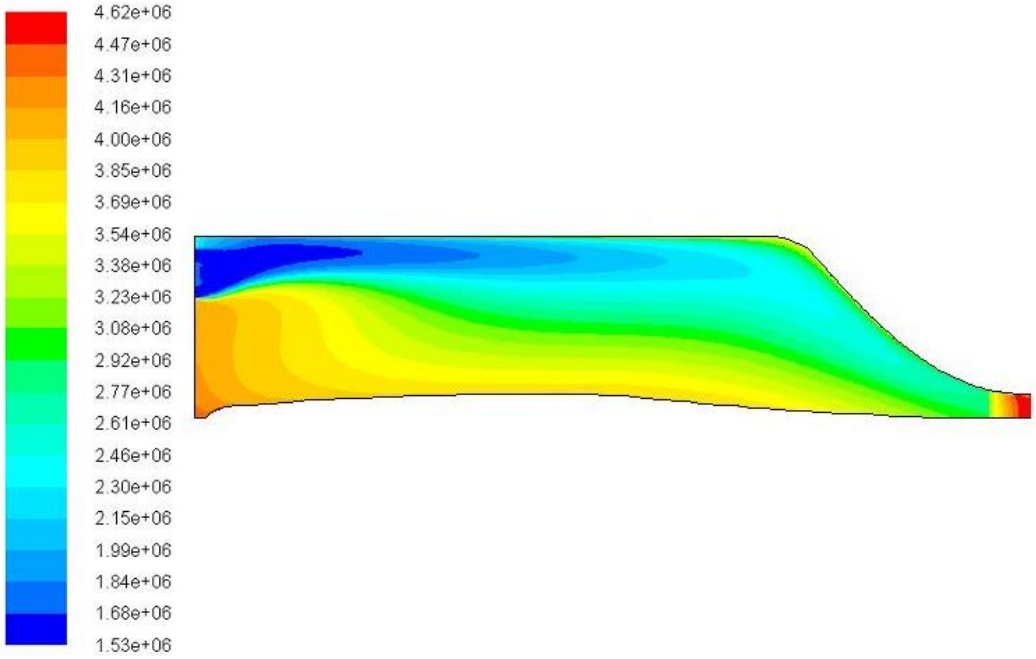

Figure 3.53: Static Pressure Variation in Case 5 with Hydrogen Propellant

In case 5 the operating pressure obtained is in the range of 1.53 Mpa to 4.62 Mpa and the maximum pressure is obtained at the throat section of the GCR chamber. The variation in the radiative and the convective heat fluxes changes the behavior at the exit of the reactor. Whereas the radiative heat fluxes increases the wall temperature at the center of the core, due to less absorption coefficents of the hydrogen used in the reactor chamber. The incident radiation is shown in the figure below which indicates the uniform distribution of the temperature compared to the other cases in the current analysis. This is due to the reduction the source temperature due to the less enriched GCR core.

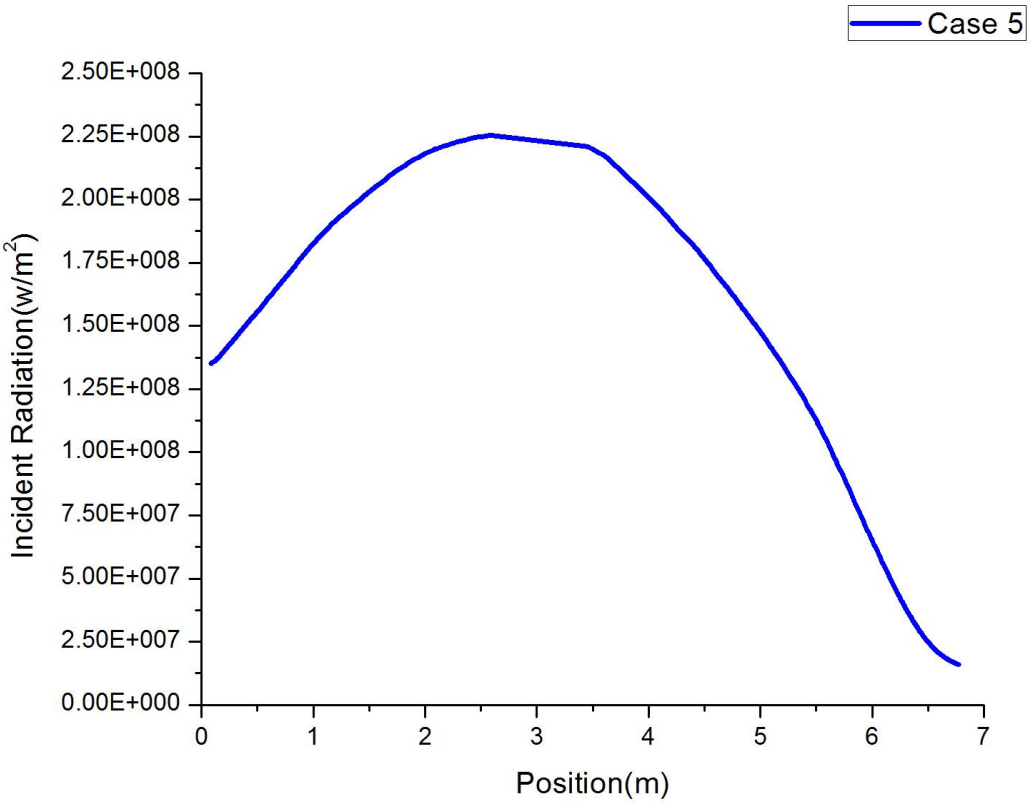

Figure 3.54: Incident Radiation in Case 5 with Hydrogen Propellant

In case 6 Helium is considered as a propellant and the heat generation rate is considered for the 5 % enriched gaseous fuel source and the same heat generate used in the case five with 280 Mw/m^3. The behavior of the propellant is examined under the similar operating conditions for both the cases. In case of hydrogen the thermal conductivity is high and the rate at which heat is transferred through convection is creating higher Temprature in the flow stream. In the current case the static Temprature and total Temprature variations are shown in the figures below. In case of helium as a working fluid the total temperature variation is visible from the inlet temperature to the maximum value of 4650 K at the source. Whereas the stagnation temperature is variation is high and which is touching 4900 K due to the back flow temperature from the pressure outlet.

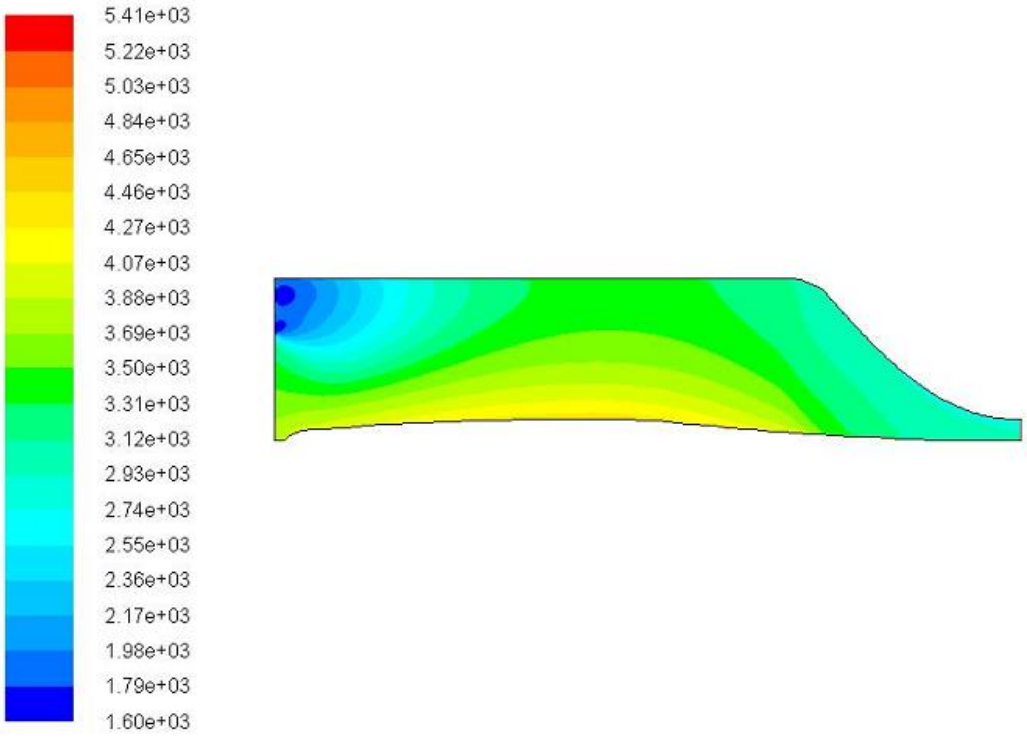

Figure 3.55: Static Temperature in Case 6 Helium as a Working Fluid

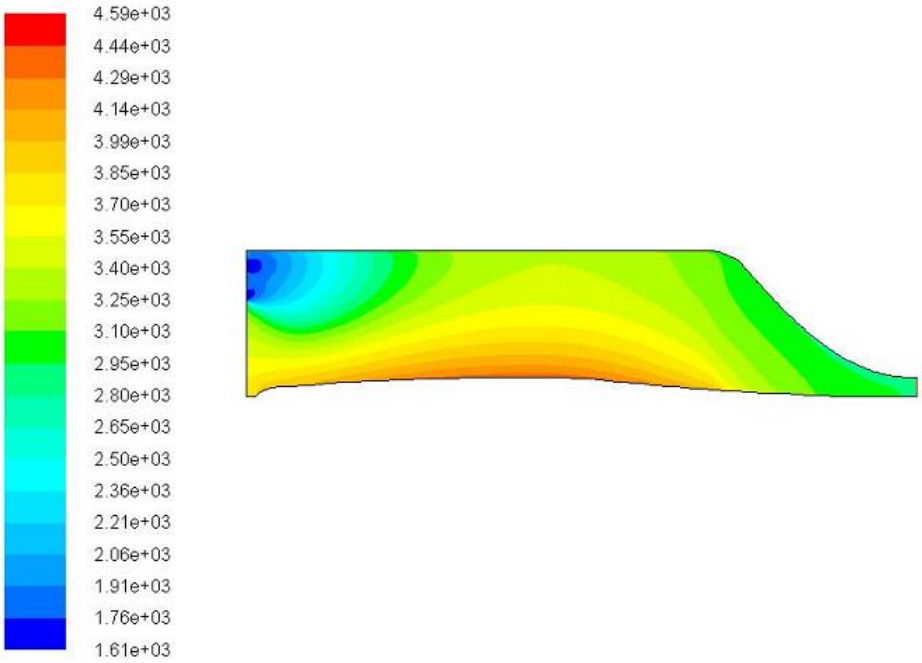

Figure 3.56: Total Temperature in Case 6 with Helium as a Working Fluid

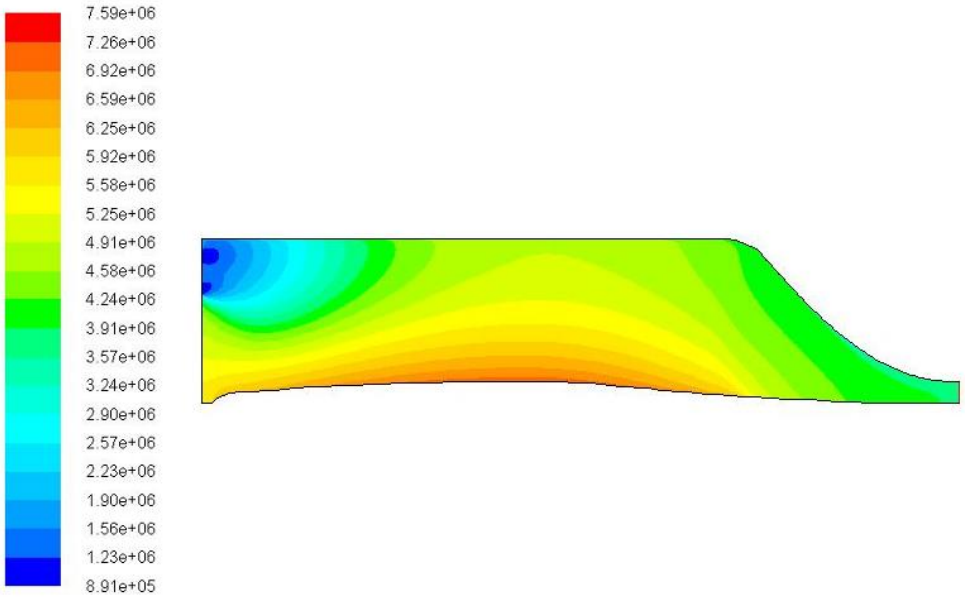

Figure 3.57: Enthalpy Variation in Case 6 with Helium Working Fluid in J/kg

The total enthalpy variation is presented in the figure, the maximum rise in enthalpy is occurring at the source with a 7.50MJ/kg. The variation in the enthalpy shows the uniform distribution of atomic density along the core, so that the pre fission conditions are met. A calculation of the actual atomic ratios at every location as per variation in the fuel gas density is not possible with the current solver. Since the resulting fuel gas mixtures with change in atomic density affects fission rate, so that total heat generation varies along the length of the core. Due to the limitations with the computational fluid dynamics solvers the uncoupled analysis need to be done as per the fission energy to heat levees inside the core and the constant generation rate need to be considered. This method of solving the problem needs a coupled solver which can predict the atomic variations as per the fuel gas mixture changes in the length of the core. This is beyond the scope of this particular research.

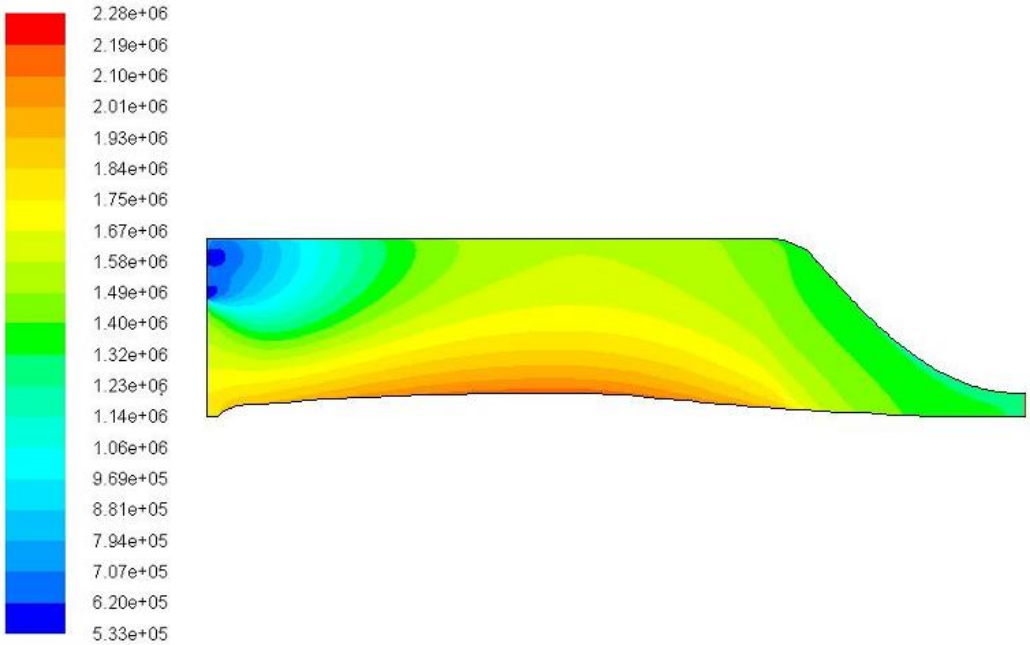

Figure 3.58: Total Energy Variation in Case 6 with Helium as a Working Fluid

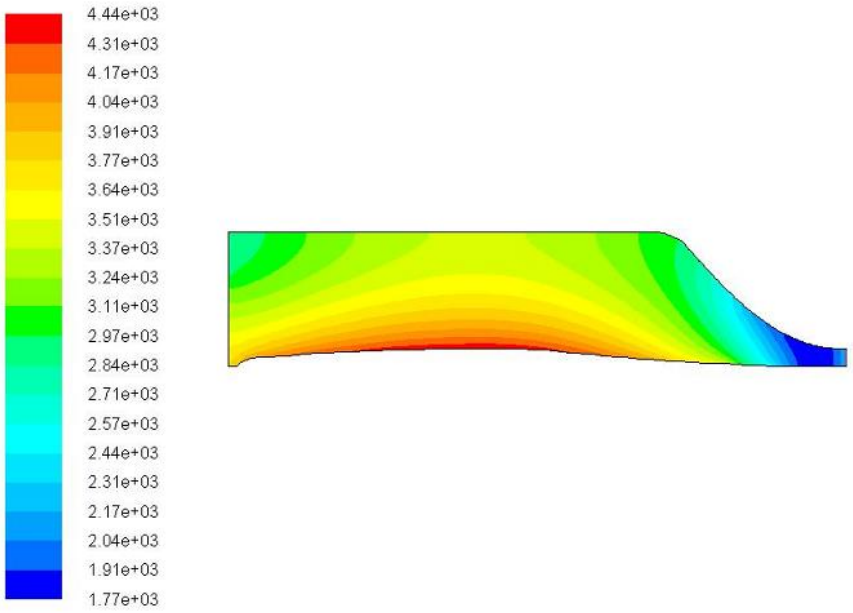

Figure 3.59: Radiative Temperature in Case 6 with Helium as a Working Fluid

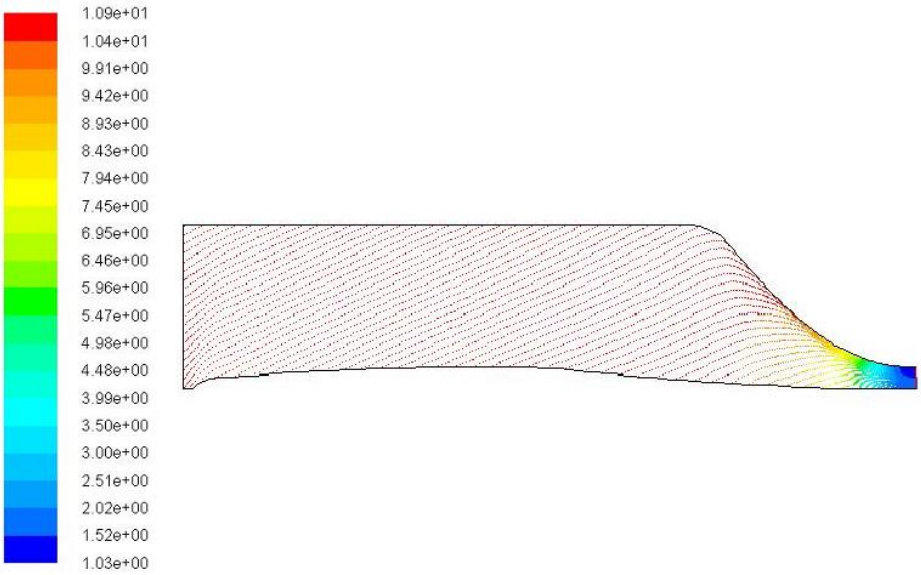

Figure 3.60: Vector Plot of Velocity Magnitude in Case 6 with Helium

The radiation temperature variation is shown in the figure, the maximum temperature is at the source and it is reaching 4400k since the inlet temperature of the propellant is comparatively low. In case six the inlet temperature maintained is at 1600 K, due to the limitation of the reflector wall temperature at 1200 K. The thermal boundary condition applies at the reflector wall is limited to 1600K as an iso thermal wall temperature condition. The velocity of the propellant at the reservoir region can be obtained from the figure 3.60, in the current case inlet mass flow rate is given at 3m/s and the targeted mass flow also calculate din the solution. In case gas core nuclear reactors which are used in propulsion applications the usage of propellant and the fuel gas should be optimum for given conditions. In case of hydrogen the molecular weight of the propellant is low so that more volume can be carried in the mission along with the pay load. In case of helium the limited propellant need to be used to obtain long distance travel.

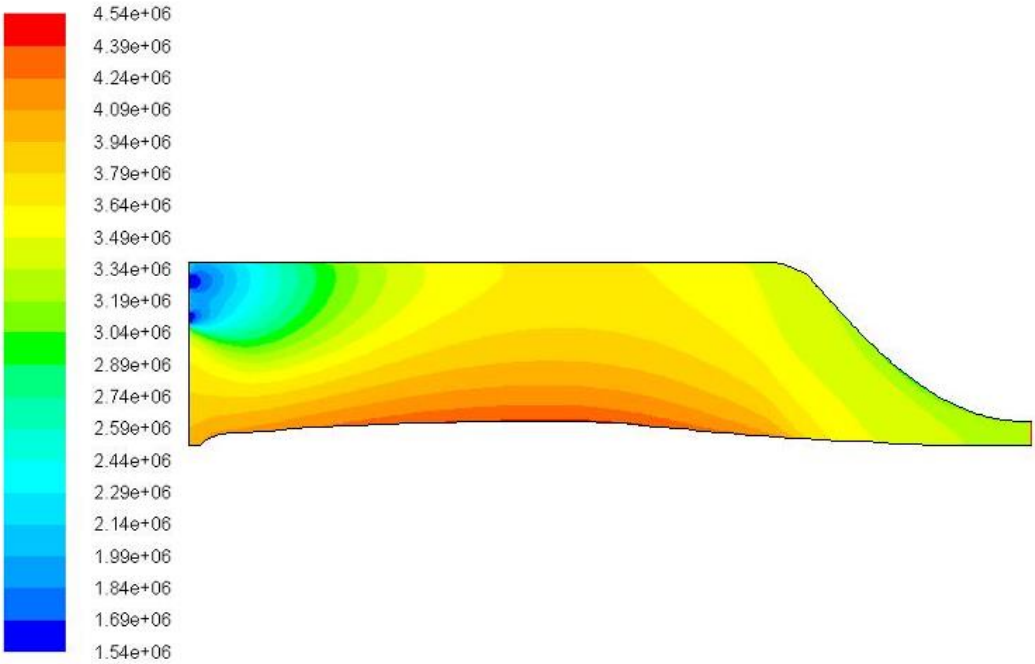

Figure 3.61: Static Pressure Variation in Case 6 with Helium as Working Fluid

The static pressure variation in the current case is shown in the current figure 3.61, in case of helium propellant with 280 Mw/m^3 heat generation rate is used. The static pressure variation is in the range of 1.54 Mpa to 4.54 Mpa, the maximum pressure is attained at the source wall and the region distributed with the convective heat flux. The buffer region is maintained in the pressure range of 3.94 Mpa and the throat is having higher pressure. The incident radiation profile is shown along the length of the core at the fuel interface in the figure 3.62. The maximum incident radiation in the case of helium is at 8.5 Mw/m^2, in case of hydrogen the variation is uniform along the core. The variation is peak in case of helium due to less scattering coefficents in the flow field. The incident radiation is less at the reservoir and the throat region.

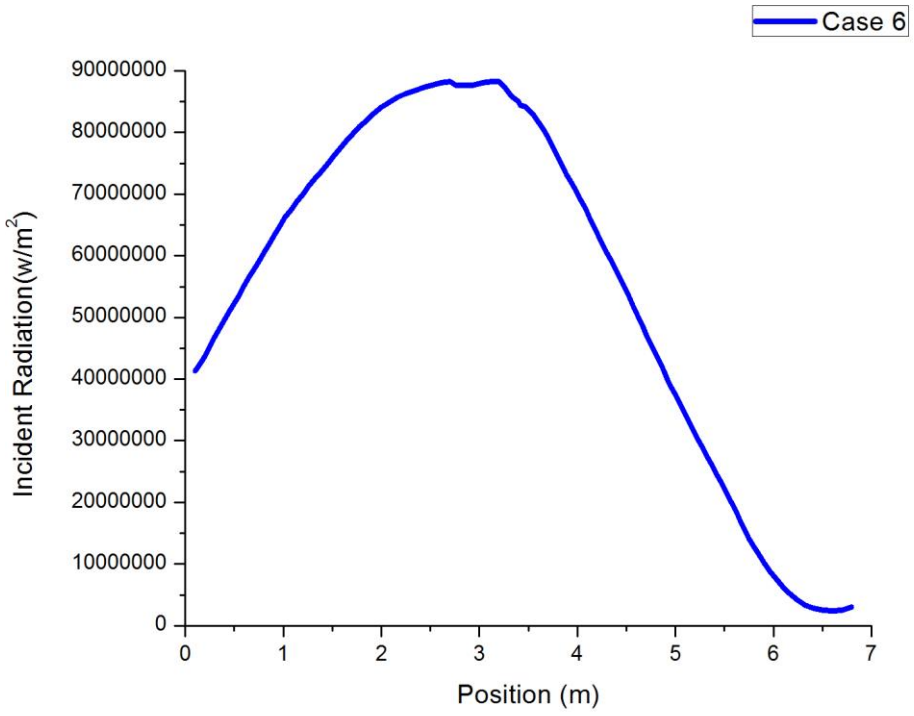

Figure 3.62: Incident Radiation along Core in case 6 with Helium

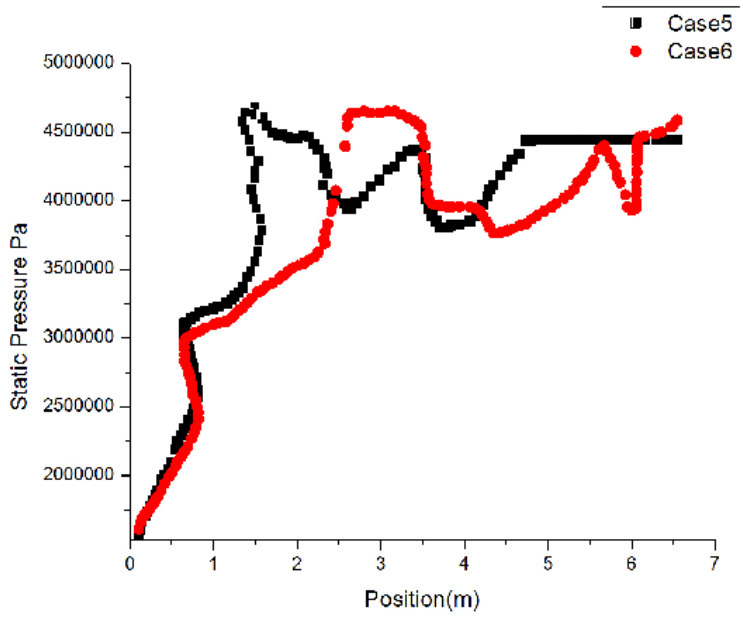

Figure 3.63: Static Pressure Variation in Case 5 and Case 6

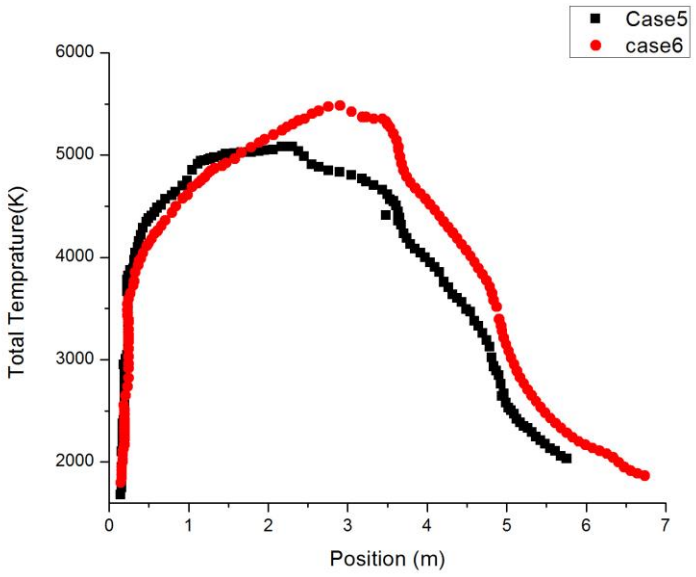

Figure 3.64: Total Temperature Variation Case 5 and Case 6

In the case 5 and 6 the minimum enriched GCR core is considered, which can be practically implemented within the current means of the technology. The temperature and pressure profiles in both the cases indicate the material requirements to handle high tempratures and the core dimensions chosen for the fission is more comparable. In case 5 the static pressure is becoming constant after the reservoir region since the heat addition is comparatively after the mean free path length. The obtained results are comparable with the Dam, 1996 and the selection of graphite thickness and the core dimensions are more productive in heat transfer and the effective core pressure development. The total pressure and temperature profile between both the cases are shown in the figure 3.64.

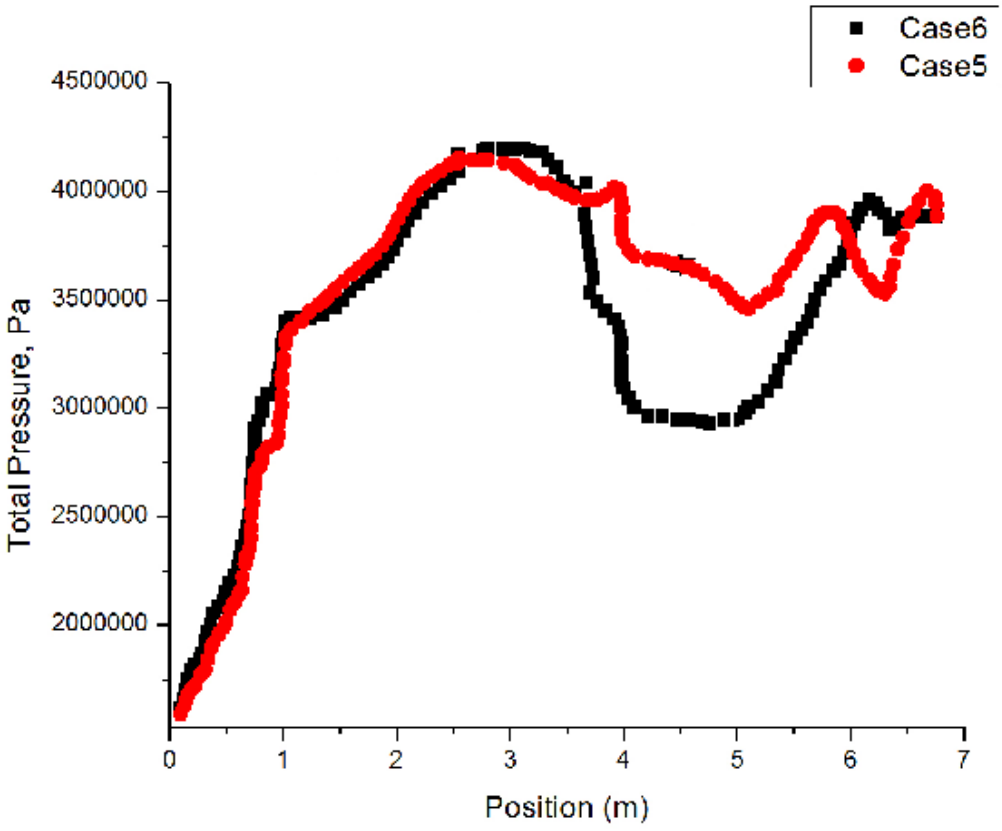

Figure 3.65: Total Pressure Variation Case 5 and Case 6

The total pressure variation in both the cases maintains similar trends, whereas the case 5 the back flow pressure high so that the fall in pressure at the reservoir region can be observed from the figure 3.65. The above accomplishments clearly demonstrate the numerical model for convective and radiative heat transfer who has the ability to develop better specific impulse and the power density. The comparison of incident radiation in both the cases shows that the difference in absorption coefficents and the scattering do effect the radiative heat transfer at the core so that the difference in fluxes are Cleary justified. The power densities obtained at the core is in the range of 100 W/cc at the given generation rate. The analysis shows that the generation rate is strongly dependent on gas temperature. This behavior is due to the limitation on the wall temperature and the radiative heat fluxes dominate the phenomena.

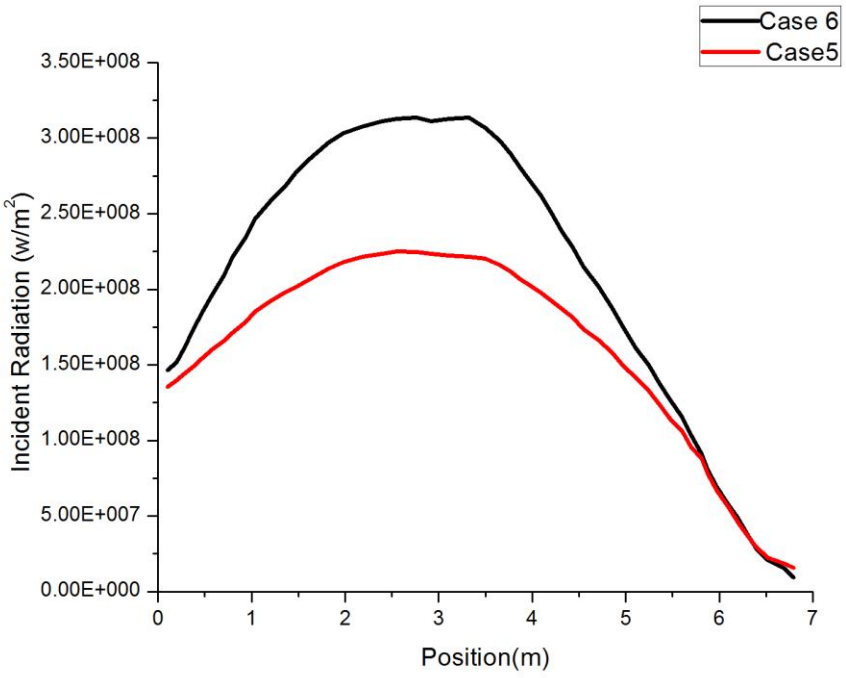

Figure 3.66: Incident Radiation in Case 5 and Case 6

The enthalpy rebalancing is visible in all the cases and comparison of various heat generation rates with the two different propellants in six cases gives an effective idea over the convective radiative heat fluxes along the fuel wall. The behavior of the propellant is more important to investigate the neutronics and the heat removal process and core walls cooling are more important in case of super critical reactors. The results compared in all the cases are plotted between the hydrogen cases and the helium cases in the figure 3.67- 3.73, it indicates helium behavior at higher temperature is more suggestible for GCR core and whereas at lower tempratures the heat transfer is not so effective. Helium is more advisable in case graphite core due to less reactions with the wall.

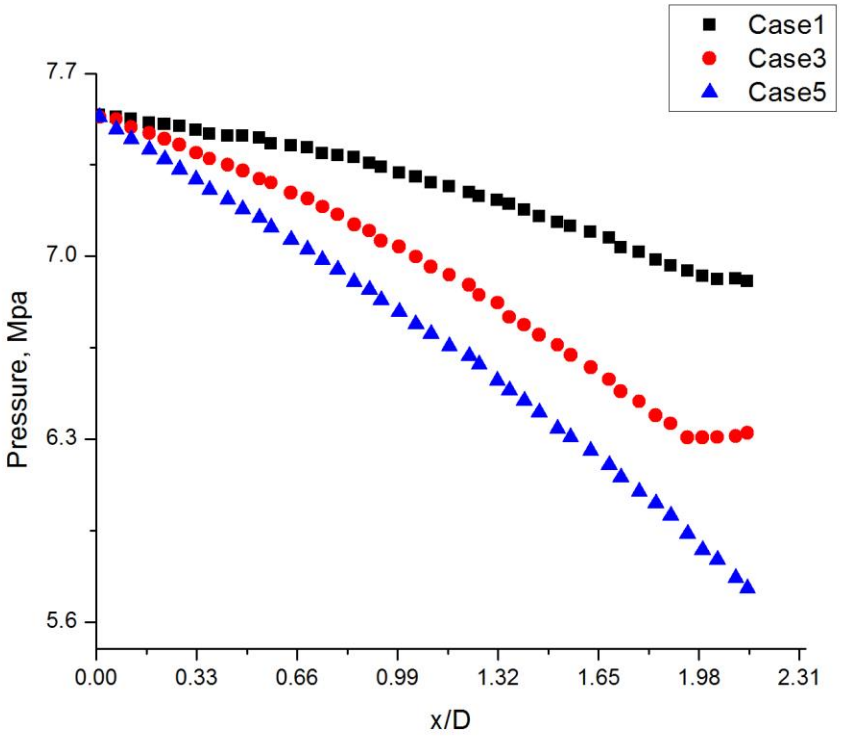

Figure 3.67: Pressure Variation along the Non-Dimensional Length

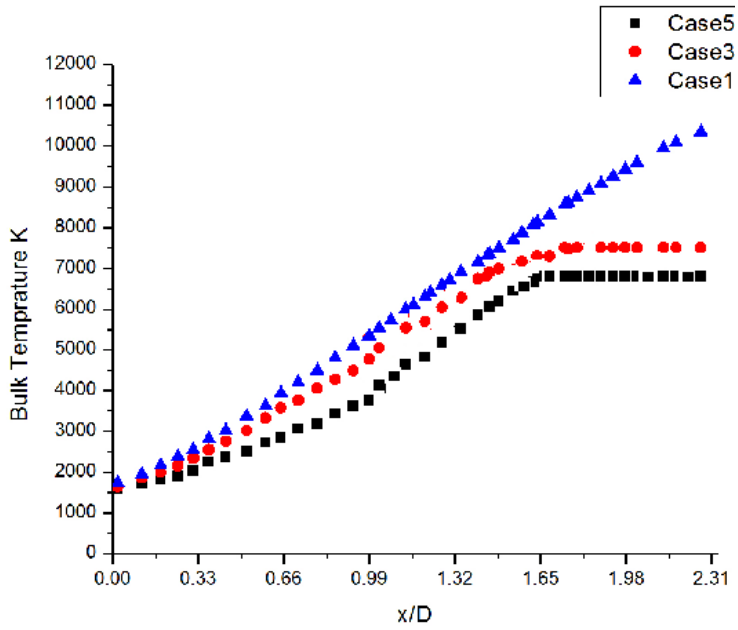

Figure 3.68: Bulk Temperature Variation along the Non-Dimensional Length

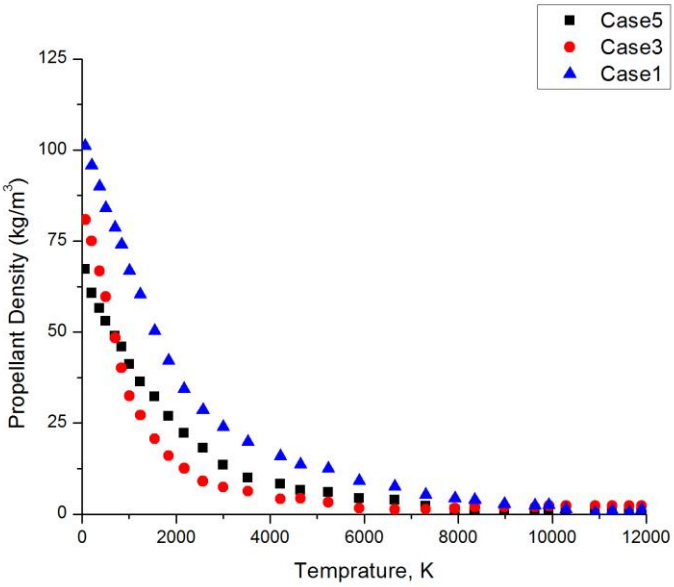

Figure 3.69: Density Variation in Hydrogen Used GCR Core for Different Cases

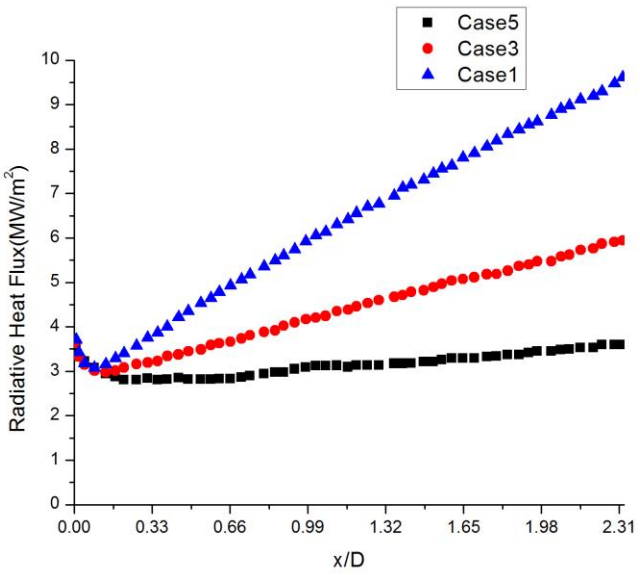

Figure 3.70: Radiative Heat Fluxes along the Non-Dimensional Length

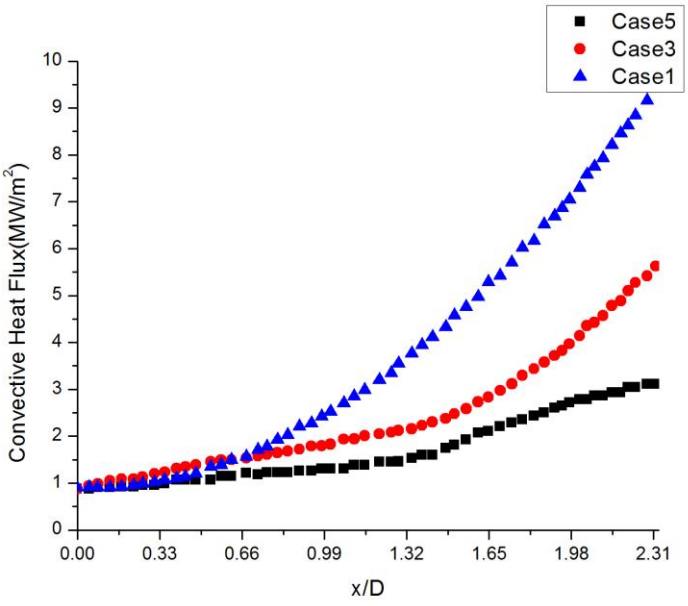

Figure 3.71: Convective Heat Fluxes along the Non-Dimensional Length

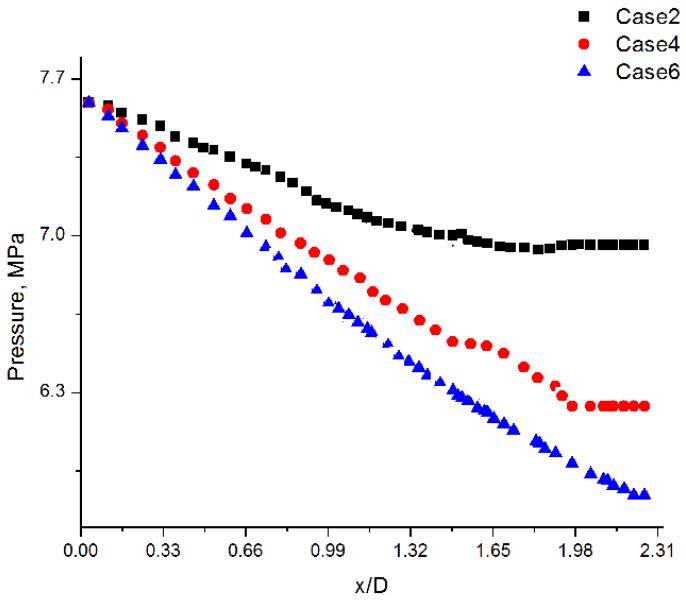

Figure 3.72: Pressure Variation along the Non-Dimensional Length

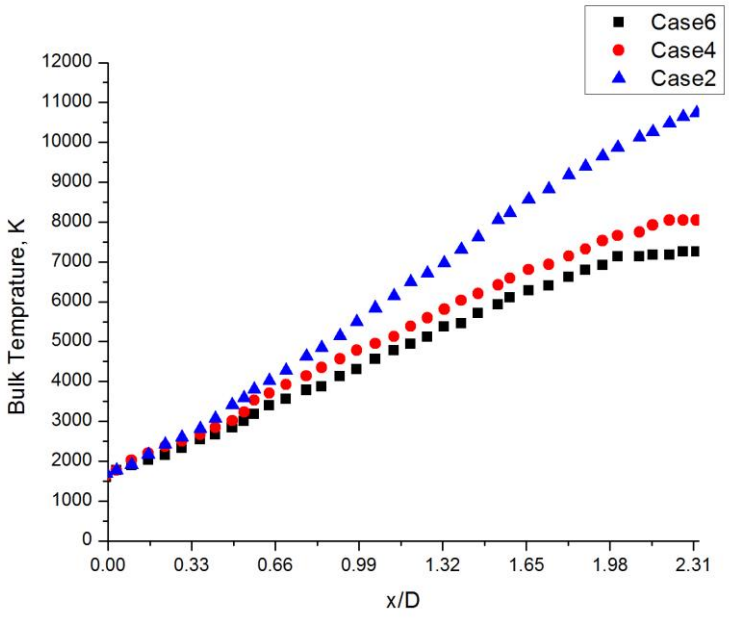

Figure 3.73: Bulk Temperature along the Non-Dimensional Length

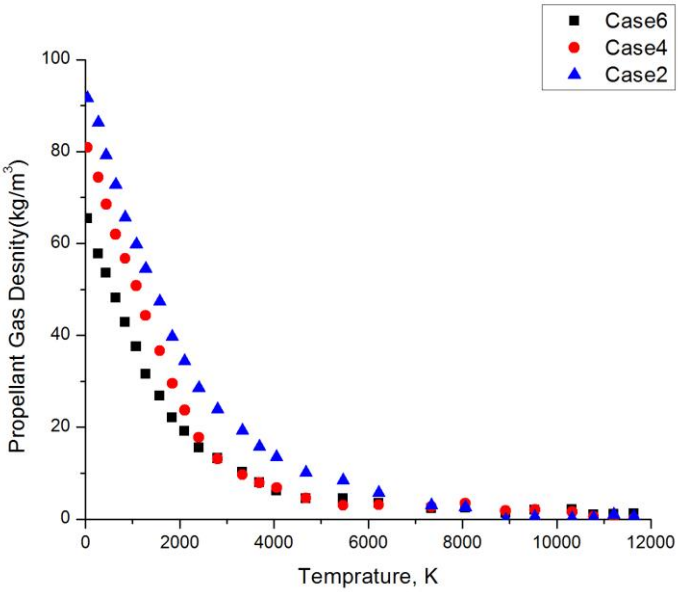

Figure 3.74: Propellant Gas Density variations along the Core Temperature

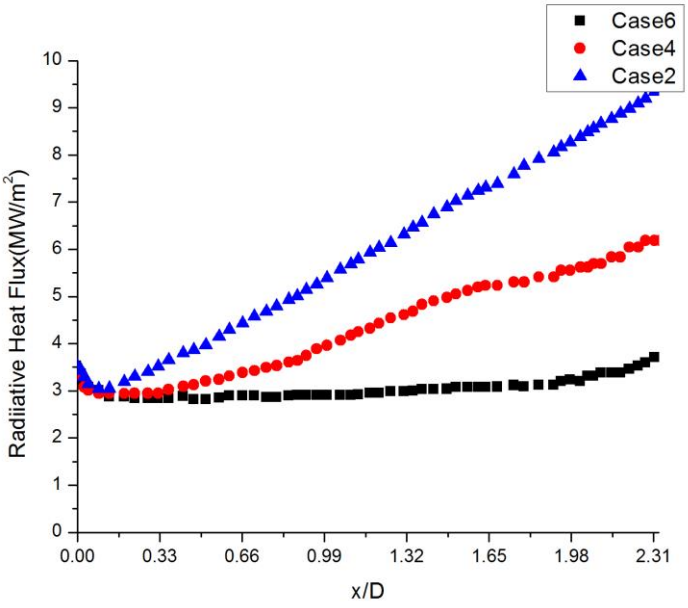

Figure 3.75: Radiative Heat Flux Variation in Hydrogen Propellant GCR

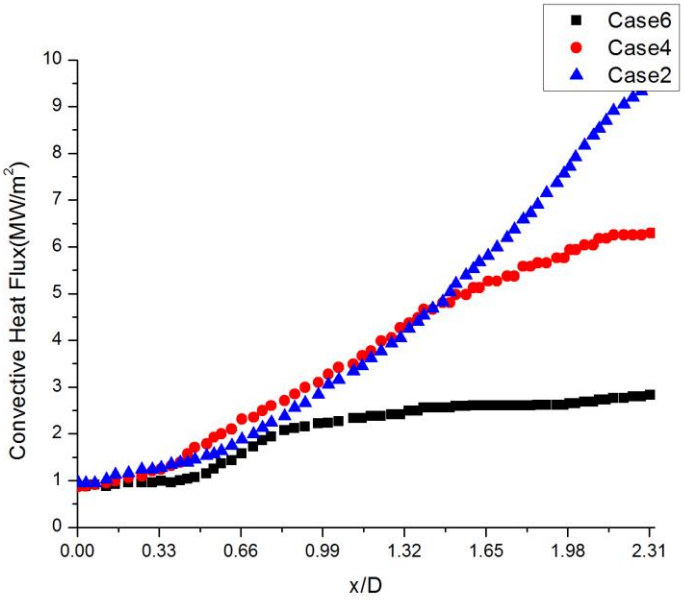

Figure 3.76: Convective Heat Flux Variation in Hydrogen Propellant GCR

The total temperature variation and the total pressure variations are compared in the figure 3.74 and 3.55, due to the flow filed with high Reynolds numbers the thin layer Navior- Stoke equations are used in the solver with a k-epsilon turbulence model. In all the cases convective and radiative heat fluxes are obtained, in all the cases the results shows in the below figures that the radiation heat transfer is mode dominant GCR core. The bulk tempratures and the pressure variations are shown in the figures, which show when there is a change in the behavior of the fuel gas inside the core reactivity changes with the neutron multiplications factor. Because of above reasons there are few portions where the pressure profile started fluctuating. This depression in the pressure in the reservoir region indicates the back flow of the fluid due to the change in resection and due to the throat area. Convective heat flux in case of 50 % enriched GCR core is very high in both the case.

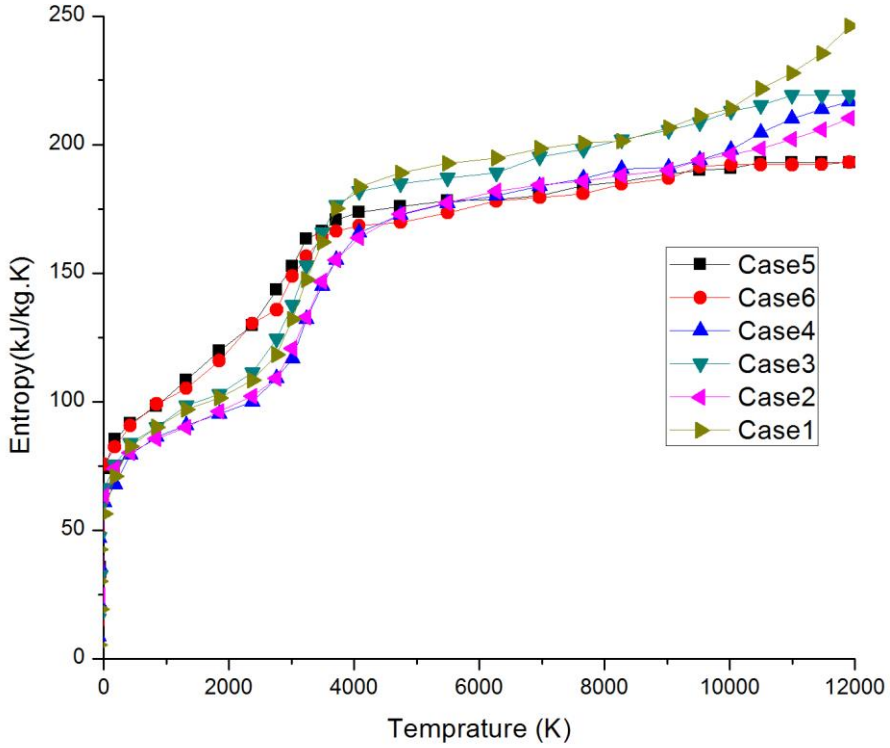

Figure 3.77: Variation of Entropy for Different Heat Generation Rates

In the heat transfer analysis of a GCR the variation of entropy due to heat generation at various operating parameters is compared for the six cases in the figure 3.77. The maximum entropy generated in the higher enriched fuel core with the highest temperature and pressure variations with higher power density. The results obtained in this work on hydrogen and helium propellants convective and radiative heat transfer indicates the behavior of the core at various conditions. In all the cases radiation intensity dominated the convective heat fluxes. Which indicate the core operation without allowing the propellant and fuel gas mixing, along the center of the core in an axisymmetric model; Iso thermal boundary condition is more effective a constant heat generation source and to maintain the wall temperature with in the considered limit.

CHAPTER 4: NEUTRONICS OF GASEOUS CORE REACTORS

The preliminary design of any reactor system depends on the behavior of the neutrons and their energy levels within the specified geometries. Since gaseous core reactors will be operated at supercritical conditions to support rocket applications, the power densities will be comparatively high. The idea of investigation of neutronics in gaseous core reactors which can be used for rocket applications will be based on fission process, where self-sustained fission reaction generates the require energy. In the fission process heavy nucleus absorbs a neutron and reaches an exited state from which it can be escaped by radiative decay or by fission. In the advancement of nuclear reactor technology has addressed reactor neutronics with moderated power densities. When it comes to reactor systems that will be designed for interstellar rocket applications will have high-power density with compact geometries, this approach is more challenging in flyable reactor systems design with effective safety considerations. This chapter deals with two-group analysis in which two kinds of neutronics, like fast and thermal groups are considered over various reflector systems with varying thickness.

The effective parameters like Keff and energy flux densities will be investigated using Monte Carlo based two group diffusion models code. The results will be used to obtain input parameters for the heat transfer analysis between the propellant and the fission region. Validation to the code will be done for the case of solid core reactors experimental data available from Los Almas Space laboratory model investigated for fuel channels with hydrogen propellant based system. The geometry that was considered in the current work is give in the figure 4, the reflector thickness considered is 10 cm with a core radius of 1.5. For

simplification pup uses the core geometry model was scaled when grid was read into the neutronics code. The gas considered as fuel inside the reactor is U-C-F and enrichment levels are varied continuously with the different cases. The overall thickness of the core structure is considered as 100 cm.

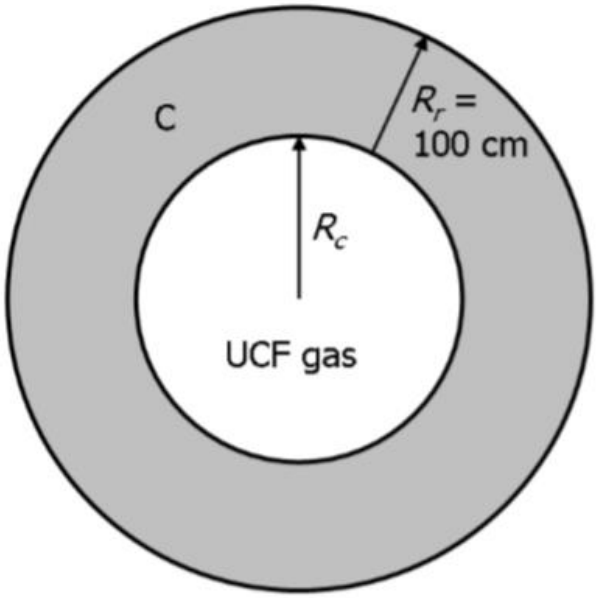

Figure4.1: Geometry of GCR Model Consider for Analysis

The reactor model operates with the vortex generation through the pressure difference created by radial flow. Since these reactors are not having the control rods the reaction is controlled by the pressure difference created in the flow. If the outlet temperature of the propellant reaches its maximum design value the flow rate increase thought he wall to create extra cooling as a same time the reactor core is going to have more concentration of hydrogen. The propellant itself starts slowing down the neutrons and the reactivity is controlled (Glasston, 1955). The schematic diagram of actual reactor core system used in nuclear rockets is given in the fig. 4.2. Buffer region is created in the core to improve the reactivity time

between the neutrons and the isotopic material, since the nuclear fuel is a so costly the flow rate need to be regulated at 100:1 ratio so that travel distance can increase. The designs parameters are considered for generating reactor core geometry are taken from Van douman, 1996 reactor analysis work. In the present thesis three reactor models are investigate with a variation in percentage of enrichment of the fuel. The mixture of U-C-F gas is also varied with the enrichment levels.

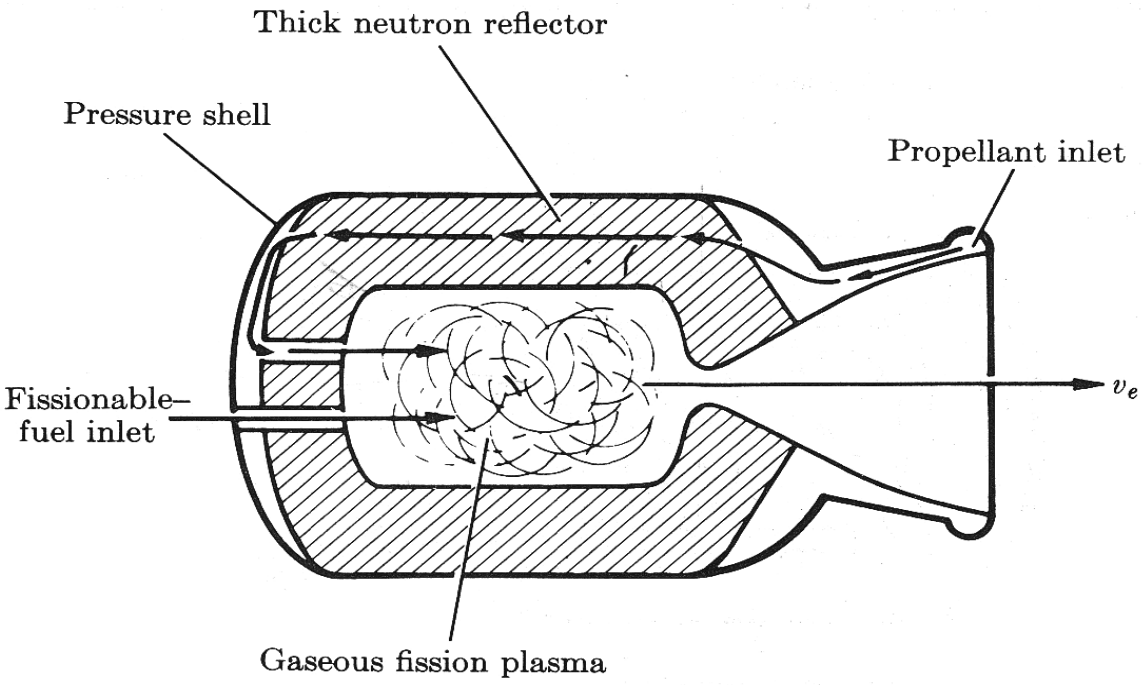

Figure 4.2: The hydrogen fuel (propellant) is injected in gaseous form, as well as the Uranium fuel in gaseous form

In the reactor core the fision process takes place with neutron interactions, besides the energy produced in the process there are various fragments released along with the neutrons. In the order of priority neutrons are the interesting elements int he core to maintain self sustained fission reaction. Along with the neutrons γ rays

are relesed. The fast neutrons whoes energy levels are high compared to thermal neutrons they are also going to obstrict the intractions. The propallent or the moderator or the reflector starts slowing down the fats neutrons so that neutron populations increase with the added quantity. Some of the neutrons get scattered due to collisions (Ragsdale, 1993). The complete fission process in the reactor core is given below with the level of extraction of different particles. Some of the neutrons starts getting absorbed with reflector material , so the total number of neutron population need to be randomized.

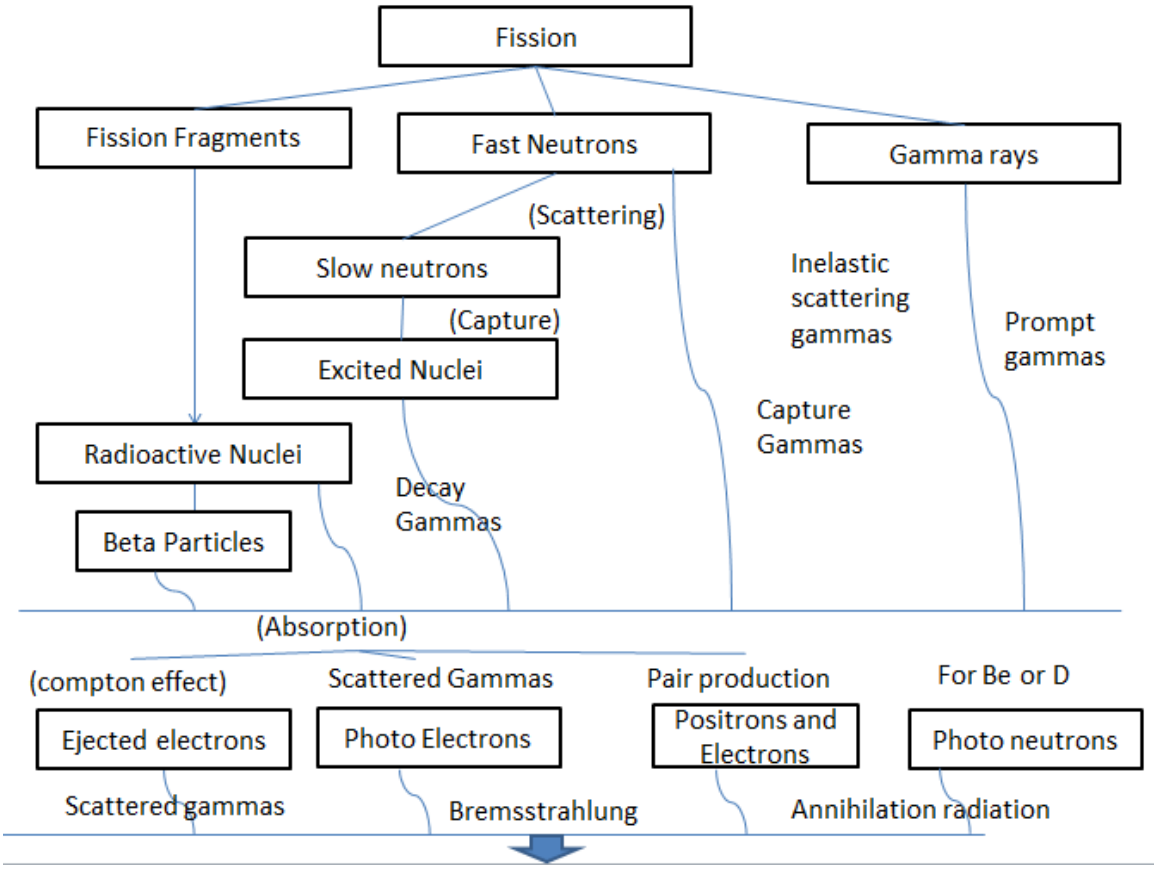

Figure 4.3: The process of fission along with the by-products

4.1 NEUTRON BEHAVIOR IN REACTOR CORE

The process of fission reaction can occur due to interactions of neutrons with nuclei and it absorbs the neutron and splits into two different fragments. In this process six new neutrons are released. These neutrons again start participating in the process and the reaction becomes chain process. In the reactor core this reaction can be self-sustained with the neutron production and their interactions with the radioactive materials (Runback, 1964). This process can continue with supplying nay external energy and the stable environment can be maintained with the heat produced during the process. The behavior of the neutrons depends on the materials used in the core and neutron reflector thickness and its selection differentiates the process.

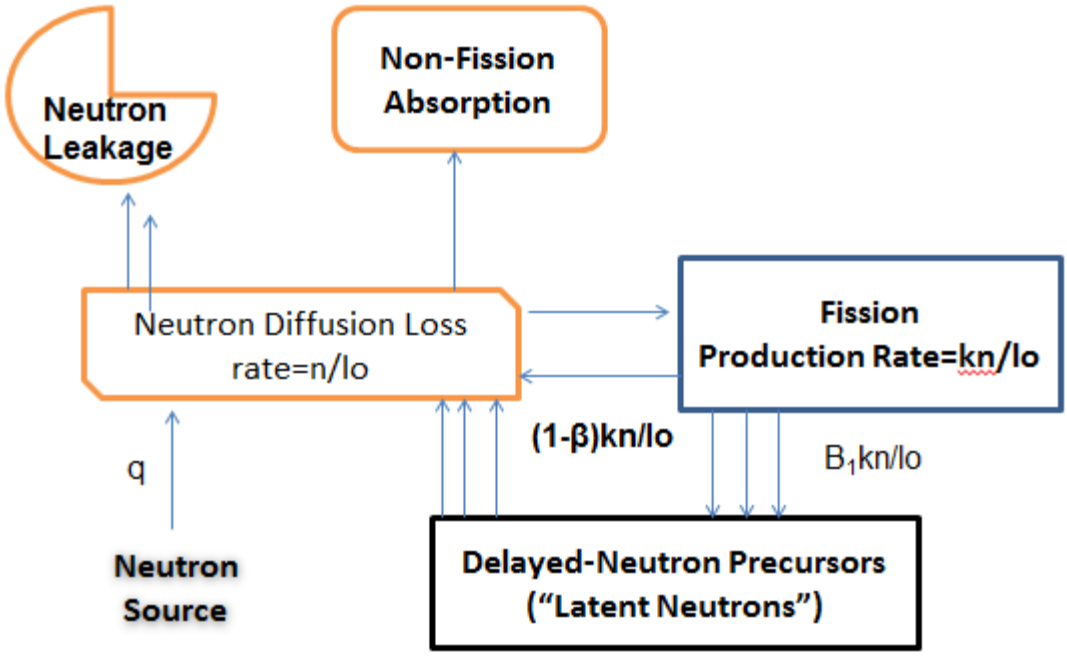

Figure 4.4: Simplified Neutron Cycle

The neutrons generated in the fission process will be normally in the energy range between 0.1 to 10 Mev, with a mean energy between 1 and 2 Mev. The generated neutrons will have different energy levels and different behavior based on its form of emitting. The fast neutrons move unimpeded through space until they interact with other nuclei (poorer, 1954). The complete cycle of the neutrons in the reactor core is given in the below figure 4.4.

4.2 APPROXIMATE METHOD OF ANALYSIS

Neutronics analysis is going to change with the reactor configuration to the operational conditions. The basic difference starts with the atomic ratio of the fuel which is going to use in the fission process, the reflector materials used, reflector thickness, Moderator usage, reactor type like fast reactor, breeder reactor, power reactor, reactors used for propulsion applications. The design criteria for any reactors depend on the parameters given in the table 4.1. The investigation conducted on neutronics of any reactor system is differentiated by its keff factor. In case of gaseous core reactors the design is based on mission time and the rocket operational conditions like the expected specific impulse, thrust of the system intended to operate. The temperature limitations over the reflector materials and the reactor chamber are going to set the upper limit over the system. The critical value of keff can be selected for the temperature of operation. In case of controlling the reactor for safety purposes the design is made based on the selected keff factor based on the maximum assurance limit (Robert, 1989). The keff accident condition is taken a reference for the safety maximum limit. The neutronics analysis is mainly conducted to estimate the neutron flux and the neutron density in a core. So that reactivity can be estimated.

Table 4.1: THE PARAMETERS FOR REACTOR CRITICALITY ANALYSES

Category	**Requirement**	**Ref Value**
Reactivity	Lifetime/Mission Assurance	Keff
Safety	Maximum Assurance of Credibility	Keff for accident Cond
Control	Leakage control, reactivity control	Neutron Flux, Density
Fuel	Enrichment, Proper Mixing	Fuel Composition, peak central temp
Operational	Power Coefficient over mission time	N flux, Topr, Popr
Shield	Dosage Limit	Shadow Angle

If the probability of neutrons are getting leaked though the core then the reflector thickness and the material need to be reconsidered. In reaching the desired keff value the reactor system need to be supplied with effective fuel composition. In case of solid core reactor systems the fuel composition varies with the material used in preparing fuel rods. Since the GCRs fuel composition depends upon the atomics ratios in which fuel gas is processed. In case of this thesis the fuel mixture is prepared from Uranium and floride compounds, the percentage of enrichment is directly proposal to the keff value. The core where is fission process is occurring the peak temperature value is measured and the distributed temperature profile depends on the effectiveness of the heat transfer with the

reactor buffer region. In most of the cases while designing the gas core nuclear reactors the neutron reflector and the external radiation shielding is selected on a single configuration to reduce the total weight of the system.

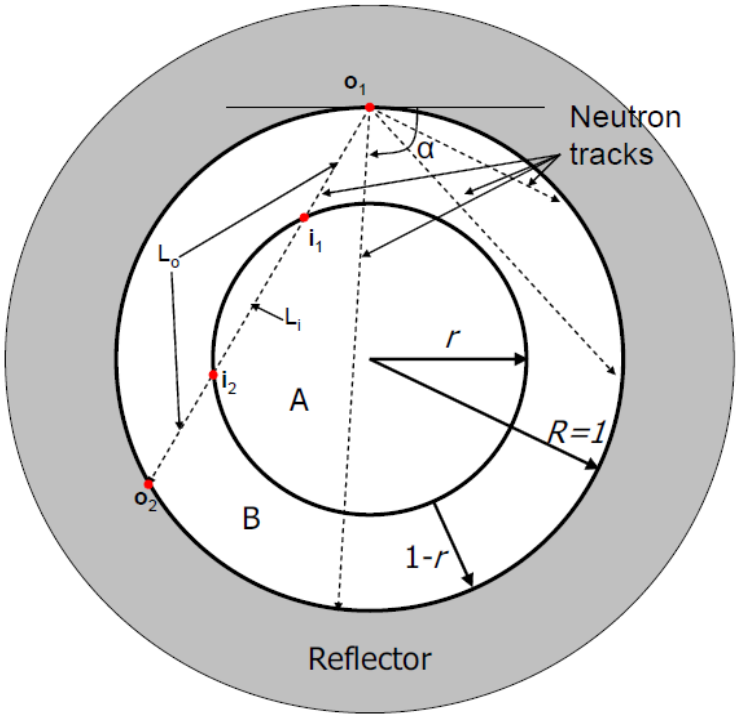

Figure 4.5: Neutron Tracks Leaving the Reflector with Angle Compared to the Reactor Surface

In case of shielding design and analysis the dosage limit is mentioned in reactor systems design. In case of space reactors the considerations will change for a manned mission or space vehicle which travels the longer distance. The reactor selection for the rocket vehicles is done based on the specific power density of the designed system. Since the total power requirement to attain required gravitational acceleration is a major interest.

4.3 CODE DEVELOPMENT FOR NEUTRONICS INVESTIGATION

The code is developed for solving time-independent two groups discrete originates in the form of Boltzmann Transport Equations for different geometries defined by the user. The grid used in solving this problem is based on standard diamond differencing method for space angle discretization, and for spatial and angle discretization adaptive weighed diamond differencing method was used. The Monte Carlo method and the functions generated for solving the two group neutron equations detailed in 4.3.1 and the input model is attached in appendix A, the code is also attached in Appendix B,. This code developed with the help Dr.Ozoner from Los Almost Space Laboratory and the neutron groups are used from the common format which can be used for MCNP, the code has grid libraries the name space step 28 class is created. This class is capable of reading the fission neutron groups and the probability functions are created with the unsigned materials. The distance for the cell zones are given as an input and it can solve for the reflector surfaces. MaterialData Xs object is created to store the material properties of each fission group and the reflector configurations. The isotopic material data is written in Material ID get_fission spectrum and the variation of fuel composition is varied through the input. To distinguish the neutron spectra energy group class is created along with the identified cell zones. The flow chart describes the user input details required to run the code and the final data to analyses the reactor criticality format can be identified. The data generated with the code is processed through Statistical number crunching system and the required values can be extracted, the data is plotted using gnu plot for the parameters required to explain the behavior in gas core reactors.

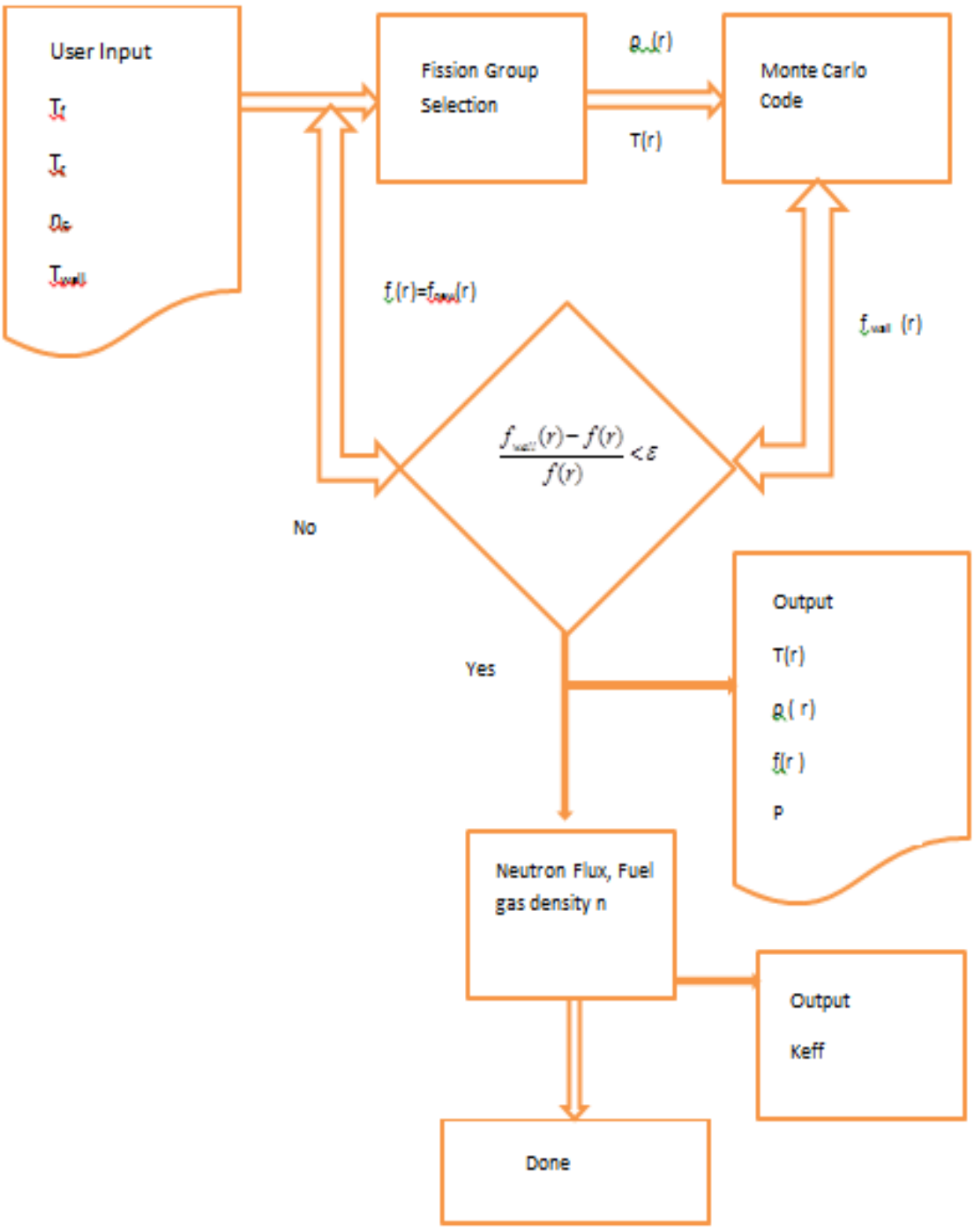

Figure 4.6: Flow Chart for the Code Developed to Solve Two Group Model

4.3.1 MONTE CARLO NEUTRON TRANSPORT

In the analysis of reactor physics neutrons play an important role to obtain self-sustain fission reaction. Mote Carlo codes are used to analyst the radiation shielding problems, neutron interactions with the nuclei, reflector modulator problems, and safety criticality analysis. Besides neutron transport equations the fundamental particles behavior also studies using Monte Carlo method. These codes accept physical geometries to analyses major interactions by the particles with input data conditions. The neutron transport equations are solved using stochastic method by Monte Carlo code. The second method that can be used for solving the neutron interaction by using Boltzmann equations, this method takes a statistical averaging of net leakage of neutrons from the core and assuming that all the neutrons in the reactor are with uniform energy levels and are taking part in the fission reaction.

$$\nabla \cdot \phi(r,\Omega) + \sum_a \phi(r,\Omega) + \sum_a \phi(r,\Omega) = \int_{\Omega'} P(\Omega' \cdot \Omega)\phi(r,\Omega')d\Omega' + S(r,\Omega) \qquad (4.1)$$

The above equation explains the loss rate of neutrons from a unit volume with a unit angle around a point. The neutron balance can be obtained by quantifying the neutron loss rate by absorption, reflection; scattering and the loss of energy by neutrons can be balanced. The integral equation on the right side will express the scattered neutrons quantity in all directions. S indicates the source of fission neutrons that are liberated in each chain for a specific location in the given volume. The difficulty with the above method lies with solving the flux distribution and which needs high computational power as well as the specific geometrical models to solve. In case of Monte Carlo algorithms the development of statistical model and the average rate of interactions can be defined base on the geometrical considerations. Monte Carlo algorithm performs the calculation on a

specific neutron and its path throughout grid at a time. The collection results are based on discreet events with the individual neutron behavior. The code developed in this thesis is not concentrated on adjoin calculations, since the running time to reverse the process is a parallel algorithm development approach. The energy variation is taken as a continuous function to describe neutron interactions in a 1 D cylindrical geometry. The code takes random selection individual neutrons to solve for required parameters. The rest of the analysis based on infinasimal cylinder with a one dimensional cross-section behaves as a complete physical system and generates the data for the reactor criticality.

The probability distribution functions considered in selecting the neutrons is taken from probability distribution f(x) where x as a variable. The event of interactions occurrence predicated between xs and x+dx

$$dP = f(x)\,dx \tag{4.2}$$

The probability density function was generated using a montecalro integration method for the following equation in the interval of [a,b] for a variable in the interactions.

$$P(a < x < b) = \int_a^b dP = \int_a^b f(x)dx \tag{4.3}$$

The behavior of the equation with a probability function will vary with the intervals and the values become infinity at a certain point of time. The convergence criteria given under boundary conditions to take the intervals for which the solution is obtained. This can be calculated from cumulative distribution function by a direct integral.

$$F(x) = P(x' < x) = \int_{-\infty}^{x} f(x')dx' \tag{4.4}$$

The limit defined in the code to solve the cumulative probability function space must yield P=1 and hence

$$\lim_{x\to\infty} F(x) = 1 \tag{4.5}$$

In case of solving this problem the random variables are distributed between the a and b the function is written in the form of

$$f(x) = \begin{cases} \dfrac{1}{b-a} when \ldots a \le x \le b \\ 0 \ldots\ldots when \ldots x < a \ldots or \ldots x > b \end{cases} \tag{4.6}$$

Now the cumulative distribution function is going to change in the form of

$$F(x) = \begin{cases} 0 \ldots\ldots\ldots when \ldots x < a \\ \dfrac{x-a}{b-a} \ldots\ldots when \ldots a \le x \le b \\ 1 \ldots\ldots\ldots when \ldots\ldots x > b \end{cases} \tag{4.7}$$

When the uniform distribution of the neutrons are considered in the geometry the limits are set for a=0 and b=1. Then the function is going to generate random variable which can be uniformly distributed in the given interval. In case of solving complete geometry Pseudo-random number generation method is used to create the sample for various intervals inside the geometry, the other random number is derived from an inversion method of sampling. The cumulative distribution function is solved at a uniformly distributed variable at unit interval. With the obtained data sample a uniformly distributed variable is generated called

ζ. This is used to apply the sampling method the CDF by using the value at 0.8979.

$$F(x) = \varsigma \Leftrightarrow x = F^{-1}(\varsigma) \tag{4.8}$$

At a given CDF the corresponding value of the x is set at 7.1552, the data samples given in the neutron groups can be randomized in the similar process and the functions are generated at each specific location of the geometry. In case of the values outside the interval the solver identifies the group as a different function and obtains the samples by using rejection technique. In simpler terms the density function g(x) and the constant of rejection limit is set for f(x) at c≥1 and the f(x) is generated through the following relation

$$f(x) \le cg(x) \tag{4.9}$$

In this case the uniformly distributed variable is obtained from the relation given below

$$\zeta < \frac{f(x)}{cg(x)} \tag{4.10}$$

If the inequality does not hold then the value will be discarded and the procedure is going to repeat from the beginning with the help a loop this function was considered and the if- else statement is used to differentiate the variable limit. If the values are acceptable with in the domain the f(x) follows exactly the same relation and data can be generated. The method of selection of sampling is done based on a specific relation given by dividing both the integrals with an infinity limits.

$$E = \frac{\int_{-\infty}^{\infty} f(x)dx}{\int_{-\infty}^{\infty} cg(x)dx} \tag{4.11}$$

The difference between the functions are relatively small and the ratio of integral have a possibility of reaching unity, since the functions are used to generate random data this factor will not affect the solution accuracy. The above method can only generate the distribution inside the core; in case of fission reaction the third method is used to account for energy and the neutrons emission in the fission reaction. The consideration taken for the two-body scattering with equip-probability interval of 12 and 14.The random variable x is generated from the following equation to integrate the function.

$$x = x_n + (N\zeta - n)(x_{n+1} - x_n) \tag{4.12}$$

The sampling algorithm starts with integrating the function between $x_n<x<x_{n+1}$

$$\int_{x_n}^{x_{n+1}} f(x)dx = \frac{1}{N} \tag{4.13}$$

The first interval sample is taken from the relation given below to solve the integral part

$$n = N\zeta + 1 \tag{4.14}$$

In most scattering reactions the cosine interval is chosen as 32 and the solution, number of intervals considered differentiates the accuracy of the solution with the functions used for creating the random data points in the reactor core. The reactor core is divided into different geometrical regions to track the single neutron in

each of the region. The path traced by each neutron is said to be a track and the path is traced once the set points on the geometry given by a specified path of neutrons are attributed to the generation point to the escape point. The total tacks traced by each neutron create a neutron history for that particular core. The free path length between the collision points need to be defined with the help of user input, the sample input values are defined in the Appendix I, which described the set points and the paths traced are chosen from eighteen value matrix. The matrix generated with different set points using a trace angle is directly read by the code. The subroutines used in the code are having the functions to generate the eighteen values for the path tracing. This values can be tallied with the number of neutrons emitted at the source and the number of histories generated.

To estimate the keff value to probability of interactions by neutrons with the nuclei can be found by sampling the free path length. The geometrical cross section is set to the nuclei and the track history can be generated for the microscopic interaction of the neutrons. This can be obtained from the constant interaction probability with the homogenous medium traveled by the neutron; the homogenous medium can be a reflector or a propellant as well as gaseous uranium (Feisbee, 2003). The probability that the neutron can undergo interaction with the nuclei surface with a distance change to dx can be obtained from Σ_t.

$$dP = \sum_t dx \tag{4.15}$$

This can trace the path from x to dx and the probability of interaction in the nuclei region. An arbitrary zero position is considered and the probability needs to be found for the intial track of the neutron path. The idea of creating intial probability function is to find out the chance of reaching x distance without any interactions and also to find out the probability with which the interactions takes place within the given interval.

$$dP_0 = -P_0(x)dP = -P_0(x)\Sigma_t dx \tag{4.16}$$

The non-interaction probability also can be found from the differential equation given by

$$P_0(x) = e^{-x\Sigma t} \tag{4.17}$$

The first move distance can be identified from then function given below with a specific cross section

$$P_0(x) = P_0(x)\sum_t dx = \sum_t e^{-x\Sigma_t} dx \tag{4.18}$$

The free path length can be written as

$$f(x) = \sum_t e^{-x\Sigma_t} \tag{4.19}$$

This can be included in cumulative probability function written to the microscopic cross-section

$$F(x) = \int_0^x \sum_t e^{-x'\Sigma_t} dx' = 1 - e^{-x\Sigma_t} \tag{4.20}$$

The intial length characteristics can be found using x and the function that can be expressed based on cross sections selected in solving the defined problem. The cross sections that can solve are up to the limit of 0.3188 cm^{-1}.

$$x = -\frac{1}{\sum_t}\ln(1-\zeta) = -\frac{1}{\sum_t}\ln\zeta \tag{4.21}$$

The mean free path, l can be used identified to calculate the non-interaction probability and the code written is with the values that can solve up to the limit of

3.1364 cm. The interactions found are at a distance of 0.004 to 0.006, it can be a good method of solving the mentioned possibilities with the functions generated. Deta Tracking probability method was used to identify the neutron path length probabilities. The generated data is interpreted with the homogeneous mediums, since the solution of non-homogeneous region needs multiple integration solutions which will become complex in developing the code. It takes ample amount of time to solve integral equation; more over the probability functions becomes closed form equations. In real cases the geometry is considered as regions by counting the cell zones. The diamond differencing method used to create the specific cell zones to number them in terms of groups.

$$l = \int_0^\infty x e^{-x\Sigma_t} dx = \frac{1}{\Sigma_t} \tag{4.22}$$

The problem in generalizing solution in case of neutron mean free path changes with the materials and the region of interest. The cell zones are identified based on spatial neutron coordinates and the boundary surfaces are excluded from the cell zones, in such cases the re-sampling the remaining distance to the next collisions. This approach is included in a subroutine by using ray coding method. The non-interaction probability can be expressed as

$$e^{-x_2\Sigma_{t_2}} = e^{-(x_1-d)\Sigma_{t_1}} \Rightarrow -\Sigma_{t_2 x_2} = -(x_1 - d)\Sigma_{t1} \tag{4.23a}$$

$$\Rightarrow x_2 = (x_1 - d)\frac{\Sigma_{t1}}{\Sigma_{t2}} \tag{4.23 b}$$

In case of non-interactive probability the path length changes to

$$x = d + x_2 = d + (x_1 - d)\frac{\Sigma_{t1}}{\Sigma_{t2}} \tag{4.24}$$

In this case infinite circular cylinder of radius R, is considered in a Cartesian coordinate system with three direction vectors, and the distance d can be resolved by using the equation below

$$d = \sqrt{\frac{(\Omega_x^2 + \Omega_y^2) r^2 - [\Omega_x (y - y_0) - \Omega_y (x - x_0)]^2}{\Omega_x^2 + \Omega_y^2}} \tag{4.25}$$

Based on the line of site the distances between the cell zones are identified so that the nearest surface can be integrated and shortest distance can be found. The microscopic total cross section of the isotopic material needs to be identified to generate a probability distribution for the isotope channels

$$P_m = \frac{\sum_{t,m}}{\sum_t} \tag{4.26}$$

The conditional probability is written to indicate a selecting reaction in the ith group if m isotopes are written as

$$P_{i,m} = P_i P_m = \frac{\sum_{i,m}}{\sum_{t,m}} \frac{\sum_{t,m}}{\sum_t} = \frac{\sum_{i,m}}{\sum_t} \tag{4.27}$$

In the fission process the truncated integer values are considered for N of ν and the probability was determined with the decimal fractions. In reality if the neutron absorbed by isotopic material the neutron history comes to termination and the new source of generation led to neutron release. The number of emitted neutrons in this process can be identified by a fission nubar ν.

$$No..of\,..emitted\,..neutrons = \begin{cases} N+1 ... if \zeta \le \bar{\nu} - N \end{cases} \tag{4.28}$$

The time of emission is exponentially distributed and it can be similar to the neutron free path length

$$t = -\frac{1}{\lambda_j} \ln \zeta \tag{4.29}$$

The distributions need to be made for neutron energy levels independent of its decay, the variation in the energy levees differentiate the total group emission time.

4.3.2 GRID GENERATION USING DIAMOND DIFFERENCING METHOD

The method used in solving the neutronics in an infinite cylinder was discretized using a finite volume based diamond difference method which creates non uniform grid. Since the specified geometry is divided into regions to identify fission groups, so structured grids are not so accurate in such kind of applications to perform analysis, the number of grid elements generated are100,000 and the number of geometrical zones divided are 250, four groups are taken on each zone to analyses the changes with respect x+dx. The data used to specify neutron secondary interaction are given in the Appendix c.To estimate the quality of the mess generate and the accuracy of the solution a relation is generated to figure of marite.

$$FOM = \frac{1}{R^2 T} \tag{4.30}$$

R indicates relative error and T indicates the computer run time, in the current problem three different cases are solved on a single grid. This identification of the error need to be compared with the each set of solution, in order to get more accurate solution when FOM value increase the R values starts decreasing. The

most accurate solution can be obtained at unity. The estimated error is obtained to generate a profile in calculating keff value with the help of code and generated grid. The error range started coming down with the increased iterations.

4.3.3 CODE CAPABILITIES

This particular code can take input in the form of ASCII text with a free field format, a sample input is given in the appendix-I. It can be developed for solving in vacuum, reflective, periodic and surface source boundary conditions. It can generate data for inhomogeneous source fixed or Keff calculation as well as time absorption of alpha, nuclide concentration can be investigated. The code is capable of solving one dimensional and two dimensional geometries with different shapes and the range of the solution domain depends on cell zones identified.

4.4 METHODOLOGY

Nuceutronic analysis is conducted under uniform temperature and density distributions. In Gas core reactors the mean free path length of the neutrons are very high under such cases the investigation of neutron criticality in a one dimensional geometry needs certain assumptions. The tempratures variations are considered to be very small and the density distributions are taken as a reference. Criticality analysis is conducted to estimate the reflector thickness and the cylindrical core effects on neutron behavior by solving two-group, two- region calculations for specified 1-D geometry. The computational facility needed to solve multi group diffusion theory to investigate the complete three dimensional core model with a completely reflected material cross-section are out of the scope for this assignment. The energy range for neutrons, all reactions given in a particular cross-section data evaluation are accounted for, and cover the energy

range between 10−5 eV and 20 MeV. The nuclear data library was used to apply neutron-induced cross- sections at different tempratures. Thermal correction in the phonon band requires separate cross-section evaluation, the so-called S(α,β) cross-sections that are available for BeO, graphite and hydrogen at a temperatures varying from 294 K -15000K used in the present calculations. The S (α, β) thermal scattering treatment is a complete representation of thermal neutron scattering by molecules and crystalline solids. Two processes are allowed: (1) inelastic scatter ing with cross-section σin and a coupled energy-angle representation derived from an S(α,β) scattering law and (2) elastic scattering with no change in the out- going neutron energy for solids with cross-section σel and an angular treatment derived from lattice parameters. The elastic scattering treatment is chosen with a probability of σel/(σel +σin).The representation of Thermal neutrons through Maxwellian Distribution is represented in the figure below.

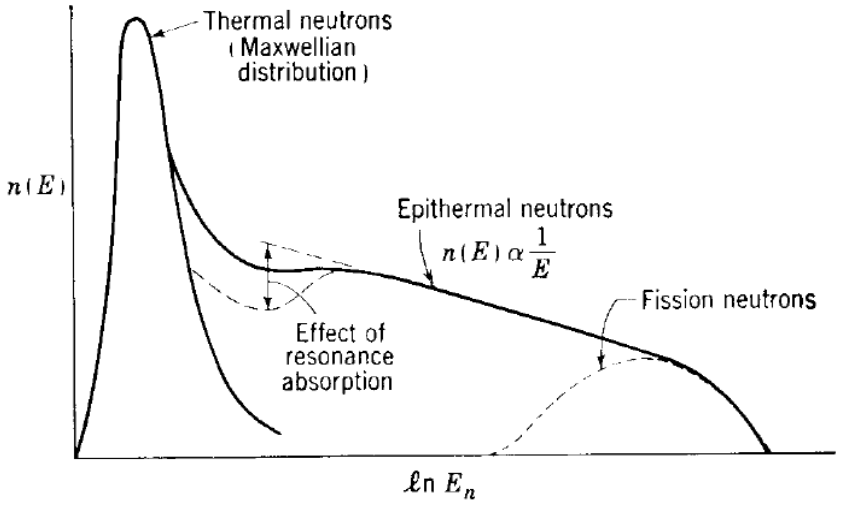

Figure 4.7: Maxwellian Distribution of Neutron Energies

The reactor core was taken to be a homogenous mixture of propellant gas and the U-C-F, the propositions are obtained from the computational fluid dynamic analysis conducted on the core. The resonance escape probability is considered as one and the fast fission was neglected. The thickness of the beryllium reflector and the graphite reflectors are varied from the consideration made by Lafyatis near optimum value 0.6. The distance at which the neutrons are traveled is considered as a neutron track, in the current solution individual neutrons are traced for its path and probability function is used to estimate the number of neutrons interacted with the source and the neutron interaction regions are formed. The figure 4.8 shows the neutron trajectory between the source and the point of absorption.

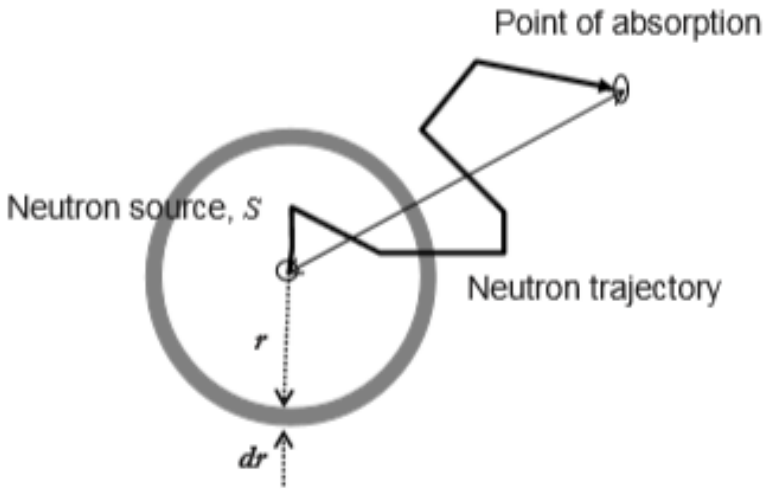

Figure 4.8: Distance and Neutron Trajectory between the Points of Neutron Source to the Point of Neutron Absorption

In this work neutron investigation is conducted in a cylindrical core system with infinite length to consider the geometry as a one dimensional system. The analysis

is conducted through a code written on two group neutron transport theory using Monte Carlo method, the detailed analysis on neutron behavior in a GCR core can give the neutron balance from the production to mean by which neutron is getting utilized. This balance can give us an account for neutron production to the neutron loss. Also for analyzing thermal hydraulics this balance will help in estimating the total heat produced by the system. Neutron diffusion theory is used to describe the neutron flux density and the neutron production, leakage, fission and absorption. Solving multi group diffusion equations are very much complex and time consuming. Inters of computational power required to analyze the reactor geometries are even more complex. In the real analysis of reactor design simple apaches are taken to solve the diffusion equations like one-speed neutron transport theory or two group diffusion equations are solved to attribute the neutron behavior to the complete system. This is not a new process, most of the validation studies are conducted on the similar aspects and the results comparison is satisfactory, the similar approach is used to complete the analysis. The infinity multiplication factor is a notation for the reactor criticality analysis and which can be written in the equation below. This indicates the number of neutrons produced in the absorption of neutron per fission.

$$k_{\infty} = \frac{Neutron \quad production \quad rate}{Neutron \quad absorption \quad rate} \tag{4.31}$$

In gaseous core reactors neutronics analysis the geometry considered is in infinity in length, in such cases the neutron leakage from the system is neglected. The only way of neutron getting lost depends on the absorption. In case of finite geometries with a specific dimensions when a core diameter is specified the effective neutron multiplication factor can be found from the following equation.

$$k_{eff} = \frac{Neutron \quad production \quad rate}{Neutron \quad absorption \quad rate + Neutron \quad lekage \quad rate} \tag{4.32}$$

The ration of infinite multiplication factor to the effective multiplication factor can be found by using source as S and the leakage as L, absorption as A

$$\frac{k_{eff}}{k_{\infty}} = \frac{A}{A+L} \tag{4.33}$$

The above relation represents the non-leakage neutron probability for a given system. In case of critical reactors the neutron multiplication factor should be above unity. If the size of the system is defined by a, and the radial distance is taken as a measure for identifying the neutron leakage with respected to the surface a proposal relation can be used.

$$\frac{L}{S} \alpha \frac{SA}{V} \alpha \frac{a^2}{a^3} \alpha \frac{1}{a} \tag{4.34}$$

The infinite multiplication factor is a function coolant used and the meteor material selected along with the propellant used inside the system. In general cases the value varied from 0 to 1.2 in case of space reactor. Neutron source in case of homogenous system is represented by S(r) and it can be found from the balance written for the diffusion equation

$$S(\vec{r}) = \sum_a k_{\infty} \Phi(\vec{r}) \tag{4.35a}$$

Lekage+absorption=Production (4.35b)

$$-D\nabla^2 \Phi(\vec{r}) + \overline{\sum_a} \Phi(\vec{r}) = S = \sum_a k_{\infty} \Phi(\vec{r}) \tag{4.35c}$$

The non-leakage probability needs to be found from the given relation to generate the functions through the cumulative functions in Monte Carlo Method.

$$\nabla^2\Phi(\vec{r})+\frac{\overline{\Sigma_a}(k_\infty-1)}{D}\Phi(\vec{r})=0 \tag{4.36}$$

$$\nabla^2\Phi(\vec{r})+B^2\Phi(\vec{r})=0 \tag{4.37}$$

Here geometrical bulking is added to specify the region to generate the functions

$$1=k_\infty\left[\frac{1}{B^2{}_mL^2+1}\right] \tag{4.38}$$

$$P_{non-leakage}=\left[\frac{1}{B^2{}_mL^2+1}\right] \tag{4.39}$$

$$P_{non-leakage}=\left[\frac{1}{B^2{}_mL^2+1}\right]=\frac{\overline{\Sigma}_a\Phi(\vec{r})}{\overline{\Sigma}_a\Phi(\vec{r})+B^2{}_m\phi}=\frac{\overline{\Sigma}_a\Phi(\vec{r})}{\overline{\Sigma}_a\Phi(\vec{r})+(-D\nabla^2\Phi(\vec{r})} \tag{4.40}$$

In two-group diffusion theory the considerations are made based on thermal energy group as well as the fast neutron group. The boundary set between these groups is given as 1 e. The fast neutrons can be thermalized with the help of moderator; fast neutrons are will be last in absorption. The neutron fluxes can be expressed for both the groups.

$$Fast:\Phi(\vec{r})=\int_{1ev}^{10Mev}\Phi(E,\vec{r})dE \tag{4.41}$$

$$Thermal:\Phi(\vec{r})=\int_{0ev}^{1ev}\Phi(E,\vec{r})dE \tag{4.42}$$

The complete set of equations used in two group neutron diffusion theory to explain the complete neutron process is given in the figure 4.9 based on the energy spectra.

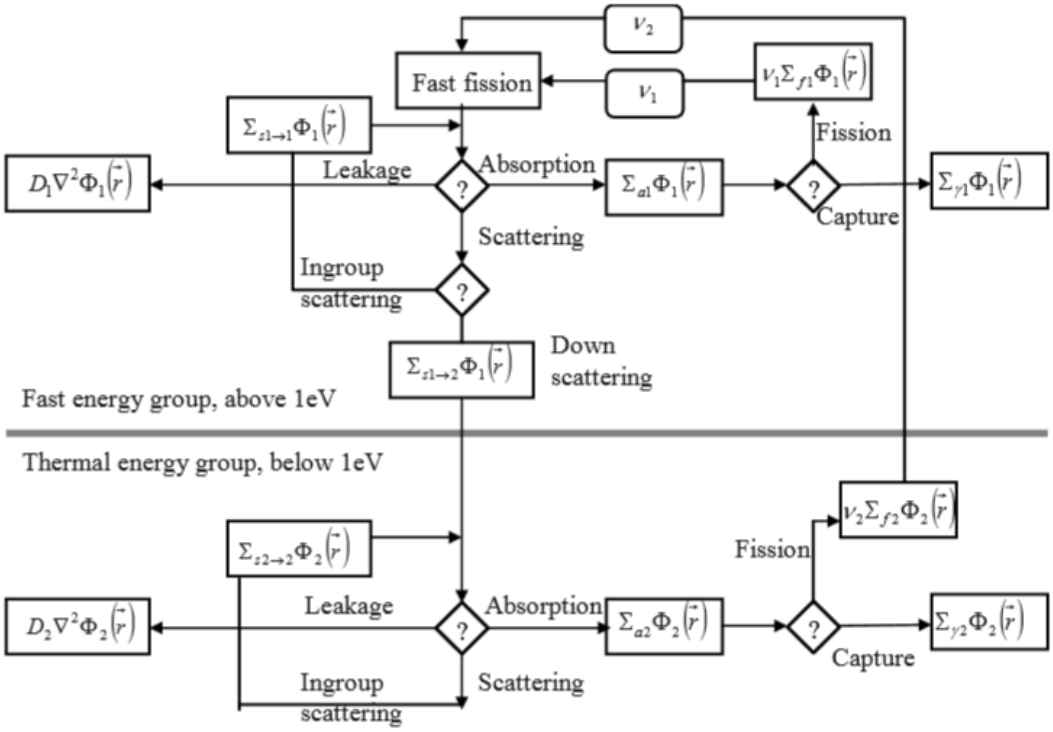

Figure 4.9: Schematic Representation of Two-Group Diffusion Equations

The keff factor by considering the two groups can be expressed from the fast energy group balance which can be written as

$$D_1\nabla^2\Phi_1(\vec{r}) - \sum_{a1}\Phi_1(\vec{r}) + S_1(\vec{r}) = 0 \qquad (4.43)$$

The balance is written as the fast neutrons produced from the source and the fast neutrons getting thermalize along with the neutrons leaked.

$$k_{eff} = \frac{\nu_1 \sum_{f_1} \Phi_1(\vec{r}) + \nu_2 \sum_{f_2} \Phi_2(\vec{r})}{-D_1 \nabla^2 \Phi_1(\vec{r}) - D_2 \nabla^2 \Phi_2(\vec{r}) + \sum_{a1} \Phi_1(\vec{r}) + \sum_{a2} \Phi_2(\vec{r})} \qquad (4.44)$$

In the process of fission the thermal neutrons are absorbed and some of the fast neutrons are thermalized and the population gets balanced this relationship can be expressed as k_{inf}/p and the source term can be replaced with the help population balance and the equation four is converted in the form of equation 4.45 and this is used to ass in the code to develop fast neutron balance

$$D_1 \nabla^2 \Phi_1(\vec{r}) - \sum_{a1} \Phi_1(\vec{r}) + \frac{k_\infty}{p} \sum_{a2} \Phi_2(\vec{r}) = 0 \qquad (4.45)$$

Thermal energy group neutrons balance can be written in the similar pattern for the balance of source and the absorption and interaction with the nuclei.

$$D_2 \nabla^2 \Phi_2(\vec{r}) - \sum_{a2} \Phi_2(\vec{r}) + S_2(\vec{r}) = 0 \qquad (4.46)$$

In case of converting the fast neutrons into the thermalized neutrons, along with the source some extra neutrons are also added to the group. The probability of which the fast neutrons converted into thermal neutrons can be written as

$$D_2 \nabla^2 \Phi_2(\vec{r}) - \sum_{a2} \Phi_2(\vec{r}) + p \sum_{a_1} \Phi_1(\vec{r}) = 0 \qquad (4.47)$$

To calculate thermal and fast flux distribution of the neutrons inside the reactor system can be expressed as

$$\nabla^2 \Phi_1(\vec{r}) + B^2 \Phi_1(\vec{r}) = 0 \qquad (4.48)$$

$$\nabla^2 \Phi_2(\vec{r}) + B^2 \Phi_2(\vec{r}) = 0 \qquad (4.49)$$

The bulking of both the systems is quite similar since the effect of buckling calculated for geometries but not for the neutron groups, In the current woke single buckling effect is consider in the forms given below

$$-(D_1B^2+\sum_{a1})\Phi_1(\vec{r})+\frac{k_\infty}{p}\sum_{a_2}\Phi_2(\vec{r})=0 \qquad (4.50)$$

$$-(D_2B^2+\sum_{a2})\Phi_2(\vec{r})+\frac{k_\infty}{p}\sum_{a1}\Phi_1(\vec{r})=0 \qquad (4.51)$$

Keff is calculated from the buckling relations and it is equated to one

$$k_{eff}=\frac{k_\infty}{(1+L_1^2B^2)(1+L_2^2B^2)}=1 \qquad (4.52)$$

Where,

$$L_1^2=\frac{D_1}{\sum_{a1}} \qquad (4.53)$$

$$L_2^2=\frac{D_2}{\sum_{a2}} \qquad (4.55)$$

The groups considered for calculating in three cases in the form of fast neutrons and the thermal neutrons are given in the table 4.2. The fuel is used in the form of Uranium-Carbon-Fluorides mixture and the atomic configurations are given the table 4.3, and the enrichment levels considered in the case 1 is practically difficult to design a system. Since the availability of highly enriched gaseous form is difficult and the temperature control within the material contains is not possible. Since the enrichment percentage is high the core diameter is reduced to 110 cm and in the other cases the core diameter kept at 150 cm. The fuel temperature are

varied different cases, intial case is kept at 10000k and the other analysis is conducted at 4400 K, since the temperature is essaly attainable and thermal-hydraulic management is comfortable. The model selected for GCR to investigate neutronics is based on mass distribution and uniform tempratures.

Table 4.2: The Neutrons Groups Considered In the Analysis of Three Cases

Parameter	Group 1	Group 2	Group 1	Group 2	Group 1	Group 2
D (cm)	1.35	1.08	1.4	0.4	1.3	0.5
Σ_a (cm^{-1})	0.001382	0.0054869	0.01	0.15	0.008	0.05
ν (neutrons)	2.41	2.41	2.4	2.4	2.4	2.4
Σ_f(cm^{-1})	0.000242	0.00408	0.0035	0.1	0.0015	0.03
$\Sigma_{s\ g,\ g+1}$(cm-	0.0023	0.0	0.01	0.0	0.01	0.0
v (cm/s)	3.0×10^7	$2.2 \times 10^{5`}$	10^7	$2 \times 10^{5`}$	10^7	$2 \times 10^{5`}$
λ(s^{-1})	0.08	0.08	0.08	0.08	0.08	0.08
B	0.0064	0.0066	0.0075	0.0076	0.0074	0.0074

The reactivity coefficients of various properties are investigated, uniform reflector tempratures is assumed and the relation with the reflector temperature and the multiplication factor variations are studied.The model consider in the investigation is from Dam and Hoogen boom. In the analysis three different core setups are considered in analyzing the effects, the calculations are conducted using the code given in the appendix b. The enrichment levels are varied with the

notion that the gaseous form of uranium with high percentage of enrichment is a costly affair. The models are divided into three cases and here after the reference moves to case1, case 2 and case 3. The fuel enrichment variation creates huge impact on the reactor thermal power, and the behavior of neutron and the reactor energy levels.

Table 4.3: The Core Models Used for Analysis with Change in Enrichment

	Fuel Mixture	Fuel Enrichment	R_c (cm)	T_f	T_r
Case 1	0.7:0.3:4.0	50 %	118	10000	2200
Case 2	0.7:0.18:4.0	30 %	150	6400	1900
Case 3	0.7:0.18:4.0	5%	150	4400	1200

The neutron reflector thickness optimization and the wall temperature need to be maintained are two important aspects of the analysis. In this work graphite reflector is selected with uniform temperature density. The fuel composition used in this work is with 50 % enrichment, derived fuel from U235, the U-C-F system contains a specific percentage of UF_4 and in molar fraction of CF_4 composition. The pressure obtained in the system from the heat transfer analysis is at 100 bars and variation of pressure with temperature does not affect the criticality and neutron behavior for a specific configuration. Since the variation is throughout all the parameters of the system. Using the Monte Carlo method probability functions is generated and the Eigen values are created in the form of matrix for thermal group and also with the fast neutron group. The code follows individual neutron tracing technique and identifies the interactions.

4.4.1 CRITICAL DENSITY CALCULATION

The total atoms density of the fuel gas is to be evaluated and the critical fuel density factor need to be evaluated for all the cases and the data is read by the code from the data libraries in the form of UF_4, UF_5 and UF_6. The critical density varies with the temperature of the gas composition at which the reactor system is operated. In this evaluation three different cases are analyzed at two different temperatures. The critical density is denoted by n_c, in order to estimate the neutron criticality the fuel density need to be evaluated. Using the data available at the given temperature for three cases the uranium fuel density is estimated by

$$n_U = \frac{f_U}{f_U + f_C + f_F} n_c \times 10^{30} \tag{4.56}$$

The molecular structure of the uranium and carbon and floride are bonded together to form uranium floride compositions and the floride bonding becomes more in terms of atomic ration UC_4 compound will form. The molecular fuel density is represented by nand which can be found from critical density.

$$n = n_U + n_C = \frac{f_U}{f_U + f_C + f_F} n_c \times 10^{30} \tag{4.57}$$

In evaluation of core pressure the molecular density n plays an important role since p is calculated from $p=nkT_f$, k is Boltzmann Constant

4.4.2. NEUTRON MEAN FREE PATH

The source term is considered in the calculation of neutron mean free path. In GCR the length of source is distributed along the center of the reactor. Since the gaseous form of fuel is used the neutron mean free path is comparatively high with solid core reactors. In the investigation of keff variations in the reactor the

calculated data supports with identifying the variations in the reactor system. The neutron mean free path length is different for the source term, leakage term, as well as absorption term. The neutron reaction rate accounts in the investigation of the multiplication factor. In the calculation of neutron men free path four neutron energy levels are considered at 2.8 ev, 4.32 Kev, 112 keV and 20 Mev. The neutron mean free path length for the source can be calculated from the microscopic cross section.

$$\sum_i = \frac{RR_i}{\phi} \tag{4.58}$$

$$l_i = \frac{1}{\sum_i} = \frac{\phi}{RR_i} \tag{4.59}$$

4.4.3 SPECIFIC POWER DENSITY

The specific power density indicates the power produced per specific quality of fuel inside the reactor system. With the input values of the fuel temperature and the reactor core temperature distribution is useful in calculating specific power density. The values can be compared with the radial position of the core since the generation rate difference from different radial positions. The reactor radial power if given by

$$P_s[kW/kg] = \frac{\mathrm{Re}actor..Thermal..Power}{Total..Mass..of..fissionable..material} \tag{4.60}$$

The specific power density is also calculated based on the specific power caluclated along the radial direction of the reactor.

$$f(r)[W/kg] = \frac{Fission..Power..Density..at..r}{Uranium.Density..at..r} \tag{4.61}$$

The reactor core where fuel occupies the cells is divided into specific power zones and in the current analysis 10 zones are considered to calculate the total power distribution along the cells.

4.4.4 FUEL DENSITY REACTIVITY COEFFICIENT

In the criticality analysis the fuel density of a reactors place an important role, since the pressure and the temperature are continuously varying with the reactivity and the number of neutrons present at a particular instant. In order to account the neutron production and the criticality the fuel density reactivity coefficient need to be calculated. The keff values are calculated for corresponding fuel densities. The coefficient of fuel density is express in terms of atomic fuel density and reactivity coefficient.

$$\alpha_n^{'} = \frac{n_f}{k}\frac{\partial k}{\partial n_f} \tag{4.62}$$

The absolute reactivity coefficient is expressed in equation 4.63, but throughout the work the normalized values are interpreted, since the units are not so reasonable for understanding.

4.4.5 FUEL TEMPERATURE REACTIVITY COEFFICIENT

For a reactor to operate at stable conditions the reactivity temperature should be maintained at a stable value. In gas core reactors the idea of maintain stable fuel tempratures reactivity coefficient is to operate the reactor at a specific criticality. The reactivity coefficient is expressed as

$$\alpha_{T_f}^{'} = \frac{\partial k}{\partial n_f} \tag{4.63}$$

In case of highly enriched fuels the reactivity coefficient varies with small changes in the reactivity, in the reactor core besides the fuel. The propellant is also entered into the reactor, but the molecular weight balances the flow and the pressure deference maintained in the process of really supports the reactivity. The velocity ratios maintained in the fuel flow rate are at 100:1, so that the fuel flow rate is regulated.

4.4.6 REFLECTOR TEMPERATURE REACTIVITY COEFFICIENT

The reflector plays an important role in reactivity inside the core; the reflector tempratures is inversely proposal to the reactor criticality. The tempratures reactivity coefficients define the stability of the reactor system; the coefficient of the reflector tempratures is given below.

$$\alpha T_r = \frac{\partial k}{\partial T_r} \tag{4.62}$$

The thickness of the reflector material affects the neutron absorption and the criticality of the reactor operation.

4.5. RESULT AND DISCUSSIONS

The analysis conducted for three cases at different enrichment levels to investigate the behavior of the neutrons inside the reactor and the effect of various parameters like reactivity coefficients, multiplication factors are investigated for the same geometry. The grid generated in this particular solution is of high accuracy. The results are converged at higher degrees of freedom and within less amount of time. The residual plots in calculating the keff values with respect to degree of freedom are given in the figure 4.10. In the analysis case got converged a very fast rate since the percentage of enrichment is high and the neutron

distribution is enormous in count. So the criticality values are easily above 1 so that the percentage of error in his case is comparatively less and the error level almost all went to the level 0000.2 and in the other cases the error levels are also less but in case of case three the enrichment levels are very low so the error obtained in keff calculation is reached to 0.0005 and all these results are satisfactory and can be comparable with the real time models.

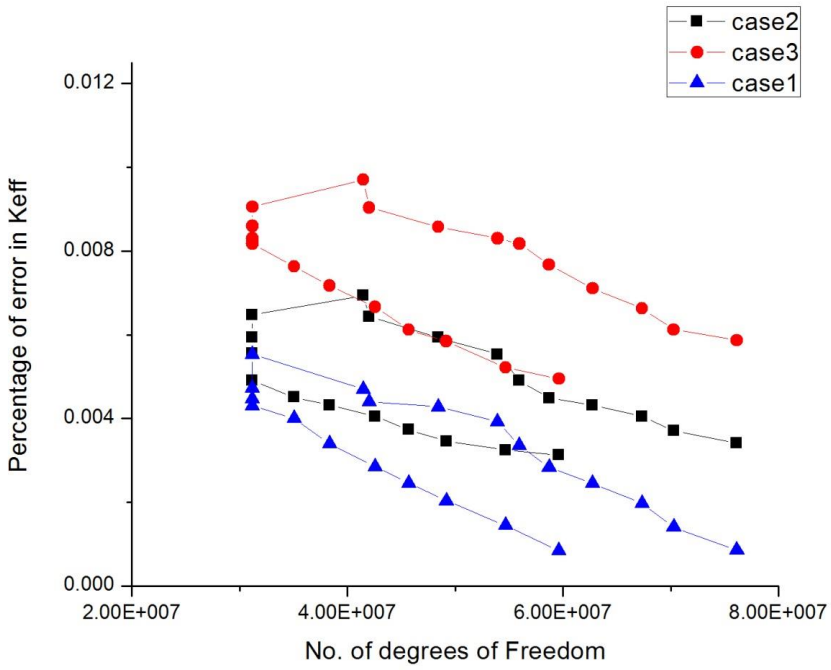

Figure 4.10: Residuals of the Code for Three Cases

The initialization of the solution started with the guess values from the boundary conditions inputted from the input desk file and the error obtained in the intial iterations are comparatively low. The convergence criteria is not set for the keff maximum value rather it was obtained from the specific density value based on the Temprature value given as a input.

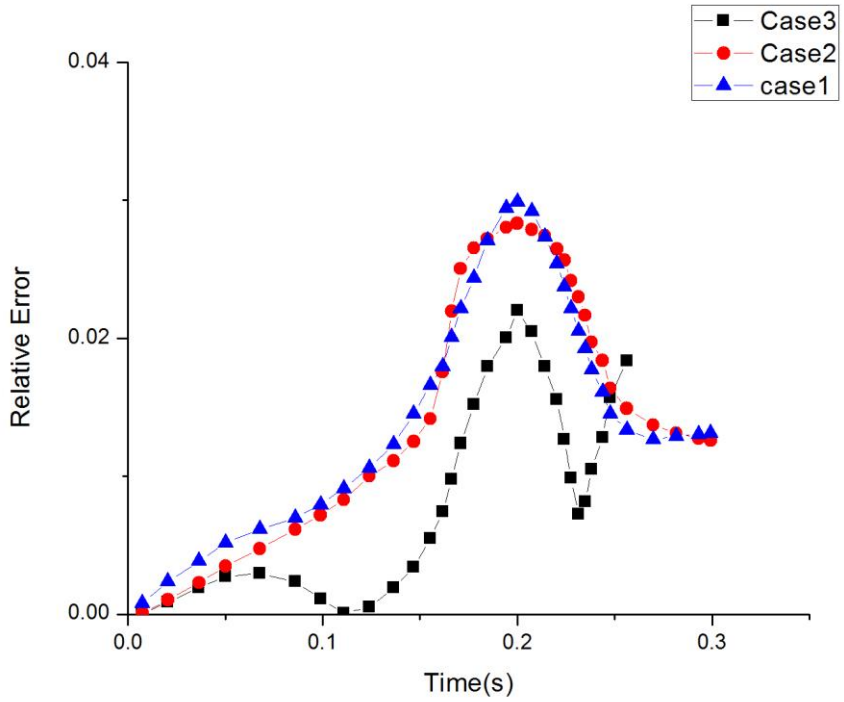

Figure 4.11: The Solution Accuracy and Change of Relative Error through Time

The accuracy of the solutions depends upon the time at which the relative error stars coming down and the where it stabilized. In case of high enriched uranium based case initially it went up and the value has come down very fast and at 0.25 seconds the value starts stabilizing. In case of 30 % enrichment levels the solution got stabilized with in the similar time lines. In the calculation of third case the time initially has come down and the error levels increased and then stabilized at 0.28 sec. The overall results obtained from the Monte Carlo based code are satisfactory and the results are discussed in his chapter with the merits in the reactor model.

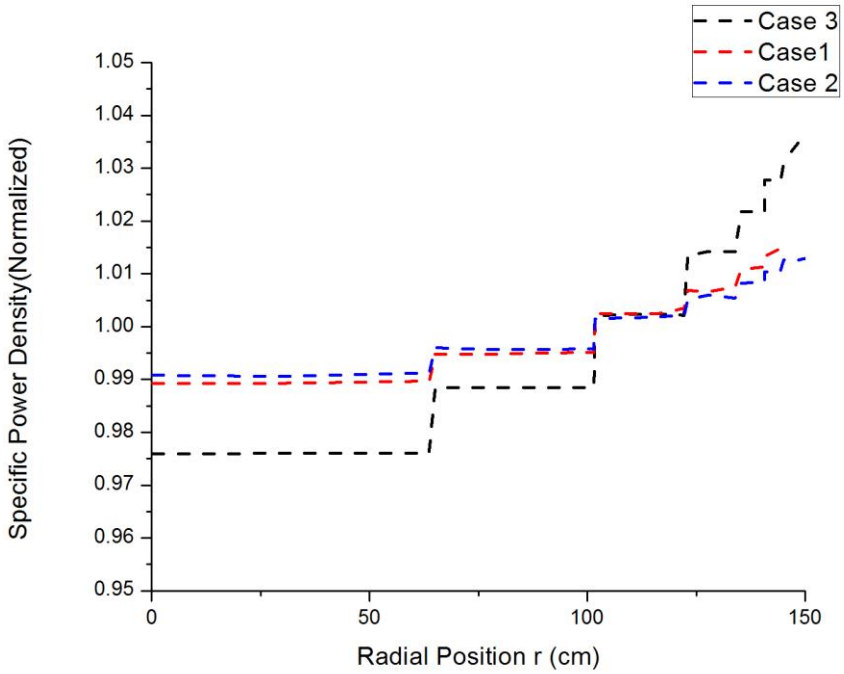

Figure 4.12: Normalized Specific Power Density for three cases

In all the three cases the normalized specific power density with respect to the radial position is calculated as per the enrichment levels mentioned. In case of 5 % enriched fuel the specific power density is comparatively low for the specified geometry configuration and it is touching 0.99 at the 100 cm radial position. In case of high enrichment levels the specific power density maintained at 0.99 at the intial stage and later stages the value started growing with the radial position. Since the enrichment levels and the atomic compositions vary in case of 30 % enrichment and in case of 50% the relative effects are comparatively low in case of 50 % enrichment. The radial distance place an important role in handling the heat transfer. The calculations are done for cell difference in specific power density for all the cases. The normalized values are plotted to compare all the three cases aginest the change in radial position.

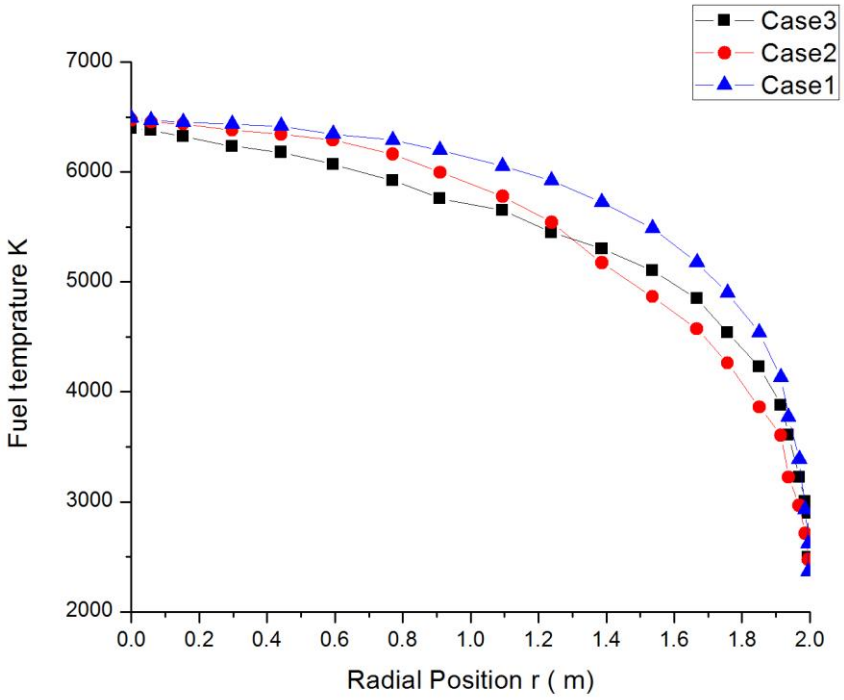

Figure 4.13: Effect of Radial position on fuel Temperature in Three Cases

The fuel tempratures is calculated with respective to the radial position for three cases , in case one the fuel tempratures is maximum at 100 cm and reaching above 6800 k and the tempratures starts decline when the buffer interactions starts transferring the heat. Since the fission zone liberates the heat and transfers to the propellant in case three the fuel tempratures initially high and it starts decline when the radial position varies. In the core estimated. The figure 4.13 explains the radial position effects on fuel tempratures along the core. The idea is that when it cross the buffer zone the overall heat is effectively transferred to the propellant. The effect of fuel gas density on neutron density is calculated using the cumulative probability functions inside the core for three cases. Since the enrichment levels different in three cases the plots are generated individually, and the result are taken on a residual scale to indicate the neutron fluctuations.

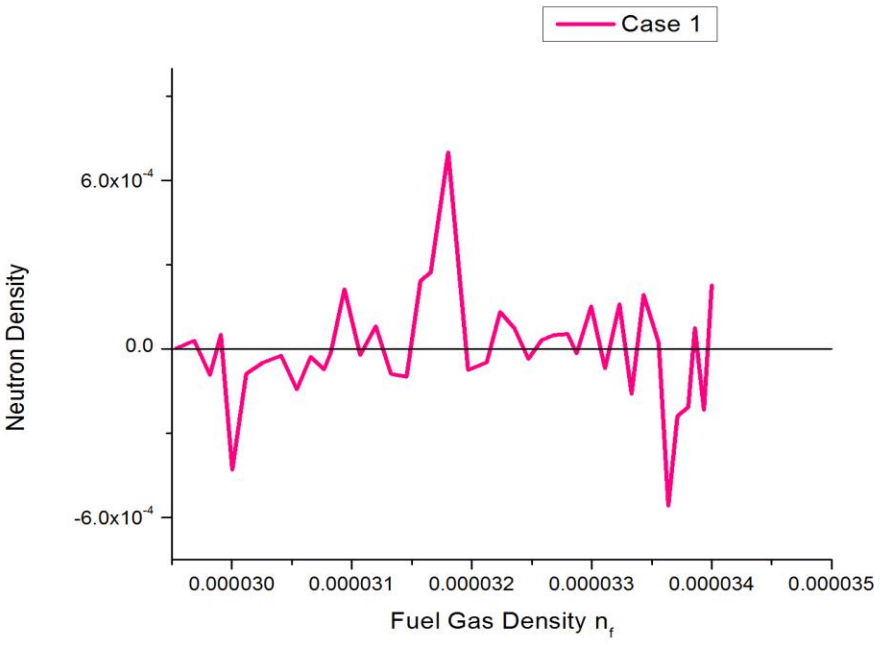

Figure 4.14: Effect of fuel gas on neutron density for Case 1 with 50% enrichment

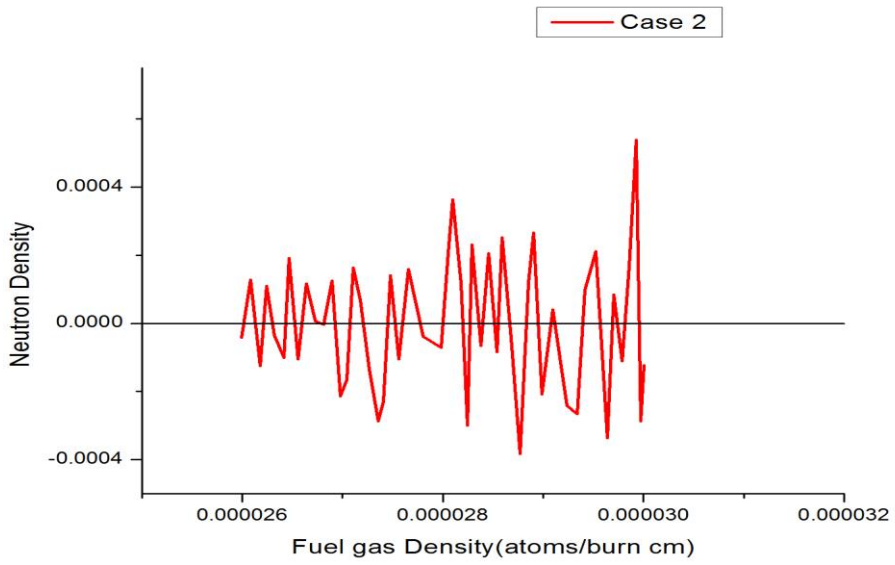

Figure 4.15: Effect of fuel gas on neutron density for Case 2 with 30% enrichment

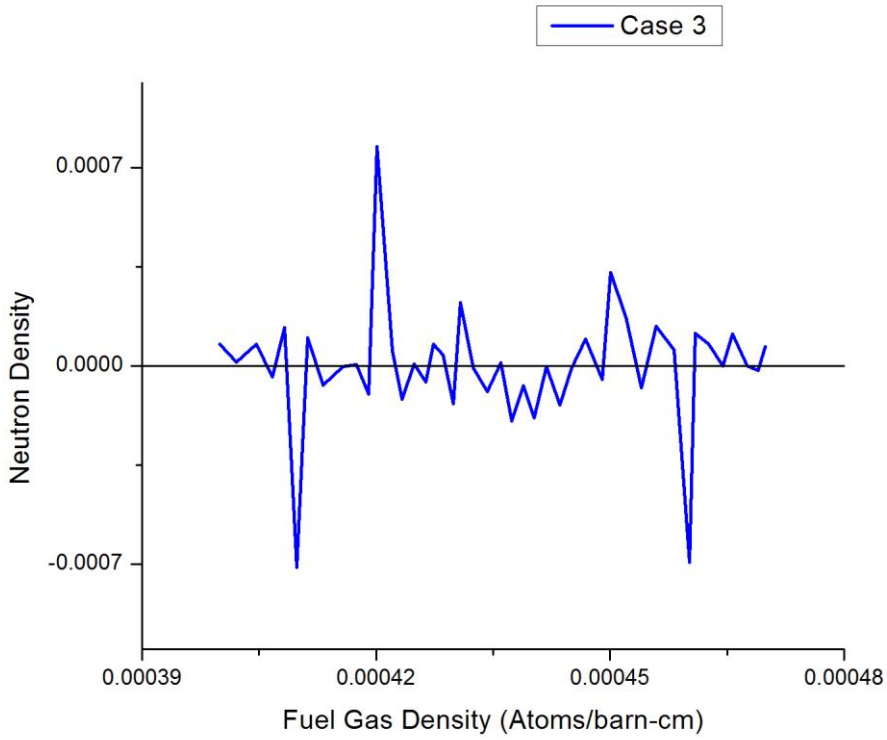

Figure 4.16: Effect of fuel gas on neutron density for Case 3 with 5% enrichment

In case 1 the enrichment levels are 50 % the neutron density fluctuations are comparatively low and the peak value is obtained at 0.000315 since the criticality and the tempratures levels do effect the neutron population. In case 2 the enrichment levels considered is at 30% and the fluctuations are high since the core geometry is not changed and the maximum values reached at 0.00030 atoms/barn-cm. In case 3 the enrichment levels are maintained at 5 and which is more nearer to the real life reactor operations. The fuel gas densities variation is also an effect of radial Temprature distribution along the length of the core. Due to the neutron mean free path length the interaction can continue till the heat reservoir region.

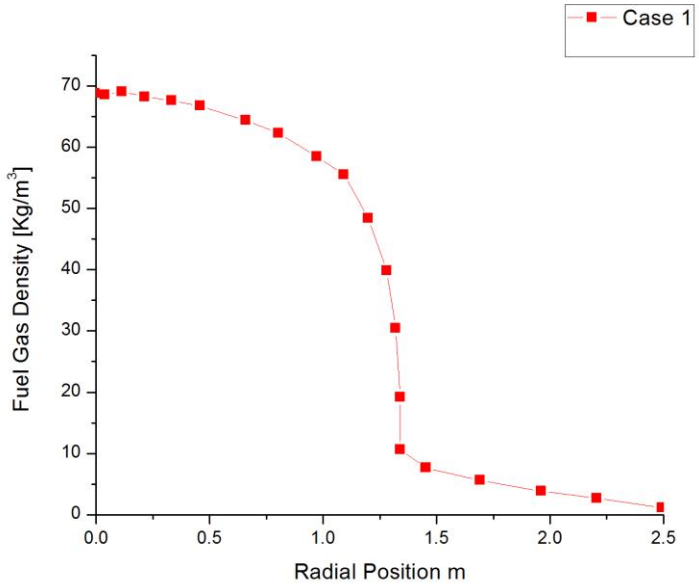

Figure 4.17: Variation in fuel gas density through radial position for Case 1

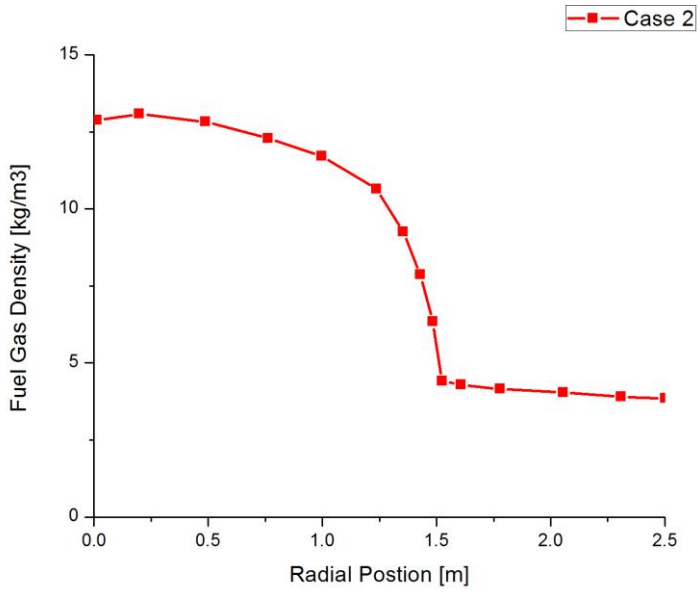

Figure 4.18: Variation in fuel gas density through radial position for Case 2

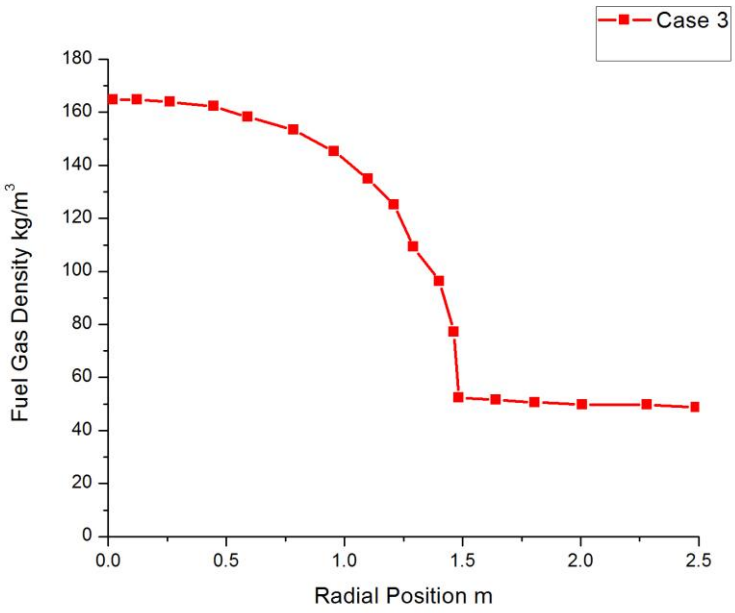

Figure 4.19: Variation in fuel gas density through radial position for Case 3

Variation in fuel gas density is calculated for the gas core reactor system and the results are plotted its change over radial position for three cases. In case one the critical density is considered at 3.18×10^{-5} atoms /burn-cm and the calculations are done up to the tempratures range of 10000 K and the reactor power obtained in this case is at 962.2 Kw with a chamber pressure of 48.49 and the maximum tempratures that can be attainable under highest value of fuel gas density at60 kg/m^3 and tempratures resulted in 14624 K. in case of 30 % enrichment the atoms/ Burn-cm is chosen as 2.833×10^{-5} and the fuel tempratures maintained inside the core is at 4400k at which the reactor is able to produce 104.4 kW of power at 8.477 bars of pressure and the maximum attainable tempratures at peak fuel density is 6048. In case of 5 % enrichment levels the reactor system operated at the same tempratures with critical density of 4.37×10^{-4} atoms/ b-cm with

power levels of 40.5 and the pressure maintained is relatively high at 96.84, the peak value of the tempratures attainable at 162 kg/m^3 fuel density.

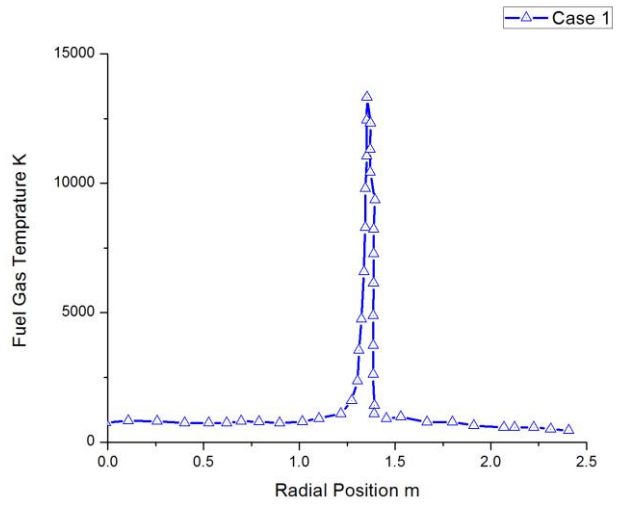

Figure 4.20: Fuel Gas temperature along the radial direction of the core for case 1

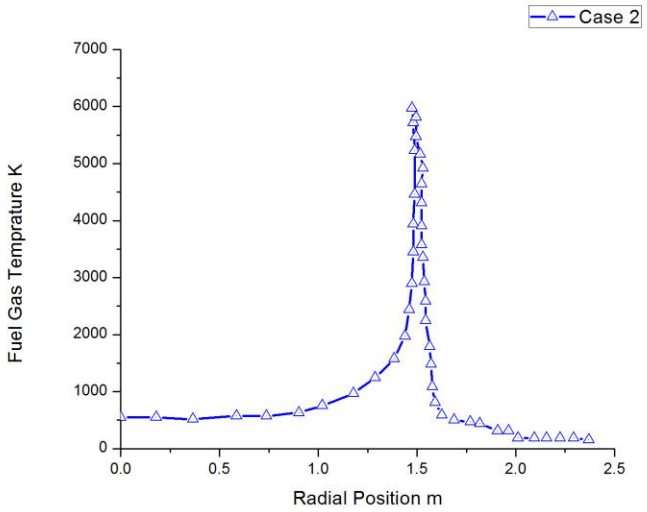

Figure 4.21: Fuel Gas temperature along the radial direction of the core for case 2

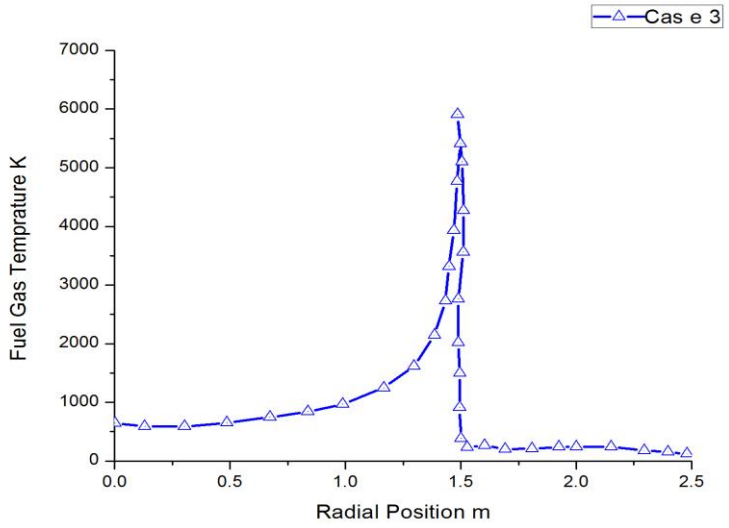

Figure 4.22: Fuel Gas temperature along the radial direction of the core for case 3

The variation in fuel gas density with respect to the radial position is studied for the three cases with the variation in tempratures. The fuel gas tempratures also affects overall reactor power and the criticality of the reactor system. In case of 50% fuel enrichment the maximum fuel gas tempratures. In the intial stage the fuel enters the reactor core and the start gaining the heat due to the core conditions and starts participating in the fission reaction. In the process the fuel gas tempratures reaches the peak and then transfers the heat to the propellant and then the fragments tempratures comes down. In case one the maximum tempratures reaches to 10000 k at the center of the geometry in radial direction. In case of 30 % enrichment the level falls down to the 7000 K, in case of 5% enrichment the maximum fuel gas tempratures is in the range of 6000 K. The variation in fuel gas tempratures affects the reactivity in the core, the uniform temperature assumed in calculating neutronics by considering its peak value at a specified radial distance. In case of coupled solutions the results obtained from

the neutronics of the system can be taken in a computational fluid dynamics code to obtain complete radial distribution.

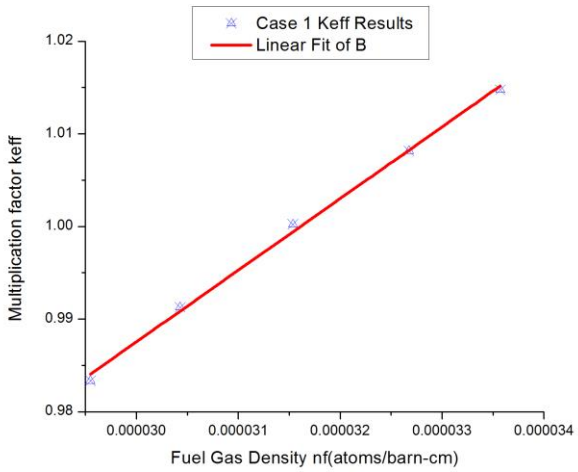

Figure 4.23: Keff variation with the change in Fuel Gas Density for Case 1

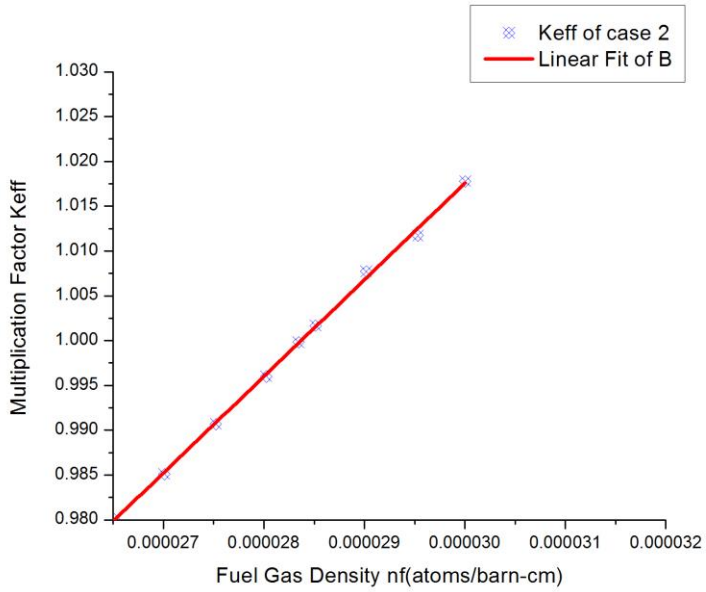

Figure 4.24: Keff variation with the change in Fuel Gas Density for Case 2

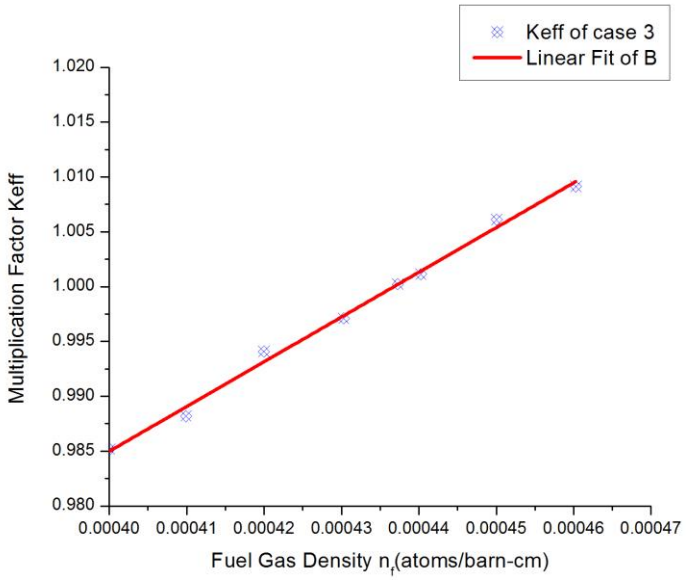

Figure 4.25: Keff variation with the change in Fuel Gas Density for Case 3

The multiplication factor keff is calculated for the relations mentioned in the methodology 4.2, and the effect of various parameters on the criticality of the reactor is studied. These effects are studied for three cases and the results are compared by curve fitting and critical points are identified in case of keff. In case 1the critical point can be found at 0.28 specific reactivity coefficients at 3.18×10^{-5} atoms/b-cm. These plots are used to find the critical density point by creating the linear fit for all the three cases. In case 2 the critical fuel density is at 0.31 with specific reactivity coefficients 2.833×10^{-5} In case three the critical fuel density is at 0.18 with a specific reactivity coefficient of 4.370×10^{-4}. In all the three cases the least value is to the less enriched fuel due so that the multiplication factor also is less for reactor operated at 5% enrichment. The variation in fuel density occurs due to the change in reactor pressure and tempratures. Radius of the core varied in case of 50 % enrichment and other cases the radius considered for the core is at

150 cm, in case one it is 118 cm. In order to handle larger core the fuel need to be supplied and the reactor criticality are too high.

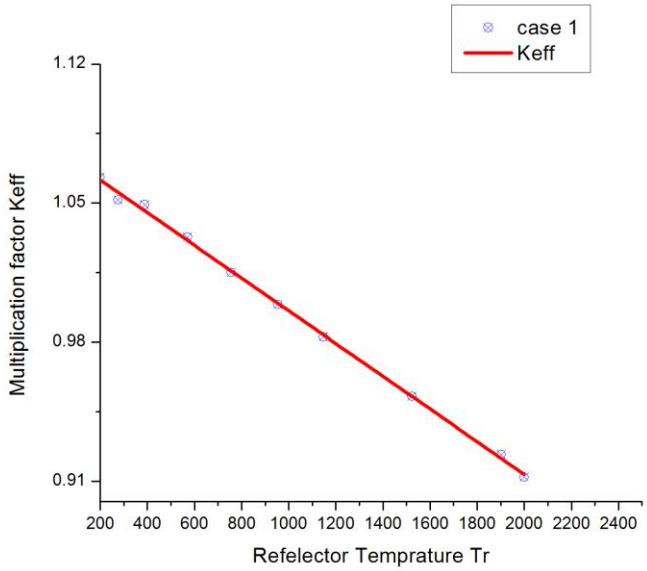

Figure 4.26: Effect of Reflector Temperature on Keff in case 1

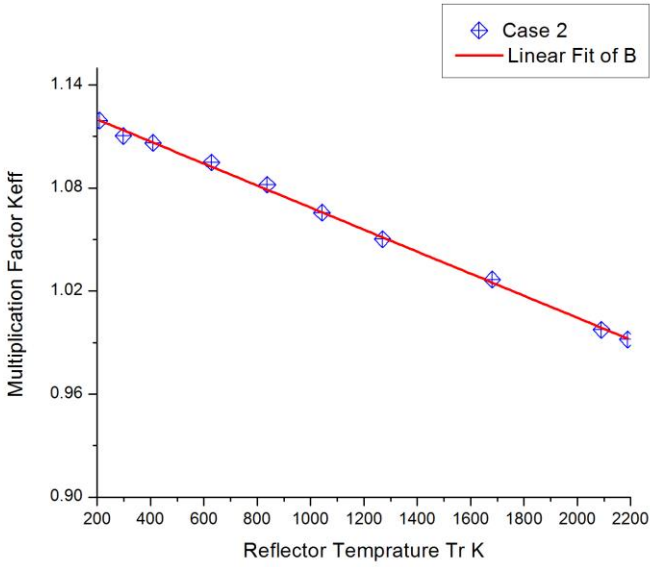

Figure 4.27: Effect of Reflector Temperature on Keff in case 2

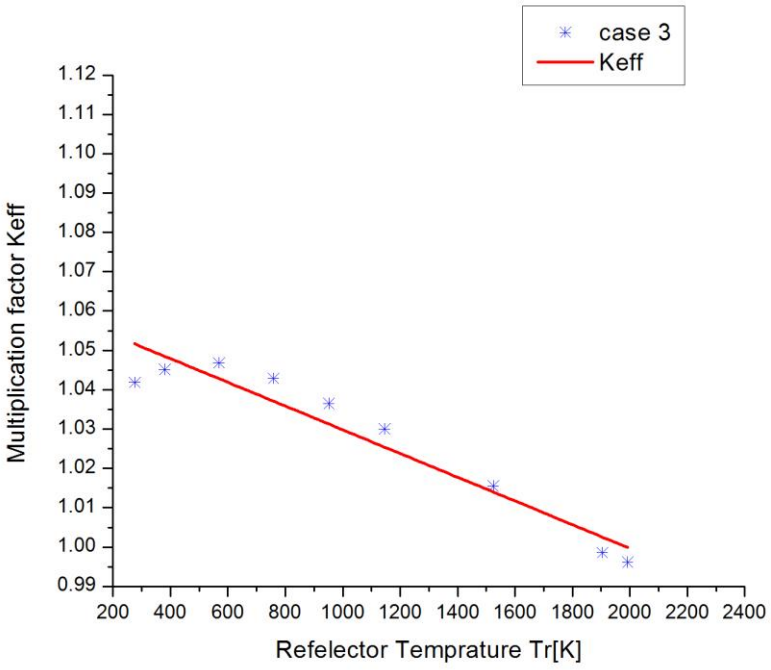

Figure 4.28: Effect of Reflector Temperature on Keff in case 2

Reflector plays an important role in core design of the reactor system. In case of highly enriched fuels the thickness of the reflectors should be high, this is represented in the graph 4.30 and it illustrates for the three cases the effect of reflector thickness on the reactor criticality. The reflector tempratures plays an important role in neutron absorption, in order to maintain the reactor core at the required criticality it should be operated at lower reflector tempratures. In case of gas core reactors creating a specific cooling cycle to the reflector walls improve the complexity of the system and which is not a feasible solution. In such cases the propellant flow Chanel is passes thought he reflector walls so that the desired reflector tempratures is maintained. In case 1 the reflector tempratures need to be maintained within the range of 1900 k to have higher keff factor since the neutron absorption leads to decrease in reactivity. In case 2 this can even manageable to reach 2200 k of the reflector tempratures. In case three the effect is not because of

the tempratures rather the most significant parameter can be reflector thickness and then the tempratures upper limit can be at 2200 K to 2400 K.

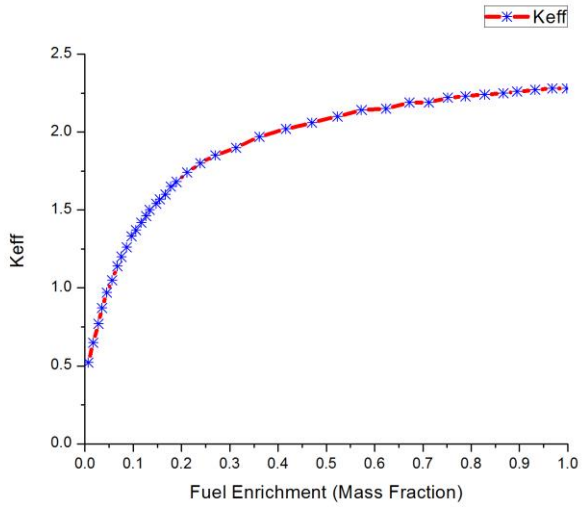

Figure 4.29: Enrichment vs. Keff for Representative Core

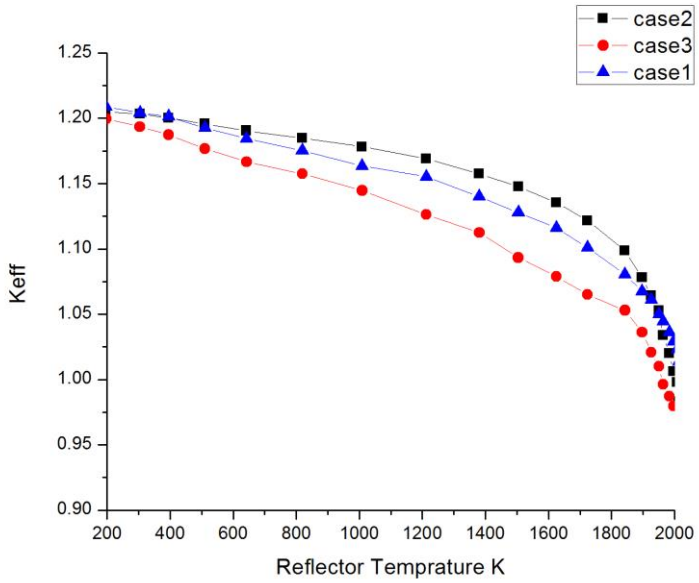

Figure 4.30: Change of Keff with the Increase in reflector Temperature

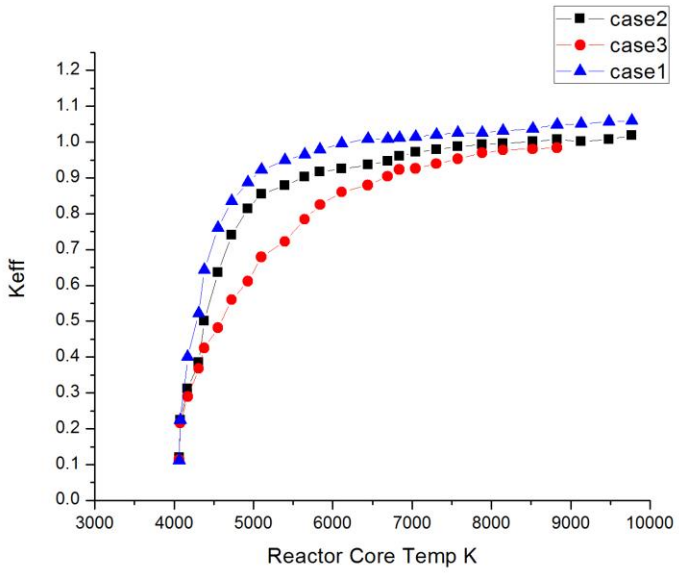

Figure 4.31: Change of Keff with the Increase in reactor core Temperature

The major factors that affect the reactor criticality are reactor core tempratures, fuel enrichment and the reflector tempratures. In all the three cases the results are compared with the parameters that can affect the system stability. A generalized relation is drawn to the fuel enrichment and the keff values for three cases since the fuel enrichment is different and it do effects the reactor criticality under similar radial positions. The major effect on criticality by reactor core tempratures is calculated for three cases and the results are plotted in 4.29, which represent the increase in criticality at higher reflector tempratures. In case one the peak keff value is obtained at 6000 K and the variation is very much limited till 10000 K. Since Keff is just not dependent on reactor core tempratures rather many factor like reflector tempratures and the critical fuel density also affect them. More interestingly the results indicate the enrichment levels differentiate the level of criticality reached by a reactor system with a specified operating tempratures. In case two and three the keff value of 1.02 is reached at 6000K at the same core

radius. In case 3 the enrichment level are low so the tempratures variations are very much effective.

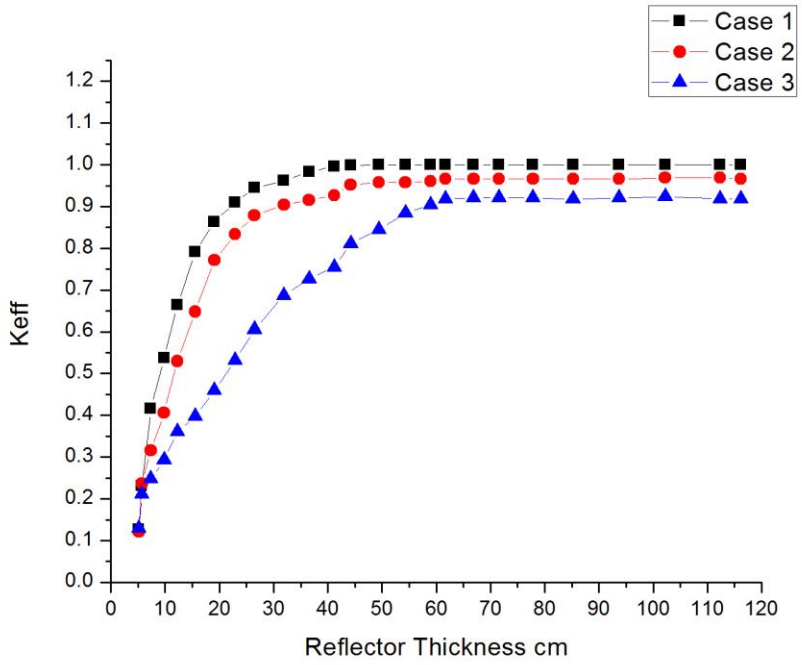

Figure 4.32: Change of Keff with the Increase in Reflector Thickness

The material of the reflector and its thickness are two important parameters in designing a reactor core. The effective reflector thickness suggest for case 1 with graphite as a reference can be at 40 cm to 100 cm based on the reflector tempratures at which reactor core is exposed. Besides the reflector thickness the wall tempratures limitations also play an important role in neutron criticality analysis. In case 2 the reflector thickness is effected the keff and get stabilized with the maximum operational tempratures of the reactor core. In competition with the various cases with effecting parameters are giving an idea how criticality is maintained in a reactor so that higher power densities are investigated in the reactor system.

CHAPTER 5: CONCLUSIONS AND POSSIBILITIES FOR FUTURE WORK

In the previous chapters both the neutronics and heat transfer analysis results are presented with a detailed explanation. This chapter deals with the specific conclusion obtained from the work and the future developments that can be possible for GCR experimentation. The important parameters that affects the reactor criticality is studied in neutronics in a confined geometrical shape with a variation the fuel enrichment and the composition. The specific idea is to choose the best model for the interstellar travel or such kind of long distances in light years by using current technological possibilities. The kinetic heat transfer and dissociation of heat affects the stability of the reactor and the neutron generation rate. In such cases the fission reaction in a core is uncontrollable; in case of ground reactors different mechanisms are used. The core Temprature and pressure control impacts the reactor operation and its criticality.

5.1 CONCLUSIONS

The flow and criticality analysis conducted on gas core nuclear reactor to quantify the effects of fuel and propellant tempratures and densities on both the generation rate as well as on neutronics are given a particular attention. The effects are considered from an uncoupled fission zones and the maximum heat generation rates with in the design parameters. This work completely determined the fuel gas density effects and reflector Temprature variations on the criticality of a gas core nuclear reactor with an infinite length. The large reactivity coefficient of the fuel gas affected the criticality and density variations also affect the neutron flux in a given core. The reflector temperature affects the neutron spectra because of large mean free path of the GCR core. The Temprature distributions in the radial directions affect the isotropic interactions there by reactivity steps down in case of

less enriched fuels. In case of highly enriched uranium fuel the coefficient of fuel density varied from 0.36 pcm/K to -6.4 pcm/K, whereas in case of 5 % enriched fuel the variation is at 0.21 Pcm/ K to the -0.3 pcm/K. This indicates in case of higher enrichment GCR core the density fluctuations create a variation in the reactivity interactions. In case of 5 % enrichment there is a sharp rise of the keff due to the density fluctuation in the reactor core and the thickness of the reflector also affected the reactivity coefficient. In case of higher enriched fuel usage with an effective thickness of graphite reflector has shown a neutron prompt removal time in 0.03 sec it may improve the reactivity and some time it can reach maximum criticality values. At the maximum thickness suggested in the results has a peak value of criticality at 0.98 and can be improved by a fraction of 0.02 with the change of material. In case of 30 % enrichment the U-C-F composition need to be taken as proposed whether the atomic ratio of U and F are high and can be a suggestible compound in the form of UF_6 so the results shown in the neutronics analysis supports the operation with higher criticality factor.

In heat transfer analysis the dissociation effects and kinetic heat transfer through convection and radiation are studied to develop conclusions on maximum heat transfer rate and the effectiveness of the core design at a given fuel enrichment. The flat Temprature profile has been observed in the case of higher generation rates at 50 % fuel enrichments. The decrease in fuel enrichment effected the radial Temprature distribution along the core and the maximum fuel gas Temprature reached in the case of 5 % enrichment is around 4500 K with a reactor pressure of 2.4 Mpa. The difference in overall pressure and Temprature distribution is not much in case of hydrogen and helium, whereas effects are more on the side of the reflector wall Temprature. The Temprature correction that can be made by using helium can be of 1% decrease in reflector wall Temprature. The same fraction can be obtained through using different cooling channel mechanism for the input of

propellant into the core. In the benchmark calculations conducted on different generation rates resulted in creating a variation profile between the core pressure rise and the dissociation energy along the center of the core. The difference is visible in first two cases in a fraction of two and then the difference has reached of order 10. This indicates the radiative fluxes dominate the overall heat transfer in a reactor core.

5.2 DISCUSSION FOR FUTURE WORK

The code can be future developed to add one speed neutronics equation, multi group diffusion equations to solve on different geometries. Creating mode libraries to solve different grids for different geometries can be considered. A coupling can be written to analyze coupled neutronics and the thermal-Hydraulics for every fission zone; more fission groups can be analyzed with such kinds of libraries in the code. The current work focused on uranium gaseous fuel derived from U-235 in the composition of U-C-F, in the future studies there can be a great potential in comparing U-233 for nuclear rocket and conversion methods into gaseous state. In case of Am-239 very limited work is available, but there is a greater potential with the compound to develop most powerful rocket reactors. In case of reflector selection graphite was considered due to its characteristics of both reflecting ability as well as to use it as a moderator to slow down the neutrons. In case of manned missions nuclear rockets needs external radiation shields, in such cases Beo is used because it can act as a reflector and shielding material. The neutronics analysis can be conducted with a coupled approach to investigate the core behavior with the Beo reflector without having much moderating ability.

In order to develop a GCR system experimentally hydrogen, helium handling need to be studied completely for chamber parameters design in later stage

neutron investigations can be done. In the current developments only experimental facilities available for handling hydrogen till 3500 K and the where are the helium is tested experimentally at 1200 K Temprature since it has common practice for gas cooled reactors. In the development of GCR rocket systems the experimental testing on propellant behavior changes the design base done its flow properties and behavior in moderated environments. Before a rocket reactor development some work can be carried out to develop a ground based power generation system with research reactor capabilities to understand its neutronics.

APPENDIX A: SAMPLE INPUT DESK FOR CODE

```
  <! -- Parameters for k-eigenvalue calculation -->
  <Eigenvalue>
    <Batches>15</batches>
    <Inactive>5</inactive>
    <Particles>10000</particles>
  </eigenvalue>

  <! -- Starting source -->
  <Source>
    <space type="box">
      <Parameters>-4 -4 -4 4 4 4</parameters>
    </space>

 </source>
<! -- Parameters for k-eigenvalue calculation -->
  <Eigenvalue>
    <Batches>20</batches>
    <Inactive>10</inactive>
    <Particles>10000</particles>
  </eigenvalue>

  <! -- Starting source -->
  <Source>
    <space type="box">
      <Parameters>-1 -1 -1 1 1 1</parameters>
    </space>
  </source>
<Materials>


  <! -- By default, use 600K cross sections -->
  <defaults>71c</default_xs>

  <!--
      Since O-18 is not present in ENDF/B-VII, it was necessary
to combine the
      atom densities for O-17 and O-18 in any materials
containing Oxygen.
  -->

  <!-- UO2 fuel at 2.4 wt% enrichment -->

  <material id="1">
    <density value="10.29769" units="g/cm3" />
```

```
  <nuclide name="U-234"  ao="4.4843e-06" />
  <nuclide name="U-235"  ao="5.5815e-04" />
  <nuclide name="U-238"  ao="2.2408e-02" />
  <nuclide name="O-16"   ao="4.5829e-02" />
  <nuclide name="O-17"   ao="1.1164e-04" />
</material>

<!-- Helium for gap -->
<material id="2">
  <density value="0.001598" units="g/cm3" />
  <nuclide name="He-4"   ao="2.4044e-04" />
</material>

<!-- Zircaloy 4 -->
<material id="3">
  <density value="6.55" units="g/cm3" />
  <nuclide name="O-16"   ao="3.0743e-04" />
  <nuclide name="O-17"   ao="7.4887e-07" />
  <nuclide name="Cr-50"  ao="3.2962e-06" />
  <nuclide name="Cr-52"  ao="6.3564e-05" />
  <nuclide name="Cr-53"  ao="7.2076e-06" />
  <nuclide name="Cr-54"  ao="1.7941e-06" />
  <nuclide name="Fe-54"  ao="8.6699e-06" />
  <nuclide name="Fe-56"  ao="1.3610e-04" />
  <nuclide name="Fe-57"  ao="3.1431e-06" />
  <nuclide name="Fe-58"  ao="4.1829e-07" />
  <nuclide name="Zr-90"  ao="2.1827e-02" />
  <nuclide name="Zr-91"  ao="4.7600e-03" />
  <nuclide name="Zr-92"  ao="7.2758e-03" />
  <nuclide name="Zr-94"  ao="7.3734e-03" />
  <nuclide name="Zr-96"  ao="1.1879e-03" />
  <nuclide name="Sn-112" ao="4.6735e-06" />
  <nuclide name="Sn-114" ao="3.1799e-06" />
  <nuclide name="Sn-115" ao="1.6381e-06" />
  <nuclide name="Sn-116" ao="7.0055e-05" />
  <nuclide name="Sn-117" ao="3.7003e-05" />
  <nuclide name="Sn-118" ao="1.1669e-04" />
  <nuclide name="Sn-119" ao="4.1387e-05" />
  <nuclide name="Sn-120" ao="1.5697e-04" />
  <nuclide name="Sn-122" ao="2.2308e-05" />
  <nuclide name="Sn-124" ao="2.7897e-05" />
</material>

<!-- Borated water at 975 ppm -->
<material id="4">
  <density value="0.740582" units="g/cm3" />
  <nuclide name="B-10"  ao="8.0042e-06" />
  <nuclide name="B-11"  ao="3.2218e-05" />
  <nuclide name="H-1"   ao="4.9457e-02" />
  <nuclide name="H-2"   ao="7.4196e-06" />
```

```
    <nuclide name="O-16"  ao="2.4672e-02" />
    <nuclide name="O-17"  ao="6.0099e-05" />
    <sab name="lwtr" xs="15t" />
  </material>

</materials>

  <!-- Define how many particles to run and for how many batches
-->
  <eigenvalue>
    <batches>100</batches>
    <inactive>10</inactive>
    <particles>1000</particles>
  </eigenvalue>

  <!-- The starting source is a uniform distribution over the
entire pin
       cell. Note that since this is effectively a 2D model, the
z coordinates
       are inconsequential -->
  <source>
    <space type="box">
      <parameters>
        -0.62992 -0.62992 -1.
         0.62992  0.62992  1.
      </parameters>
    </space>
  </source>

  <!-- To assess convergence of the source distribution, we need
to define the
       bounds for a mesh over which the Shannon entropy should be
       calculated. The extent in the z direction is made
arbitrarily large. -->
  <entropy>
    <lower_left>-0.39218 -0.39218 -1.e50</lower_left>
    <upper_right>0.39218  0.39218  1.e50</upper_right>
    <dimension>10 10 1</dimension>
  </entropy>

</settings>

<tallies>

  <mesh id="1" type="rectangular">
    <dimension>100 100 1</dimension>
    <lower_left>-0.62992 -0.62992 -1.e50</lower_left>
    <upper_right>0.62992  0.62992  1.e50</upper_right>
  </mesh>
```

```
  <tally id="1">
    <filter type="mesh" bins="1" />
    <filter type="energy" bins="0. 4.e-6 20.0" />
    <scores>flux fission nu-fission</scores>
  </tally>

</tallies>
```

C cell cards

1 1 2.9262299E-02-1 2-3 imp:n=1 tmp=6.662234E-08

2 2 8.898912E-02-1 2 3 -4 imp:n=1 tmp=6.662234E-08

99 0 1:-2:4 imp:n=0

C end of cell cards

C surface cards

*1 Beo 50

*2 Beo 50

3 C-F-C 150

4 C-F-C 240

C end of reflector cards

C material cards

C material 1: Inner core, Material 2: Reflector

C Material 3: reflector, Material 4: cladding

M1 6000.60c 8.849109E-03 $C

56136.96c 0.000605532

56130.96c 8.72244E-06 56132.96c 7.78695E-06 56135.96 c 0.000508236

56134.26c 0.000187356 65137.62c 0.00086597 56138.60c 0.005527809

82000.50c 3.8549226E-03 $pb

92235.60c 1.163166E-03

92238.60c 7.685943E-03

M2 28000.50c 8.898912E-02 $Ni

C reflector material follows (39 ACT+100 FP)

C 100 fission products, m701 to m800

C ksr 0 0 0

Mode n

Kcode 3000 1.107 5 120

Prdmp 120 120 120

Print

```
$ MCODE, UF6 fuel, GCR core matrix, H2 propellant, cold condition

TTL Test case    $define title

CEL 1  1  1   2.751209912E+07    7.06858e+06    FFTFC.LIB

$total volume of modeling systems (cm3)

VOL  7.06858E+06

$ ORIGEN files def.

$ Normalization method, 1=flux, 2=power

NOR2

$predictor- corrector (OFF)

COR 0

$ Power Density, opt:WGC=W/gIHM, KWL=kW/(liter core)

PDE 10.61033475 KWL
$points   0  1   2   3   4   5   6   7   8    9   10   11   12   13   14    15   16   17
DEP E     0   5    10   15   20    30   40    50    60   70 80 90  100  120   140   180
200
NMD       40 40 40   40   40    40    40   40    40    40   40   40   40    40    40
40
STA 0    $ Starting point
END 17 $ ending point
```

APPENDIX B: CODE FOR CALCULATING NEUTRONICS

```
/* Author: Gurunadh Velidi, Univ. of Petroleum and Eneergy Studies, 2012-2013 */
/* Supervisor: Dr. Ugur Guven, ITU, 2012-2013 */
/* Run on ITU Server Cray Computer with Permission of Nuclear Energy Institute */
/* Neutron Diffusion Analysis for GCR */

/* @f$Id: @ref step_28 "step-28".cc 28798 2013-03-07 17:00:02Z maier @f$ */
/* */
/* Gurunadh Velidi PhD Thesis */
/* Los Alamos Laboratory Subroutines used by Permission of Dr. Ozgener */
/* */
#include <deal.II/base/timer.h>
#include <deal.II/base/quadrature_lib.h>
#include <deal.II/base/function.h>
#include <deal.II/base/logstream.h>
#include <deal.II/base/thread_management.h>
#include <deal.II/base/parameter_handler.h>
#include <deal.II/lac/vector.h>
#include <deal.II/lac/full_matrix.h>
#include <deal.II/lac/sparsity_pattern.h>
#include <deal.II/lac/sparse_matrix.h>
#include <deal.II/lac/solver_cg.h>
#include <deal.II/lac/precondition.h>
#include <deal.II/lac/constraint_matrix.h>
#include <deal.II/grid/tria.h>
#include <deal.II/grid/grid_refinement.h>
#include <deal.II/grid/grid_out.h>
#include <deal.II/grid/grid_generator.h>
#include <deal.II/grid/tria_accessor.h>
#include <deal.II/grid/tria_iterator.h>
#include <deal.II/grid/tria_boundary_lib.h>
#include <deal.II/dofs/dof_handler.h>
#include <deal.II/dofs/dof_accessor.h>
#include <deal.II/dofs/dof_tools.h>
#include <deal.II/fe/fe_q.h>
#include <deal.II/fe/fe_values.h>
#include <deal.II/numerics/vector_tools.h>
#include <deal.II/numerics/matrix_tools.h>
#include <deal.II/numerics/data_out.h>
```

```
#include <deal.II/numerics/error_estimator.h>
#include <fstream>
#include <iostream>
#include <deal.II/base/utilities.h>
#include <deal.II/lac/block_vector.h>
#include <deal.II/numerics/solution_transfer.h>
#include <deal.II/grid/grid_tools.h>
#include <list>
#include <iomanip>
namespace Step28
{
using namespace dealii;
class MaterialData
{
public:
MaterialData (const unsigned int n_groups);
double get_diffusion_coefficient (const unsigned int group,
const unsigned int material_id) const;
double get_removal_XS (const unsigned int group,
const unsigned int material_id) const;
double get_fission_XS (const unsigned int group,
const unsigned int material_id) const;
double get_fission_dist_XS (const unsigned int group_1,
const unsigned int group_2,
const unsigned int material_id) const;
double get_scattering_XS (const unsigned int group_1,
const unsigned int group_2,
const unsigned int material_id) const;
double get_fission_spectrum (const unsigned int group,
const unsigned int material_id) const;
private:
const unsigned int n_groups;
const unsigned int n_materials;
Table<2,double> diffusion;
Table<2,double> sigma_r;
Table<2,double> nu_sigma_f;
Table<3,double> sigma_s;
Table<2,double> chi;
};
MaterialData::MaterialData (const unsigned int n_groups)
:
n_groups (n_groups),
n_materials (8),
```

```
diffusion (n_materials, n_groups),
sigma_r (n_materials, n_groups),
nu_sigma_f (n_materials, n_groups),
sigma_s (n_materials, n_groups, n_groups),
chi (n_materials, n_groups)
{
switch (n_groups)
{
case 2:
{
for (unsigned int m=0; m<n_materials; ++m)
{
diffusion[m][0] = 1.2;
diffusion[m][1] = 0.4;
chi[m][0] = 1.0;
chi[m][1] = 0.0;
sigma_r[m][0] = 0.03;
for (unsigned int group_1=0; group_1<n_groups; ++group_1)
for (unsigned int group_2=0; group_2<n_groups; ++ group_2)
sigma_s[m][group_1][group_2] = 0.0;
}
diffusion[5][1] = 0.2;
sigma_r[4][0] = 0.026;
sigma_r[5][0] = 0.051;
sigma_r[6][0] = 0.026;
sigma_r[7][0] = 0.050;
sigma_r[0][1] = 0.100;
sigma_r[1][1] = 0.200;
sigma_r[2][1] = 0.250;
sigma_r[3][1] = 0.300;
sigma_r[4][1] = 0.020;
sigma_r[5][1] = 0.040;
sigma_r[6][1] = 0.020;
sigma_r[7][1] = 0.800;
nu_sigma_f[0][0] = 0.0050;
nu_sigma_f[1][0] = 0.0075;
nu_sigma_f[2][0] = 0.0075;
nu_sigma_f[3][0] = 0.0075;
nu_sigma_f[4][0] = 0.000;
nu_sigma_f[5][0] = 0.000;
nu_sigma_f[6][0] = 1e-7;
nu_sigma_f[7][0] = 0.00;
nu_sigma_f[0][1] = 0.125;
```

```
nu_sigma_f[1][1] = 0.300;
nu_sigma_f[2][1] = 0.375;
nu_sigma_f[3][1] = 0.450;
nu_sigma_f[4][1] = 0.000;
nu_sigma_f[5][1] = 0.000;
nu_sigma_f[6][1] = 3e-6;
nu_sigma_f[7][1] = 0.00;
sigma_s[0][0][1] = 0.020;
sigma_s[1][0][1] = 0.015;
sigma_s[2][0][1] = 0.015;
sigma_s[3][0][1] = 0.015;
sigma_s[4][0][1] = 0.025;
sigma_s[5][0][1] = 0.050;
sigma_s[6][0][1] = 0.025;
sigma_s[7][0][1] = 0.010;
break;
}
default:
Assert (false,
ExcMessage ("Presently, only data for 2 groups is implemented"));
}
}
double
MaterialData::get_diffusion_coefficient (const unsigned int group,
const unsigned int material_id) const
{
Assert (group < n_groups,
ExcIndexRange (group, 0, n_groups));
Assert (material_id < n_materials,
ExcIndexRange (material_id, 0, n_materials));
return diffusion[material_id][group];
}
double
MaterialData::get_removal_XS (const unsigned int group,
const unsigned int material_id) const
{
Assert (group < n_groups,
ExcIndexRange (group, 0, n_groups));
Assert (material_id < n_materials,
ExcIndexRange (material_id, 0, n_materials));
return sigma_r[material_id][group];
}
double
```

```
MaterialData::get_fission_XS (const unsigned int group,
const unsigned int material_id) const
{
Assert (group < n_groups,
ExcIndexRange (group, 0, n_groups));
Assert (material_id < n_materials,
ExcIndexRange (material_id, 0, n_materials));
return nu_sigma_f[material_id][group];
}
double
MaterialData::get_scattering_XS (const unsigned int group_1,
const unsigned int group_2,
const unsigned int material_id) const
{
Assert (group_1 < n_groups,
ExcIndexRange (group_1, 0, n_groups));
Assert (group_2 < n_groups,
ExcIndexRange (group_2, 0, n_groups));
Assert (material_id < n_materials,
ExcIndexRange (material_id, 0, n_materials));
return sigma_s[material_id][group_1][group_2];
}
double
MaterialData::get_fission_spectrum (const unsigned int group,
const unsigned int material_id) const
{
Assert (group < n_groups,
ExcIndexRange (group, 0, n_groups));
Assert (material_id < n_materials,
ExcIndexRange (material_id, 0, n_materials));
return chi[material_id][group];
}
double
MaterialData::get_fission_dist_XS (const unsigned int group_1,
const unsigned int group_2,
const unsigned int material_id) const
{
return (get_fission_spectrum(group_1, material_id) *
get_fission_XS(group_2, material_id));
}
template <int dim>
class EnergyGroup
{
```

```
public:
EnergyGroup (const unsigned int group,
const MaterialData &material_data,
const Triangulation<dim> &coarse_grid,
const FiniteElement<dim> &fe);
void setup_linear_system ();
unsigned int n_active_cells () const;
unsigned int n_dofs () const;
void assemble_system_matrix ();
void assemble_ingroup_rhs (const Function<dim> &extraneous_source);
void assemble_cross_group_rhs (const EnergyGroup<dim> &g_prime);
void solve ();
double get_fission_source () const;
void output_results (const unsigned int cycle) const;
void estimate_errors (Vector<float> &error_indicators) const;
void refine_grid (const Vector<float> &error_indicators,
const double refine_threshold,
const double coarsen_threshold);
public:
Vector<double> solution;
Vector<double> solution_old;
private:
const unsigned int group;
const MaterialData &material_data;
Triangulation<dim> triangulation;
const FiniteElement<dim> &fe;
DoFHandler<dim> dof_handler;
SparsityPattern sparsity_pattern;
SparseMatrix<double> system_matrix;
Vector<double> system_rhs;
std::map<unsigned int,double> boundary_values;
ConstraintMatrix hanging_node_constraints;
private:
void
assemble_cross_group_rhs_recursive (const EnergyGroup<dim> &g_prime,
const typename DoFHandler<dim>::cell_iterator &cell_g,
const typename DoFHandler<dim>::cell_iterator &cell_g_prime,
const FullMatrix<double> prolongation_matrix);
};
template <int dim>
EnergyGroup<dim>::EnergyGroup (const unsigned int group,
const MaterialData &material_data,
const Triangulation<dim> &coarse_grid,
```

```
const FiniteElement<dim> &fe)
:
group (group),
material_data (material_data),
fe (fe),
dof_handler (triangulation)
{
triangulation.copy_triangulation (coarse_grid);
dof_handler.distribute_dofs (fe);
}
template <int dim>
unsigned int
EnergyGroup<dim>::n_active_cells () const
{
return triangulation.n_active_cells ();
}
template <int dim>
unsigned int
EnergyGroup<dim>::n_dofs () const
{
return dof_handler.n_dofs ();
}
template <int dim>
void
EnergyGroup<dim>::setup_linear_system ()
{
const unsigned int n_dofs = dof_handler.n_dofs();
hanging_node_constraints.clear ();
DoFTools::make_hanging_node_constraints (dof_handler,
hanging_node_constraints);
hanging_node_constraints.close ();
system_matrix.clear ();
sparsity_pattern.reinit (n_dofs, n_dofs,
dof_handler.max_couplings_between_dofs());
DoFTools::make_sparsity_pattern (dof_handler, sparsity_pattern);
hanging_node_constraints.condense (sparsity_pattern);
sparsity_pattern.compress ();
system_matrix.reinit (sparsity_pattern);
system_rhs.reinit (n_dofs);
if (solution.size() == 0)
{
solution.reinit (n_dofs);
solution_old.reinit(n_dofs);
```

```
solution_old = 1.0;
solution = solution_old;
}
boundary_values.clear();
for (unsigned int i=0; i<dim; ++i)
VectorTools::interpolate_boundary_values (dof_handler,
2*i+1,
ZeroFunction<dim>(),
boundary_values);
}
template <int dim>
void
EnergyGroup<dim>::assemble_system_matrix ()
{
const QGauss<dim> quadrature_formula(fe.degree + 1);
FEValues<dim> fe_values (fe, quadrature_formula,
update_values | update_gradients |
update_JxW_values);
const unsigned int dofs_per_cell = fe.dofs_per_cell;
const unsigned int n_q_points = quadrature_formula.size();
FullMatrix<double> cell_matrix (dofs_per_cell, dofs_per_cell);
Vector<double> cell_rhs (dofs_per_cell);
std::vector<unsigned int> local_dof_indices (dofs_per_cell);
typename DoFHandler<dim>::active_cell_iterator
cell = dof_handler.begin_active(),
endc = dof_handler.end();
for (; cell!=endc; ++cell)
{
cell_matrix = 0;
fe_values.reinit (cell);
const double diffusion_coefficient
= material_data.get_diffusion_coefficient (group, cell->material_id());
const double removal_XS
= material_data.get_removal_XS (group,cell->material_id());
for (unsigned int q_point=0; q_point<n_q_points; ++q_point)
for (unsigned int i=0; i<dofs_per_cell; ++i)
for (unsigned int j=0; j<dofs_per_cell; ++j)
cell_matrix(i,j) += ((diffusion_coefficient *
fe_values.shape_grad(i,q_point) *
fe_values.shape_grad(j,q_point)
+
removal_XS *
fe_values.shape_value(i,q_point) *
```

```
fe_values.shape_value(j,q_point))
*
fe_values.JxW(q_point));
cell->get_dof_indices (local_dof_indices);
for (unsigned int i=0; i<dofs_per_cell; ++i)
for (unsigned int j=0; j<dofs_per_cell; ++j)
system_matrix.add (local_dof_indices[i],
local_dof_indices[j],
cell_matrix(i,j));
}
hanging_node_constraints.condense (system_matrix);
}
template <int dim>
void EnergyGroup<dim>::assemble_ingroup_rhs (const Function<dim>
&extraneous_source)
{
system_rhs.reinit (dof_handler.n_dofs());
const QGauss<dim> quadrature_formula (fe.degree + 1);
const unsigned int dofs_per_cell = fe.dofs_per_cell;
const unsigned int n_q_points = quadrature_formula.size();
FEValues<dim> fe_values (fe, quadrature_formula,
update_values | update_quadrature_points |
update_JxW_values);
Vector<double> cell_rhs (dofs_per_cell);
std::vector<double> extraneous_source_values (n_q_points);
std::vector<double> solution_old_values (n_q_points);
std::vector<unsigned int> local_dof_indices (dofs_per_cell);
typename DoFHandler<dim>::active_cell_iterator
cell = dof_handler.begin_active(),
endc = dof_handler.end();
for (; cell!=endc; ++cell)
{
cell_rhs = 0;
fe_values.reinit (cell);
const double fission_dist_XS
= material_data.get_fission_dist_XS (group, group, cell->material_id());
extraneous_source.value_list (fe_values.get_quadrature_points(),
extraneous_source_values);
fe_values.get_function_values (solution_old, solution_old_values);
cell->get_dof_indices (local_dof_indices);
for (unsigned int q_point=0; q_point<n_q_points; ++q_point)
for (unsigned int i=0; i<dofs_per_cell; ++i)
cell_rhs(i) += ((extraneous_source_values[q_point]
```

```
+
fission_dist_XS *
solution_old_values[q_point]) *
fe_values.shape_value(i,q_point) *
fe_values.JxW(q_point));
for (unsigned int i=0; i<dofs_per_cell; ++i)
system_rhs(local_dof_indices[i]) += cell_rhs(i);
}
}
template <int dim>
void EnergyGroup<dim>::assemble_cross_group_rhs (const EnergyGroup<dim>
&g_prime)
{
if (group == g_prime.group)
return;
const std::list<std::pair<typename DoFHandler<dim>::cell_iterator,
typename DoFHandler<dim>::cell_iterator> >
cell_list
= GridTools::get_finest_common_cells (dof_handler,
g_prime.dof_handler);
typename std::list<std::pair<typename DoFHandler<dim>::cell_iterator,
typename DoFHandler<dim>::cell_iterator> >
::const_iterator
cell_iter = cell_list.begin();
for (; cell_iter!=cell_list.end(); ++cell_iter)
{
FullMatrix<double> unit_matrix (fe.dofs_per_cell);
for (unsigned int i=0; i<unit_matrix.m(); ++i)
unit_matrix(i,i) = 1;
assemble_cross_group_rhs_recursive (g_prime,
cell_iter->first,
cell_iter->second,
unit_matrix);
}
}
template <int dim>
void
EnergyGroup<dim>::
assemble_cross_group_rhs_recursive (const EnergyGroup<dim> &g_prime,
const typename DoFHandler<dim>::cell_iterator &cell_g,
const typename DoFHandler<dim>::cell_iterator &cell_g_prime,
const FullMatrix<double> prolongation_matrix)
{
```

```
if (!cell_g->has_children() && !cell_g_prime->has_children())
{
const QGauss<dim> quadrature_formula (fe.degree+1);
const unsigned int n_q_points = quadrature_formula.size();
FEValues<dim> fe_values (fe, quadrature_formula,
update_values | update_JxW_values);
if (cell_g->level() > cell_g_prime->level())
fe_values.reinit (cell_g);
else
fe_values.reinit (cell_g_prime);
const double fission_dist_XS
= material_data.get_fission_dist_XS (group, g_prime.group,
cell_g_prime->material_id());
const double scattering_XS
= material_data.get_scattering_XS (g_prime.group, group,
cell_g_prime->material_id());
FullMatrix<double> local_mass_matrix_f (fe.dofs_per_cell,
fe.dofs_per_cell);
FullMatrix<double> local_mass_matrix_g (fe.dofs_per_cell,
fe.dofs_per_cell);
for (unsigned int q_point=0; q_point<n_q_points; ++q_point)
for (unsigned int i=0; i<fe.dofs_per_cell; ++i)
for (unsigned int j=0; j<fe.dofs_per_cell; ++j)
{
local_mass_matrix_f(i,j) += (fission_dist_XS *
fe_values.shape_value(i,q_point) *
fe_values.shape_value(j,q_point) *
fe_values.JxW(q_point));
local_mass_matrix_g(i,j) += (scattering_XS *
fe_values.shape_value(i,q_point) *
fe_values.shape_value(j,q_point) *
fe_values.JxW(q_point));
}
Vector<double> g_prime_new_values (fe.dofs_per_cell);
Vector<double> g_prime_old_values (fe.dofs_per_cell);
cell_g_prime->get_dof_values (g_prime.solution_old, g_prime_old_values);
cell_g_prime->get_dof_values (g_prime.solution, g_prime_new_values);
Vector<double> cell_rhs (fe.dofs_per_cell);
Vector<double> tmp (fe.dofs_per_cell);
if (cell_g->level() > cell_g_prime->level())
{
prolongation_matrix.vmult (tmp, g_prime_old_values);
local_mass_matrix_f.vmult (cell_rhs, tmp);
```

```
prolongation_matrix.vmult (tmp, g_prime_new_values);
local_mass_matrix_g.vmult_add (cell_rhs, tmp);
}
else
{
local_mass_matrix_f.vmult (tmp, g_prime_old_values);
prolongation_matrix.Tvmult (cell_rhs, tmp);
local_mass_matrix_g.vmult (tmp, g_prime_new_values);
prolongation_matrix.Tvmult_add (cell_rhs, tmp);
}
std::vector<unsigned int> local_dof_indices (fe.dofs_per_cell);
cell_g->get_dof_indices (local_dof_indices);
for (unsigned int i=0; i<fe.dofs_per_cell; ++i)
system_rhs(local_dof_indices[i]) += cell_rhs(i);
}
else
for (unsigned int child=0; child<GeometryInfo<dim>::max_children_per_cell; ++child)
{
FullMatrix<double> new_matrix (fe.dofs_per_cell, fe.dofs_per_cell);
fe.get_prolongation_matrix(child).mmult (new_matrix,
prolongation_matrix);
if (cell_g->has_children())
assemble_cross_group_rhs_recursive (g_prime,
cell_g->child(child), cell_g_prime,
new_matrix);
else
assemble_cross_group_rhs_recursive (g_prime,
cell_g, cell_g_prime->child(child),
new_matrix);
}
}
template <int dim>
double EnergyGroup<dim>::get_fission_source () const
{
const QGauss<dim> quadrature_formula (fe.degree + 1);
const unsigned int n_q_points = quadrature_formula.size();
FEValues<dim> fe_values (fe, quadrature_formula,
update_values | update_JxW_values);
std::vector<double> solution_values (n_q_points);
double fission_source = 0;
typename DoFHandler<dim>::active_cell_iterator
cell = dof_handler.begin_active(),
endc = dof_handler.end();
```

```
for (; cell!=endc; ++cell)
{
fe_values.reinit (cell);
const double fission_XS
= material_data.get_fission_XS(group, cell->material_id());
fe_values.get_function_values (solution, solution_values);
for (unsigned int q_point=0; q_point<n_q_points; ++q_point)
fission_source += (fission_XS *
solution_values[q_point] *
fe_values.JxW(q_point));
}
return fission_source;
}
template <int dim>
void
EnergyGroup<dim>::solve ()
{
hanging_node_constraints.condense (system_rhs);
MatrixTools::apply_boundary_values (boundary_values,
system_matrix,
solution,
system_rhs);
SolverControl solver_control (system_matrix.m(),
1e-12*system_rhs.l2_norm());
SolverCG<> cg (solver_control);
PreconditionSSOR<> preconditioner;
preconditioner.initialize(system_matrix, 1.2);
cg.solve (system_matrix, solution, system_rhs, preconditioner);
hanging_node_constraints.distribute (solution);
}
template <int dim>
void EnergyGroup<dim>::estimate_errors (Vector<float> &error_indicators) const
{
KellyErrorEstimator<dim>::estimate (dof_handler,
QGauss<dim-1> (fe.degree + 1),
typename FunctionMap<dim>::type(),
solution,
error_indicators);
error_indicators /= solution.linfty_norm();
}
template <int dim>
void EnergyGroup<dim>::refine_grid (const Vector<float> &error_indicators,
const double refine_threshold,
```

```
const double coarsen_threshold)
{
typename Triangulation<dim>::active_cell_iterator
cell = triangulation.begin_active(),
endc = triangulation.end();
for (unsigned int cell_index=0; cell!=endc; ++cell, ++cell_index)
if (error_indicators(cell_index) > refine_threshold)
cell->set_refine_flag ();
else if (error_indicators(cell_index) < coarsen_threshold)
cell->set_coarsen_flag ();
SolutionTransfer<dim> soltrans(dof_handler);
triangulation.prepare_coarsening_and_refinement();
soltrans.prepare_for_coarsening_and_refinement(solution);
triangulation.execute_coarsening_and_refinement ();
dof_handler.distribute_dofs (fe);
solution.reinit (dof_handler.n_dofs());
soltrans.interpolate(solution_old, solution);
solution_old.reinit (dof_handler.n_dofs());
solution_old = solution;
}
template <int dim>
void
EnergyGroup<dim>::output_results (const unsigned int cycle) const
{
{
const std::string filename = std::string("grid-") +
Utilities::int_to_string(group,1) +
"." +
Utilities::int_to_string(cycle,1) +
".eps";
std::ofstream output (filename.c_str());
GridOut grid_out;
grid_out.write_eps (triangulation, output);
}
{
const std::string filename = std::string("solution-") +
Utilities::int_to_string(group,1) +
"." +
Utilities::int_to_string(cycle,1) +
".gmv";
DataOut<dim> data_out;
data_out.attach_dof_handler (dof_handler);
data_out.add_data_vector (solution, "solution");
```

```
data_out.build_patches ();
std::ofstream output (filename.c_str());
data_out.write_gmv (output);
}
}
template <int dim>
class NeutronDiffusionProblem
{
public:
class Parameters
{
public:
Parameters ();
static void declare_parameters (ParameterHandler &prm);
void get_parameters (ParameterHandler &prm);
unsigned int n_groups;
unsigned int n_refinement_cycles;
unsigned int fe_degree;
double convergence_tolerance;
};
NeutronDiffusionProblem (const Parameters &parameters);
~NeutronDiffusionProblem ();
void run ();
private:
void initialize_problem();
void refine_grid ();
double get_total_fission_source () const;
const Parameters &parameters;
const MaterialData material_data;
FE_Q<dim> fe;
double k_eff;
std::vector<EnergyGroup<dim>*> energy_groups;
};
template <int dim>
NeutronDiffusionProblem<dim>::Parameters::Parameters ()
:
n_groups (2),
n_refinement_cycles (5),
fe_degree (2),
convergence_tolerance (1e-12)
{}
template <int dim>
void
```

```
NeutronDiffusionProblem<dim>::Parameters::
declare_parameters (ParameterHandler &prm)
{
prm.declare_entry ("Number of energy groups", "2",
Patterns::Integer (),
"The number of energy different groups considered");
prm.declare_entry ("Refinement cycles", "5",
Patterns::Integer (),
"Number of refinement cycles to be performed");
prm.declare_entry ("Finite element degree", "2",
Patterns::Integer (),
"Polynomial degree of the finite element to be used");
prm.declare_entry ("Power iteration tolerance", "1e-12",
Patterns::Double (),
"Inner power iterations are stopped when the change in k_eff falls "
"below this tolerance");
}
template <int dim>
void
NeutronDiffusionProblem<dim>::Parameters::
get_parameters (ParameterHandler &prm)
{
n_groups = prm.get_integer ("Number of energy groups");
n_refinement_cycles = prm.get_integer ("Refinement cycles");
fe_degree = prm.get_integer ("Finite element degree");
convergence_tolerance = prm.get_double ("Power iteration tolerance");
}
template <int dim>
NeutronDiffusionProblem<dim>::
NeutronDiffusionProblem (const Parameters &parameters)
:
parameters (parameters),
material_data (parameters.n_groups),
fe (parameters.fe_degree)
{}
template <int dim>
NeutronDiffusionProblem<dim>::~NeutronDiffusionProblem ()
{
for (unsigned int group=0; group<energy_groups.size(); ++group)
delete energy_groups[group];
energy_groups.resize (0);
}
template <int dim>
```

```
void NeutronDiffusionProblem<dim>::initialize_problem()
{
const unsigned int rods_per_assembly_x = 17,
rods_per_assembly_y = 17;
const double pin_pitch_x = 1.26,
pin_pitch_y = 1.26;
const double assembly_height = 200;
const unsigned int assemblies_x = 2,
assemblies_y = 2,
assemblies_z = 1;
const Point<dim> bottom_left = Point<dim>();
const Point<dim> upper_right = (dim == 2
?
Point<dim> (assemblies_x*rods_per_assembly_x*pin_pitch_x,
assemblies_y*rods_per_assembly_y*pin_pitch_y)
:
Point<dim> (assemblies_x*rods_per_assembly_x*pin_pitch_x,
assemblies_y*rods_per_assembly_y*pin_pitch_y,
assemblies_z*assembly_height));
std::vector<unsigned int> n_subdivisions;
n_subdivisions.push_back (assemblies_x*rods_per_assembly_x);
if (dim >= 2)
n_subdivisions.push_back (assemblies_y*rods_per_assembly_y);
if (dim >= 3)
n_subdivisions.push_back (assemblies_z);
Triangulation<dim> coarse_grid;
GridGenerator::subdivided_hyper_rectangle (coarse_grid,
n_subdivisions,
bottom_left,
upper_right,
true);
const unsigned int n_assemblies=4;
const unsigned int
assembly_materials[n_assemblies][rods_per_assembly_x][rods_per_assembly_y]
=
{
{
{ 1, 1, 1, 1, 1, 1, 1, 1, 1, 1, 1, 1, 1, 1, 1, 1, 1 },
{ 1, 1, 1, 1, 1, 1, 1, 1, 1, 1, 1, 1, 1, 1, 1, 1, 1 },
{ 1, 1, 1, 1, 1, 5, 1, 1, 5, 1, 1, 5, 1, 1, 1, 1, 1 },
{ 1, 1, 1, 5, 1, 1, 1, 1, 1, 1, 1, 1, 1, 5, 1, 1, 1 },
{ 1, 1, 1, 1, 1, 1, 1, 1, 1, 1, 1, 1, 1, 1, 1, 1, 1 },
{ 1, 1, 5, 1, 1, 5, 1, 1, 5, 1, 1, 5, 1, 1, 5, 1, 1 },
```

```
{ 1, 1, 1, 1, 1, 1, 1, 1, 1, 1, 1, 1, 1, 1, 1, 1, 1 },
{ 1, 1, 1, 1, 1, 1, 1, 1, 1, 1, 1, 1, 1, 1, 1, 1, 1 },
{ 1, 1, 5, 1, 1, 5, 1, 1, 7, 1, 1, 5, 1, 1, 5, 1, 1 },
{ 1, 1, 1, 1, 1, 1, 1, 1, 1, 1, 1, 1, 1, 1, 1, 1, 1 },
{ 1, 1, 1, 1, 1, 1, 1, 1, 1, 1, 1, 1, 1, 1, 1, 1, 1 },
{ 1, 1, 5, 1, 1, 5, 1, 1, 5, 1, 1, 5, 1, 1, 5, 1, 1 },
{ 1, 1, 1, 1, 1, 1, 1, 1, 1, 1, 1, 1, 1, 1, 1, 1, 1 },
{ 1, 1, 1, 5, 1, 1, 1, 1, 1, 1, 1, 1, 1, 5, 1, 1, 1 },
{ 1, 1, 1, 1, 1, 5, 1, 1, 5, 1, 1, 5, 1, 1, 1, 1, 1 },
{ 1, 1, 1, 1, 1, 1, 1, 1, 1, 1, 1, 1, 1, 1, 1, 1, 1 },
{ 1, 1, 1, 1, 1, 1, 1, 1, 1, 1, 1, 1, 1, 1, 1, 1, 1 }
},
{
{ 1, 1, 1, 1, 1, 1, 1, 1, 1, 1, 1, 1, 1, 1, 1, 1, 1 },
{ 1, 1, 1, 1, 1, 1, 1, 1, 1, 1, 1, 1, 1, 1, 1, 1, 1 },
{ 1, 1, 1, 1, 1, 8, 1, 1, 8, 1, 1, 8, 1, 1, 1, 1, 1 },
{ 1, 1, 1, 8, 1, 1, 1, 1, 1, 1, 1, 1, 1, 8, 1, 1, 1 },
{ 1, 1, 1, 1, 1, 1, 1, 1, 1, 1, 1, 1, 1, 1, 1, 1, 1 },
{ 1, 1, 8, 1, 1, 8, 1, 1, 8, 1, 1, 8, 1, 1, 8, 1, 1 },
{ 1, 1, 1, 1, 1, 1, 1, 1, 1, 1, 1, 1, 1, 1, 1, 1, 1 },
{ 1, 1, 1, 1, 1, 1, 1, 1, 1, 1, 1, 1, 1, 1, 1, 1, 1 },
{ 1, 1, 8, 1, 1, 8, 1, 1, 7, 1, 1, 8, 1, 1, 8, 1, 1 },
{ 1, 1, 1, 1, 1, 1, 1, 1, 1, 1, 1, 1, 1, 1, 1, 1, 1 },
{ 1, 1, 1, 1, 1, 1, 1, 1, 1, 1, 1, 1, 1, 1, 1, 1, 1 },
{ 1, 1, 8, 1, 1, 8, 1, 1, 8, 1, 1, 8, 1, 1, 8, 1, 1 },
{ 1, 1, 1, 1, 1, 1, 1, 1, 1, 1, 1, 1, 1, 1, 1, 1, 1 },
{ 1, 1, 1, 8, 1, 1, 1, 1, 1, 1, 1, 1, 1, 8, 1, 1, 1 },
{ 1, 1, 1, 1, 1, 8, 1, 1, 8, 1, 1, 8, 1, 1, 1, 1, 1 },
{ 1, 1, 1, 1, 1, 1, 1, 1, 1, 1, 1, 1, 1, 1, 1, 1, 1 },
{ 1, 1, 1, 1, 1, 1, 1, 1, 1, 1, 1, 1, 1, 1, 1, 1, 1 }
},
{
{ 2, 2, 2, 2, 2, 2, 2, 2, 2, 2, 2, 2, 2, 2, 2, 2, 2 },
{ 2, 3, 3, 3, 3, 3, 3, 3, 3, 3, 3, 3, 3, 3, 3, 3, 2 },
{ 2, 3, 3, 3, 3, 5, 3, 3, 5, 3, 3, 5, 3, 3, 3, 3, 2 },
{ 2, 3, 3, 5, 3, 4, 4, 4, 4, 4, 4, 4, 3, 5, 3, 3, 2 },
{ 2, 3, 3, 3, 4, 4, 4, 4, 4, 4, 4, 4, 4, 3, 3, 3, 2 },
{ 2, 3, 5, 4, 4, 5, 4, 4, 5, 4, 4, 5, 4, 4, 5, 3, 2 },
{ 2, 3, 3, 4, 4, 4, 4, 4, 4, 4, 4, 4, 4, 4, 3, 3, 2 },
{ 2, 3, 3, 4, 4, 4, 4, 4, 4, 4, 4, 4, 4, 4, 3, 3, 2 },
{ 2, 3, 5, 4, 4, 5, 4, 4, 7, 4, 4, 5, 4, 4, 5, 3, 2 },
{ 2, 3, 3, 4, 4, 4, 4, 4, 4, 4, 4, 4, 4, 4, 3, 3, 2 },
{ 2, 3, 3, 4, 4, 4, 4, 4, 4, 4, 4, 4, 4, 4, 3, 3, 2 },
```

```
{ 2, 3, 5, 4, 4, 5, 4, 4, 5, 4, 4, 5, 4, 4, 5, 3, 2 },
{ 2, 3, 3, 3, 4, 4, 4, 4, 4, 4, 4, 4, 4, 3, 3, 3, 2 },
{ 2, 3, 3, 5, 3, 4, 4, 4, 4, 4, 4, 4, 3, 5, 3, 3, 2 },
{ 2, 3, 3, 3, 3, 5, 3, 3, 5, 3, 3, 5, 3, 3, 3, 3, 2 },
{ 2, 3, 3, 3, 3, 3, 3, 3, 3, 3, 3, 3, 3, 3, 3, 3, 2 },
{ 2, 2, 2, 2, 2, 2, 2, 2, 2, 2, 2, 2, 2, 2, 2, 2, 2 }
},
{
{ 6, 6, 6, 6, 6, 6, 6, 6, 6, 6, 6, 6, 6, 6, 6, 6, 6 },
{ 6, 6, 6, 6, 6, 6, 6, 6, 6, 6, 6, 6, 6, 6, 6, 6, 6 },
{ 6, 6, 6, 6, 6, 6, 6, 6, 6, 6, 6, 6, 6, 6, 6, 6, 6 },
{ 6, 6, 6, 6, 6, 6, 6, 6, 6, 6, 6, 6, 6, 6, 6, 6, 6 },
{ 6, 6, 6, 6, 6, 6, 6, 6, 6, 6, 6, 6, 6, 6, 6, 6, 6 },
{ 6, 6, 6, 6, 6, 6, 6, 6, 6, 6, 6, 6, 6, 6, 6, 6, 6 },
{ 6, 6, 6, 6, 6, 6, 6, 6, 6, 6, 6, 6, 6, 6, 6, 6, 6 },
{ 6, 6, 6, 6, 6, 6, 6, 6, 6, 6, 6, 6, 6, 6, 6, 6, 6 },
{ 6, 6, 6, 6, 6, 6, 6, 6, 6, 6, 6, 6, 6, 6, 6, 6, 6 },
{ 6, 6, 6, 6, 6, 6, 6, 6, 6, 6, 6, 6, 6, 6, 6, 6, 6 },
{ 6, 6, 6, 6, 6, 6, 6, 6, 6, 6, 6, 6, 6, 6, 6, 6, 6 },
{ 6, 6, 6, 6, 6, 6, 6, 6, 6, 6, 6, 6, 6, 6, 6, 6, 6 },
{ 6, 6, 6, 6, 6, 6, 6, 6, 6, 6, 6, 6, 6, 6, 6, 6, 6 },
{ 6, 6, 6, 6, 6, 6, 6, 6, 6, 6, 6, 6, 6, 6, 6, 6, 6 },
{ 6, 6, 6, 6, 6, 6, 6, 6, 6, 6, 6, 6, 6, 6, 6, 6, 6 },
{ 6, 6, 6, 6, 6, 6, 6, 6, 6, 6, 6, 6, 6, 6, 6, 6, 6 },
{ 6, 6, 6, 6, 6, 6, 6, 6, 6, 6, 6, 6, 6, 6, 6, 6, 6 }
}
};
const unsigned int core[assemblies_x][assemblies_y][assemblies_z]
= {{{0}, {2}}, {{2}, {0}}};
for (typename Triangulation<dim>::active_cell_iterator
cell = coarse_grid.begin_active();
cell!=coarse_grid.end();
++cell)
{
const Point<dim> cell_center = cell->center();
const unsigned int tmp_x = int(cell_center[0]/pin_pitch_x);
const unsigned int ax = tmp_x/rods_per_assembly_x;
const unsigned int cx = tmp_x - ax * rods_per_assembly_x;
const unsigned tmp_y = int(cell_center[1]/pin_pitch_y);
const unsigned int ay = tmp_y/rods_per_assembly_y;
const unsigned int cy = tmp_y - ay * rods_per_assembly_y;
const unsigned int az = (dim == 2
?
```

```
0
:
int (cell_center[dim-1]/assembly_height));
Assert (ax < assemblies_x, ExcInternalError());
Assert (ay < assemblies_y, ExcInternalError());
Assert (az < assemblies_z, ExcInternalError());
Assert (core[ax][ay][az] < n_assemblies, ExcInternalError());
Assert (cx < rods_per_assembly_x, ExcInternalError());
Assert (cy < rods_per_assembly_y, ExcInternalError());
cell->set_material_id(assembly_materials[core[ax][ay][az]][cx][cy] - 1);
}
energy_groups.resize (parameters.n_groups);
for (unsigned int group=0; group<parameters.n_groups; ++group)
energy_groups[group] = new EnergyGroup<dim> (group, material_data,
coarse_grid, fe);
}
template <int dim>
double NeutronDiffusionProblem<dim>::get_total_fission_source () const
{
std::vector<Threads::Thread<double> > threads;
for (unsigned int group=0; group<parameters.n_groups; ++group)
threads.push_back (Threads::new_thread (&EnergyGroup<dim>::get_fission_source,
*energy_groups[group]));
double fission_source = 0;
for (unsigned int group=0; group<parameters.n_groups; ++group)
fission_source += threads[group].return_value ();
return fission_source;
}
template <int dim>
void NeutronDiffusionProblem<dim>::refine_grid ()
{
std::vector<unsigned int> n_cells (parameters.n_groups);
for (unsigned int group=0; group<parameters.n_groups; ++group)
n_cells[group] = energy_groups[group]->n_active_cells();
BlockVector<float> group_error_indicators(n_cells);
{
Threads::ThreadGroup<> threads;
for (unsigned int group=0; group<parameters.n_groups; ++group)
threads += Threads::new_thread (&EnergyGroup<dim>::estimate_errors,
*energy_groups[group],
group_error_indicators.block(group));
threads.join_all ();
}
```

```
const float max_error = group_error_indicators.linfty_norm();
const float refine_threshold = 0.3*max_error;
const float coarsen_threshold = 0.01*max_error;
{
Threads::ThreadGroup<> threads;
for (unsigned int group=0; group<parameters.n_groups; ++group)
threads += Threads::new_thread (&EnergyGroup<dim>::refine_grid,
*energy_groups[group],
group_error_indicators.block(group),
refine_threshold,
coarsen_threshold);
threads.join_all ();
}
}
template <int dim>
void NeutronDiffusionProblem<dim>::run ()
{
std::cout << std::setprecision (12) << std::fixed;
double k_eff_old = k_eff;
Timer timer;
timer.start ();
for (unsigned int cycle=0; cycle<parameters.n_refinement_cycles; ++cycle)
{
std::cout << "Cycle " << cycle << ':' << std::endl;
if (cycle == 0)
initialize_problem();
else
{
refine_grid ();
for (unsigned int group=0; group<parameters.n_groups; ++group)
energy_groups[group]->solution *= k_eff;
}
for (unsigned int group=0; group<parameters.n_groups; ++group)
energy_groups[group]->setup_linear_system ();
std::cout << " Numbers of active cells: ";
for (unsigned int group=0; group<parameters.n_groups; ++group)
std::cout << energy_groups[group]->n_active_cells()
<< ' ';
std::cout << std::endl;
std::cout << " Numbers of degrees of freedom: ";
for (unsigned int group=0; group<parameters.n_groups; ++group)
std::cout << energy_groups[group]->n_dofs()
<< ' ';
```

```
std::cout << std::endl << std::endl;
Threads::ThreadGroup<> threads;
for (unsigned int group=0; group<parameters.n_groups; ++group)
threads += Threads::new_thread
(&EnergyGroup<dim>::assemble_system_matrix,
*energy_groups[group]);
threads.join_all ();
double error;
unsigned int iteration = 1;
do
{
for (unsigned int group=0; group<parameters.n_groups; ++group)
{
energy_groups[group]->assemble_ingroup_rhs (ZeroFunction<dim>());
for (unsigned int bgroup=0; bgroup<parameters.n_groups; ++bgroup)
energy_groups[group]->assemble_cross_group_rhs (*energy_groups[bgroup]);
energy_groups[group]->solve ();
}
k_eff = get_total_fission_source();
error = fabs(k_eff-k_eff_old)/fabs(k_eff);
std::cout << " Iteration " << iteration
<< ": k_eff=" << k_eff
<< std::endl;
k_eff_old=k_eff;
for (unsigned int group=0; group<parameters.n_groups; ++group)
{
energy_groups[group]->solution_old = energy_groups[group]->solution;
energy_groups[group]->solution_old /= k_eff;
}
++iteration;
}
while ((error > parameters.convergence_tolerance)
&&
(iteration < 500));
for (unsigned int group=0; group<parameters.n_groups; ++group)
energy_groups[group]->output_results (cycle);
std::cout << std::endl;
std::cout << " Cycle=" << cycle
<< ", n_dofs=" << energy_groups[0]->n_dofs() + energy_groups[1]->n_dofs()
<< ", k_eff=" << k_eff
<< ", time=" << timer()
<< std::endl;
std::cout << std::endl << std::endl;
```

```
}
}
}
int main (int argc, char **argv)
{
try
{
using namespace dealii;
using namespace Step28;
deallog.depth_console (0);
std::string filename;
if (argc < 2)
filename = "project.prm";
else
filename = argv[1];
const unsigned int dim = 2;
ParameterHandler parameter_handler;
NeutronDiffusionProblem<dim>::Parameters parameters;
parameters.declare_parameters (parameter_handler);
parameter_handler.read_input (filename);
parameters.get_parameters (parameter_handler);
NeutronDiffusionProblem<dim> neutron_diffusion_problem (parameters);
neutron_diffusion_problem.run ();
}
catch (std::exception &exc)
{
std::cerr << std::endl << std::endl
<< "----------------------------------------------------"
<< std::endl;
std::cerr << "Exception on processing: " << std::endl
<< exc.what() << std::endl
<< "Aborting!" << std::endl
<< "----------------------------------------------------"
<< std::endl;
return 1;
}
catch (...)
{
std::cerr << std::endl << std::endl
<< "----------------------------------------------------"
<< std::endl;
std::cerr << "Unknown exception!" << std::endl
<< "Aborting!" << std::endl
```

```
<< "--------------------------------------------------"
<< std::endl;
return 1;
}
return 0;
}
```

APPENDIX C: NEUTRON GROUPS

Table C-1:.Physical Constants

S.No	Physical Constant	Symbol	Value
1.	Universal gas constant	R_u	8.314 abs joules/(^{0}K)(gmole) 1.987 cal/(^{0}K)(gmole) 1,545.33 ft-lb/(lb mole)(^{0}R) 1.986 Btu/(lb mole)(^{0}R)
2.	Gravitational conversion factor	g_c	32.2 (lb mass/lb force)ft/sec^2
3.	Acceleration due to gravity at sea level	g_0	32.2 ft/sec^2 980.7 cm/sec^2
4.	Mechanical equivalent of heat	J	778.2 ft-lb/Btu
5.	Boltzmann's constant	K	1.3804×10^{-16} erg/^{0}K 8.61×10^{-5} ev/^{0} K
6.	Velocity of light	C	2.998×10^{10} cm/sec 9.835×10^{8} ft/sec
7.	Avogadro number	N_0	6.02×10^{23} nuclei/ g atom
9.	Stefan-Boltzmann Constant	Σ	5.67×10^{-5} erg/(cm^2)(^{0}K)^4(sec) 0.171×10^{-8} Btu/(ft^2) (^{0}R)^4(hr)
10.	Planck's constant	H	6.625×10^{-27} erg-sec

Table C-2: Neutron Continuous-energy and Discrete Reactions

MT	FM	Microscopic Cross-Section Description
1	-1	Total
2	-3	Elastic
16		(n,2n)
17		(n,3n)
18		Total fission(n.fx) if and only if MT=18 is used to specify fission in the original evaluation
	-6	Total fission cross section, (equal to MT=18 if MT=18 exits; otherwise equal to the sum of MTs 19,20,21 and 38
19		(n,f)
20		(n,n,f)
21		(n,2nf)
22		(n,n'α)
28		(n,n'p)
32		(n,n'd)
33		(n,n't)
38		(n,3nf)
51		(n,n') to 1st excited state
52		(n,n') to 2nd excited state
90		(n,n') to 40 th excited state
91		(n,n') to continuum
101	-2	Absorption: sum of MT=102-117 (Neutron disappearance; does not include fission)
102		(n, γ)
103		(n,p)
104		(n,d)
105		(n,t)
106		(n^3, He)
107		(n, α)

APPENDIX D: DATA FOR HEAT TRANSFER CALUCULATIONS

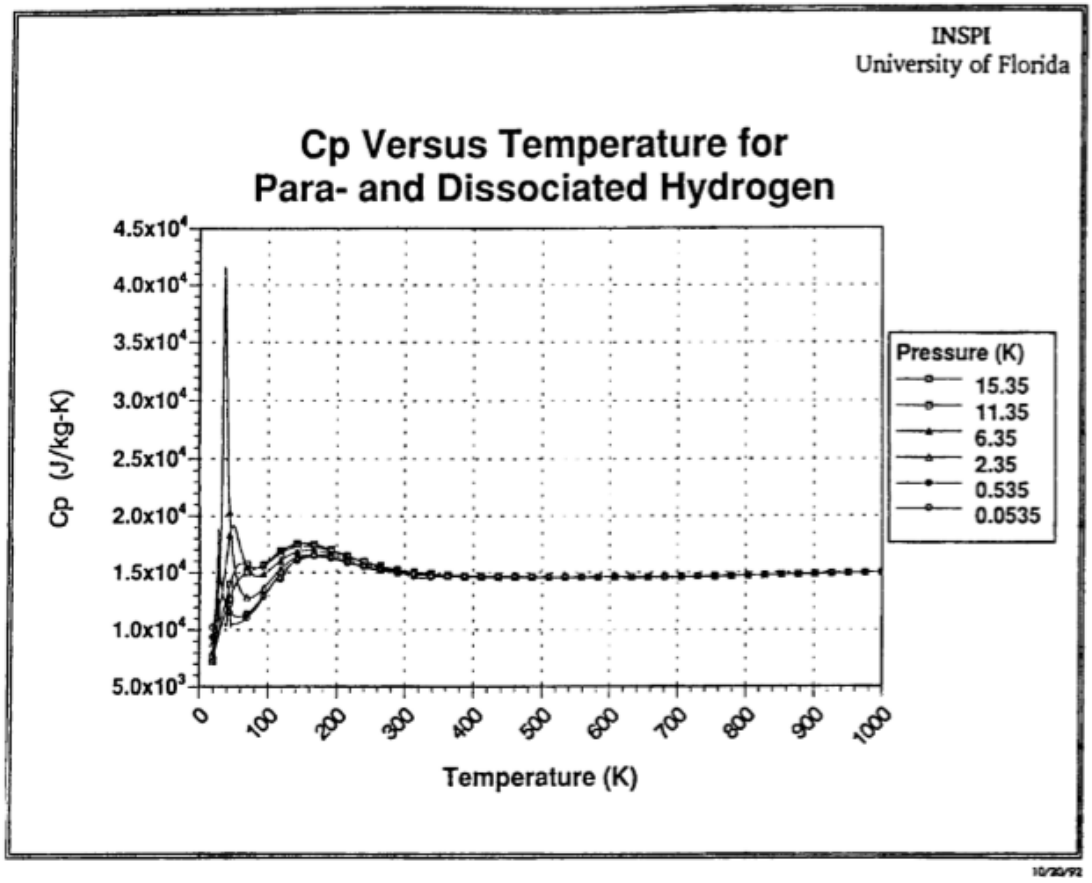

Figure D-1: Heat capacity of hydrogen near the critical point shows large gradient and oscillatory behavior. At p = 2.35 MPa the property package indicates a sharp peak for Cp.

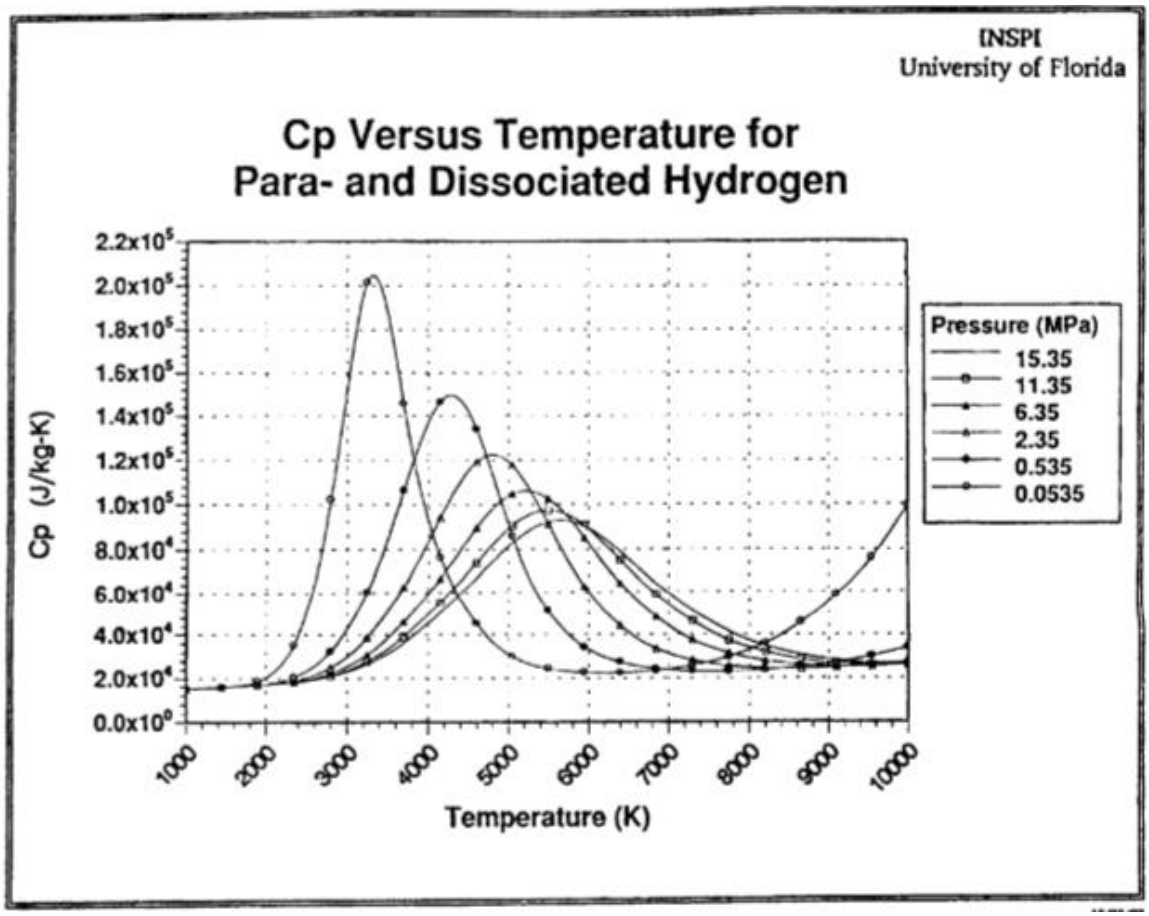

Figure D-2: At higher temperatures, the heat capacity data displays smooth behavior. The sharp increase in C, value at temperatures above 2000 K is due to hydrogen dissociation.

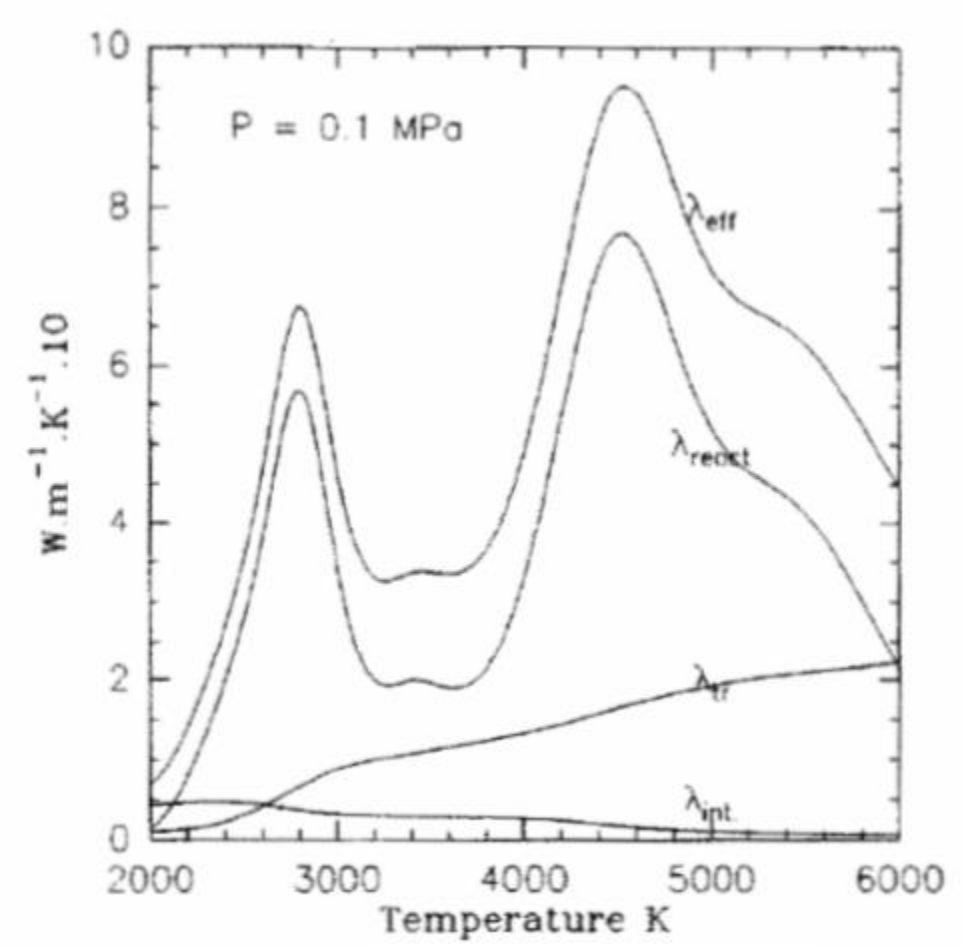

Figure D-3: At higher temperatures, the heat capacity data displays smooth behavior. The sharp increase in C, value at temperatures above 5000 K is due to hydrogen dissociation.

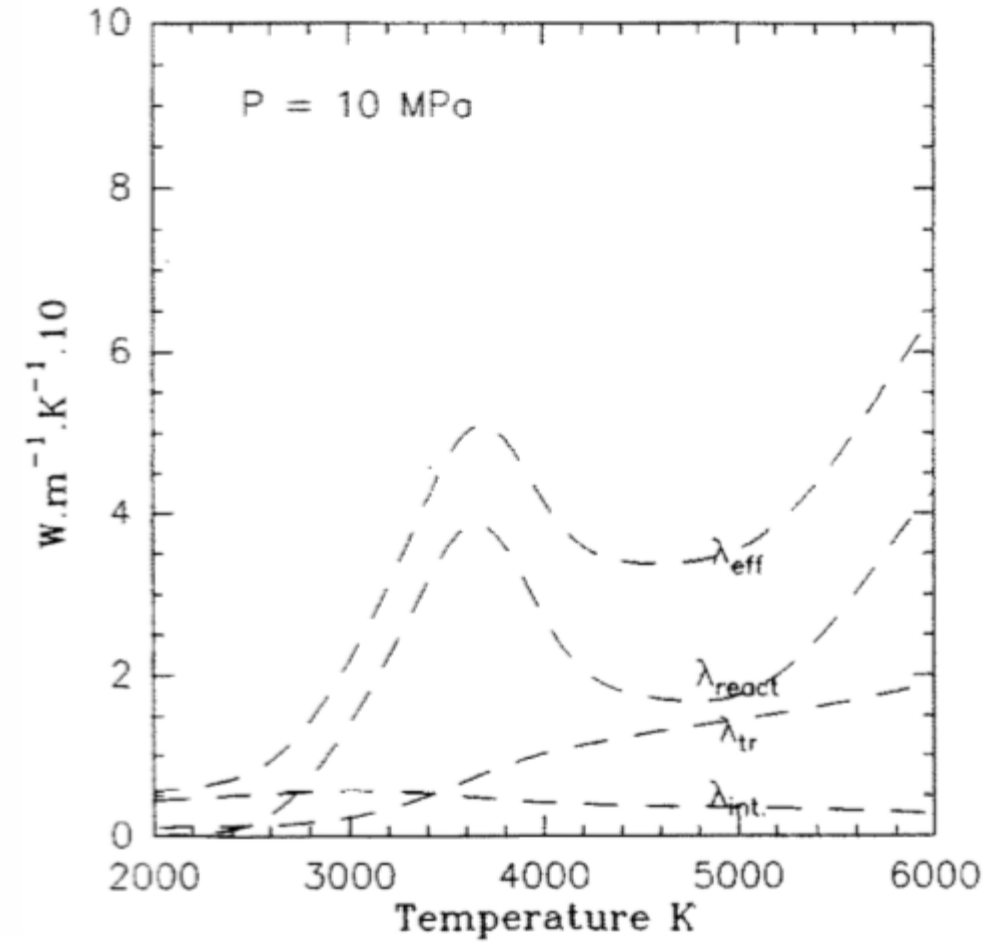

Figure D-4: Kinetic thermal conductivty components at p = 0.1 MPa and p = 10 MPa from Klein. λeff is the total kinetic thermal conductivity λkin.

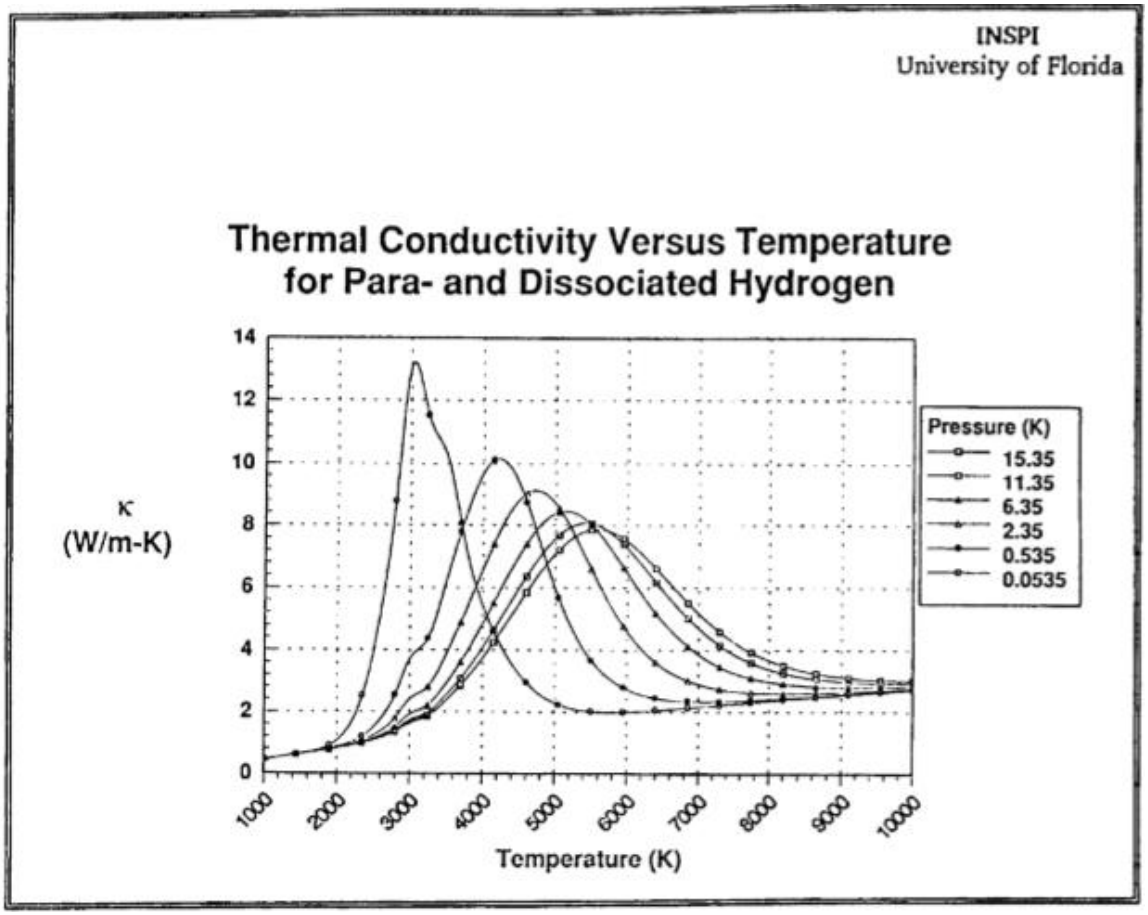

Figure D-5: The hydrogen property package is a combination of two sub packages covering the temperature ranges 10 - 3000 K and 3000 - 10,000 K, respectively. The large change of gradients in hydrogen viscosity at 3000 K indicates a non-physical flaw in the model.

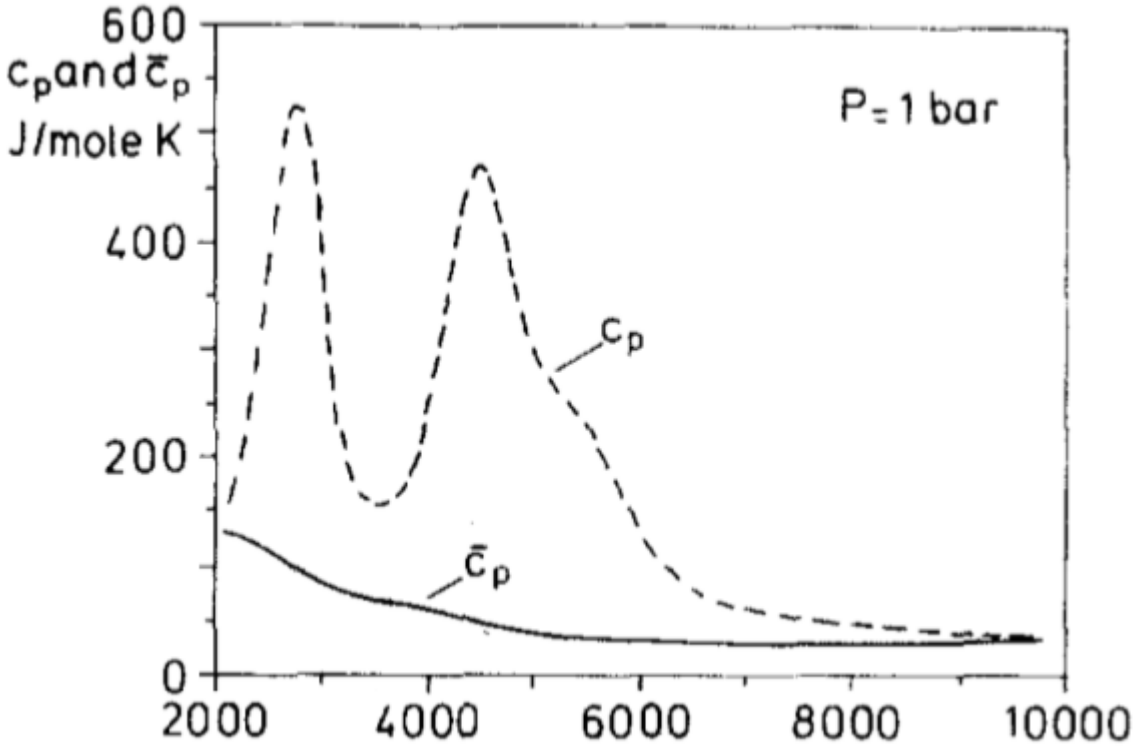

Figure D-6: Heat Capacity of the UCF fuel gas at a Pressure of 0.1 Mpa from Klein, with Right the Evaluated Data Evaluated Points and Liner Interpolated Function

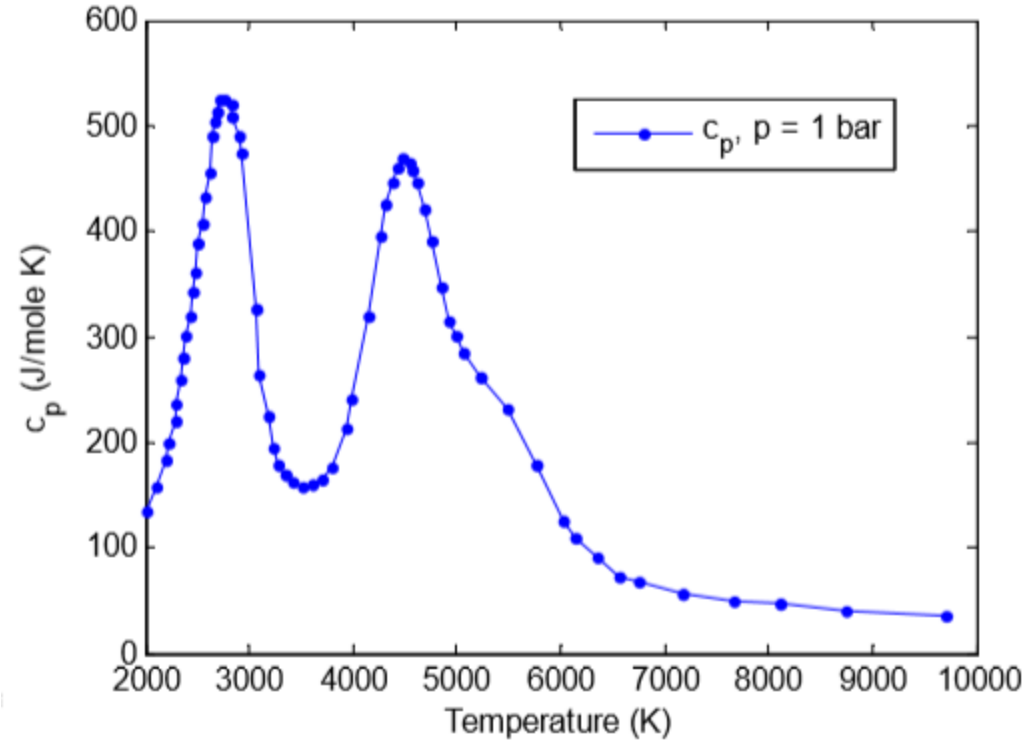

Fugure D-7: The Interpolated Values of the Specific Heat at 1 Bar Along with Variation Tempratures

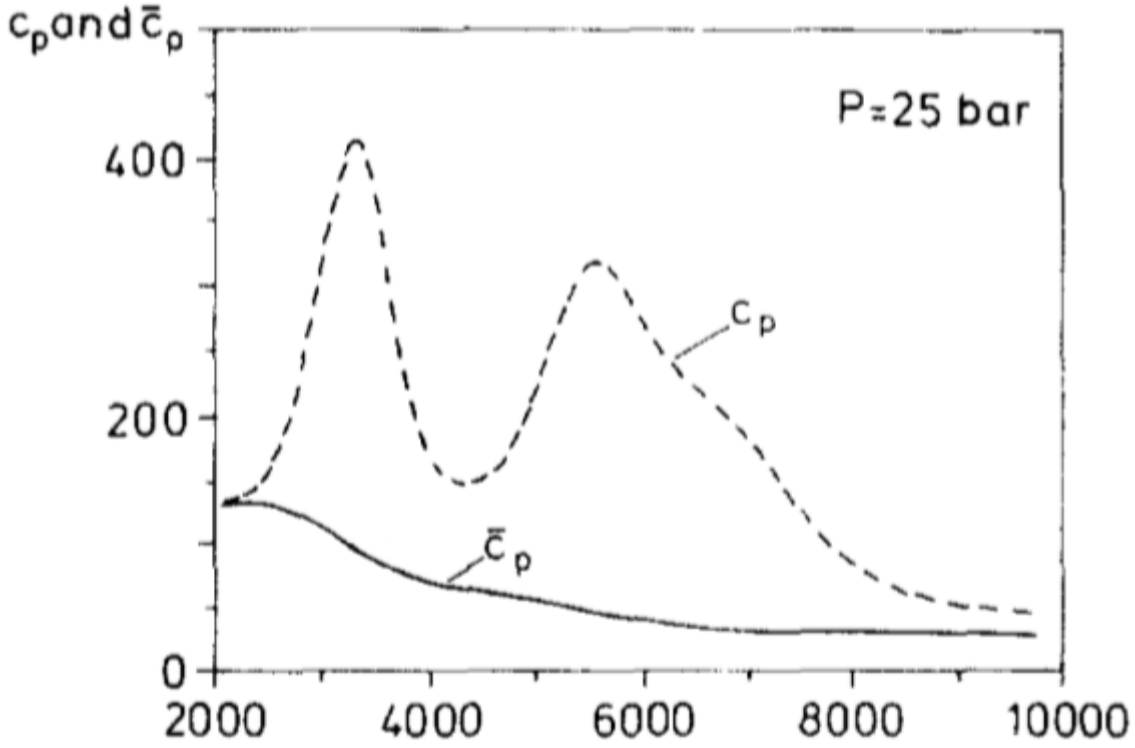

D8: Heat Capacity of the UCF Gas at 25 bar Pressure

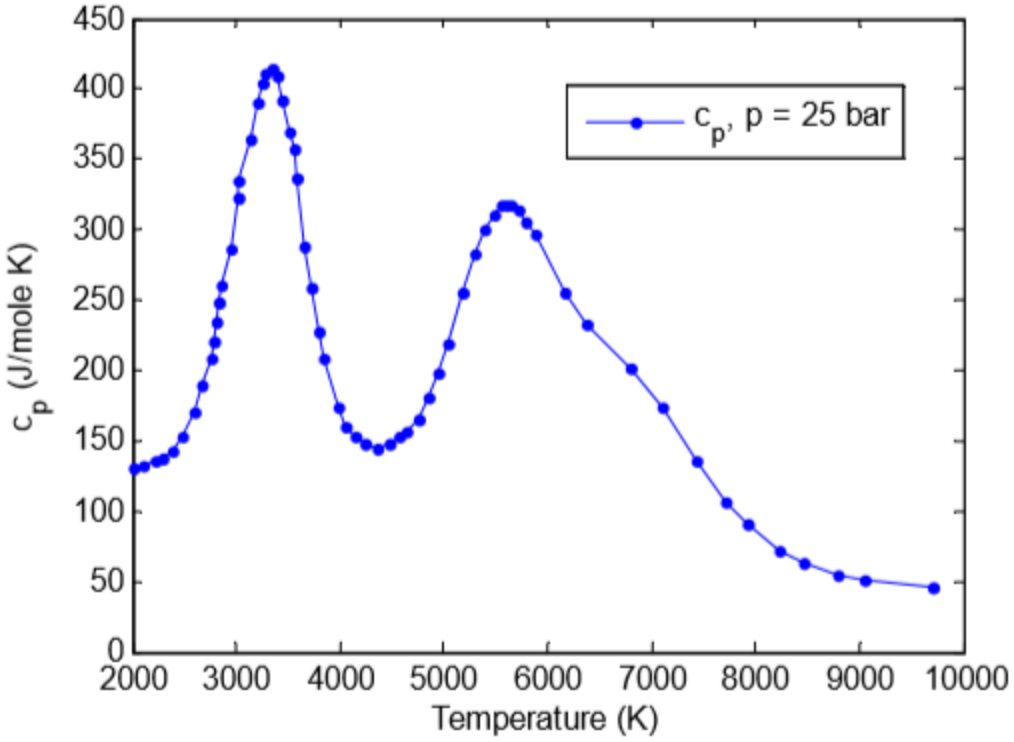

Figure D-9 : Heat capacity of the UCF fuel gases at a pressure of 2.5 MPa from Klein, with right the evaluated data points and linear interpolated function.

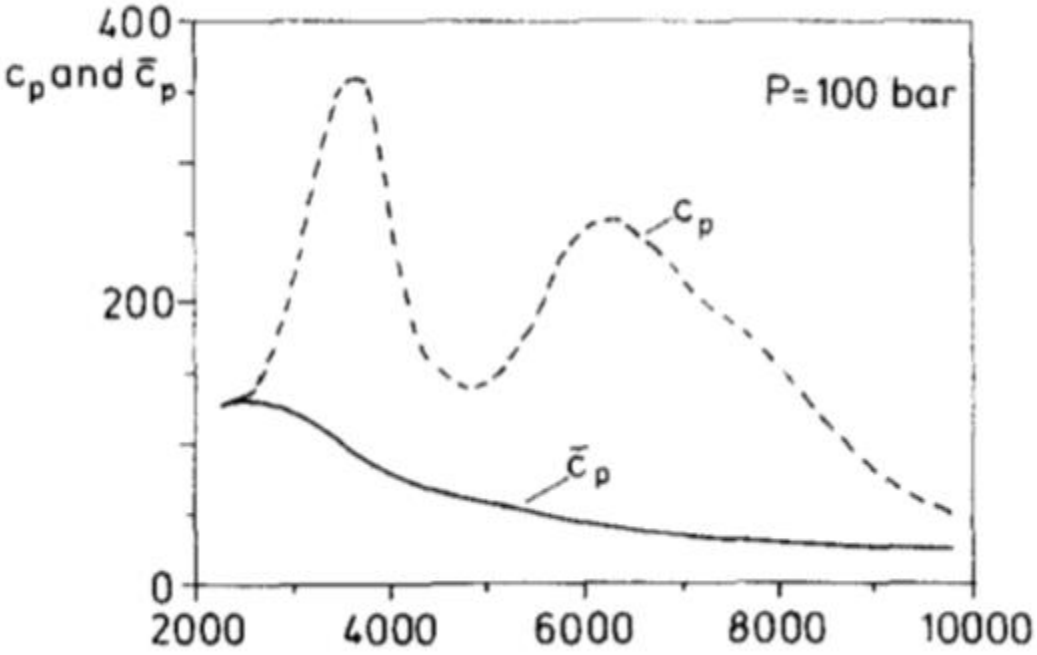

Figure D-10: Heat Capacity of UCF Gas at 100 bar

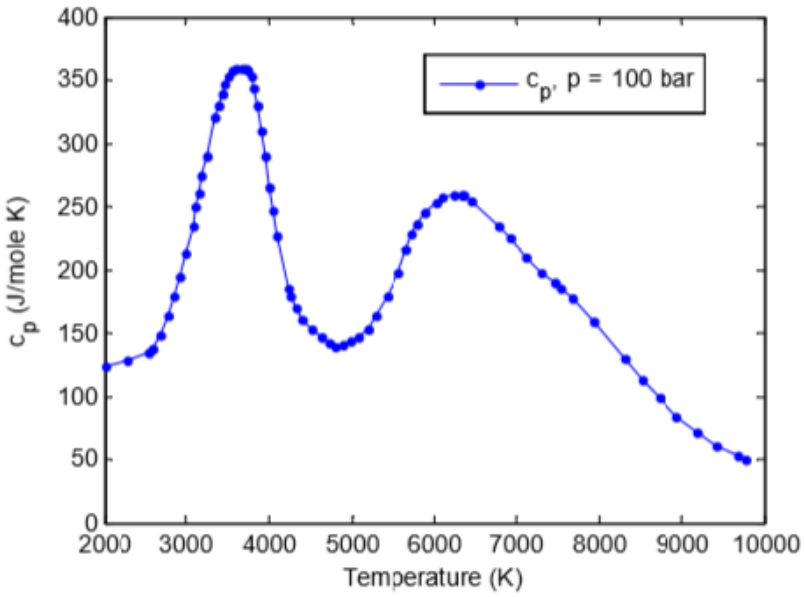

D-11: Heat Capacity of the UCF gas at a Pressure of 10 Mpa

BIBLIOGRAPHY

Adler, D., Bazin, M., and Schiffer M., "Introduction to General Relativity", International Student Edition, McGraw-Hill, 1975.

Anghaie, S., Pickard, P., Lewis, D. "Gas Core & Vapor Core Reactors- Concept Summary" , NASA Technical Report, 1986.

B G Schnitzler, "Gas Core Reactor for Direct Nuclear Propulsion", Idaho National Engineering Lab, Report #EGG-NE-9087

Bissel W R, Gunn SV, "Turbo Pump Options for Nuclear Thermal Rockets", AIAA paper No. 91-3858, July 1992.

Black DL, Gunn SV, " A Technical Summary of Engine and Reactor Subsystem Design Performance during the NERVA Program", AIAA paper No.91-3450, September 1991.

Brengle R G, Gunn SV, " Nuclear Thermal Rocket Engine Exhaust Conditioning in Open Cycle and Closed Cycle Systems", Semipalatinsk-21, Kazakhstan, September 22-26, 1992.

Bussard, R. W., and DeLauer, R. D., *Nuclear Rocket Propulsion*, McGraw-Hill, New York, 1958.

Dana G. Andrews, "Interstellar Propulsion Opportunities using near-term Technology", Acta Astronautica, 55 (2004) 443-451.

D.F Spencer, L.D. Jaffe, " Feasibility of Interstellar Travel", Astronautica Acta 9(1963) 49-58

Del Rossi, A., and Bruno, C., "Safety Aspects in Nuclear Space Propulsion," International Astronautical Congress, Paper IAC-04-R.4/S.7.07, Oct. 2004.

Dewar, J. A., *To the End of the Solar System – The Story of the Nuclear Rocket*, Univ. Press of Kentucky, Lexington, KY, 2004.

D I Poston, T Kammash, "Heat Transfer Model for an Open-Cycle Gas Core Nuclear Rocket", Proc. 9th Symposium on Space Nuclear Power Systems", American Institute of Physics, AIP Conf. Proc No-246, 3, 1083-1088

D I Poston and T Kammash, " Hydrodynamic Fuel Containment in an Open Cycle Gas Core Nuclear Rocket", Proc of 11th Symposium on Space Nuclear Power and Propulsion, American Institute of Physics, AIP Conf. Proc.No.301,1 437:479.

D I Poston and T Kammash, "A Comprehensive Thermal-Hydraulic Model of an Open-Cycle Gas Core Nuclear Rocket", Proc 11th Symposium on Space Nuclear Power and Propulsion, American Institute of Physics AIP Conf. Proc No. 30, 3:1415-1520.

Dunn C, Kaith I, "Design of High Performance Bell Rocket Nozzle for a High Pressure and Thrust NTR", AIAA Paper No. 91-3627, September 1991.

Edelman R B, "Scramjet Technology Assessment", Vol. I. Technical Review, AFWAl-TR-88-2015, May 1989. 1981, 19(5) 601-09.

Edelman R B, Harsha P T, "Modeling Techniques for the Analysis of Ramjet Combustion Process", AIAA Journal

E.Sappel, "Relativity and Clocks near Earth Observations of Spacelab Experiment NAVEX", Naturwissenschaften 77(1990) 325-327

Frank H.Winter, Michael J. Neufeld, Kerrie Dougherty, "Was the Rocket invented or Accidentally Discovered? Some New Observations on its Origins", Acta Astronautica, 77(2012) 131-137.

Frank H.Winter, "The Rocket in India from Ancient Times to the 19th Century", JBIS 32 (1979) 467-471

G.A. Robertson, D.W.Webb, "The Death of Rocket Science in the 21th Century",

Physics Procedia 20(2011) 319-330

George P. Sutton, Oscar Biblarz, Rocket Propulsion Elements. 7th ed. New York: Wiley Inter Science Publications, 2011

Glasstone,S. "Principles of Nuclear Reactor Engineering", D. Van Nostrand company, Inc., Princeton, N.J.,1955

G.L Bennett, "Historical Overview of the US Use of Space Nuclear Power", Space Power, 8-3(1989) 259-284.

G.L.Bennett, R.J. Hemler and A.Schock, "Development and Use of the Galileo and Ulysses Power Sources", Proc. of 45th Congress of the International Astronautical Federation, 1994, IAF-94-R.1.362

G.L. Bennett, S.R. Graham, and K.F. Harer, "Back to the Future: Using Nuclear Propulsion to Go to Mars", Proc. of 27 th Joint Proplsion Conference of AIAA/SAE/ASME, (1991) 91-1888.

G.L Bennett, H.B.Finger, T.J.Miller, W.H.Robbins and M.Klein, "Prelude to the Future: A Brief History of Nuclear Thermal Propulsion in the United States", A Critical Review of Space Nuclear Power and Propulsion (1984-1993), American Institute of Physics, 1994.

G.Marx, The Mechanical Efficiency of Interstellar Vehicles, Acta Astronautica 9 (1963) 131-139

G.M.Gryaznov, “Nuclear Power for Space Vechiles: A new Division in the Energy technology of the Future”, Lzvestiya Akademii Nauk SSSR Energetika I transport, UDC 620.92; 629.786, vol.29.No 6, pp.24-33,1991.

Goel P. Barson, S.Halloran, “The Effect of Combustor Flow Nonuniformity on the Performance of Hypersonic Nozzle”, AGARD-CP-479, Paper No.32, Hypersonic Combined Cycle Propulsion, 1990.

Gurunadh Velidi, Ugur Guven, “Usage of Nuclear Reactors in Space Applications: Space Propulsion and Power Concepts”, Applied Mechanics and Materials, 110-116(2012) 2252-2259.

Gurunadh Velidi, Ugur Guven, “Design of Nuclear Power Plant Using Gas Turbine Modular Helium Cooled Reactors”, Journal of Nuclear Technology, 1(2011) 1-15.

Gurunadh Velidi, Ugur Guven, “Usage of Nuclear Power as a Powerful Source for Space Stations and for Space Development Missions, *Proc. of* International Astronautical Congress, 2011, IAC-11.D4.1.7.

G. Vulpetti, “ Maximum Terminal Velocity of Relativistic Rocket”, Acta Astronautica 12 (1985) 81-90.

Gunn, S. V., and Ehresman, C. M., “The Space Propulsion Technology Base Established Four Decades Ago for the Thermal Nuclear Rocket is Ready for Current Applications,” AIAA Paper 2003-4590, July 2003.

Gunn SV, “Development of Nuclear Rockets Engine Technology”, AIAA Paper No. 89-2386, July 1989.

Gunn SV, “Design of Second-Generation Nuclear Thermal Rocket Engines”, AIAA Papers No. 90-1954, July 1990.

Gunn Sv, Dunn C, “Feed Systems and Nozzle for Phoebus Reactor Experiments”, AIAA Paper No. 67-478, July 1967.

G.M. Anderson, D.T Greenwood, “Relativistic Rocket Flight with Constant Acceleration”, AIAA Journal 7 (1969) 343-344

G. M. Anderson, D.T Greenwood, “Relativistic Rocket Flight with a Constant Rocket Thrust”, Astronautica Acta 16 (1971) 153-158

G. M Piacentino, “Prospects of Nuclear Propulsion for Space Physics”, Jouranl-Ref: Presented at the 2008 SIF Conference Genua, Italy.

Harsha PT, Edelman RB, “Fundamental Combustion Technology for Ramjet Applications”, CPIA-PUB-363, Vol.II, September 1982.

Howe, S. D., DeVolder, B., Thode, L., and Zerkle, D., “Reducing the Risk to Mars: the Gas Core Nuclear Rocket,” *Space Technology and Applications International Forum-1998*, edited by Mohamed S. El-Genk, Publication CP-420, American Inst. Of Physics, New York, 1998, p. 1138.

Howell, John R, Strite, Mary K, “Analysis of Heat-Transfer Effects in Rocket Nozzle Operating with Very High-Temperature Hydrogen, NASA TR R-220, 1965.

Hsia Y-C, Daso EO, “FNS Analysis of a 3-D Scramjet Inlet”, AIAA Paper 91-0129, January 1991.

J. E. HOOGENBOOM, H. V. DAM, and J. C. KUIJPER, “The Temperature Distribution in a Gas Core Fission Reac- tor,” Ann. Nucl. Energy, 18,-4 183, 1991.

J. M. J Kooy, On Relativistic Rocket Mechanics, Astronutica Acta 4(1958) 31-58.

J. Huth, “Relativistic Theory of Rocket Flight with Advanced Propulsion Systems”, ARS Journal (1960) 250-253.

Kerrebrock, Jack L, and Meghreblian, Robert V, "Vortex Containment for the Gaseous-Fission Rocket, Rept. No. TR 34-205, Jet Prop. Lab., C.I.T., Sept.1961.

Koroteev, A. S. (ed.), *Rocket Engines and Power plants Based on Gas-Core Nuclear Reactor*, Mashinostroenie, Moscow, 2002 (in Russian).

L.A.Walton and J.D. Malloy, "Nuclear Propulsion Tradeoffs for Manned Mars Missions", Proc. of 8th Symposium on Space Nuclear Power Systems, Part-II, American Institute of Physics, 1991

L.Nasi , J.-L Raimbault, " A Generalization of the Rocket Formula and its Applications to Advance Space Propulsion Systems", Acta Astronautica, 68 (2011) 34-38.

Lawrence, T. J., Witter, J. K., and Humble, R. W., "Nuclear Rocket Propulsion Systems," *Space Propulsion Analysis and Design*, edited by R.W. Humble, G. N. Henry, and W. J. Larsen, McGraw-Hill, New York, 1995, Chap. 8.

Michael Cook, Howard D. Curtis, ed.l, Aerospace Engineering Desk Reference, First Edition Butterworth- Heinemann imprint of Elsevier. Oxford: 2009

Michal Plavec, "Beginning of Rocket Development in the Czech", Acta Astronautica 69(2011) 905-910.

Mclafferty, G.H: Analytical Study of Moderator Wall Cooling of Gaseous Nuclear Rocket Engines. Rept. No. C-910093-9, United Aircraft Corp, 1964

Palaniswamy S, Ota DK, Chakravartthy, "Some Reacting-Flow Validation Results for USA-Series Codes", AIAA Paper, AIAA-91-0583, January 1991.

Pelaccio, D., Perry, F,, Oeding, "Nuclear Engine Design Technical Assessment Considerations, AIAA 90-1950, AIAA-SAE-ASME-ASEE, 26th Joint Propulsion Conference, Orland .

Powell.J, Paniagua, J. Maise, "High Performance Nuclear Thermal Propulsion System near term Exploration Missions to 100AU and beyond", Acta Astronautica, 44-2(1999) 159-166

Ragsdale.R, "Open Cycle Gas Core Nuclear Rockets", Proceedings of the Nuclear Thermal Propulsion Workshop, NASA Lewis Research Center, 343-357.

R.Serber, "The Use of Atomic Power for Rockets", Douglas Aircraft Company, 5 July 1946.

Robbins WH, Finger HB, "An History Perspective of the NERVA Nuclear Rocket Engine Technology Program", AIAA Paper No.91-3451, September 1991.

Rom, Frank C, Ragsdale and Robert G, "Advanced Concepts for Nuclear Rocket Propulsion", NASA SP-20, 1962, pp. 3-25.

Rosenzweig, Martin L. Lewellen, W.S, "The Feasibility of Turbulent Vortex Containment in the Gaseous Fission Rocket", Preprint No.1516A-60, ARS, Dec. 1960.

Robert Rosen and A Dan Schnyer , "Civilian Usage of Nuclear Reactor in Space", Volume pp, 147-164, Science & Global Security, 1989.

R.Esnault-Pelterie, "Astronutik and Relativitatstsheorie. Die Rakete 2 (1928) 114.

R. H Feisbee, How to Build an Antimatter rocket for interstellar missions, 39th AIAA/ASME/SAE/ASEE Joint Propulsion conference and Exhibit, Huntsville Alabama, July 20-23, 2003.

Roback, R, “Thermodynamics Properties of Coolant Fluids and Particle Seeds for Gaseous Nuclear Rockets. Rept. No. C-9100092-3, United Aircraft Corp., Sept. 1964.

S. Anghaie, G.Chen, “A Computational Fluid Dynamics and Heat Transfer Model for Gaseous Core and Gas Cooled Space Power and Propulsion Reactors”, University of Florida, Prepared for Lewis Research Center, NAS3-26314, 1996.

Sforza, P.M., Cresci, R.J., & Girlea, F, “Fuel Efficient Hydrodynamic Containment for Gas Core Fission Reactor Rocket Propulsion”, IAF 93-R.1.427, 44Th International Astronutical Federation Congress, Graz, Austria, October, 1-11.

Sforza, P.M., Shooman, “A Safety and Reliability Analysis for Space Nuclear Thermal Propulsion Systems”, Acta Astrounatica, 30(67-83) 1992.

Smith, B., and Anghaie, S., “Gas Core Reactor with Magnetohydrodynamic Power System and Cascading Power Cycle,” *Nuclear Technology*, Vol. 145, No. 3, 2004, pp. 311–318.

Seetesh Pande, Ugur Guven, Gurunadh Velidi, “ Interstellar Space Flight Using Nuclear Propulsion and Advanced Techniques”, *Proc. of* International Astronautical Congress, 2011, IAC-11.D4.1.7.

Spence R W, Durham RP, “The Los Alamos Nuclear Rocket Program “, Astronautics and Aeronautics, June 1965. pp.42-46.

S.V Gunn “Development of Nuclear Rocket Engine Technology”, Proc.of 25th Joint Propulsion Conference of AIAA/ASME/SAE/ASEE, (1989) 89-2986

Stanley Gunn, “Nuclear Propulsion-a Historical Perspective”, Space Policy, 17(2001) 291-298.

Taub J M, “ A Review of Fuel Element Development for Nuclear Rocket Engines”, LASL LA-5931, June 1975.

Thomas J Miller, Dr.Gary L. Bennett, “Nuclear Propulsion for Space Exploration”, Acta Astronautica, 30 (1993) 143-149.

Ugur Guven, Gurunadh Velidi, “Nuclear Propulsion in Spacecraft as a Unique Solution for log Range Mission”, *Prof. of* International Astronautical Congress, 2011, IAC-11.A3.3A.6.

Way, K., and E.Winger, “The Rate of Decay of Fission Products, Phys.Rev., vol.73-11(1948) 1318.

Wetch J R, Goldin, LY Koroteev, “Development of Nuclear Rocket Engines in the USSR”, AIAA Paper No.91-3648, September 1991.

W.L. Smith G.L Bennett and T.J. Miller, “Nuclear Thermal Propulsion: Mission Benefits”, Proc. of 30th Joint Propulsion Conference of AIAA/ASME/SAE/ASEE, (1994) 94-2758

W.L Bade, Relativistic Rocket Theory, American Journal of Physics 21 (1953) 310.

Shepherd, L. R., and Cleaver, A. V., “The Atomic Rocket-2 and -3,” *Journal of the British Interplanetary Society*, Vol. 7, No. 6, 1948, pp. 237–240; also Vol. 8, No. 1, 1949, p. 30 also Bussard, R. W. and DeLauer, R. D., *Nuclear Rocket Propulsion*, McGraw-Hill, New York, 1958, p. 319.

PUBLICATIONS FROM THE AUTHOR

Gurunadh Velidi, Ugur Guven, "Usage of Nuclear Reactors in Space Applications: Space Propulsion and Power Concepts", Applied Mechanics and Materials, 110-116(2012) 2252-2259.

Gurunadh Velidi, Ugur Guven "Utilization of Gas Core Nuclear Reactors for Nuclear Safety and Efficient Nuclear Waste Management ", Asian Journal of Science and Technology 12 (2011) 48-66.

Gurunadh Velidi, Ugur Guven "Usage Of Nuclear Power as a Powerful Source for Space Stations And For Space Development Missions", *Proc. of International Astronautical Congress, 2011, Cape town, IAC-11-C4.7.-C3.5.*

Ugur Guven**, Gurunadh Velidi**, "Nuclear Propulsion in Spacecraft as a Unique Solution for a Mars Mission", *Proc. of International Astronautical Congress, 2011, Cape town*, IAC-11.A3.3A.6.

Seetesh Pande, Ugur Guven, **Gurunadh Velidi,** "Interstellar Spaceflight Using Nuclear Propulsion and Advanced Techniques", *Proc. of International Astronautical Congress, 2011, Cape town, IAC-11.D4.1*

Gurunadh Velidi , Ugur Guven, Aakankash Dhar, " Gas Core Reactors as Technological Break Through for Long Range Space Missions", ", *Proc. of Global Space Exploration Conference 2012 , GLEX-2012,09,2,7,x1240.*

Gurunadh Velidi , Ugur Guven, Aakankash Dhar, Yachna Gola " Nuclear Power As a Powerful Solution in Supporting Systems and Mission Components for

International Space Station ", *Proc. of Global Space Exploration Conference 2012 , GLEX-2012,01,P,1,p,1,x1244.*

Gurunadh Velidi , Seetesh Pande, Ugur Guven, Samaksh Bhel, Alpha Centauri Mission Using Interstellar Flight: Technological Possibilities and its Limitations , *Proc. of Global Space Exploration Conference 2012 , GLEX-2012,05,P,6.p1,x12396,* 9.

Ugur Guven, **Gurunadh Velidi,** Harisha Emmadi, Aakankash Dhar, " Space As a Dream Destination to a Mankind: Space Tourism Flight design with Economical and Technological Feasibility, ", *Proc. of Global Space Exploration Conference 2012 , GLEX-2012,-14,P,5.p1,x12416*

Ugur Guven**, Gurunadh Velidi,** Pavan Kumar Nanduri, Seetesh Pande, "The Utilization of Robotic Space Probes in Deep Space Missions: Case Study of AI Protocols and Nuclear Power Requirements", *Proc. of International Conference on Mechanical Engineering, Robotics and Aerospace*, 2011.

Ugur Guven, Piyush Kuchhal**, Gurunadh Velidi**, " Extraction of Strategic Raw Materials and Helium 3 from the Moon and from the Asteroids for Clean Fusion Energy", *Proc. of Global Space Exploration Conference 2012 , GLEX-2012,11,1,12,X12437*

Ugur Guven, Mrinal Sharma, Surbhi Sacklecha, **Gurunadh Velidi,** " Mining Rights of Developing Nations on Quest for the Moon: Case Study of Helium 3 Mining Rights", *Proc. of Global Space Exploration Conference 2012 , GLEX-2012,12,2,2,x12447*

Ugur Guven, **Gurunadh Velidi**, Sampath Emani, *" Effect of Boundary Layer Formation on Fuel Pebbles in Gas cooled Reactor" Advancements in Fluid Dynamics and Thermodynamics Conference, Singapore, 2012*

Ugur Guven, Pavan Kumar Nanduri**, Gurunadh Velidi,** Seetesh Pande, "Interstellar Communication Techniques for Long Range Mission Spacecraft", *proc. of International Astronautical congress 2012,* IAC-12- B2,1,5,x12898

Ugur Guven, **Gurunadh Velidi,** Seetesh Pande "Interstellar Mission to Lalande 21185: Possibilities for the Future", ", *proc. of International Astronautical congress 2012,* IAC-12-D4,1,7,x15192.

Rajesh Yadav**,** Ugur Guven, **Gurunadh Velidi,** Karthik Sundarraj "Effect of Eccentricity on the Heat Transfer Rates of a Re-entry Vehicle with Concave Windward Surface", ", *proc. of International Astronautical congress 2012,* IAC-12, C2,7,9x12902

Rajesh Yadav, Ugur Guven**, Gurunadh Velidi,** "Aerothermodynamics of Generic Reentry Vehicle with a Series of Aero spikes at Nose, ", *proc. of International Astronautical congress 2012,* IAC-12, D2,5,9x12903

Rajesh Yadav, **Gurunadh Velidi,** Ugur Guven, " Aerothermodynamics of a Hemispherical-Cylindrical Blunt Vehicle with a Flow through Duct", ", *proc. of International Astronautical congress 2012,* IAC-12, C2,7,11x12904

Karthik Sundaraj, Linsu Sabastine, Ugur Guven, Rajesh Yadav, **Gurunadh Velidi**, " Effect of Nose Cavity on the Heat Fluxes to Reentry Vehicle in Titan's Atmosphere", ", *proc. of International Astronautical congress 2012,* IAC-12- A3,5,13.p1,x12886

Gurunadh Velidi, Ugur Guven, Seetesh Pande, Pavan Kumar Nanduri, "Analysis of Radiation Effects on Astronauts for a Manned Mission to Mars Using Nuclear Space Propulsion", ", *proc. of International Astronautical congress 2012,* IAC-12-A1,4,19.p1,x13727

Sourabh Bhat, Ugur Guven, Rajesh Yadav, **Gurunadh Velidi,** "Effect Of Nose Cavity On Heat Transfer Rates To The Surface Of An Aeroshell Descending Through The Martian Atmosphere", ", *proc. of International Astronautical congress 2012,* IAC-12- A3,3A,13.p1,x12885

Ugur Guven, **Gurunadh Velidi**, Seetesh Pande, Pavan Kumar Nanduri, "Analytical Exploration of Manned Space Mission to Heliopause", *Proc. of International Astronautical congress 2012.*

Gurunadh Velidi, Ugur Guven, "Design of Nuclear Power Plant Using Gas Turbine Modular Helium Cooled Reactors", Journal of Nuclear Technology, 1(2011) 1-15.

Rajesh Yadav, **Gurunadh Velidi**, Ugur Guven, "Aerothermodynamics of Generic Reentry Vehicle with A Series of Aerospikes At Nose", Acta Astronutica, 11 (2013) 43-57.